joint research centre
EUROPEAN COMMISSION

Annual Report

Institute for Transuranium Elements

1999

Institute for Transuranium Elements Annual Report 1999

EUROPEAN COMMISSION
JOINT RESEARCH CENTRE

Report EUR 19054 EN

Institute for Transuranium Elements (ITU)

The mission of ITU is to protect the European citizien against risks associated with the handling and storage of highly radioactive elements. ITU's prime objectives are to serve as a reference centre for basic actinide research, to contribute to an effective safety and safeguards system for the nuclear fuel cycle, and to study technological and medical applications of transuranium elements.

ANNUAL REPORT 1999

Institute for Transuranium Elements

EUROPEAN COMMISSION
JOINT RESEARCH CENTRE

EUR 19054 EN

Published by the

EUROPEAN COMMISSION

Directorate-General Joint Research Centre

INSTITUTE FOR TRANSURANIUM ELEMENTS

LEGAL NOTICE

Neither the European Commission nor any person acting on behalf of the Commission is responsible for the use which might be made of the following information

This report was compiled and edited by
R. Schenkel, J. Richter, J. Magill, D. Pel

Inquiries for more details should be addressed to the Programme Office,
Institute for Transuranium Elements, P.O. Box 2340, D-76125 Karlsruhe,
Phone ++49-7247-951287, Fax ++49-7247-951591
E-mail: joseph.richter@jrc.org

This publication and more information on the Institute may be found on the Web site:

http://www.jrc.org/

Graphic design:
Wilhelm Stober GmbH, Druckerei und Verlag · Eggenstein

A great deal of additional information of the European Union is available on the Internet.
It can be accessed through the Europa server (http://europa.eu.int).

Cataloguing data can be found at the end of this publication.

EUR 19054 EN

Luxembourg: Office for Official Publications of the European Communities, 2000

ISBN 92-828-8985-8

Printed in Germany

Foreword

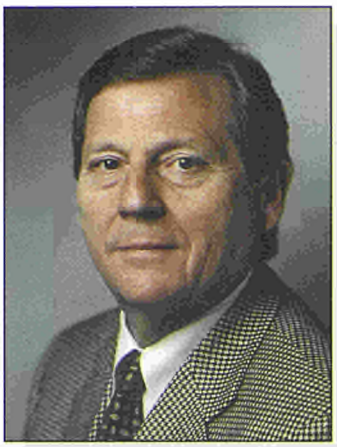

J. van Geel
Director

Once again, it is a great pleasure for me to present the Annual Report of the Institute for Transuranium Elements. I do this with somewhat mixed feelings, since 1999 is the last year of my almost 14 year period as Director.

During this period at the Institute there have been many changes. In a time where we have seen interest in nuclear energy wane, the Institute has equipped itself to face a much more competitive environment, to venture into new areas, and to support the policies of the European Union.

We have seen "third party" work introduced, and this now accounts for about 15% of the Institute's total budget. Our customer base comprises of research organisations, industry, authorities, and inspectorates. This is a major achievement and a great credit to the staff. To achieve this, quality management techniques have been introduced. This has led to certification of standards in our laboratories and to a "stamp of approval" which enables us to compete effectively and guarantee quality in the work for our customers.

ITU supports increasingly Commission Directorates in the areas of nuclear safety for Eastern countries (DG External Relations), radioactivity in the environment (DG Environment) and safeguards (DG Energy). A milestone in this respect has been the inauguration this year of the "On-site-Laboratory" at Sellafied (U.K) for safeguards measurements. The design and installation work for this laboratory for nuclear material accountancy was carried out by ITU staff.

During 1999, new experimental facilites have been developed and reflect a concentration of our mainstream activities. Of great interest here is the ability to investigate advanced aqueous and pyroprocessing techniques for processing spent fuel to separate or partition the more harmful radioactive by-products from nuclear waste. Once separated, these by-products can then be fabricated into targets in a new Minor Actinide laboratory. Thereafter, they will be irradiated in dedicated reactors in which they will be converted into less harmful products. Success in these activities may have considerable impact on the problem of radioactive waste disposal and ultimately lead to better acceptance of nuclear energy.
A spin-off activitiy, i.e. alpha-immunotherapy, continue to expand to meet increasing interest from hospitals. This activity underlines again the beneficial effects that radiation can have - in this case the treatment of patients with cancer.
Our mainstream in-house activities in the field of basic actinide research continues to provides the necessary scientific platform upon which such new activities can be launched. We attract a large number of young researchers through our reputation and publications in actinide science and the first class research facilities that ITU has at its disposal.

Finally, I feel deeply satisfied that I leave with the Instititue in a healthy state. The new 5th Framework Programme of the European Union will require once again a shifting of priorities within the Institute programme and demand a continuing flexibility among the co-workers. I do not hesitate when I say that ITU will rise to meet these challenges with all the energy and fervour that have been so apparent over these last 14 years.

Institute for Transuranium Elements Annual Report 1999

A - The Institute in Overview

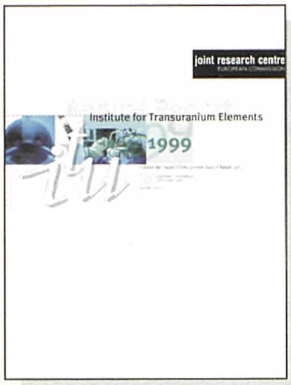

B - Activities in Progress

ITU's Contribution to the 5th Framework Programme

Economy and acceptability remain keywords for long-term nuclear developments. Acceptability implies safety, proliferation resistance, low or negligible health impact. In response to these remarks made by the Scientific Audit Team in their report on the Institute's activities, ITU scientists will continue to concentrate their efforts on making a useful contribution in the 5th Framework Programme.

Changes were introduced into the new research programme, following extensive discussions with other Commission Directorates who were involved in the conception, monitoring and implementation of nuclear related EU policies. One result of these consultations was the establishment of a new research direction, i.e. Radioactivity in the Environment.

In support of the European Commission's programme "Serving the Citizen" through Medical and Health Applications, ITU performs

- Alpha-Immunotherapy studies.

In support of the EAEC (Euratom) programme "Nuclear Fission Safety", ITU activites centre on

- Basic Actinide Research
- Safety of Nuclear Fuel
- Partitioning and Transmutation
- Measurement of Radioactivity in the Environment
- Spent Fuel Characterisation in View of Long-Term Storage.

In the interest of Euratom's "Control of Nuclear Materials and Safeguards" and the EC's non-proliferation commitments, ITU does

- Safeguards Research & Development work.

ITU continues to provide services to other Directorates-General, to network with other research centres, to do work for third parties. With these activities ITU earns some 15% of its budget.

ITU's ambitions, in line with the Audit team's recommendations are to:

- remain a source of advice in the sensitive field of nuclear technology and
- remain a centre of excellence in research,

with a view of guaranteeing quality service for the benefit of the European citizen.

More details on ITU's activities over the reporting period can be found in the following pages.

Alpha-Immunotherapy

Developing, testing, and validating a new type of drug against various forms of cancer presents a challenge to scientists and raises hope in patients. ITU has been studying the use of high-energy low-range alpha particles, coupled to suitable antibodies. Bismuth-213, a daughter product of actinium-225, has been packed into a "magic bullet" to combat cancer.

Collaboration with universities, hospitals and the pharmaceutical industry in Europe and in the U.S. was intensified in the search for additional suitable alpha-emitting nuclides, cancer-specific carriers, e.g. antibodies or peptides, and appropriate chelators (the "glue" holding the nuclide and the carrier together).

With demand for alpha-emitters for clinical tests rising, large-scale production of actinium-225 from radium-226 has become necessary. Therefore, ITU is exploring new production paths for these radionuclides. Facilities were created for preparing radium targets, treating them after irradiation in a cyclotron, and separating the actinium. A sufficient number of actinium / bismuth generators can be sent to hospitals in Europe and elsewhere once the ongoing tests have been successfully completed.

The short half-life (45 minutes) of bismuth-213 has proved a handicap in certain assessments of the therapy's effectiveness. ITU has designed and created a novel, longer-lived mixture of other bismuth isotopes. The product is being tested at the German Cancer Research Centre, Heidelberg, where specialists are also performing pre-clinical tests with bismuth-213 for non-Hodgkin lymphoma.

Investigations to treat various other types of cancer are also underway at hospitals and universities in New York (U.S.), Nantes (F), Gent (B), Basle (CH), Göttingen, and Munich (D).

Demands are high on Roger Molinet's concentration and skills when labelling antibodies with bismuth-213 for targeted tumour therapy.

Basic Actinide Research

Good knowledge of fundamental physical, chemical and materials science data on actinides and actinide-containing products, i.e. nuclear fuels and nuclear waste, is the basis for addressing nuclear issues.

ITU scientists aim at developing an understanding of the properties, especially the electronic structure, of these actinides and actinide compounds. Activities range from preparing and purifying the elements to studying single crystals by sophisticated physical techniques, some of which involve the use of intense synchrotron beams, neutron or muon beams. Theoretical research on the electronic properties of the actinides backs up experiment and suggests new avenues for investigation.

With new fuel materials for advanced reactors under discussion, materials science data are urgently required. The supply of data such as phase diagrams, thermal properties, pressure behaviour and irradiation behaviour is a genuine task for basic actinide research. Findings of investigations can also help to answer questions arising in connection with the management of highly active waste.

Characteristics of ITU Basic Actinide Research are high-quality scientific publications, visibility at international conferences, and world-wide collaboration with academia and national research centres. The Group has traditionally hosted scientists for well-defined experiments. With the creation of the Actinide User Laboratory, its attractiveness has grown.

Particular attention is given to training the next generation of scientists, especially those from Member States which lack fissile materials handling installations. Results are encouraging with the number of students, doctorals and post-docs, spending up to three years at ITU, remaining at a constant level – despite scepticism of nuclear sciences among the general public.

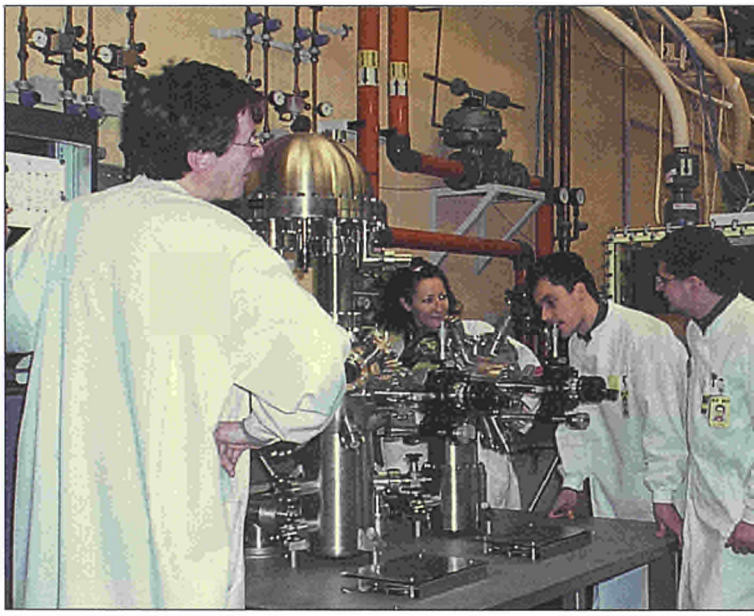

New directions in actinide science: preparation of thin films for surface studies. Valérie Ichas (right) and the doc and post-doc grantees Frédéric Miserque, Monique Idiri, Andreas Lindbaum, Karsten Litfin (from left)

Safety of Nuclear Fuel

Safety of nuclear installations is a major public concern, affecting operators of power reactors, fuel fabrication plants, national and international licensing and regulatory authorities alike. Demand on research for solutions is multi-layered: regulators insist on improved safety, plant operators strive for increased operational efficiency.

Leaving fuel rods inside the reactor for longer operation periods seems a viable compromise. However, there may be limits to subjecting fuel rods to so-called higher burn-up. ITU is, therefore, investigating these phenomena and factors that may endanger the integrity of the fuel and thus set limits to extended burn-ups.

ITU has concentrated on mechanical and chemical interactions at the fuel / cladding interface and on enhanced fission gas release and related modifications of the microstructure of the fuel.

Through participation in PHEBUS, the reactor meltdown simulation project, ITU has gained new insights into the behaviour of melted fuel rod bundles and of the behaviour of aerosol deposits in the primary circuit.

Modelling remains an integral part of safety studies. The TRANSURANUS fuel performance code has been complemented with new data. Training of users has continued, including scientists from East European countries.

Another approach to improve fuel safety and reduce civil and military stockpiles of plutonium is the development and use of advanced fuels. Together with European partners, ITU is developing advanced fuel fabrication techniques based on the Sol-Gel process and carbo-thermal reduction.

Safety-relevant studies with a bearing on advanced fuel fabrication techniques and protection of operating personnel were continued.

Safety research often needs its own instruments. ITU's latest development is a compact and user-friendly precision tool for recording a full thermal spectrum in a few milliseconds and obtaining information on the temperature of the emitting surface. The device can be used under difficult conditions, e.g. for measuring materials with high evaporation rates.

ITU specialists guiding telemanipulators in shielded hot cells: Giorgio Palgiosa and Kuno Römer (left and right); Oliver Courson (middle) monitoring his PC screen.

Partitioning and Transmutation

Lowering the radiotoxicity of waste by reducing the quantity of actinides and other long-lived radioactive elements in the fuel cycle means reducing potential long-term hazards arising from growing stockpiles of spent fuel and separated civil and military plutonium.

Separating long-lived nuclides from the waste, recycling them in reactors for transmuting or "burning" them by neutron capture or fission is considered an important waste management option.

Under its Partitioning and Transmutation programme, and in close co-operation with its European partners, ITU has been testing and evaluating processes that permit an efficient separation (partitioning) of radiotoxic elements from spent fuel with a minimum of losses. Advanced aqueous and dry reprocessing techniques have received particular attention.

ITU has also been studying techniques appropriate for processing the resultant product. It aims at optimising fuel fabrication technology for novel, minor-actinide containing fuels for the transmutation or "incineration" of long-lived actinides and fission products. It has, therefore, tested existing and new fabrication techniques for fuels and targets used in irradiation experiments. Also inert matrices, i.e., uranium-free fuels, for effective burning of excess civilian or military plutonium were produced and studied at ITU.

Further, ITU has started developing and testing new analytical techniques for measuring minor actinide fuel solutions and compounds.

Minor actinide containing materials cannot be fabricated in conventional facilities. Remote handling and shielded cells are necessary to protect operators from intense radiation. ITU's Minor Actinide Laboratory meets all of these requirements. The laboratory will be commissioned soon and can open its doors to its partners in 2001.

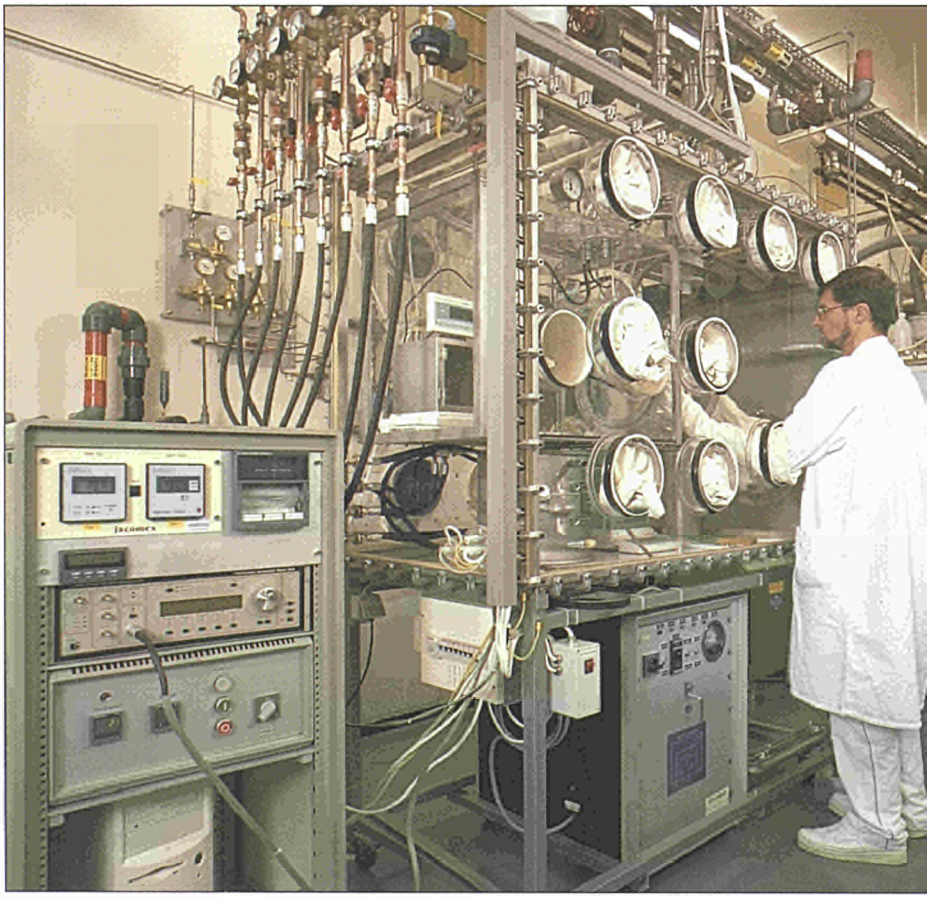

Michel Ougier testing the newly installed glove-box for pyrochemical studies on radioactive waste.

Measurement of Radioactivity in the Environment

"We agree to prevent pollution of the maritime area from ionising radiation through progressive and substantial reductions of discharges, emissions and losses of radioactive substances ...." is the objective of Art.15 of the SINTRA statement released by the Ministerial Meeting of the Oslo Paris (OSPAR) Commission on 23.7.1998 for the Protection of the Marine Environment of the North-East Atlantic.

In response to the needs, especially of the Environment DG, ITU has embarked on this new activity.

It is applying its expertise in trace analysis to tasks of verification of radioactive discharges and emissions from nuclear installations, the identification and characterisation of radioactive scrap material and sources. Work also includes studies on migration patterns of actinides in the biosphere. Also, technical assistance in radiological emergencies is foreseen under the programme.

After carefully defining the development programme among the partners and assessing the suitability of available equipment, work has started at ITU. Minute particles containing actinides were successfully selected and separated for chemical analysis.

This new project is gaining momentum. ITU scientists' ambitions are focused on becoming a European reference laboratory in this field.

Laura Aldave de las Heras preparing hot swipes in a "clean" glove box.

Spent Fuel Characterisation in View of Long-term Storage

The two approaches for waste management favoured by the Member States of the European Union are intermediate storage with subsequent conditioning for final disposal and intermediate storage with subsequent reprocessing before final disposal in geological formations.

The behaviour of irradiated fuel under conditions of direct long-term disposal requires further investigation with regard to basic processes involved. Safety relevant data on the corrosion and dissolution behaviour of waste under realistic conditions are of utmost importance to determine the radiotoxic potential and assess the consequences of storage over extended periods of time.

In this context, ITU, continues to study the leaching behaviour of real high burn-up spent fuel, including MOX material. Particular attention is given to the different types of groundwater and other parameters as they prevail under realistic conditions.

After about 500 years' storage the radioactivity of the spent fuel stems mainly from alpha decay, and alpha radiolysis plays a key role. It will damage the structure of the fuel and influence its dissolution behaviour. For studying the influence of radiolysis on spent fuel dissolution, ITU has prepared and studied samples of UO_2 containing different concentrations of short-lived actinides (mainly Pu-238). New specimens are being fabricated with the much longer lived U-233 as the source of alpha-radiolysis.

Also, the influence of agglomerates rich in plutonium oxide on the dissolution mechanisms of MOX fuels was further investigated.

In performing its work, ITU will remain in close contact with national research centres and agencies as well as Member State authorities in charge of long-term storage of waste.

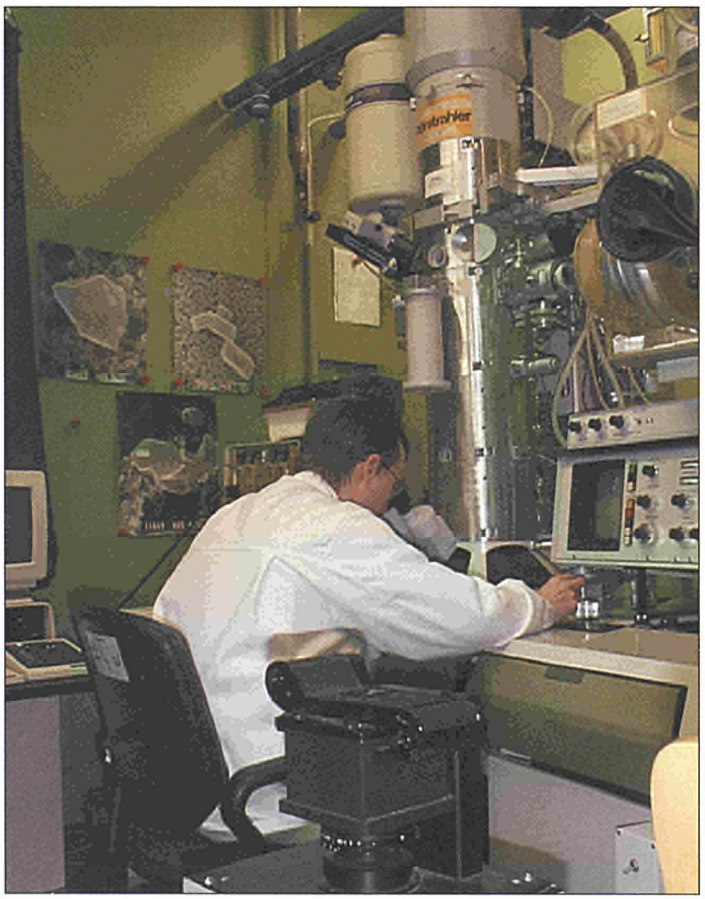

Thierry Wiss investigating α-damage accumulation in $(U,Pu)O_2$ using the Transmission Electron Microscope (TEM).

Safeguards Research and Development

Preventing proliferation of nuclear material is a world-wide task shared by the European Commission's Euratom and the International Atomic Energy Agency (IAEA) inspectorates. They are responsible for implementing safeguards measures to control the use of nuclear materials within the European Union and world-wide.

As a long-time partner, ITU has been providing assistance with expertise on plutonium handling facilities, such as reprocessing or MOX fuel fabrication plants. As the Commission's Analytical Reference Laboratory in Safeguards it has developed new analytical tools to analyse and characterise different nuclear materials, perfecting them to perform forensic analysis and identify seized, illicit material.

ITU has fulfilled its commitment for designing and installing an in situ laboratory for safeguards measurements: the first On-Site Laboratory was inaugurated at BNFL's Sellafield reprocessing plant in October. Work for a second installation of this kind at Cogema's La Hague plant is making good progress.

ITU's participation in a round robin test on nuclear forensics, organised by the P-8 International Technical Working Group, was successful with the identification of the origin of an unknown plutonium sample. In the same context, a model action plan for the seizure of nuclear material was developed and demonstrated in the Ukraine.

The ITU nuclear materials databank was extended by integrating data received from industry in the Member States.

Progress was made in the environmental monitoring field by refining analytical techniques and instrumentation. The circle of inspectors trained in safeguards on high-performance trace analysis (HPTA) has widened: the Brazilian-Argentine Agency for Accounting and Control of Nuclear Materials has sent its delegates to Karlsruhe for the ITU courses.

The first tour of the On-Site Laboratory in Sellafield after its inauguration; (from left to right): Professor Jacques van Geel together with Hans Günther Schneider (ITU), and Mr. Wilhelm Gmelin (Euratom Safeguards Office, Luxembourg).

Competitive Activities

In this first year of the 5th FWP, ITU submitted 15 new Shared-Cost Action proposals in the nuclear field. One new proposal - a "Cluster" with the JRC Institute for Health and Consumer Protection, Ispra is in the field of alpha-immunotherapy.
Four Competitive Support Activities (focussed on technology transfer and validation) were started under the competitive action scheme with several hospitals and research partners; one Innovation Programme Proposal entered the implementation phase and includes both international and regional collaboration (German Cancer Research Centre, DKFZ, in Heidelberg).

In the field of Safeguards, a large effort was made to satisfy the request for analyses by our customer DG Energy. This covers enrichment, fuel fabrication and reprocessing plants and the relatively new area of detecting clandestine or undeclared activities through the analysis of "swipes" from enrichment plants or hot cells.

In the related area of combatting illicit trafficking of nuclear materials, several PHARE / TACIS projects were completed for DG External Relations. This includes the demonstration of the on-the-spot use of the transferred know-how and equipment, such as in Hungary, Bulgaria and the Ukraine.

ITU's core competences in safety of nuclear fuel research, partitioning and transmutation, spent fuel behaviour characteristion also gave rise to a large volume of Third Party Work in 1999. Many European industrial nuclear organisations are included in ITU's customer book.

Outside Europe, ITU is collaborating with EPRI in the US and KAERI in Korea. Long-lasting relations with the Japanese CRIEPI were continued and strengthened in 1999 with a new activity in the field of pyrometallurgical processing. The addition of European research partners working for advanced / alternative reactor concepts, such as ADS, have also expressed interest in this direction.

Finally, 1999 was a year of major challenge for the installation, on-site testing, and commissioning of the on-site safeguards laboratories in Sellafield and La Hague, which, starting from 2000, will be operated by a qualified team of ITU technicians, supporting DG Energy, Luxembourg.

Fig. All smiles after signing another important contract: Dr. Mitsuo Fukushima of CRIEPI, Japan, and Professor Jacques van Geel, ITU Director.

Growth of single crystals of mixed actinide dioxides

Despite receiving considerable attention for the past 50 years, the actinide dioxides continue to provide significant scientific and technological challenges. By far the greatest effort has been made with UO_2, for which large single crystals have existed for many years. Ostensibly simple compounds with the CaF_2 face-centered cubic structure, the dioxides may exist in many stoichiometric forms with both excess and reduced oxygen content. From a technical perspective the interaction with oxygen (e.g. distribution of vacancies or interstitials, their mobility etc.) as well as how other atoms (e.g. fission products) react in UO_2 are the central questions. These problems are naturally even more complex in mixed actinide oxides [e.g. the fast neutron reactor fuel MOX, $(U_{0.8}Pu_{0.2})O_2$] and in potential fuels planned for the transmutation of the minor actinides such as Np, Am, and Cm in fast neutron reactors. A more complete knowledge and characterisation of these mixed oxides is therefore necessary, and a pre-requisite for these investigations is the availability of single crystals.

In basic research on the electronic and magnetic properties of these materials there are still major questions remaining; for example, in 1999, papers appeared on the basic properties of all three actinide dioxides UO_2 [1], NpO_2 [2], and PuO_2 [3].

Returning to a process developed some 20 years ago, we have used the vapour transport method involving $TeCl_4$ to grow a wide series of mixed actinide dioxides, as well as the stoichiometric dioxides themselves. Fig. 1 shows a single crystal of PuO_2 and Fig. 2 one of $(U_{0.88}Pu_{0.12})O_2$. Single crystals have also been achieved of other mixed oxides, e.g. $(Np,U)O_2$ and even mixtures containing small amounts of Am.

Although the crystals produced by this method are small, the crystal quality is very good. Modern techniques are able to extract a considerable amount of information from experiments on such crystals.

As an example of the studies that can be performed on these small crystals, we show in Fig. 3 the energy dependence of the magnetic scattering of x-rays from a 0.73 mg crystal of NpO_2 compared to that from a similar size crystal of $NpRu_2Si_2$ (also grown at ITU). The results from these studies have established the ground state of NpO_2, although the form of the energy dependence as shown in the Fig. 3 is not yet understood. Such studies, and others involving different techniques, will now be extended to the single crystals of mixed oxides grown at ITU.

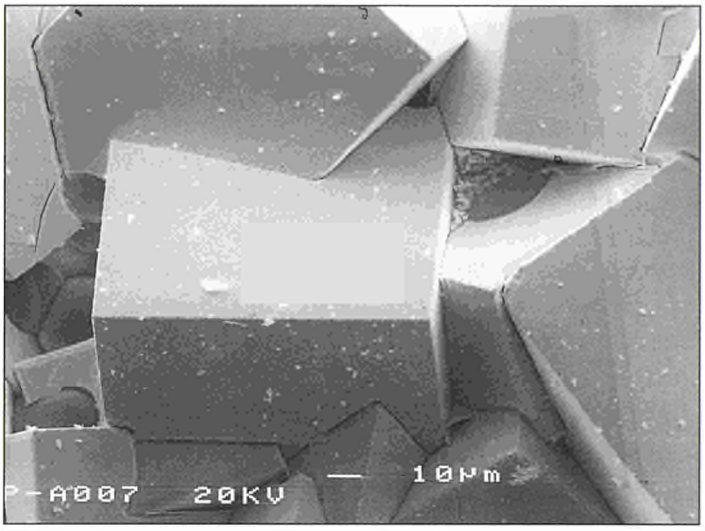

Fig. 1 Scanning electron microscope image of PuO_2 single crystals grown by the chemical vapour transport method.

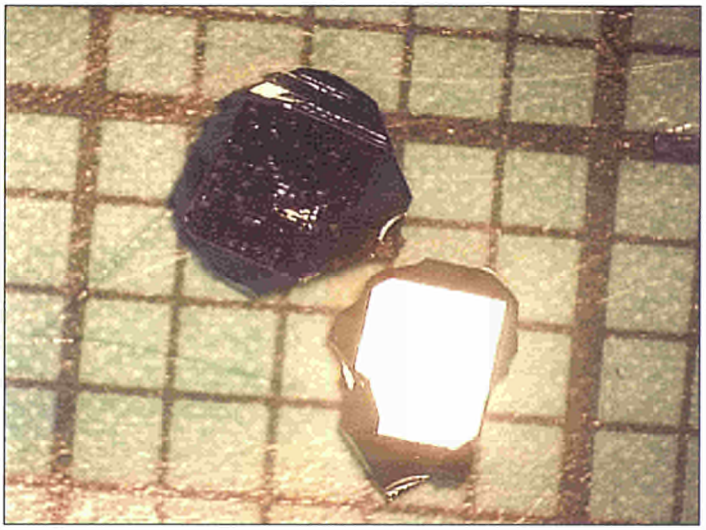

Fig. 2 Single crystal of $(U_{0.88}Pu_{0.12})O_2$ isolated from the material by mechanical fragmentation.

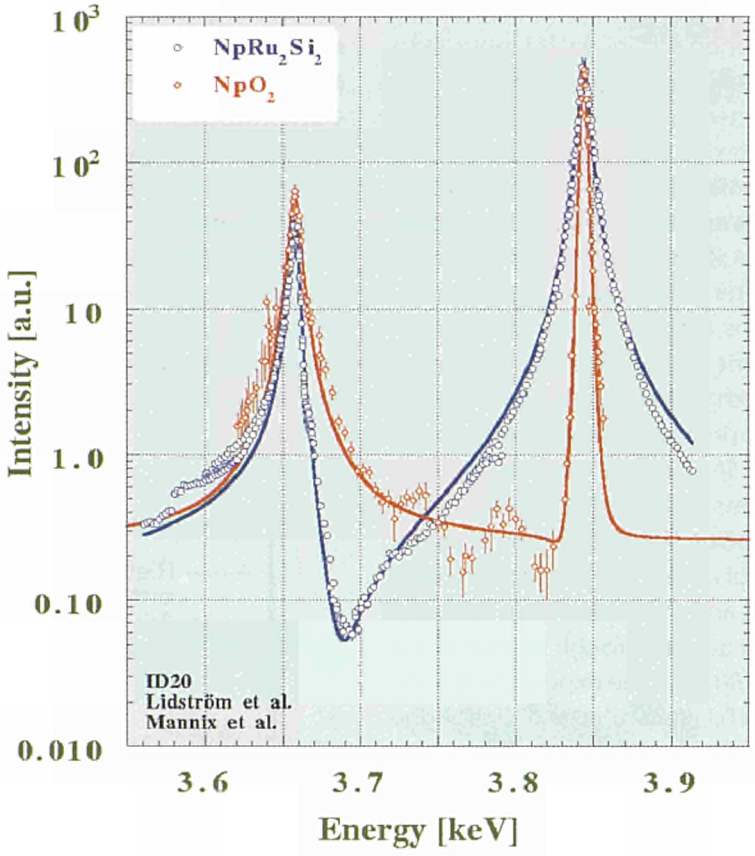

Fig. 3 The figure shows the dependence of the intensity of magnetic scattering from the antiferromagnetic arrangement in these crystals as a function of incident photon energy. The two peaks represent transitions from the spin-orbit split core 3d electron shell to the two possible 5f configurations – the M_5 at 3.66 keV, and the M_4 at 3.84 keV in the case of neptunium. The blue curve for $NpRu_2Si_2$ is similar to that found for other actinides. It consists of two interfering resonances represented by Lorentzians. The solid line is a fit to the open points. On the other hand, the shape of the resonances in NpO_2 is quite different from any previously found. At the M_4 (3.84 keV) we find that a Lorentzian-squared curve best fits (red line) the data, whereas a Lorentzian is needed at the M_5 (3.66 keV).

References

[1] R. Caciuffo et al., Physical Review B 59 (1999) 13892
[2] D. Mannix et al., Physical Review B 60 (1999) 15187
[3] S. Kern et al., Physical Review B 59 (1999) 104

New Crystal Phase of Americium Metal

The physico-chemical properties of the actinide metals at ambient pressure vary widely across the series, due largely to the changing nature of the 5f electrons. In principle, the filling of 5f orbitals begins after thorium and it is generally accepted that the 5f electrons are involved to varying degrees in the bonding (itinerant 5f electrons) for protactinium, uranium, neptunium and plutonium. These four elements display quite different properties from the elements with non-bonding (localised 5f electrons) such as americium and the remaining elements of the actinide series. In this sense americium occupies a pivotal position in the 5f series. New insights into the nature of americium's f-electrons with regard to its metallic bonding and the relationship to that in other f elements have been acquired through studies of the metal under pressure up to 100 GPa. The experiments were performed by a team from ITU, Karlsruhe and Oak Ridge National Laboratory, USA on a 5 µg sample at the ID30 beam line of the European Synchrotron Radiation Facility in Grenoble France.

The initial structure of the americium used in the high-pressure studies was the standard dhcp form ($P6_3mmc$; Am (I), a=0.3467, c=1.1240 nm). At 6.1 GPa, the dhcp form of americium converts to an fcc structure (Fm3m; Am (II), a=0.454 nm at 9.0 GPa). With additional pressure, we observed that the fcc Am (II) phase transformed to an Am (III) phase at 10.0 GPa (Fig. 1), which was retained up to 15.0 GPa.

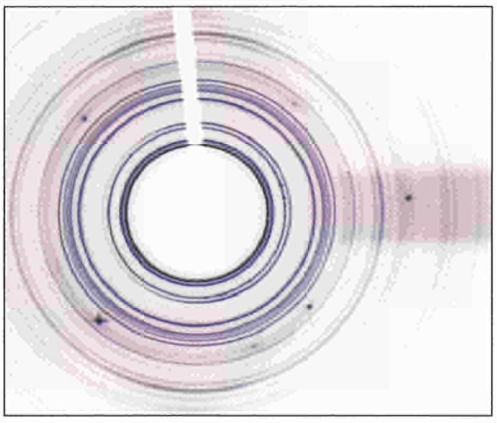

Fig. 1 2-D diffraction image of the 3rd phase of americium metal at 10.9 GPa.

Given the quality of our diffraction data for this phase, especially using N_2 as the hydrostatic pressure-transmitting medium, we determined that the structure has a face centred orthorhombic cell (space group Fddd, Am on 8a sites). At pressures above 15 GPa we observed the formation of a fourth phase Am (IV) which was accompanied by a 7% volume collapse.

Using Rietveld refinement programs, we were able to assign this Am (IV) structure as being orthorhombic, but in contrast to Am (III), with a primitive orthorhombic cell (space group Pnma, Am on 4c sites). Rietveld fits and difference profiles are shown for the Am (III) and (IV) phases in (Fig. 2).

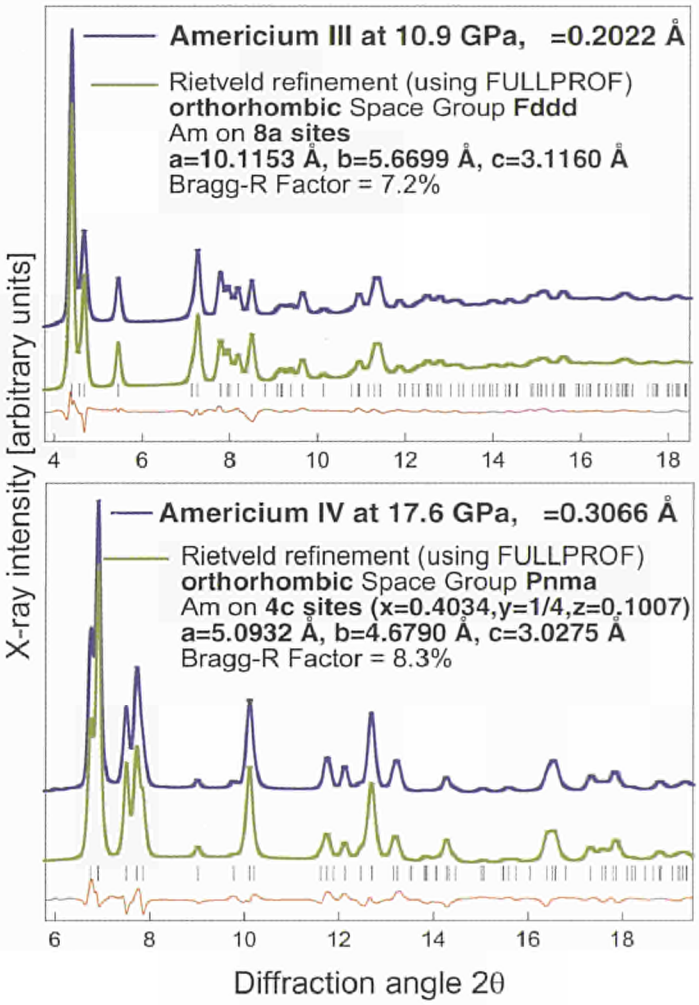

Fig. 2 Rietveld fit and difference profiles of the face centred orthorhombic Am (III) structure (space group Fddd) and the primitive orthorhombic Am (IV) structure (space group Pnma) to the integrated profiles obtained at 10.9 and 17.6 GPa. The tick marks under the profile indicate the reflections allowed for this space group.

The four different americium structures observed in this work are shown as dhcp (Am (I), fcc (Am (II), Am (III) and Am (IV) in (Fig. 3), and permit one to envision the transformation process occurring under pressure. In principle, the structures are composed of close-packed hexagonal or distorted close-packed hexagonal planes with a certain stacking sequence that changes from one structure to the next. In the case of Am (IV) there is an additional "ZIG-ZAG" bending of the hexagonal planes.

This work has established two critical findings about the Am (III) and the Am (IV) structures formed under pressure. First, the Am (III) phase has the same structure as the γ-phase of plutonium [1] where the bonding involves itinerant 5f electrons. Second, the Am (IV) structure is a primitive orthorhombic structure, rather than the base centred orthorhombic α-uranium structure as reported previously, and is stable up to at least 100 GPa. The Am (IV) structure shows a rather small compressibility with pressure, as expected for a metal having 5f-electron character in its bonding.

Reference

[1] W.H. Zachariasen and F.H. Ellinger, Acta Cryst. 8 (1955) 431-433

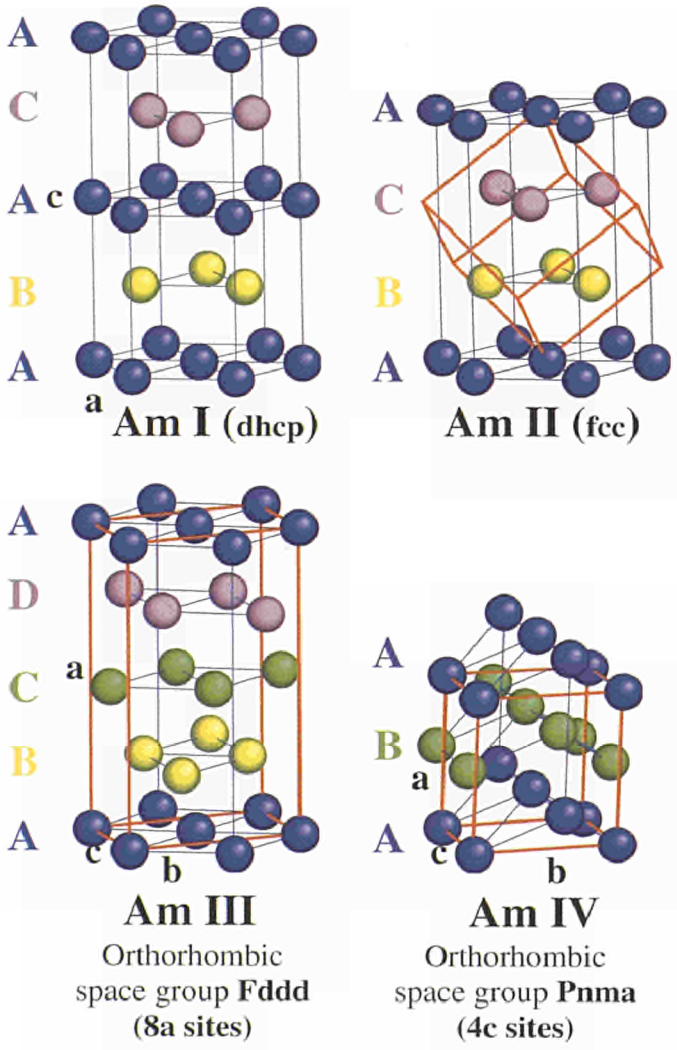

Fig. 3 Models of the four crystal structures of americium.

„Switching" on Nuclear Reactions: Laser Induced Fission of Uranium

Through a collaboration involving the Institute for Transuranium Elements, with various university groups in the U.K. (universities of Glasgow, Oxford, Imperial College, Scottish Universities Reactor Centre), and the Rutherford Appleton laboratory, laser induced fission of metallic uranium has been demonstrated using the very high power VULCAN laser. The role of ITU in this collaboration is in sample preparation and post irradiation fission track analysis. The results of these experiments have been published recently [1,2].

The possibility of accelerating electrons in focussed laser fields was first discussed by Feldman and Chiao [3] in 1971. In this work, the authors showed that in a single pass across the diffraction limited focus of a laser power of 10^{12} W, the electron could gain 30 MeV, and become relativistic within an optical cycle. With a very high transverse velocity, the magnetic field of the wave bends the particle trajectory through the Lorentz force into the direction of the travelling wave. In very large fields, the particle velocity approaches the speed of light and the electron will tend to travel with the wave, gaining energy as it does so.

In 1988, K. Boyer et al. [4] investigated the possibility that such laser beams could be focussed onto solid surfaces and cause nuclear transitions. In particular, irradiation of a uranium target could induce electro- and photo-fission in the focal region. With laser intensities of approximately 10^{21} W/cm^2, approximately 8000 electro-fission events are estimated, well above the detection limit. The authors concluded that the total neutron production is probably dominated by photofission since the active volume for photofission is much greater than that for electrofission. In the immediate focal region, however, electrofission dominates. Fission product ions leaving the surface would be the result primarily of electrofission.

These developments open the possibility of „switching" nuclear reactions on and off by high intensity ultraviolet laser radiation and providing a bright point source of fission products and neutrons [5].

A ^{238}U (depleted uranium) sample of dimensions ~10x10x2mm (~3g) with a fission fragment 3005m polycarbonate foil on the front and back sides, prepared at ITU, was targeted. This sandwich was shrink wrapped in plastic to contain any gaseous radioactivity and enclosed in an aluminium container. The sample was irradiated with 3 consecutive laser shots, twenty minutes apart, of nominally 10^{19} Wcm^{-2} intensity and analysed using the Ge detector.

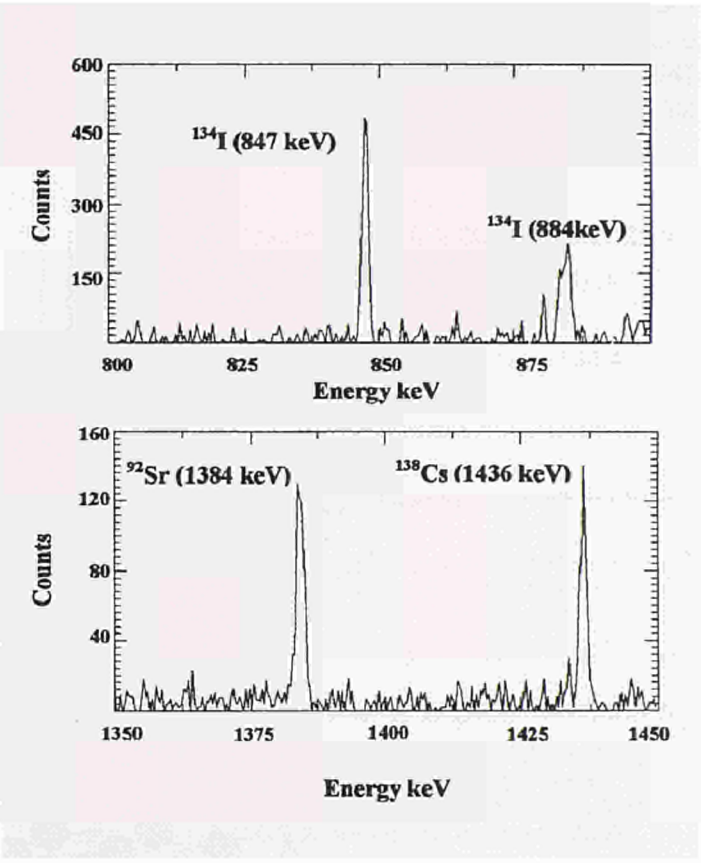

Some of the characteristic γrays emitted by three of the principal fission fragments following a ^{238}U(γ, f) reaction.

The principal fission fragments amount to about 5-6% of the total fission yield. Evidence for fission events is normally carried out by detecting the characteristic γ-rays from the principal fission fragments, detection of fission fragment tracks or fission neutrons. In the case of ^{238}U with a (γ,f) cross section which peaks at about 150mb the most abundant isotopes produced include ^{134}I, ^{138}Cs and ^{92}Sr shown in the figure with suitable γ-ray energies and half-lives. The background activity from fissile materials is normally sufficiently large that very careful background measurements must be taken.

Two Ge γ-ray spectra in the region of 850 keV and 1400 keV are shown in the figure after background subtraction was performed. The unambiguous characteristic γ-rays of the fission fragments ^{134}I, ^{138}Cs and ^{92}Sr are indicated.

Thus it has been demonstrated experimentally that a laser based source of nuclear radiation is a possibility at intensities $>10^{19}$ Wcm^{-2}. With intensities at 10^{21} Wcm^{-2} available from petawatt lasers, pion production, energetically possible with γ-rays >140 MeV, is a distinct possibility and can be demonstrated using similar activation experiments to those described in this letter.

References:

[1] P.A. Norreys et al. Phys. Plasmas 6, (1991) 2150.
[2] K.W.D. Legingham et al. Phys. Rev. Lett. 84 (2000) 899.
[3] M.J. Feldman and R.Y. Chiao, Phys. Rev A4 (1971) 352-358.
[4] K. Boyer, T.S. Luk, C.K. Rhodes, Phys. Rev. Lett. 60 (1988) 557-560.
[5] J.E. Lynn, Nature, 333 (1988) 116.

Volatile Molecule PuO_3 Observed from Subliming Plutonium Dioxide

Although plutonium can assume a hexavalent form in halides (e.g. fluorides and oxyl-chlorides) or oxo-compounds (e.g. plutonates), only valences II, III and IV are observed in solid oxides. Shortly after its discovery, several reactions of the new element with highly oxidising agents were investigated. It was found, that in the exploitable temperature and pressure range, $PuO_{2.00}$ represents the highest oxide form in the condensed phase diagram of Pu-O. Thus, at the end of the sixties, any systematic quest of plutonium oxides higher than PuO_2 was practically abandoned.

Recently, the possible existence of higher plutonium oxides was considered again, and investigated by thermochromatographic techniques. The analysis of the experimental results suggest that an oxidising gas flowing over hot plutonium dioxide may carry molecules of type PuO_n, with n>2. However, no direct proof of their existence could be produced so far.

More direct evidence was obtained, from experiments conducted at ITU in 1998-99, which corroborated the hypothesis of the existence of a volatile plutonium trioxide vapour molecule, sublimating from the solid dioxide.

Experiment

During Knudsen-effusion experiments on MOX (uranium-plutonium mixed oxide nuclear fuel), presently in progress at JRC-ITU, mass spectrometer (MS) analysis of the vapour unexpectedly revealed the presence of masses corresponding to PuO_3.

The experiment was therefore repeated with high purity stoichiometric PuO_2. The results confirm the previous observations: at temperatures of approximately 1800 K, at which the vaporisation rate of PuO_2 becomes measurable, an important component of PuO_3(g) was found in the effusing beam.

The sample was treated in the Knudsen-cell according to a thermal-annealing programme suitable for measuring the equilibrium partial pressures of the vapour as a function of temperature. The results are plotted in Fig.1: the starting total effusion rate was found to be more than one order of

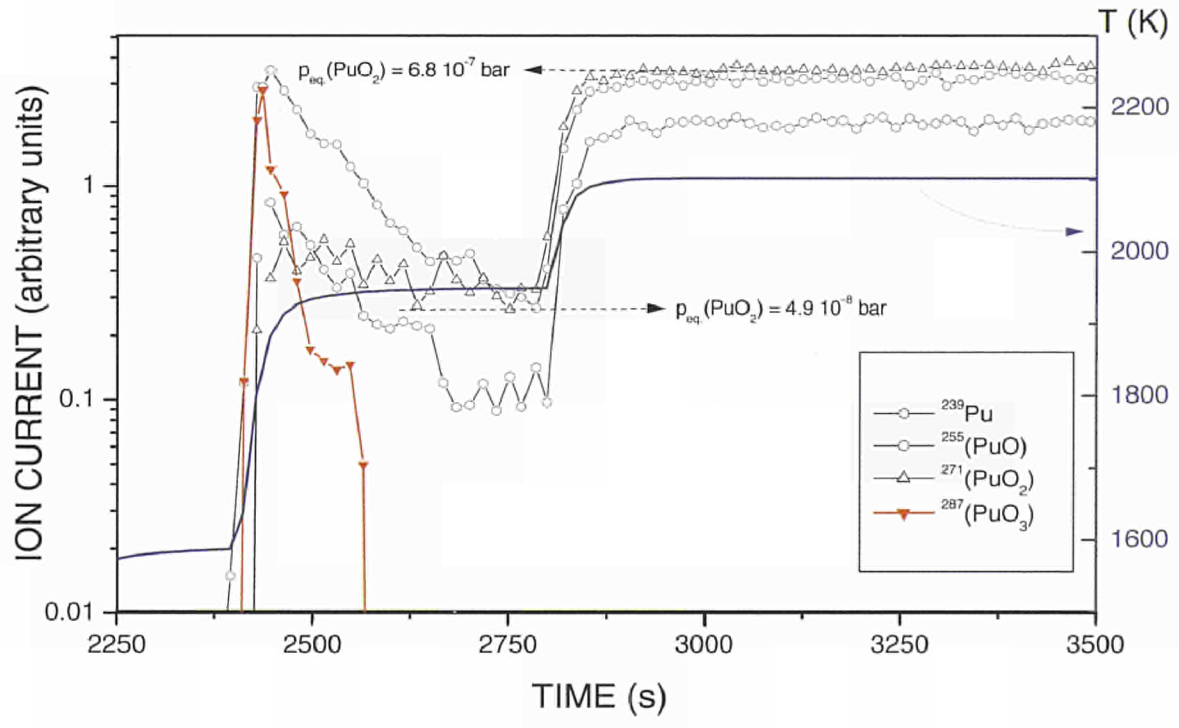

Fig. 1 Effusion studies of PuO_2 oxidised in air.

magnitude higher than in PuO_2 under thermodynamic equilibrium conditions. In the mass spectrometer, the observed ion composition is completely different from that of the equilibrium vapour. The observed effect corresponds to a transitory vaporisation stage whose nature was unknown. In fact, at constant temperature, the measured concentration of the trioxide in the vapour decreases, whilst that of PuO_2 increases in relative weight, so that when PuO_3 effectively disappears, the former becomes the major species.

Though the fractional amount of PuO_3 vaporised in these experiments is very small, it appears that, under unwanted oxidation conditions, this rather volatile oxide may represent a non negligible source of air-borne dispersion of plutonium.

To investigate this further, a second experiment was carried out: a sample of PuO_2 was heated in the Knudsen-cell at 1990 K. The electronically-controlled gas inlet valve of the cell was then opened to allow CO_2 flow, onto the sample, at the maximum rate compatible with the differential pumping system of the device. During circa 20 seconds, the vacuum in the MS chamber could be stabilised just below 10^{-5} torr, whilst in the furnace vessel the pressure was of the order of 10 torr.

The MS measurements of the effusing vapours are plotted in Fig. 2. One can see that the current of all Pu-bearing ions increases approximately by a factor of 50. This cannot be caused by a change in stoichiometry of the sample, since the total pressure over Pu_2O_3 and PuO_2 at this temperature is almost the same. Therefore, the increase in sublimation rate is due to formation of PuO_3 on the surface, whilst the other oxide ions, whose current is simultaneously increasing, are ionisation fragments of the trioxide. Contrary to the case of Fig. 1, the PuO_2 component is here larger than PuO. This is due to oxidation of PuO(g) in the gas phase.

Analysis of the vaporisation rates of the various components indicates that the oxidation conditions were far from equilibrium and only surface atoms of plutonium were involved in the formation of PuO_3.

An additional proof that only surface atoms of plutonium are involved in the detected sublimation "burst" is furnished by the signal of UO_3 – approximately 1% uranium was present in the sample as a decay product of plutonium – that is *evidently unaffected* by the applied transient conditions.
In conclusion, these results disclose new aspects of the oxidation mechanism of PuO_x. Under certain conditions, the volatility of this oxides is more complex than commonly assumed.

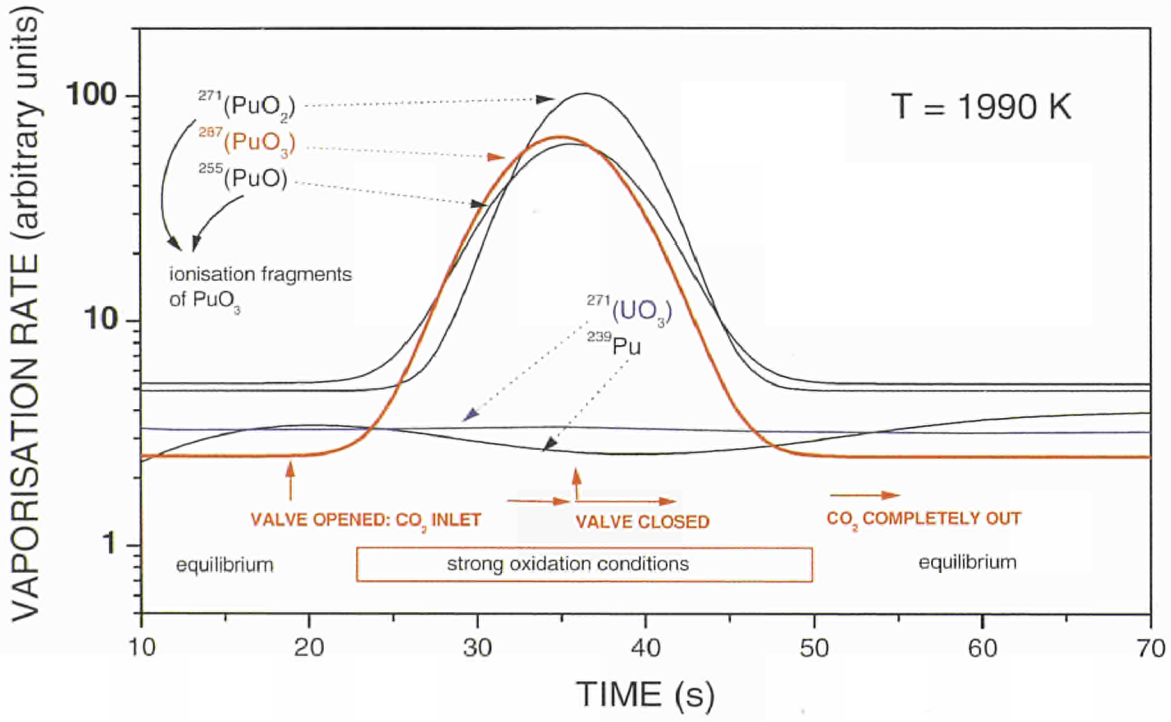

Fig. 2 Production of PuO_3 in a flux of CO_2. Oxygen potential during the transient: $\Delta G(O_2) \sim$ -30 kcal/mole.

Application of the Micro-X-ray Diffraction Technique to the Rim Zone in High Burn-up Fuels

Following the development of the Micro-X-ray Diffraction technique, reported in TUAR 96, p. 18-19, we present the first radial high resolution lattice distortion measurements in high burn-up UO_2 fuels.

The distortion of the UO_2 crystal lattice through neutron irradiation has been studied in detail in the low burn-up range 10^{-6}-1 GWd/tM [1-3] and to a lesser extent in the range 6-100 GWd/tM [4-9]. In the very low burn-up range, it was shown that neutron damage caused lattice expansion and Bragg peak-broadening that were maximum at about 0.01 GWd/tM and practically disappeared at ~1 GWd/tM [1-3]. For burn-ups above 6 GWd/tM, a renewed increase of the lattice expansion and peak-broadening has been confirmed [4-9], with a trend to a saturation around 80 GWd/tM [4,6].

The main reason for the appearance of the rim-structure at high burn-ups has been assigned to the accumulated lattice damage [5-9]. It is hence considered important to determine quantitatively the local profile of this fission damage in the fuel and to investigate any correlation with the other property changes. For this purpose, a special micro-XRD instrument was developed to allow the focusing of the primary X-ray beam in a region not wider than 30 µm, thus making possible the acquisition of non-overlapping diffraction spectra at intervals of 50 µm in the pellet radial direction. The results obtained for a fuel with 67 GWd/tM average burn-up are shown in the figure in terms of the peak shift ($\Delta\theta_{hkl}$) and the line broadening ($\Delta FWHM_{hkl}/FWHM_{hkl}$) across the pellet radius for various (hkl)-reflections.

The figure shows a more or less constant peak broadening for all (hkl)-reflections over the pellet radius, but maximum peak-shifts ($\Delta\theta_{hkl} < 0$, lattice dilatations) in the region adjacent to the rim-zone. The decrease of this lattice expansion towards the pellet centre is attributed to thermal healing effects, whereas the decrease towards the cold fuel periphery is assigned to the formation of the rim-structure. Indeed, the region of maximum lattice-strain concentration r/r_o~0.9 is found coincident with the onset of the porosity increase and the hardness decrease [10] as well as the Xe-depletion [11].

Thus, the conclusion is that during the rim-structure formation, the previously accumulated lattice strain is fully released. Studies on the connection of these results with other property changes; namely, the lattice contraction due to fission products dissolution, the pore formation, the Xe-depletion, etc., are in progress.

Thus, the conclusion is that during the rim-structure formation, the previously accumulated lattice strain is fully released. Studies on the connection of these results with other property changes; namely, the lattice contraction due to fission products dissolution, the pore formation, the Xe-depletion, etc., are in progress.

References

[1] L.E. Roberts et. al, 3rd UN Int.Conf.,P/155 Geneva, 1964,
[2] E. Wait et. al, Radiation Damage in Solids, Vol.2, IAEA (1962) p 231
[3] N. Nakae et. al., J. Nucl. Mater. 71 (1978) 314-319
[4] J.H. Davies, F.T. Ewart, J. Nucl. Mater. 41 (1971)143-155
[5] K.Une, Y. Tominaga, S. Kashibe, J. Nucl. Sci. & Technol., 28 (1991) 409-417
[6] K. Une, K. Nogita,S. Kashibe, M. Imamura, J. Nucl. Mater. 188 (1992) 65-72
[7] K. Nogita, K. Une, J. Nucl. Sci. & Technol., 30 (1993) 900-910
[8] K. Nogita, K. Une, Nucl.Inst. and Meth. in Phys.Res., B91 (1994) 301-306
[9] K. Nogita, K. Une, J. Nucl. Sci. & Technol., 31 (1994) 929-936
[10] J. Spino, K. Vennix, M. Coquerelle, J. Nucl. Mater. 231 (1996) 179-190
[11] C.T. Walker, J. Nucl. Mater. 275 (1999) 56-62

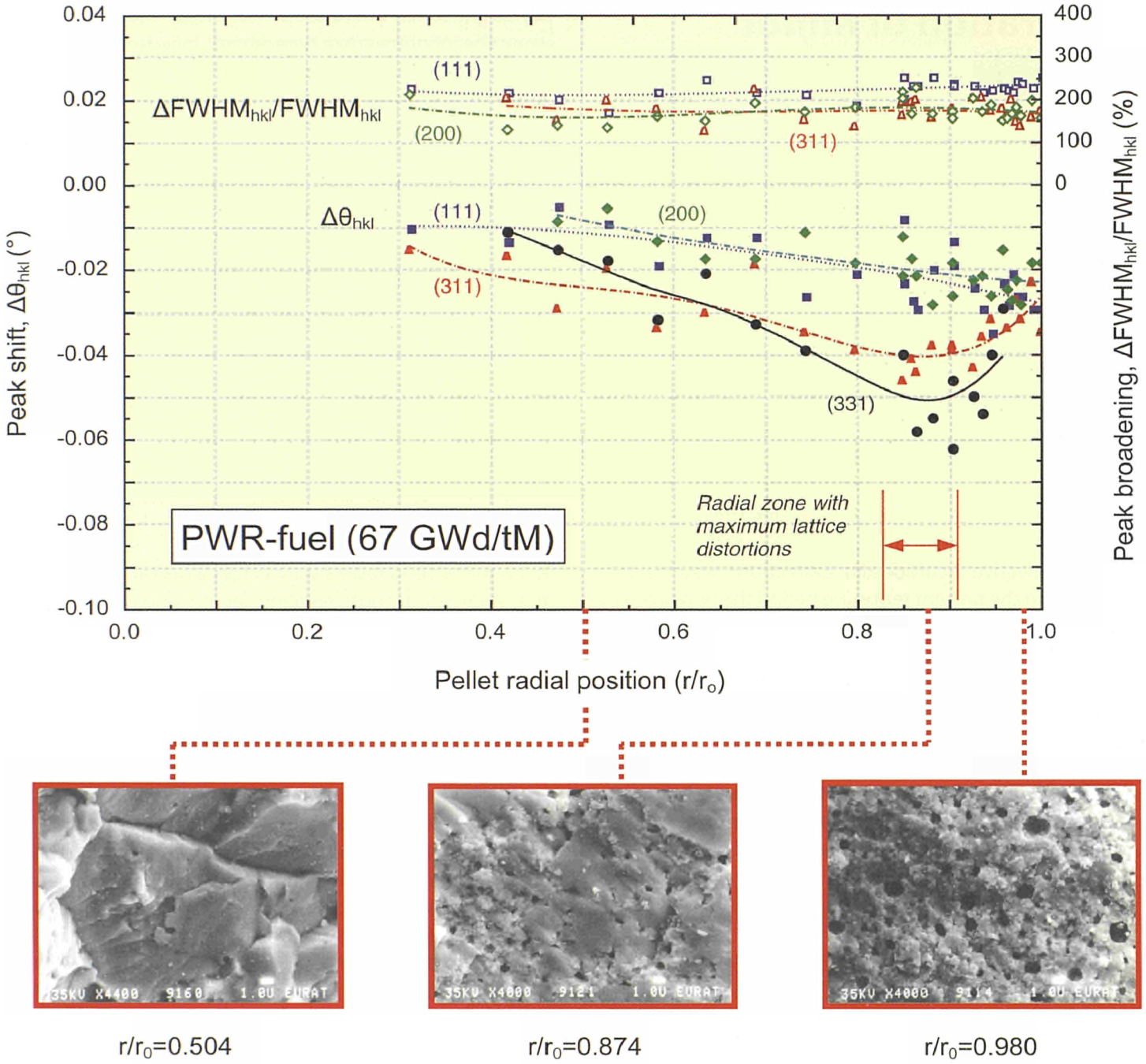

r/r_0=0.504 r/r_0=0.874 r/r_0=0.980

Bragg Peak-broadening and peak-shift for various (hkl)-reflections across the pellet radius of a high burn-up fuel, as determined by micro-XRD (30 μm-beam) and SEM micrographs at three radial positions.

Separation of Minor Actinides from Lanthanides

The potential harmfulness of the wastes generated by reprocessing and also non-reprocessed fuel reactor operation are primarily due to the presence of minor actinides. These radioactive by-products of nuclear power generation require special attention with regard to the separation (partitioning). Different systems based on liquid-liquid extraction for the purpose of minor actinides partitioning are being tested using a 16-stage continuous counter-current extractor set-up installed in the hot cells.

In the previous report (TUAR-98, p.89) the successful separation of lanthanides (Ln) from minor actinides (MA) using chlorophenyl substituted dithiophosphinic acid was described. The method was tested using a genuine MA/Ln effluent from the DIAMEX process. Recent advances in high acidity MA/Ln separation chemistry has made two more SANEX (Selective ActiNides(III) EXtraction) systems available. During the present reporting period the two processes have been tested. Both processes are based on the use of nitrogen polydendate ligands as extractants, the first system being a tri-synergistic mixture of BADPTZ, α-CNC_{10} and DMDBTDMA [1], the second a BisTriazinylPyridine (BTP) System [2]. In contrast to the dithiophosphinic acid, which is an organophosphorous sulphur bearing acid, these reagents follow the so-called CHON principal, *i. e.* they consist only of C, H, O, N atoms and are therefore completely combustible. This minimises the amount of solid secondary waste generated in a future advanced partitioning process.

A number of preparative experiments have been carried out followed by a hot verification test using a genuine DIAMEX MA/Ln fraction of the waste stream. The hydraulic behaviour was studied in inactive experiments (cold tests) using 8 centrifugal extractors (4 extraction and 4 back-extraction steps). These experiments were also carried out to investigate distribution factors and to optimise process schemes. The organic tri-synergistic mixture of 0.1M BADPTZ, 1M α-cyanodecanoic acid and 0.46M DMDBTDMA in TPH was tested with a aqueous synthetic Ln solution in 0.2M HNO_3. Due to poor phase separation, both in the extraction and the back-extraction section, this system needs further improvements before a hot verification test can be performed. For the BTP system the cold phase separation and the hydraulic behaviour was proven to be fully satisfactory, and thus a hot verification test using a flowsheet composed of 5 extraction stages, 3 acid scrubbing stages and 8 strip stages (see Figure) was carried out.

Reasonably good results were achieved as can be seen from the obtained decontamination factors and recovery rates (see Table).

For Am and Cm, decontamination factors of 122 and 64, respectively were achieved in only 5 extraction stages. The back-extraction was more efficient for Am (99.1% recovery) than for Cm (97.5%). The small amounts of co-extracted lanthanides were efficiently removed in the acid scrubbing section. However, the scrubbing efficiency decreases with the increase in the atomic number of the lanthanide. Higher

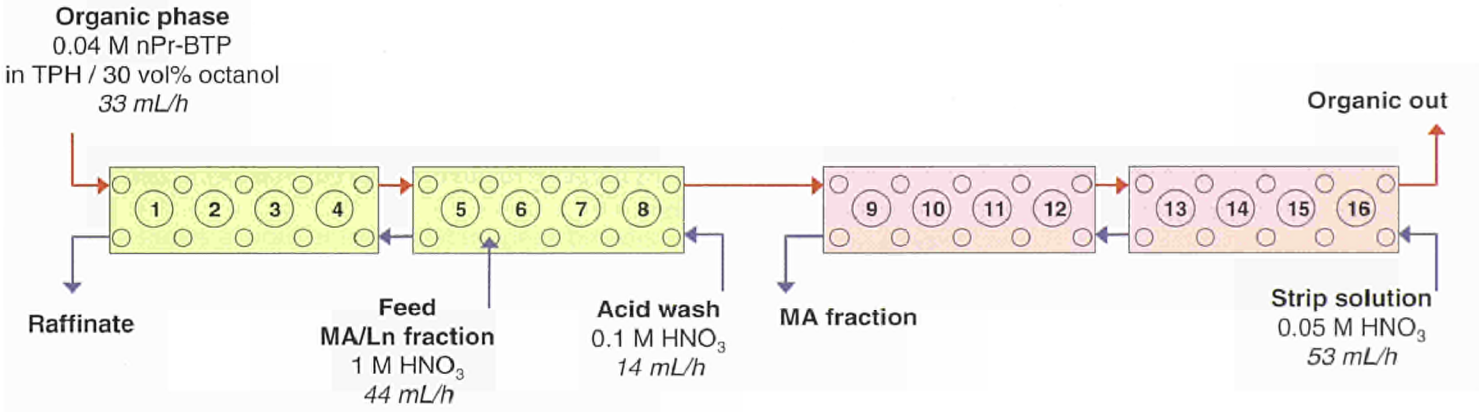

The flowsheet for the hot test verification of the BTP process.

Decontamination factors of the feed. Also tabulated are the amounts recovered of the elements in the raffinate and in the MA fraction

	Element	DF	Recovery from the Feed (%)	
			Raffinate fraction	An fraction
FP	Y	1.02	98.2	1.8
	Tc	11	9.2	8.5
	Ru	1.00	99.8	0.2
	Pd	687	0.1	4.0
Ln (FP)	La	1.00	> 99.99	–
	Ce	1.00	> 99.99	–
	Pr	1.00	> 99.99	–
	Nd	1.00	> 99.99	–
	Sm	1.00	99.9	0.1
	Eu	1.01	98.9	1.1
	Gd	1.04	96	4
An	Np	1.00	99.9	0.05
	Am	122	0.8	99.1
	Cm	64	1.6	97.5

lanthanides (Eu, Gd) were therefore to some extent back-extracted with the minor actinides. Of the lighter fission products Pd and to same small degree Tc, were accumulated in the organic phase. As a consequence, the process scheme has to be improved and optimised to increase the recovery of Cm, to decrease higher Ln co-extraction and prevent Pd accumulation in the organic phase. Nevertheless, this experiment, using the BisTriazinePyridine molecule is the first successful demonstration of the separation of MA from Ln in a genuine MA/Ln fraction with a nitric acid concentration of ca. 1M. *It represents an important breakthrough in the difficult field of minor actinide partitioning.*

References

[1] Cordier P.Y.; François N.; Bulbals N.; Madic C.; Hudson M.J.; Liljenzin O.; ISEC '99 Internat. Conf., Spain 11-16 July (1999) 54

[2] Kolarik Z.; Müllich U., Gasner F.; Solv. Extr. Ion Exch. 17 (1999) 23

α-Decay Damage in UO_2 : Long Term Storage Behaviour of Spent Fuel.

Unirradiated UO_2 containing short-lived α-emitters, the so-called α-doped UO_2, can reproduce the type (essentially α-decay) and the level of activity of the fuel after thousands of years in a final repository, i.e. at the time when the fuel surface might become exposed to groundwater (this report, chapter 6.2, TUAR-98, p. 98-100, and [1]). The accumulation of damage [2,3], and also of He, which is directly produced by the α-decays, causes modifications in the fuel, e.g. thermal conductivity, hardness, and lattice parameter changes. The impact of these modifications on the fuel performance during storage is an important issue, which is currently the object of investigations in several laboratories.

Pellets of α-doped UO_2 containing ~10 w/o ^{238}Pu with an α-activity of ~$3.76 \cdot 10^{10}$ Bqg^{-1} were fabricated and characterized (this report, chapter 6.2 [1]). Since its fabrication (November 1997), approximately $2.7 \cdot 10^{18}$ α-decays g^{-1} have occurred, corresponding to the decay of one atom in every ~800 atoms of metal present in the material and to about 0.6 displacements per atom. The α-decays have produced ~$4.4 \cdot 10^{-6}$ mol g^{-1} of He, or ~1 cm^3 of gas per cm^3 of material. Fig. 1 shows the production of He calculated using the ORIGEN2 code as a function of time of storage for different types of irradiated fuel and for α-doped UO_2. The amount of He produced in α-doped UO_2 in slightly more than two years corresponds to that for spent PWR fuel with 40 GWd/tM during several hundred years of storage, or for spent MOX fuel after several decades, depending on the burnup. The amount of He produced in α-doped UO_2 after 10 years of storage is also shown in Fig. 1, to illustrate the rapid accumulation of decay damage in this α-doped material compared to irradiated fuels. Fig. 2 reproduces Transmission Electron micrographs of the microstructure of α-doped UO_2 after 2 years of storage, showing a matrix characterized by a large concentration of dislocation loops. Nanometer-sized bubbles were also observed in the very thin regions of the specimen.

The monitoring of the evolution with time of the properties of α-doped materials will continue and will be extended to lower α-activities, to evaluate possible dose rate effects. The results will be used to integrate data obtained from the characterization of irradiated fuel with the aim to extrapolate the long-term behaviour of spent fuel during storage.

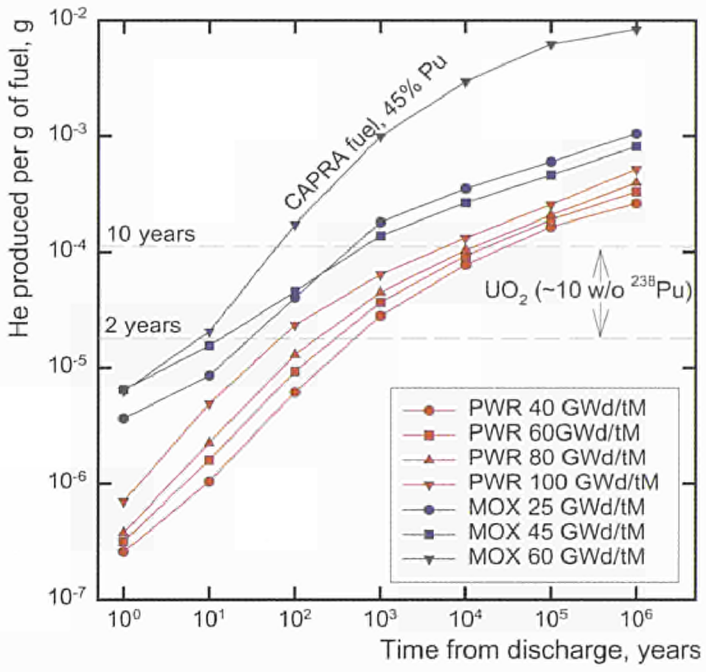

Fig. 1 Helium production in UO_2 and MOX spent fuels with different burnups, and in α-doped UO_2 (labeled UO_2-10) calculated using the ORIGEN2 code. The dashed horizontal lines represent the He produced after 2 and after 10 years in the α-doped material.

References:

[1] V.V. Rondinella, Hj. Matzke, J. Cobos, and T. Wiss, Mat. Res. Soc. Symp. Proc. 556 (1999) 447-454.

[2] J. Fuger and Hj. Matzke, Handbook on the Physics and Chemistry of the Actinides, Vol. 6, ed. A.J. Freeman and C. Keller, p. 641-684, Elsevier 1991.

[3] Hj. Matzke, J. Nucl. Mater. 270 (1999) 49-54.

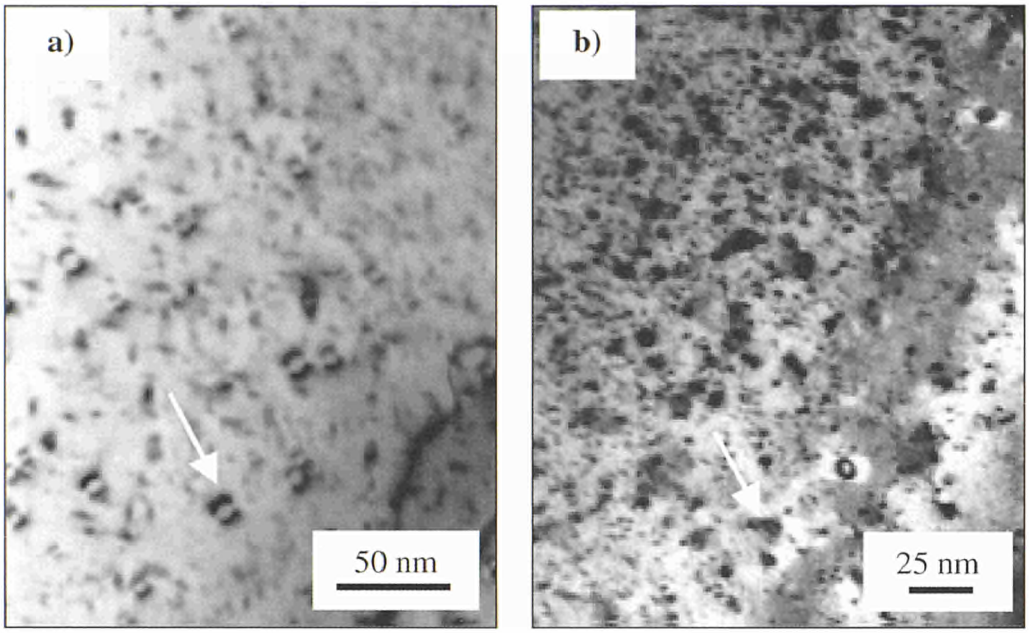

Fig. 2. Transmission Electron Microscopy micrographs showing the microstructure of α-doped UO_2 after 2 years of storage. A high density of dislocation loops with an average size of 20 nm is visible (indicated by the white arrows on the figure). Micrographs a) and b) shows loop contrast for two different tilting angles of the specimen in the electron beam. On micrograph b) a high concentration of defect clusters (black dots), precursors of the loops, can be observed.

A Milestone in Nuclear Safeguards – Inauguration of the 'On-Site Laboratory' at Sellafield

The start-up of the large reprocessing plant THORP at Sellafield represented a challenge for the Euratom Safeguards Office (ESO), particularly in view of the number of samples to be analysed. The idea of performing these measurements locally without transporting them to a specialised laboratory, resulted in the concept of the 'On-Site Laboratory' (OSL).

ITU accepted the task to design, install and commission the OSL. The project took almost a decade from the cradle to maturity, it's growth permanently being supervised and controlled by ESO, by the plant operator (BNFL), by the National Nuclear Corporation (NNC) and by the British safety authorities (NII). On 13 October 1999 the OSL came of age: the laboratory was officially inaugurated by the Directors of ESO and ITU .

The OSL is a significant contribution in improving the effectiveness and efficiency of safeguards verification measurements at the BNFL Sellafield reprocessing plant. Almost a thousand samples are planned to be analysed in the OSL using advanced measurement techniques. The OSL has gradually entered the operational phase by stepwise accepting different types of samples and by increasing their number.

Much research and development work was carried out at ITU in order to further improve measurement instrumentation and software, to streamline analytical procedures and optimize the sample flow in the laboratory. The spectrum of analytical techniques covers the following range:

- **High level neutron coincidence counting combined with-high resolution gamma spectroscopy**
  is applied for the analysis of PuO_2 and MOX samples. The samples are measured without any treatment, therefore the sample material can be returned to the plant, no waste is created.

Mr. Gmelin, Director of ESO, (front) starting a measurement of plutonium nitrate solution using the product hybrid K-edge under guidance of Mr. Ottmar (ITU).

- **K-edge absorption in combination with X-ray fluorescence, the so-called hybrid product K-edge instrument**
  measures Pu and Am concentration and the Pu isotopic composition in liquid samples. Again, any excess sample is returned to the plant.

- **Combined uranium enrichment and element assay, the COMPUCEA instrument**
  is used for the analysis of low enriched uranium from the product streams of THORP or from other installations in the UK.

- **Robotised chemical sample preparation prior to mass spectrometry**
  comprises sample spiking, the separation of U, Pu and fission products, alpha spectrometry and filament preparation.
- **Thermal Ionisation Mass Spectrometry**
  using the total evaporation technique is applied for highly accurate isotope ratio measurements in all kind of samples.

These techniques are applied by highly skilled analysts who acquired their know-how through training in the pre-OSL, a specialised facility at ITU very similar to the OSL analytical installations.

Plutonium Round-Robin Test

Nuclear forensic science is a new multidisciplinary area, which uses the characteristics inherent to a nuclear material for obtaining information on the origin and the production route of the sample under investigation. A very limited number of laboratories work in this field and exchange their experience on an international level regularly. In this context the International Technical Working Group on Nuclear Smuggling (ITWG), where ITU Karlsruhe is represented by the group's co-chairman, was established in early 1996 and holds its meetings annually.

The ITWG initiated and organized an international exercise ("Round Robin") on the analysis of nuclear material of unknown origin. Its main purpose was to compare the approaches of different laboratories and gather further experience on the most suitable experimental methods and reference data. Rather than comparing standardized procedures (as in safeguards analytics), it was intended to prioritize analytical methods stemming from a wide range of scientific areas and to make recommendations for their improvement and application. Nuclear forensic science requires a step-by-step analysis which is very case-specific and built on the principle of individual diagnosis.

The aim of the first exercise was to determine the fabrication date and location for a PuO_2 powder sample, and the Institute was one of six participating laboratories, which were identified only by volcanic codenames. All of the participating laboratories succeeded in producing a "Twenty-four Hour Report" identifying the sample as containing plutonium. This report is essential to guide the law enforcement agencies as to how the material should be handled and to establish whether an infringement against various laws in a state has been committed.

The next stage of the examination was a chemical and isotopic analysis, and the material was identified in the Institute to be PuO_2 containing Am and a characteristically high concentration of Np. The sample finally underwent a microscopic analysis by SEM and TEM to identify its "Microstructural Fingerprint", and was found to consist of a mixture of different components, as in previous real cases of seized nuclear materials.
The results obtained in the ITU enabled the fabrication plant and the fuel fabrication date, the reprocessing plant that recovered the plutonium from the spent fuel and the nuclear reactor which had discharged the fuel to be established. Further details can be found in chapter 7.

In the follow-up meeting at the Euratom Safeguards Office, Luxembourg in October the Institute emerged as the participant to have made a correct identification of the source reactor and reprocessing plant, and came closest in the estimates of the sample age. In addition the Institute provided significant work on the morphology and microstructure of the powder particles. The actual conclusions are subject to confidentiality agreements.

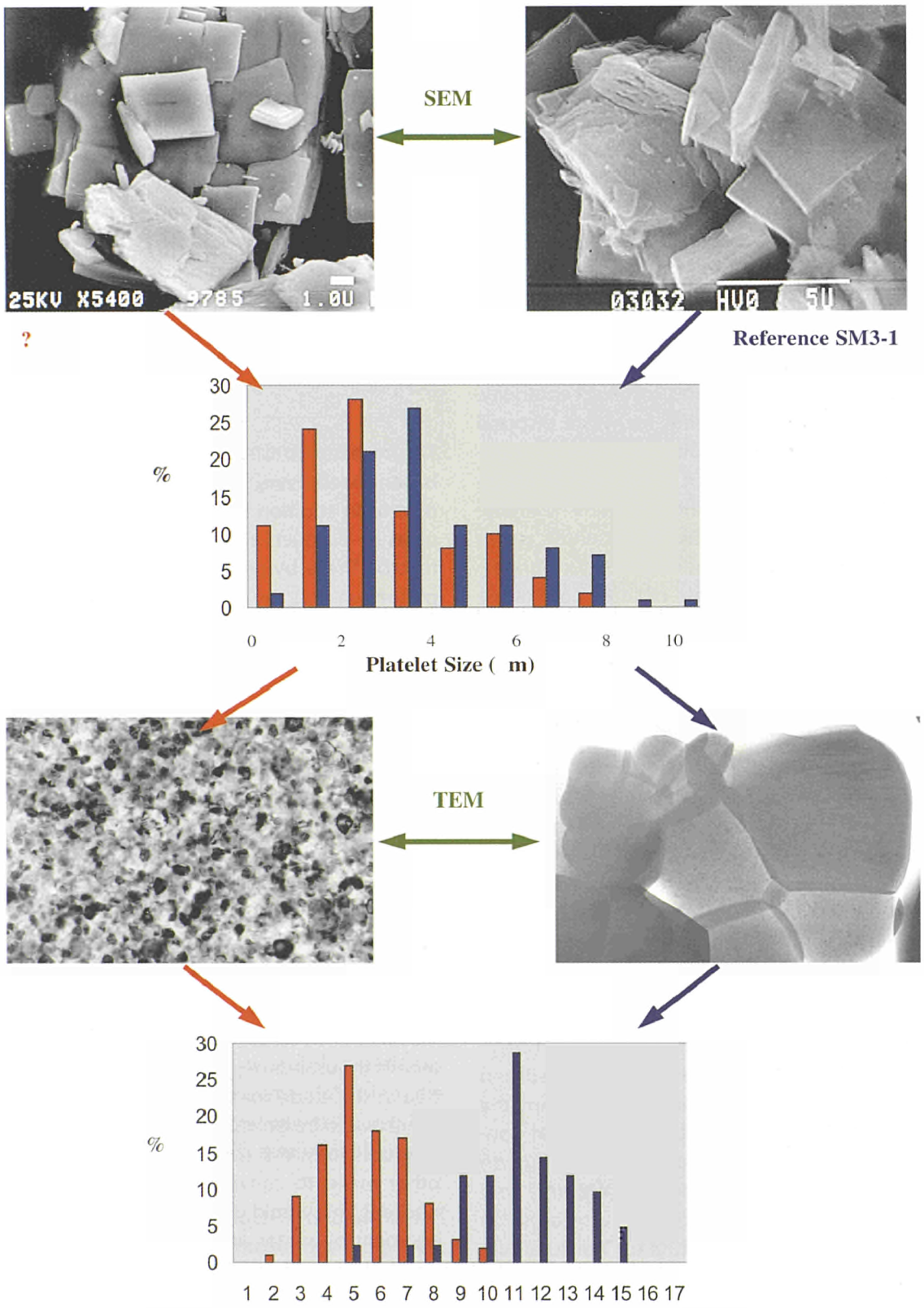

The figure illustrates a comparison of PuO_2 platelet and grain size distributions measured on an illicit sample with those from a reference material of known origin.

Partitioning and Transmutation Studies at ITU

L. Koch, J.-P. Glatz, R. J. M. Konings, J. Magill

1. Background

In this sixth decade of nuclear power, the issue of waste disposal strongly dominates public opinion. In the eyes of the public, the problem of waste disposal is not fully solved, especially in terms of environmental and social acceptability. The public attitude to developing sites for waste disposal has been succinctly summarised in suitable acronyms - NIMBY (not in my back yard), NIMTO (not in my term of office) and BANANA (build absolutely nothing anywhere near anyone) [1]. However, it must also be added that scientific issues related to the disposal problem do indeed need further clarification. Evidence given to the House of Lords Committee [2,3] by the science and engineering community clearly state that *"there is a need for developing the sciences relevant to a detailed assessment, at a fundamental level"*. The source of public attitude seems to be the very long times involving many generations during which this waste must be separated from the biosphere to avoid possible harmful effects. To address this problem, scientists are looking for ways to significantly reduce both the volumes and the radiotoxicity of the waste, and to shorten the very long times for which this waste must be stored safely. For this reason various so-called Partitioning and Transmutation (P&T) techniques are being investigated in most countries with significant nuclear power generating capacity.

In this article we describe briefly how radioactive by-products are unavoidably formed during normal reactor operation. Some of these by-products are very long-lived and *radiotoxic* and, if untreated, must be separated from the biosphere for very long times. Various international concepts on how these by-products could be separated *(partitioned)* from the waste and converted *(transmuted)* into shorter-lived, less harmful products are discussed. In sections 3 and 4 activities at the Institute for Transuranium Elements (ITU) are described. In the field of partitioning, both advanced aqueous and pyro-processing techniques are under investigation. For transmutation studies, fabrication techniques for various fuel and target concepts are being investigated.

2. Introduction

At the present level of nuclear power production in Europe, approximately 2500 tons of fuel is required each year for 145 reactors in operation in the European Union (EU). This fuel generates about 127 gigawatts of electricity (GWe) thereby providing 36% of the total electricity requirements [4,5]. Based on an average consumption of electricity in countries of the EU of approximately 6400 kilowatt-hours per capita per year [6] the amount of nuclear fuel required is approximately 14 grams per person per year. Since energy production results in an insignificant loss of mass, it follows that the waste generated is also approximately 14 grams per person per year.

The fresh fuel consists essentially of uranium oxide and heat is generated from the fissioning of uranium atoms in the reactor. In addition to heat generation from fission, various other by-products are generated by nuclear reactions in the reactor. These by-products consist mainly of the elements plutonium (Pu), the so-called **M**inor **A**ctinides (MAs) neptunium, americium, and curium, and fission products (FPs). During reactor operation, the fission products build-up to such a level that they start to "poison" and reduce the mechanical integrity of the fuel. At this stage the *spent* fuel has to be removed from the reactors and be replaced by fresh fuel. Following removal from the reactor, most of the radioactivity in the spent fuel is in the form of the fission products ^{137}Cs, ^{90}Sr and other short-lived nuclides. The radioactivity of these products decreases significantly on timescales of a few decades. Thereafter, the long-lived by-products determine the radioactivity. An estimate of the amounts of these by-products and their half-lives is given in Tab. 1.

For this reason, their disposal requires isolation from the biosphere in a stable deep geological formation for at least tens of thousands of years. Since these products are embedded in the oxide matrix, this means that all 2500 tons per year have to be isolated. If it were possible to separate these products from the spent fuel, and use nuclear reactors or other mean to convert them into stable or shorter-lived nuclides, this would greatly facilitate the disposal and management of wastes and raise public acceptance of nuclear energy.

This is the motivation behind the **Partitioning and Transmutation** activities worldwide and in particular at the Institute for Transuranium Elements.

Tab. 1 Estimated annual production rates of plutonium, minor actinides and selected fission fragments from all reactors operating in the EU.*

Element	**Amount** (tons per year)	**Half-life (years)** (most abundant isotope)
plutonium	23	2.41×10^4 (^{239}Pu)
minor actinides MA:	4	2.14×10^6 (^{237}Np) 433 (^{241}Am) 18.1 (^{244}Cm)
selected fission products		
technetium-99	2.3	2.13×10^5
iodine-129	0.8	1.57×10^7
caesium-137	2.3	30.0
strontium-90	1.0	29.1

** Burn-up assumed to be 37.2 MWd/kg, 2500 t spent fuel/y.*

2.1 How hazardous is nuclear waste?

A measure of the hazard of nuclear waste is provided by the *toxicity* of spent nuclear fuel and in particular its *radiotoxicity* (see box) arising from its radioactive quality rather than the chemical toxicity. Despite the high radiotoxicity of plutonium, americium, neptunium and curium, they contribute relatively little to the long-term *risk* posed by the geological storage of spent fuel in evolutionary scenarios where ground water transport is important. These elements *(actinides)* are relatively insoluble under anaerobic conditions and therefore not mobile. However, in human intrusion scenarios where the effect is related to the inventory (e.g. salt consumption), the actinides Am and Pu dominate the risk.

On the other hand, the activation product ^{14}C and the fission products ^{135}Cs and ^{129}I are less radiotoxic but long-lived, produced in significant quantities in the fission process, soluble, and can migrate relatively quickly through ground water. ^{99}Tc can form monovalent ions, similar to some of the actinides under oxidising conditions, and migratecorrespondingly.

These isotopes, therefore, can also contribute significantly to the long-term risk and should be considered as candidates for partitioning and transmutation. So although the hazard associated with nuclear waste is more complicated than the radiotoxicity alone, the radiotoxicity is the starting point for *risk* evaluations which account for pathways for these products into the biosphere. Tab. 2 gives the effective dose coefficients and annual limits of intake for the main radioactive by-products in nuclear waste.

The *radiotoxicity* of a nuclide is determined by the product of the activity and the *effective dose coefficient e* for a given isotope

radiotoxicity = activity × e

The activity is the number of disintegrations per second and is measured in units of Becquerel, Bq (1 Bq = 1 disintegration per second). The *effective dose coefficient e* is a measure of the damage done by ionising radiation associated with the radioactivity of an isotope. It accounts for radiation and tissue weighting factors, metabolic and bio-kinetic information. It is measured in units of Sievert per Becquerel (Sv/Bq) where the Sievert is a measure of the dose arising from the ionisation energy absorbed.

The Annual Limit of Intake (ALI) of an isotope is defined as the activity required to give a particular annual dose. This annual dose is usually taken as 0.02 Sv corresponding to that obtained from background radiation i.e.

ALI = (0.02Sv)/e

The Sievert, Sv, is the unit describing the biological effect of radiation deposited in an organism. The biological effect of radiation is not just directly proportional to the energy absorbed in the organism but also by a factor describing the *quality* of the radiation. An energy deposition of 6 J per kg of gamma radiation (quality = 1) i.e. 6 Sv is lethal. This same energy deposited in the form of heat (quality = 0) will only increase the body temperature by 1mK and is therefore completely harmless. The difference between the two types of radiation is due to the fact that biological damage arises from ionisation.

Tab. 2 Effective dose coefficients (ingestion) for adults [7] for the main radioactive by-products of nuclear waste. Also listed are the annual limits of intake (ALI) of these isotope required to give a dose (of 0.02 Sv) equivalent to that arising from background radiation.

Isotope	Committed effective dose coefficient e(50) for adults (Sv/Bq)	Annual Limit of Intake (Becquerel)	Annual Limit of Intake (mass)
plutonium-239	2.5×10^{-7}	8.0×10^{4}	30 µg
minor actinides MA:			
neptunium-237	1.1×10^{-7}	1.82×10^{5}	7 mg
americium-241	2.0×10^{-7}	1.00×10^{5}	0.8 µg
curium-244	1.2×10^{-7}	1.67×10^{5}	0.06 µg
Selected fission fragments			
technetium-99	6.4×10^{-10}	3.13×10^{7}	40 mg
iodine-129	1.1×10^{-7}	1.82×10^{5}	30 mg
caesium-135	2.0×10^{-9}	1.00×10^{7}	0.2 g

It follows that although the absolute amounts of nuclear waste are relatively small (approximately 14 g per person per year), this waste is highly radiotoxic. From the values shown in table 2 one sees that incorporation of microgram quantities into the body is sufficient to give a dose equivalent to that received from background radiation.

2.2 How can the radiotoxic by-products be separated (partitioned) from spent fuel?

If all spent fuel in the EU were to be reprocessed, approximately 2500 tons will have to be treated annually. This is by far in excess of current reprocessing capacities. Current reprocessing technology is based on the aqueous PUREX process in which the spent fuel is dissolved in nitric acid. Using an organic solvent, uranium and plutonium are recovered and can be used for fresh fuel fabrication. Thereafter, the aqueous raffinate containing the minor actinides and fission products is vitrified for disposal. The technique can also be extended for the extraction of neptunium, but americium and curium cannot be separated directly in this process.

Additional advanced aqueous processes have been proposed (TRUEX, DIDPA, TRPO, DIAMEX) in which americium, and curium can be separated. The effectiveness of these separation processes has been investigated at ITU. The results of these investigations are given in the section 3.1. where it has been shown that aqueous methods are technically feasible. Optimisation, however, is required for industrial scale operation.

So-called "dry" (in contrast to "wet" or aqueous) processing techniques on the other hand may offer a way to avoid problems encountered with aqueous processes. In these techniques the actinides are separated using electrochemical and pyro-chemical separation in molten salts. A key advantage of such processes is that higher levels of radiation can be tolerated. A consequence of this is that reprocessing becomes feasible in which spent fuel that has been cooled for short periods. In addition, pyro-processing promises compactness, simplicity, low cost (less transport when reprocessing is on-site), and proliferation resistance (due to low product purity). At ITU a pyro-processing laboratory is under construction for such investigations. The progress is reported here in the section 3.2.

2.3 How can the separated by-products be converted (transmuted)?

Already in the sixties, the transition from Light Water Reactors (LWRs) to Fast Neutron Reactors (FNRs) was foreseen in which plutonium generated in the LWRs would be separated through aqueous processing and used to fabricate fuel for fast reactors. Recent studies have shown that such an approach can be extended to the minor actinides Np, Am, Cm. However, for various technical and economical reasons, such a transition has not been realised and LWRs still are and will continue to be the preferred nuclear power generating reactors.

Accelerator driven systems (ADS) open the possibility of "burning" or incinerating the waste material from LWRs in dedicated actinide burners. These actinide burners can burn large quantities of minor actinides (in contrast to critical reactors) safely, and generate heat and electricity in doing so. In addition, schemes have been proposed, in which the long-lived fission products are also destroyed. An advantage of ADS is that, since there is no criticality condition to fulfil, almost any fuel composition can be used in the system. Although these ADS are usually based on the use of fast neutrons, epithermal neutron systems are also being considered.

2.4 Partitioning and Transmutation (P&T) Scenarios

The main international P&T concepts [8] are the following: in France [9] and Japan [10], the fast reactor concept is extended to the recycling of self generated MAs. In addition the so called Double Strata Fuel Cycles have been proposed. In these latter fuel cycles, the first stratum is based on a conventional fuel cycle and consists of standard LWRs (France) and FNRs, fuel fabrication and reprocessing plants. Also in this first stratum, the recovered plutonium is recycled as mixed oxide fuel in thermal and fast reactors. The remaining plutonium, MAs and long-lived fission products (Japan only) are partitioned from the waste and enter the second stratum where they are transmuted in a dedicated ADS.

In the second stratum, which is devoted primarily to waste reduction, the Pu, MAs, and long-lived fission products (Japanese concept, Fig.1) are fabricated into fuels and targets for transmutation in dedicated ADSs. The use of dry reprocessing in this stratum allows for multiple reprocessing of the fuel. A key advantage of this is that higher levels of radiation can be tolerated in the molten salts and allows reprocessing of spent fuel which has been cooled for periods as short as one month.

In the "Energy Amplifier" concept proposed by CERN [11], the objective is to burn actinides and fission products within the thorium fuel cycle. The advantage of using thorium lies in the fact that less transuranium elements are produced. In the Minimum Scheme [11], waste from a LWR is processed and some of the separated plutonium is recycled into the thermal reactor. The remaining plutonium, the MAs and FPs together with thorium are used to fabricate fuel for the ADS waste burner.

In the U.S. [12], P&T is foreseen for treatment of the spent fuel arising from a once-through fuel cycle. Hence, rather than being an integral part of the fuel management scheme, the spent fuel is processed (using a UREX process) to initially separate the uranium, stable and short lived FPs which are disposed of as low level waste. The remaining Pu, MAs, and FPs are then sent for transmutation in the ADS or ATW system (accelerator transmutation of waste).
By keeping the long-lived radiotoxic isotopes contained "within" the fuel cycle, they transform, by neutron induced fission and/or capture, faster into less toxic or even stable nuclides than by decay in a geological repository. This is especially true for the most toxic alpha-emitters listed in Tab. 3 where the half-life by natural decay is compared to that resulting from transmutation in a fast reactor. Generally, fast neutrons are more efficient than thermal neutrons, because the latter favour neutron capture processes which leads to the formation of higher actinides. For example, if the Pu is exclusively recycled in LWR, one third would not fission and hence be transmuted in minor actinides. However, an intermediate solution is the Double Strata Concept, where Pu is recycled in LWR and minor actinides, MAs (Np, Am, Cm) and fission products, such as ^{99}Tc, are transmuted in an accelerator driven fast reactor (see Fig. 1). The fast reactor burner, when fuelled only with minor actinides possibly in an inert matrix, has to have a sub-critical core, which is driven by neutrons from a spallation source. To obtain a sufficient strong spallation reaction in lead or lead-bismuth targets one needs accelerated protons of an energy of about 1 GeV. The need to operate a fast reactor in a sub-critical mode with such an accelerator driven system rises from the insufficient Doppler and void coefficients of minor actinide fuelled fast reactors.

Tab. 3 Half-lives (y) of actinides due to natural decay and by fission with fast neutrons (fission spectrum) [13].*

Actinide	Half-life due to natural decay	Half-life due to fission with fast neutrons
^{237}Np	2×10^{6}	2.46
^{238}Pu	88	1.61
^{239}Pu	2×10^{4}	1.76
^{240}Pu	6×10^{3}	2.35
^{241}Pu	15	1.95
^{242}Pu	4×10^{5}	2.83
^{241}Am	433	2.40
^{242m}Am	152	1.72
^{243}Am	7×10^{3}	2.89
^{242}Cm	0.45	1.93
^{243}Cm	30	1.46
^{244}Cm	18	1.97
^{245}Cm	8×10^{3}	1.60

* *note that some relatively short-lived actinides (e.g. of Cm, Pu, Am) decay to very long-lived actinides. For this reason one can regard the effective half-lives of all actinides as being very large.*

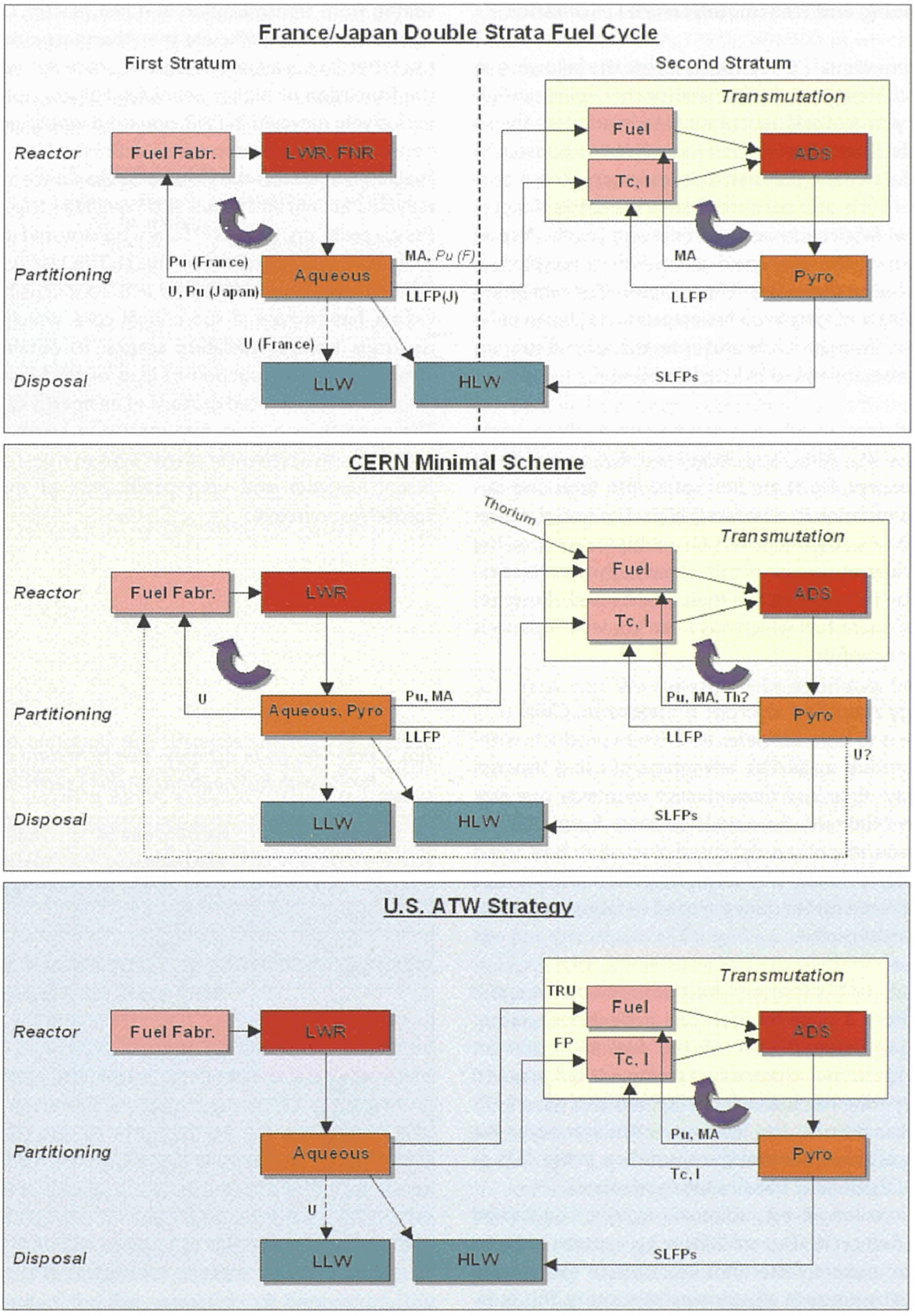

Fig. 1 International partitioning and transmutation (P&T) concepts.

3. Partitioning Studies at ITU

3.1 Aqueous Reprocessing

The partitioning of MA is normally done by advanced reprocessing of high level liquid waste (HLLW) coming from the PUREX extraction of spent nuclear fuel in a two cycle process. Group separation of lanthanides (Ln) together with MA is followed by MA separation from the Ln fraction (see Fig. 2). This separation is necessary because of the high neutron capture cross-sections of the lanthanides.
An alternative route could be the direct selective separation of MA from HLLW. At ITU the 2 cycle process has been extensively investigated up to now and will be described below. Future research will concentrate on the 1 cycle route.

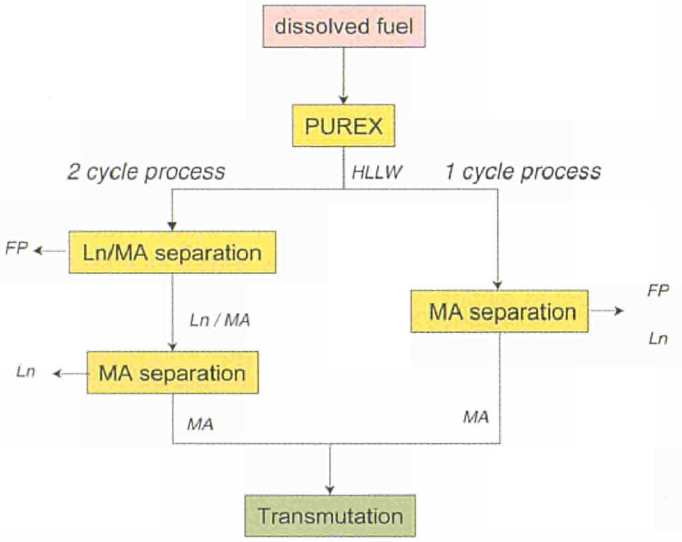

Fig. 2 Main routes for the separation of MA from HLLW

The high-level waste stream of LWR spent fuel reprocessed in a PUREX-type process was partitioned by centrifugal contactors [14] into a residual fraction containing U, Pu, and part of the Np and a fraction containing Am, Cm, lanthanides (Ln) and the remaining Np.

For the Ln/MA group separation, several extraction processes were investigated, the best known being the TRUEX process [15]. A similar process has been developed recently in the P.R. of China, the so-called TRPO process, which uses a trialkyl (C6-C8) phosphine oxide extractant [16]. Diisodecyl phosphoric acid (DIDPA) is an extractant used in a process developed at Japan Atomic Energy Research Institute (JAERI); this solvent extracts actinides from feed solutions at 0.5 M HNO_3 and thereby offers possibly the potential to achieve also a separation of Am and Cm from lanthanides [17]. The French DIAMEX process uses dimethyl-dibutyl-tetradecyl-methylen-diamide (DMDBTDMA) as reference molecule [18]. The four solvents investigated are shown in Fig. 3.

For all four extractants, continuous counter-current extraction tests were carried out in a 16 stage centrifugal extractor battery. As shown in Tab. 4, the extractants investigated have reasonably good extraction properties and should allow achievement of the target Decontamination Factors (DFs) proposed by Koch et al. [19]. The most efficient stripping and the highest recovery rates are achieved in the DIAMEX and the TRPO processes. The DIAMEX process, has the additional advantage that no acidity adjustment (denitration) of the feed solution is needed.

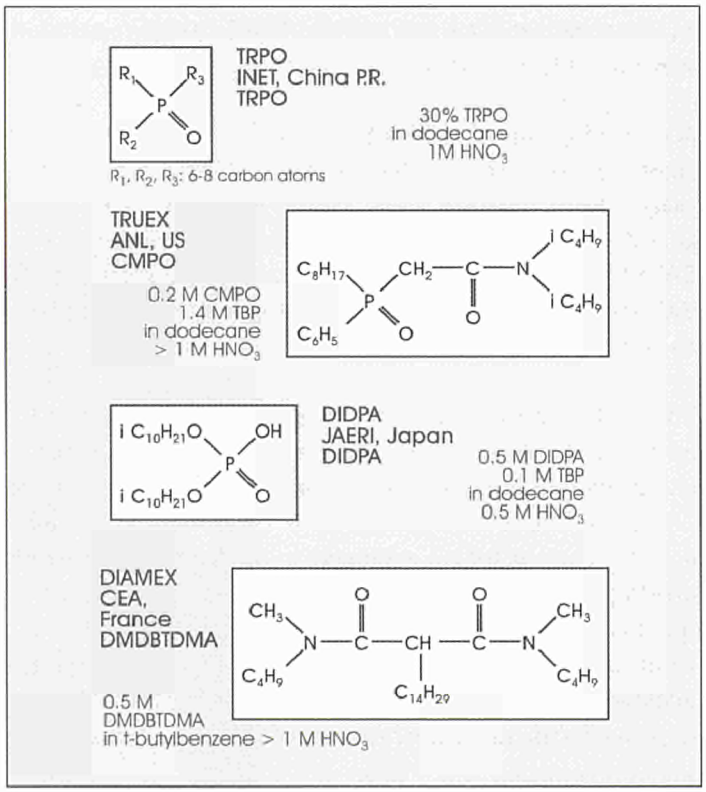

Fig. 3 Characteristics of the four solvents used for dissolving spent fuel.

As a result of this study, the DIAMEX process represents the best compromise of all four processes studied, showing good extraction and excellent stripping properties.

Tab. 4 Decontamination factors (DF) determined for the different extractants.

Isotope measured	TRUEX	DIDPA	TRPO	DIAMEX
^{99}Tc	> 180	–	> 1760	>30
^{144}Nd	> 30000	> 4000	> 22000	> 50000
^{237}Np	> 30000	> 5	12.4 (> 4100*)	> 29
^{238}U	> 100000	> 20000	> 5400	> 2300
^{239}Pu	> 4000	> 150	> 760	> 1250
^{243}Am	> 15000	> 10000	> 900	> 25100
^{244}Cm	> 1500	> 1500	> 600	> 600

** HNO_3 concentration in the feed increased from 0.7 to 1.35 M*

Unfortunately, none of these processes allow the separation of Lanthanide (Ln) fission products from MAs.

For the Ln/MA separation, a first group of methods uses low acidic selective back-extraction of MA from Ln using an aqueous complexant.

A second group of methods is based on a two step partitioning principle in which the aqueous MA/Ln fraction generated from the processes mentioned above (i.e. TRUEX, DIDPA, TRPO and DIAMEX) is subjected to the so-called SANEX process (Separation of ActiNide(III) elements by EXtraction), where the MAs are selectively extracted from the Ln/MA fraction.

The performance of several solvents was compared at ITU and excellent results were obtained for the BTP process [20] using the n Propyl-Bis-TriazinylPyridine (nPr-BTP) molecule. The experiment, carried out in a centrifugal continuous counter-current set-up, achieved an MA/Ln separation with an efficient scrubbing of Ln and produced a MA fraction almost free of Ln. MA extraction and back-extraction was efficient and a reasonably good recovery of Am (>99%) was achieved. Nevertheless, this process scheme has still to be improved to increase the recovery of Cm (at present 97.6 %).

By means of these tests it could be demonstrated, that an efficient separation of minor actinides from genuine spent fuel is possible in a 3-step process (PUREX, DIAMEX, BTP)

For transmutation in fast neutron fluxes one would not need such an extreme purification of the fissile material from thermal neutron absorbing elements (as is the case for the extended PUREX process). Enhanced parasitic neutron capture of certain fission products does not exist in a fast neutron spectrum.

3.2 Pyro-processing

Compared with aqueous methods, dry reprocessing of fuels results in less pure fractions of Pu, Np or Am. Due to the higher radiation resistance of the proposed electrolysis in molten salts, the reprocessing of short-cooled spent fuel is possible. This has two benefits: The out of pile time of the fuel is reduced and as a result the decay of ^{241}Pu producing ^{241}Am (during storage of the fuel) is reduced. Cooling times, as short as a month, of the spent fuel seem possible compared to the present seven years and longer needed for aqueous reprocessing. If the dry partitioning is made on-site, the present difficulties encountered for frequent nuclear material transportation are eliminated.

The dry reprocessing technique can be applied as well for the recycling of the homogeneously distributed minor actinides in a fast reactor fuel as in the accelerator driven systems where the minor actinides with concentrations of up to 40% as oxides, nitrides, metals or even in inert matrices. It should be pointed out however, that in order to obtain physical stability of the fuel, good separation of minor actinides from the lanthanides is needed to reduce their content in the fuel matrix. For the minor actinide fuels, containing up to 20% of minor actinides, the separation of lanthanide has to be better (by a factor of 10), compared to the homogeneous fuel cycle for fast reactors where the minor actinide content is only a few percent. There are also hybrid concepts, where for instance americium in inert matrixes is burnt in the thermalised blanket of a fast reactor.

Compared to aqueous reprocessing, pyro-processing of spent nuclear fuel is far less developed. Originally, both technologies were applied for military purposes: The PUREX process to extract pure enough Pu, the electro-refining to clean Pu-metal from in-grown Am. This latter process was extended to reprocess Zr alloy based-uranium-plutonium-alloy – a test fuel of the fast reactor prototype EBR-II. A similar approach was taken for Russian fast reactors. Here, the PuO_2 was the product instead of Pu-metal. For both the processes it is claimed that they could also separate the

minor actinides.

In the Russian DOVITA-process [21] being developed in Dimitroffgrad, the oxide fuel is converted into chlorides, and UO_2 as well as NpO_2 are separated by electrolysis in a melt of NaCl-KCl at 650 C. The transuranium elements are precipitated sequentially as the oxo-chlorides or oxides out of the NaCl-KCl melt by gassing with Cl_2/O_2 and adding Na_2CO_3. Since lanthanides and the transplutonium elements (Am, Cm) have similar behaviour, a fractionated precipitation of the chlorides is proposed in order to have a pure Am, Cm fraction. From the technological point of view, this is a cumbersome step. Therefore it was proposed to adopt the same process as outlined in the metal refining approach.

The electro-refining of minor actinide metals in molten LiCl-KCl at 450 C seems feasible except for Am. This is the result of studies carried out by CRIEPI, Japan [22] and with the University of Missouri [23]. An alternative approach will be the combination of electro-refining with the reductive multistage extraction from the molten salts into molten Bi. So far, the tests have been made on trace levels with promising yields of 99.9%.

A larger installation, shown in Fig. 4, is being set up at ITU where, jointly with CRIEPI, the technical feasibility of the electro-refining - reductive extraction concept will be demonstrated, and also the conditions to improve the electrorefining of Am from lanthanides. The installation will be the first to operate in the gram-scale (the present conditioning of the EBR-II fuel at Argonne National Laboratory in Idaho separates only uranium by electro-refining and disposes off the transuranium elements unseparated from each other, together with the fission products).

The installation at ITU consists of a stainless steel box, which fits behind the lead shielding of our cells. The atmosphere inside is pure Argon with less than 10 ppm H_2O and O_2 each. We are prepared to process MA containing alloys, described below, but also high level liquid waste from the PUREX process, which we will convert into dry halides. In order to process also oxide fuels, the actinides have to be converted into chlorides or, possibly by reduction with Li, directly to the metals. In preparing the fuel for reprocessing or during different process steps, the separation of long-lived radiotoxic fission products can be achieved. If a voloxidation of the spent oxide fuel is included in the pre-treatment, several fission products are distilled off including ^{129}I, which could be collected with 99.9 % yield. During the electrorefining process, 95% of the ^{99}Tc is collected together with the noble metal fission products in the bottom Cd layer of the electrolysis cell. For the transmutation of the two fission products, special targets have to be fabricated.

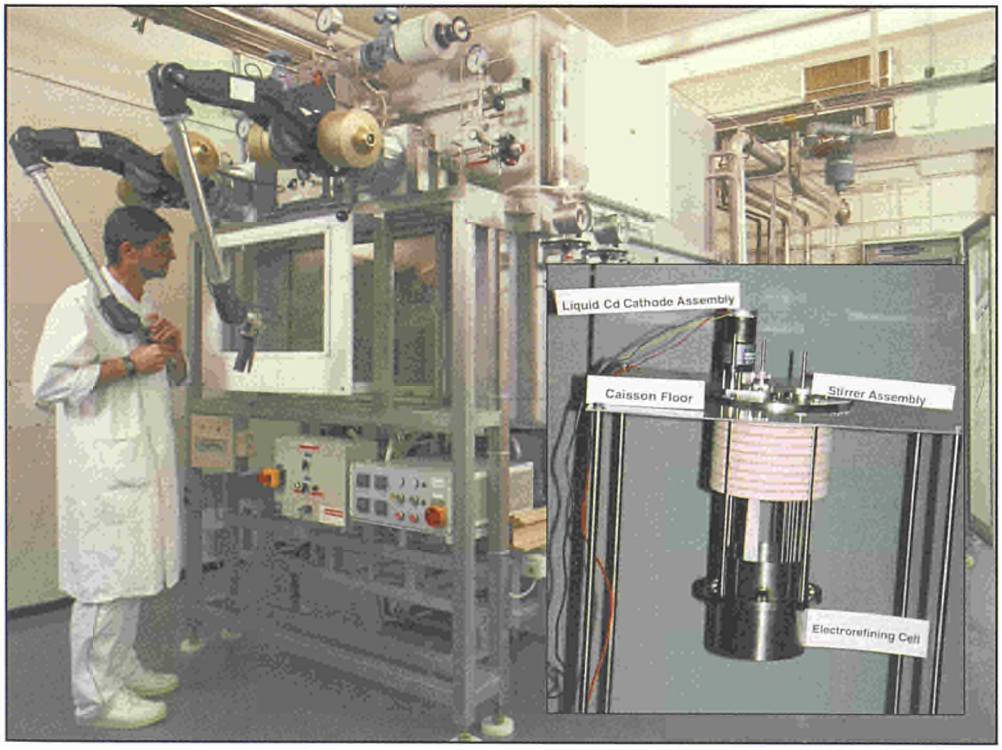

Fig. 4
Stainless steel hot cell inner box equipped with Ar purification unit. Insert shows the electro-refiner for metal fuel containing MAs. The insert (courtesy of T. Koyama, CRIEPI) shows a micro-graph of the target in which the helium-containing gas bubbles, which caused the swelling of the target pellets, are clearly visible.

4 ITU Studies on Fuels and Targets for Transmutation

At present, the research on fuels and targets for transmutation actinides is focussed mainly on three types of materials: oxides, nitrides and metals. These materials all have advantages and disadvantages, depending on the fuel cycle strategy (e.g. type of reactor, reprocessing method) that is envisaged. The research on targets for transmutation of long-lived fission products has been concentrated on technetium. ITU has strongly contributed to the development of fabrication methods for fuel and targets, as summarised in Table 5. Details of these experiments are given below.

4.1 Oxide Fuels

The fabrication of oxide fuels for MA transmutation is often based on the existing technology for UO_2 and mixed oxide $(U, Pu)O_2$ fuel, which comprises powder blending, compacting into pellets and high-temperature sintering. This technology, used commercially for LWR fuels (< 10 w/o Pu) and FNR fuels (up to 30 w/o Pu), has been tested for fuels with high Pu-content (up to 45 w/o Pu) for dedicated fuels for incineration of plutonium in fast neutron reactors in the CAPRA-TRABANT project. In principle, the minor actinides can be mixed into MOX-fuel. When existing facilities for MOX fabrication would be used, the dose to the workers would significantly increase due to increased gamma and neutron

Tab. 5 Programme on transmutation and incineration showing fuels and targets fabricated in ITU.

Programme	Reactor	Fuel/Target	Method	Status
FACT	FR2 (1981)	$(U_{0.5}Am_{0.5})O_2$	sol-gel	PIE complete
MTE2	KNK II (1984-85)	NpO_2; $(U_{0.5}Am_{0.5})O_2$	sol-gel	PIE complete
		$(U_{0.73}Pu_{0.25}Np_{0.02})O_2$	sol-gel	PIE complete
		$(U_{0.73}Pu_{0.25}Am_{0.02})O_2$	sol-gel	PIE complete
SUPERFACT1	Phenix (1986-88)	$(U_{0.74}Pu_{0.24}Np_{0.02})O_2$	sol-gel	PIE complete
		$(U_{0.74}Pu_{0.24}Am_{0.02})O_2$	sol-gel	PIE complete
		$(U_{0.55}Np_{0.45})O_2$	sol-gel	PIE complete
		$(U_{0.6}Am_{0.2}Np_{0.2})O_2$	sol-gel	PIE complete
POMPEI	HFR (1993-94)	Tc metal	casting	PIE in progress
		Tc-50% Ru metal	casting	PIE in progress
		Tc-80% Ru metal	casting	PIE in progress
TRABANT1	HFR (1995-96)	$(U_{0.55}Pu_{0.40}Np_{0.05})O_2$	sol-gel	PIE in progress
		$(Pu_{0.47}Ce_{0.53})O_{2-x}$ [two O/M]	sol-gel	PIE in progress
EFTTRA-T1	HFR (1994-95)	Tc metal [three pins]	casting	PIE complete
EFTTRA-T4	HFR (1996-97)	$MgAl_2O_4$-12% Am	INRAM (pellets)	PIE complete
EFTTRA-T4bis	HFR (1997-99)	$MgAl_2O_4$-12% Am	INRAM (pellets)	PIE in progress
TRABANT2	HFR	$(U_{0.55}Pu_{0.45})O_2$	sol-gel	Irrad. to be started
		$(U_{0.6}Pu_{0.4})O_2$ [two pins]	mech. mix.	Irrad. to be started
ANTICORP	Phenix	Tc metal	casting	Irrad. to be started
METAPHIX	Phenix	U,Pu,Zr	casting	Irrad. to be started
		UPuZrMA2%RE2%	casting	Irrad. to be started
		UpuZrMA5%RE5%	casting	Irrad. to be started

emission rates, especially in case of americium and curium. Therefore special shielded facilities are needed for the fabrication of minor actinide fuels, and this leads to increased fabrication costs. Under these circumstances it might be more practical to fabricate a limited number of fuel pins/elements with higher content of minor actinides (e.g. 20 w/o) rather than adding small quantities (≤ 2 w/o) to each fuel pin. In that case, one could also consider the use of dust-free aqueous processes for the powder fabrication such as the SOL-GEL technique. At ITU, the feasibility of the fabrication of such fuels has been demonstrated in the SUPERFACT experiments and the fuels have been irradiated successfully in the Phénix reactor [24].

Alternatively, the minor actinides could be mixed with an inert matrix such as MgO, $MgAl_2O_4$ or ZrO_2. This would enhance the radiotoxicity reduction by avoiding production of new minor actinides from uranium-free host materials or with thorium oxide in which smaller quantities of minor actinides are bred. However, one has to consider that in critical reactors the absence of uranium has an impact on reactivity and kinetic parameters such as Doppler and moderator void coefficients and delayed neutron fraction. In an ADS this would be less problematic. In addition, not every inert matrix allows for multiple recycling because the reprocessing of some of these materials (e.g. $MgAl_2O_4$ or ZrO_2) by either aqueous or pyro-chemical methods will be difficult. In any case, such fuels would require the development of a new and separate fuel cycle.

Inert matrix concepts are being investigated experimentally in Europe and ITU is participating in the fabrication of targets for irradiation experiments. For these targets, dust-free fabrication methods are being developed and tested. In addition to SOL-GEL, infiltration of actinide solutions into ceramic hosts is being considered. The latter method has been used for the fuels of the only irradiation experiment on an americium-containing inert-matrix target, the EFTTRA-T4 experiment [25]. In this experiment, a target of americium in magnesium aluminate spinel $MgAl_2O_4$, fabricated at ITU by the infiltration method, was irradiated in the HFR-Petten. During 358 full power days 96% of the ^{241}Am was transmuted, mainly to curium and plutonium isotopes of which about 28% were destroyed by fission [25]. Post-irradiation examinations revealed significant swelling of the target due to the accumulation of helium, produced by the decay of ^{242}Cm (see Fig. 5). This effect was also observed to a lesser extent in the americium-rich targets of the SUPERFACT experiment [24].

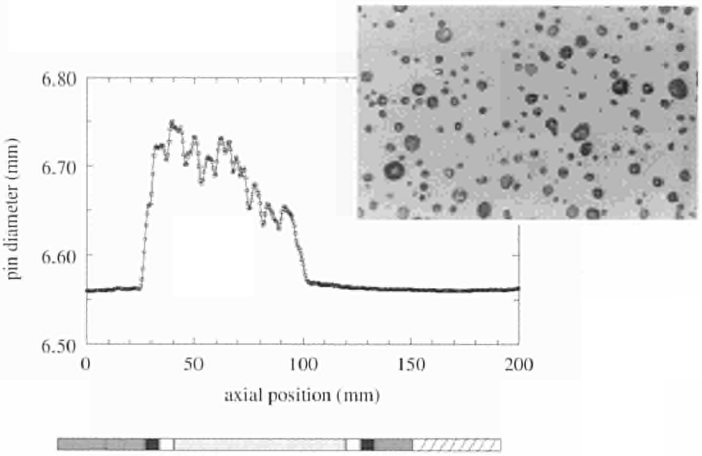

Fig. 5 The change in the diameter of the cladding of the EFTTRA-T4 target showing its expansion in the area where the target pellets were located (curve reproduced by courtesy of NRG).

4.2 Nitride Fuels

The actinide nitrides, which can only be used in LMRs, have a higher thermal conductivity than actinide oxides whereas the melting temperatures are similar. This results in a lower central fuel temperature or, alternatively, allows a higher actinide content in the target. This makes them attractive as fuel material. Moreover, the actinide mono-nitrides form a cubic solid solution in the complete composition range. However, to avoid the production of ^{14}C through (n,p) reactions, the targets or fuels should be produced with nitrogen enriched in the isotope ^{15}N. This raises the cost of the fuel pins although, when pyro-chemical reprocessing of the fuel is used, a significant part of the enriched ^{15}N can be recycled.

The fabrication of actinide nitrides is generally done by carbo-thermic reduction of the oxides. This is a high-temperature process that produces powders with relatively low sintering activity. As a result, high pellet density is difficult to achieve. The process has been applied successfully for (U, Pu)N fuels with low oxygen (< 1000 ppm) and carbon content (< 1000 ppm) in the NILOC, NIMPHE and POMPEI programmes at ITU. For the minor actinide nitrides, researchers of JAERI have shown that NpN can be prepared in a similar way as UN and PuN [26]. For AmN, however, uncertainty exists due to the much poorer thermal stability of AmN compared to the other actinide nitrides [27].

As for the oxides, mixing of the actinide nitrides with an inert nitride matrix could enhance the radiotoxicity reduction of the actinides. ZrN is considered to be one of the most interesting matrices as it forms a solid solution with the actinide mono-nitrides and has favourable properties.

4.3 Metallic Fuels

Actinide metals (similar to the nitrides) have a much better thermal conductivity than the actinide oxides. They cannot, however, be used in water reactors but are suitable for liquid metal and gas-cooled reactors. Due to the complex allotropy of the actinide metals, the alloys of pure actinides undergo several phase transitions in the temperature range of operation of the fuel that results in swelling starting at relatively low burn-up. This can be avoided by increasing the space between the fuel and the cladding. This has only small penalties with respect to temperature of the fuel because of the excellent thermal properties of the metallic fuel and the possibility of applying sodium bonding. The swelling can be limited by adding a non-fissile metal to the alloy (e.g. molybdenum or zirconium), which has the additional advantages that the chemical compatibility of the fuel is further improved and the melting point of the alloy is increased (raising the margin to melting). In the framework of the fast breeder programme in the USA and the evolving IFR concept of Argonne National Laboratory, U-Pu-Zr fuels have been tested successfully in the EBR-II reactor [28]. Irradiation tests with minor actinide containing alloys have not been done. CRIEPI is preparing the METAPHIX irradiation test of (U, Pu, Zr) with up to 5% minor actinides in the Phenix reactor. The metallic fuel for this experiment was fabricated at ITU [29].

The most common fabrication process for metallic fuel is injection casting of the alloy. If pyro-chemical reprocessing is applied, the cathode product obtained is already an alloy of uranium, plutonium and the minor actinides. This can be relatively easily processed to new fuel pins. However, in the case of americium-containing alloys this method poses some problems since Am metal is relatively volatile and may evaporate. Powder metallurgy is therefore also being considered for the fabrication. Because the cathode product contains small amounts of fission products, the fabrication requires remote handling.

4.4 Targets for transmutation of long-lived fission products

The long-lived fission products that are most frequently considered in transmutation studies are ^{99}Tc, ^{129}I and ^{135}Cs. They can be transformed into stable isotopes by a single neutron capture.

Technetium metal has been found to be an excellent target material for transmutation in reactors. As part of the EFTTRA collaboration, irradiation tests of this material were performed in the High Flux Reactor (HFR) at Petten and an irradiation test in the Phénix reactor is in preparation. The fabrication of the targets for these tests was done at ITU where a technique was developed to make cylinders/pellets by casting liquid technetium metal in a water-cooled copper mould. The targets each contained two such cylinders. The EFTTRA-T1 and T2 irradiation tests [30-33] showed good behaviour of the technetium in which about 18% was transmuted to the stable ^{100}Ru isotope. In the rim of the cylinders the extent of transmutation was considerable higher (30-40%) due to contribution of neutrons from the resonance region, where neutron capture cross section of ^{99}Tc is much larger than for thermal or fast energies, typical for LWRs and FNRs, respectively. To make use of this effect, at CERN experiments on the transmutation of ^{99}Tc were performed [34,35] applying the adiabatic resonance crossing (ARC) method in lead where neutrons lose their energy in small decrements. This allows access to the resonance energy region and, thus, the efficiency of the transmutation process may be increased. The CERN researchers have shown that ^{99}Tc can be introduced in the lead volume of an ADS in a parasitic mode, and transmuted without affecting the operation in a significant way.

For iodine targets, metal iodides such as NaI and CeI_3 are being considered and have been tested in irradiation experiments by the EFTTRA group [30,36]. However, they do not seem to be very well suited for transmutation in reactors. Caesium transmutation in reactors does not seem feasible from the point of view of the neutron economy. The neutron absorption cross section of ^{135}Cs is low and separated cesium is not a single isotope but a mixture of the long-lived ^{135}Cs, the short-lived ^{137}Cs and the stable ^{133}Cs, as a result of which parasitic neutron capture in especially ^{133}Cs will occur.

5. Partitioning and Transmutation – The Way Forward

The extent to which partitioning and transmutation technologies can reduce the burden placed on geological disposal (in terms of volumes, decay heat, radiotoxicity, isolation times, etc.) cannot at present be fully assessed. Before this can be done, three key issues have to be resolved:

1. Suitable "back-end" technology to separate the MA and LLFP by-products from the spent fuel.

   At ITU, aqueous processing of MA at laboratory scale by partitioning of genuine spent fuel has been demonstrated. Pyro-processing of simulated fuel containing trace amounts of MAs has also been achieved. Future efforts must concentrate on pyro-processing of irradiated fuels and on the scaling-up of both aqueous and dry processes.

2. Development of dedicated fuels and targets to host MAs, and LLFPs for irradiation in transmutation reactors.

   Fabrication of advanced fuels and actinide targets is being tested at present in various laboratories and many different options (oxides, metals, nitrides, homogeneous, inhomogeneous) are under investigation. Because limited information from irradiation experiments is available to evaluate these options and, moreover, such experiments are relatively time-consuming and expensive, it is not yet possible to concentrate the international efforts in this field, as one would wish. It is thus clear that this area requires much effort and attention in the coming years.

3. The design and testing of transmutation devices such as FNRs or ADSs.

   The very promising ADS require reliable, high intensity accelerators and associated spallation sources for neutron production. Experiments on the coupling of accelerator and spallation source are a major requirement to demonstrate engineering feasibility.

   For the already developed FNRs, ITU and CRIEPI have fabricated MA containing fuel that would allow transmutation in a homogeneous recycling scheme i.e. the self-generated MAs will be returned to the reactor without affecting criticality safety. Nine fuel pins will be testet after the restart of Phénix.

Some of these issues were addressed in the 4th Framework Programme (1995-1998) of the European Commission, and specific results have been reported in this paper. In the 5th Framework Programme (1999-2002), an extension of these activities can be expected and ITU will participate in several key projects in the field of fuel and reprocessing technology. In addition to the framework programme activities, eight European countries and the Joint Research Centre have formed a Technical Working Group (TWG) on ADS to:

- Develop a "roadmap" for a European waste transmutation facility
- Pursue and extend the present co-ordination activities of the TWG to a European Network
- Co-ordinate European participation in emerging projects, mainly outside Europe
- Propose the planning, design, and construction steps for adequate funding in the 6th Framework Programme

Only with such a common European approach can the complex and innovative technology for P&T be transferred from the scientific arena to mature industrial technology.

6. Conclusions

Partitioning and transmutation techniques offer the possibility of removing those by-products from spent nuclear fuel that contribute to the long-term risks of storage, and transmuting them in fast breeders and dedicated waste burners to less harmful products. Research in this area could have a considerable impact on the long-term technical demands placed upon sites for the disposal of radioactive waste, because the radiotoxicity of the by-products, and the very long times that they need to be separated from the biosphere, can be reduced. This may also lead to a better acceptance of nuclear energy.

The ongoing activities at the Institute for Transuranium Elements are closely related to the development of schemes for partitioning and transmutation of these by-products. Partitioning activities involve the investigation of advanced aqueous and pyroprocessing techniques for separation of plutonium and minor actinides from the spent fuel. Transmutation activities deal with the development of techniques for fabrication of dedicated fuels and minor actinide targets and involves the fabrication of materials for irradiation experiments and their post-irradiation analysis.

These activities, which are described in more detail in this report, will continue as a main line of research at the Institute during the current 5th Framework Programme.

Acknowledgements

The authors would like to thank Mr. J. Richter for help in preparation of the manuscript. In addition, J.M. would like to thank Dr. Enrique Miguel González Romero for discussion on the CERN ADS concept, Dr. Francesco Venneri for comments on the U.S. ATW concept, and Dr. Massimo Salvatores regarding the French Double Strata concept.

References

[1] D. R. Williams, What is Safe? The Risks of Living in a Nuclear Age, The Royal Society of Chemistry, Cambridge, 1998.

[2] The Royal Society, Nuclear Energy, The Future Climate, p27, 1999.

[3] Management of nuclear wastes, Volume II (Evidence) (Select Committee on Science and Technology House of Lords, para 925, p146, March 1999.)

[4] 1999 World Nuclear Industry Handbook, Nuclear Engineering International, p. 12. (European Union countries with nuclear power are Belgium, Finland, France, Germany, Netherlands, Spain, Sweden, and UK).

[5] Assuming a conversion efficiency of 35% thermal to electrical energy.

[6] Informations Utiles, 1999, p. 16, CEA, ISBN 2-11-091547-1.

[7] International Commission For Radiological Protection, Age-dependent Doses to Members of the Public from Intake of Radionuclides: Part 5 Compilation of Ingestion and Inhalation Dose Coefficients, Annals of the ICRP publications 72 (1996), Pergamon Press.

[8] J. Magill, P Peerani, J. van Geel, Closing the Fuel Cycle with ADS, International Workshop on the Physics of Accelerator-Driven Systems for Nuclear Transmutation and Clean Energy Production, 29th Sept. - 3rd Oct. 1997, Trento, Italy.
http://itumagill.fzk.de/ADS/trento/trento.html
also
OECD/NEA, Actinide and Fission Product Partitioning and Transmutation, OECD 1999.

[9] M. Salvatores, Studies at CEA-France on the Role of Accelerator-Driven systems in Waste Incineration Scenarios, Proceedings of the I.A.E.A. Technical Committee Meeting on: Feasibility and Motivation for Hybrid Concepts for Nuclear Energy Generation and Transmutation, Madrid, Spain, 17-19 September 1997, to be published.

[10] T. Mukaiyama, et al., Omega Program & Neutron Science Project for Development of Accelerator Hybrid System at JAERI, Proceedings of the I.A.E.A. Technical Committee Meeting on: Feasibility and Motivation for Hybrid Concepts for Nuclear Energy Generation and Transmutation, Madrid, Spain, 17-19 September 1997, to be published.

[11] C. Rubbia, CERN Concept of ADS, Proceedings of the I.A.E.A. Technical Committee Meeting on: Feasibility and Motivation for Hybrid Concepts for Nuclear Energy Generation and Transmutation, Madrid, Spain, 17-19 September 1997, to be published.

[12] Department of Energy, A Roadmap for Developing Accelerator Transmutation of Waste (ATW) Technology: A Report to Congress. October 1999, DOE/RW-0519.
http://www.pnl.gov/ATW/ReportToCongress/

[13] Data on half-lives taken from Nuclides 2000:
An Electronic Chart of the Nuclides (see website at
http://itumagill.fzk.de/nuclides_2000/).
This data is based on the JEF 2.2 datafile. The fission half-life was calculated using the relation $\tau_{1/2} = 2/(\sigma,\phi)$ where is the fission cross section and the neutron flux. The cross section data is based on the JEF 2.2 datafile. The values used, for a fission spectrum, were taken from JEF Report 14, NEA/OECD, 1994. The neutron flux was assumed to be $5x10^{15}$ $cm^{-2}s^{-1}$.

[14] Institute for Transuranium Elements Annual Report 1992, TUAR '92, p 81.

[15] E.P Horwitz,. D.G. Kalina, H. Diamond,. G. Vendegrift, W.W. Schulz, Solvent Extr. Ion Exch. 3 (1985) 75.

[16] J.-P. Glatz, C. Song, X. He, H. Bokelund, L. Koch, Partitioning of Actinides from HAW in a Continuous Process by Centrifugal Extractors, Proc. of the Special Symposium on Emerging Technologies in Hazardous Waste Management, September 27-29, 1993, Atlanta, Georgia, D.W. Tedder ed., ACS, Washington, DC.

[17] M. Kubota, I. Yamaguchi, Y. Morita, Y. Kondo, K. Shirahashi, I.Yamagishi, T. Fujiwara, "Development of a Partitioning Process for the Management of High-Level Waste", Proc. of GLOBAL '93, Seattle (WA), USA (1993) Vol.1, p.588

[18] C. Madic, P. Blanc, N. Condamines, P. Baron, L. Berthon, C. Nicol, C. Pozo, M. Lecomte, M. Philippe, M. Masson, C. Hequet, M.J. Hudson, Actinide Partitioning from HLLW using the Diamex Process, Proc. of the Fourth Int. Conf. on Nuclear Fuel Reprocessing and Waste Management, "RECOD '94", April 24-28 1994, London, UK

[19] L. Koch, J.-F. Babelot, J.-P. Glatz and G. Nicolaou, OECD/NEA, Proc. of the 3rd International Information Exchange Meeting on Actinide and Fission Product Separation and Transmutation, Cadarache France, Nov. 11-13, 1994

[20] O. Courson, R. Malmbeck, G. Pagliosa, K. Römer, B. Sätmark, J.-P. Glatz, Separation of Minor Actinides from a Genuine An/Ln Fraction, Proceedings Euradwaste'99 - Radioactive Waste Management Strategies and Issues – 15.-18. November 1999 – Luxembourg

[21] A.V. Bychkov, S.K. Vavilov, O.V. Skiba, P.T. Porodnov, A.K. Pravdin, G.P. Popkov, K. Suzuki, Y. Shoji, T. Kobayashi, Pyroelectrochemical processing of irradiated FBR MOX fuel. III. Experiment on high burn-up fuel of the BOR-60 reactor; Proceedings of the Int. Conf. on Future Nuclear Systems, GLOBAL '97, Yokohama, Japan, 1997, vol.2 , p. 912-917

[22] T. Inoue, H. Tanaka, Recycling of actinides produced in LWR and FBR fuel cycles by applying pryrometallurgical process;. Proceedings of the Int. Conf. on Future Nuclear Systems, GLOBAL '97, Yokohama, Japan, 1997, vol.1 p. 646-652

[23] S.P. Fusselman, R.L. Gay, D.L. Grimmett, J.J. Roay, C.L. Krueger, C.R. Nabelek, T.S. Storvick, T. Inoue, K. Kinoshita, N. Takahashi, Dry separation process for actinide removal from PUREX waste; Proceedings of the Int. Conf. on Future Nuclear Systems, GLOBAL '97, Yokohama, Japan, 1997, vol.2. p. 816-819

[24] J.-F. Babelot, N. Chauvin, Joint CEA/ITU synthesis report of the experiment SUPERFACT 1. Institute for Transuranium Elements Technical Note JRC-ITU-TN-99/03, 1999

[25] R.J.M. Konings, R. Conrad, G. Dassel, B. Pijlgroms, J. Somers, E. Toscano, The EFTTRA-T4 experiment on americium transmutation. EUR Report, in press.

[26] Y. Suzuki and Y. Arai, Thermophysical and thermodynamic properties of actinide mononitrides and their solid solutions. J. Alloys. Comp. 271-273 (1998) 577-582

[27] M. Takano, A. Itoh, M. Akabori, T. Ogawa, S. Kikkawa and H Okamoto, Synthesis of americium mononitride by carbothermic reduction method. In : Proceedings GLOBAL'99.

[28] L.C. Walters, G.L. Hofman, T.H. Bauer and D.C. Wade, Metallic fuels for fast reactors. In: Proceedings Workshop Advanced Reactors with Innovative Fuels, 21-23 October 1998, Villigen, Switzerland. OECD/NEA, 1999.

[29] M. Kurata, A. Sasahara, T. Inoue, M. Betti, J.-F. Babelot, J.-C. Spirlet, L. Koch, Fabrication of U-Pu-Zr metallic fuel containing minor actinides; Proceedings of the Int. Conf. on Future Nuclear Systems, GLOBAL '97, Yokohama, Japan, 1997 vol.2 p. 1384-1389

[30] R.J.M. Konings, W.M.P. Franken, R. Conrad, J.-F. Gueugnon and J.-C. Spirlet, Transmutation of technetium and iodine – Irradiation tests in the frame of the EFTTRA cooperation. Nucl. Technol. 117 (1997) 293-298

[31] R.J.M. Konings, J.L. Kloosterman, J.A. Hendriks and H. Gruppelaar, Transmutation of technetium in the Petten HFR: a comparison of measurements and calculations. Nucl. Sci. Eng. 128 (1998) 70-75

[32] R.J.M. Konings, A.D. Stalios, C.T. Walker and N. Cocuaud, Transmutation of technetium - Results of the EFTTRA-T1 experiment. J. Nucl. Mat. 254 (1998) 122-128.

[33] R.J.M. Konings, R. Conrad, Transmutation of technetium – Results of the EFTTRA-T2 experiment. J. Nucl. Mat. 274 (1999) 336-340

[34] H. Arnould et al. Neutron-driven nuclear transmutation by adiabatic resonance crossing. Report EUR 19117 en.

[35] H. Arnould et al., Experimental verification of neutron phenomenology in lead and transmutation by adiabatic resonance crossing in accelerator driven systems. Phys.Lett. (1999), B458, 167-180

[36] R.J.M. Konings, Transmutation of iodine: results of the EFTTRA-T1 irradiation test. J. Nucl. Mat. 244 (1997) 16-21

Glossary/Acronyms

ADS Accelerator Driven System. An essential feature of the fission process is that more neutrons are produced than absorbed. This opened the possibility of arranging the fissile material to produce a chain reaction and led to the design "critical" reactors to extract energy on a large scale. There is, however, an alternative way of extracting energy from the nucleus. By bombarding heavy nuclei with high-energy protons from an accelerator, a high yield of neutrons results. These neutrons can then interact with fissile material, to produce energy. With such an accelerator driven system, the arrangement of fissile material in the reactor need not be critical. A key advantage of ADSs over conventional critical reactors lies in the fact that large amounts of MAs can be transmuted safely.

ALI Annual Limit of Intake

ANTICORP Américium, Neptunium, Technétium Incinérés dans Couvertures Radiales de Phénix

ATW Accelerator Transmutation of Waste usually refers to the U.S. ADS programme

BTP process using Propyl-Bis-TriazinylPyridine for separation of antinides from lanthanides

CAPRA is the acronym for Consommation Acrue de Plutonium dans réacteurs Rapides. It is the name of the programme of the French Commissariat à l'Energie Atomique (CEA) on plutonium incineration in fast reactors. TRABANT is the name of an irradiation experiment in the HFR-Petten.

CERN Conseil Européen pour la Recherche Nucléaire or European Organization for Nuclear Research in Geneva, Switzerland.

CRIEPI Central Research Institute of the Electric Power Industry, Tokyo, Japan

DIAMEX Diamide Extraction Process. An advanced aqueous process for separating americium and curium from spent fuel.

DF Decontamination Factor of an element is the concentration of that element in the feed divided by that in the raffinate.

DIDPA Diisodecyl phosphoric acid: an extractant used in advanced aqueous processing to separate actinides.

DOVITA Dry reprocessing, Oxide fuels, Vibropac, Integral, Transmutation of Actinides, Dimitroffgrad, Russia

EFTTRA is the acronym for Experimental Feasibility of Targets for Transmutation. It is a co-operation between CEA, EDF (France), Forschungszentrum Karlsruhe (Germany), NRG (Netherlands), JRC-IAM and JRC-ITU (European Commission) .

Extraction removal of elements from the aqueous solution to the organic solvent. See stripping, the opposite process.

FACT Formation of actinides in pile

fp or **FP** fission products

HLW High Level Waste refers to the liquid waste from reprocessing which contains fission products and the minor actinides and, as a result, requires massive shielding and provision for cooling.

IFR Integral Fast Reactor – a compact reactor design based on metallic fuel fabrication and pyro-chemical reprocessing at the reactor site.

ILW Intermediate Level Waste: The nuclear cycle also generates materials described as intermediate waste "ILW". An example is the cladding around the fuel. ILW materials are sufficiently radioactive as to require a barrier between them and the biosphere. Cooling is not required.

JAERI Japan Atomic Energy Research Institute

LLW Low Level Waste: a mixed bag of items such as protective clothing, which can be safely disposed of by shallow burial.

LLFP Long-lived fission products

LMR Liquid metal reactor

LWR Light Water Reactor

MA Minor Actinides – This expression refers mainly to the elements neptunium, americium and curium. These minor actinides (MA) are produced as radioctive by-products in nuclear reactors. The term "minor" refers to the fact that they are produced in smaller quantities in comparison to the "major" actinide plutonium.

METAPHIX Metal Transmutation of Actinides in Phénix

NIMPHE Nitrures Mixtes dans Phenix à joint Helium.

NILOC Nitride fuel with Low Oxygen and Carbon content (irradiation experiment).

POM An irradiation capsule for mixed oxide pellets (Pellets Oxyde Mixte), where the pellet axis is not parallel but transverse to the fuel pin axis. This device was used in the past for oxide fuel experiments in the BR2, Mol (BE) and later for nitride fuel in the HFR, Petten (NL) test reactors.

POMPEI POM Petten Irradiation experiment to study the structure of nitride fuel.

PUREX An aqueous process for Plutonium and Uranium Recovery by Extraction from spent fuel.

SUPERFACT minor actinide irradiation in Phénix (follow up of FACT).

Raffinate the refined fraction which results after removal of the actinides by solvent extraction.

SLFP Short-lived fission products.

Spallation refers to the process in which a particle with high energy strikes a nucleus. The particle imparts some of its energy to the nucleons which may then be ejected from the nucleus. Above 100MeV, a dozen or more nucleons may escape.

Stripping removal of elements from the organic solvent to the aqueous solution. See extraction, the opposite process.

TRABANT Transmutation and Burning of Actinides in Triox
(Triox is an irradiation capsule used in the HFR test reactor, Petten, NL).

TRPO Trialkyl Phosphine Oxide: an extractant used in advanced aqueous processing to separate americium and curium.

TRUEX An advanced aqueous process for Trans-Uranium Extraction from spent fuel

UREX An Aqueous process for Uranium Extraction from spent fuel

Institute Staff

The staff situation as of December 1999 is presented in the chart below. The total statutory staff, i.e. employees of the European Commission, was 194. In addition 12 post-docs and 10 doctoral grantholders worked during 1999 in the Institute.

The distribution of staff by category and status is given in the chart below. Category A grade means scientists and engineers with an university degree, category B corresponds to technicians and category C/D means laboratory attendants or craftsmen.

Statutory staff by category and status 194

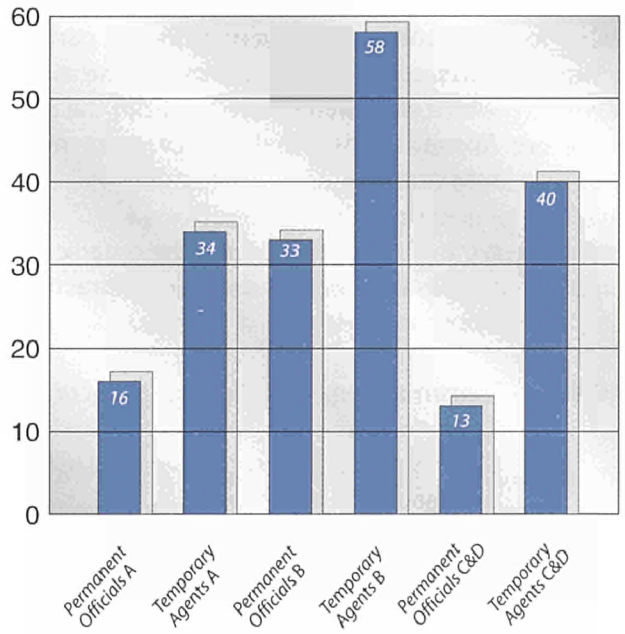

Staff Situation

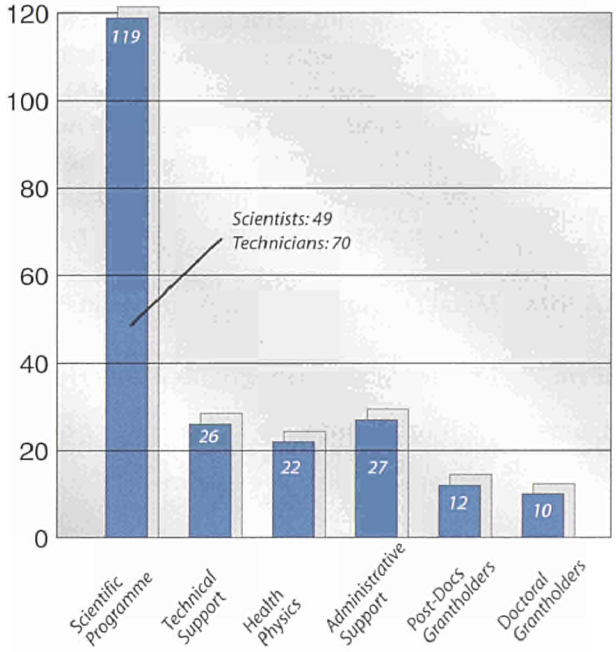

Budget

Two major categories of activities are performed in the Institute. So-called "institutional" activities are activities carried out on behalf of the European Union and paid by the European Commission. These activities include research in the area of alpha-immunotherapy, fuel cycle safety, nuclear safeguards and scientific technical support to the different Directorate Generals of the Commission.

The second category of activities comprises so-called "competitive" work, covers activities performed against payment. This category includes work for third parties, technology transfer actions, shared cost actions (DG Research) and work for other Directorate Generals of the Commission following a call for tender.

The distribution of the institutional budget to the different research and support activities and the source of competitive income for 1999 is shown below.

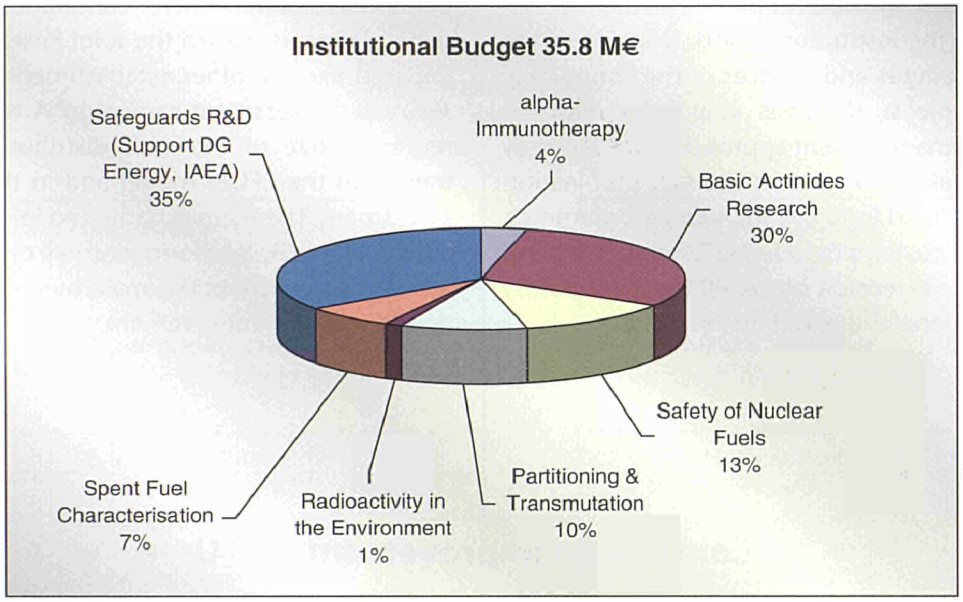

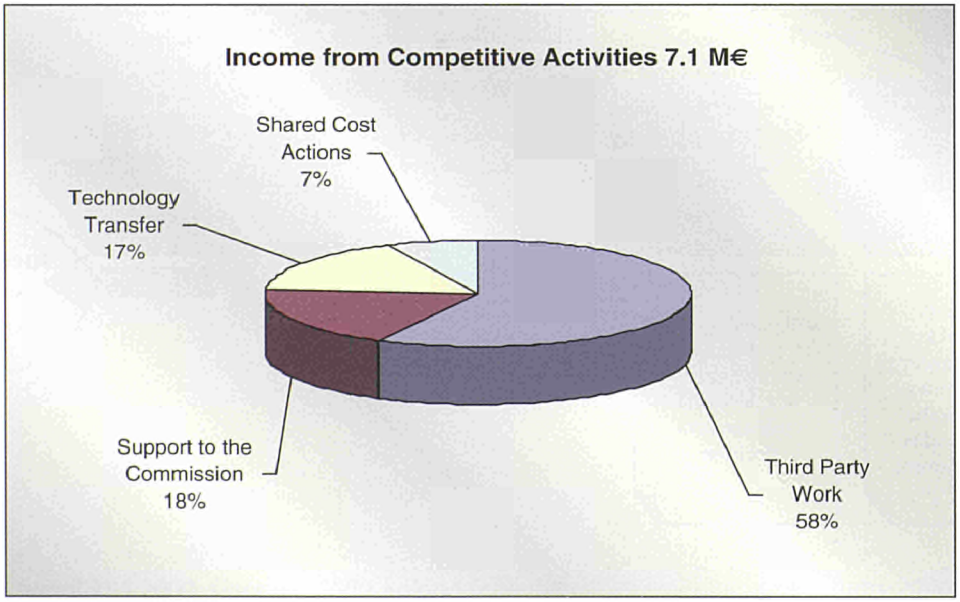

Quality Management

Following a control audit, the 'Deutsche Gesellschaft zur Zertifizierung von Qualitätssicherungssystemen' (DQS) confirmed its certification that the Quality Management (QM) system at ITU fulfils the requirements of the ISO 9001 norm for contractual work. Considering the positive effects of the system in terms of transparency and efficiency in solving problems, and for reasons of internal coherence, it was decided to continue the implementation of the system to cover all activities of the Institute. In particular, the QM system now extends to the institutional work; because of the many common procedures and services of the contractual and institutional projects, this was straightforward. For example, the project management approach had to be only slightly adapted to take into account the fact that institutional projects are defined from the JRC work programmes, and not directly from customer requests. Concretely, a good way of achieving this extension of the QM system was by including the institutional projects in the audit plan.

The control audit was completed by a so-called "delta-audit", consisting of an evaluation of the QM system at ITU with respect to the new ISO 9001:2000 norm, which is in preparation. Following this evaluation, six adaptation actions were defined, and are now being implemented. They will be reviewed at the next control audit.

Finally, and in agreement with the quality policy defined by the Directorate-General, stating that the EFQM model will be used as a framework for continuous improvement in the general organisation of the Joint Research Centre (JRC), ITU initiated, like the other establishments and services of the JRC, a self-assessment campaign. A team was constituted, representative of the staff distribution of the ITU, and trained in the EFQM model and in the technique of self-assessment. The team is gathering information on the nine criteria of the EFQM model, and will evaluate the Institute in a two-day workshop. The main outcome will be the definition of areas for improvement.

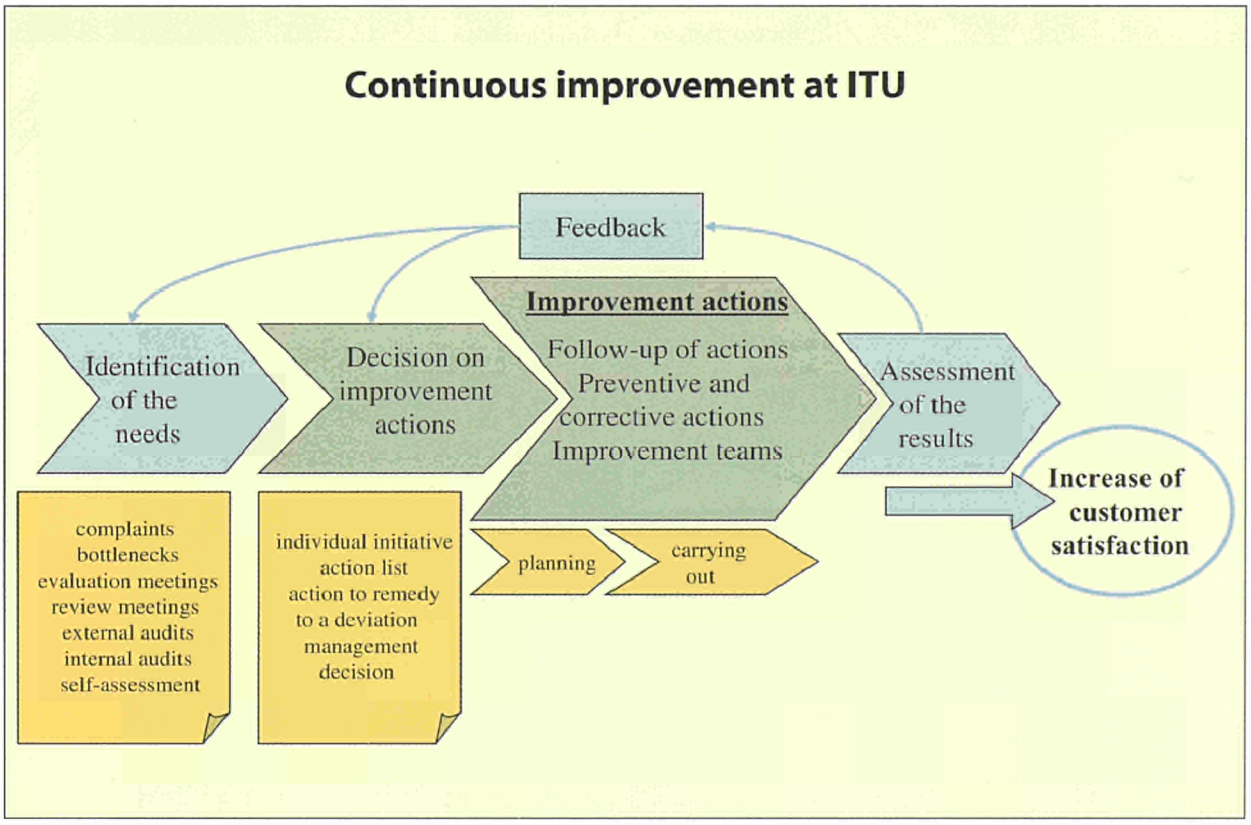

Institute Organigram

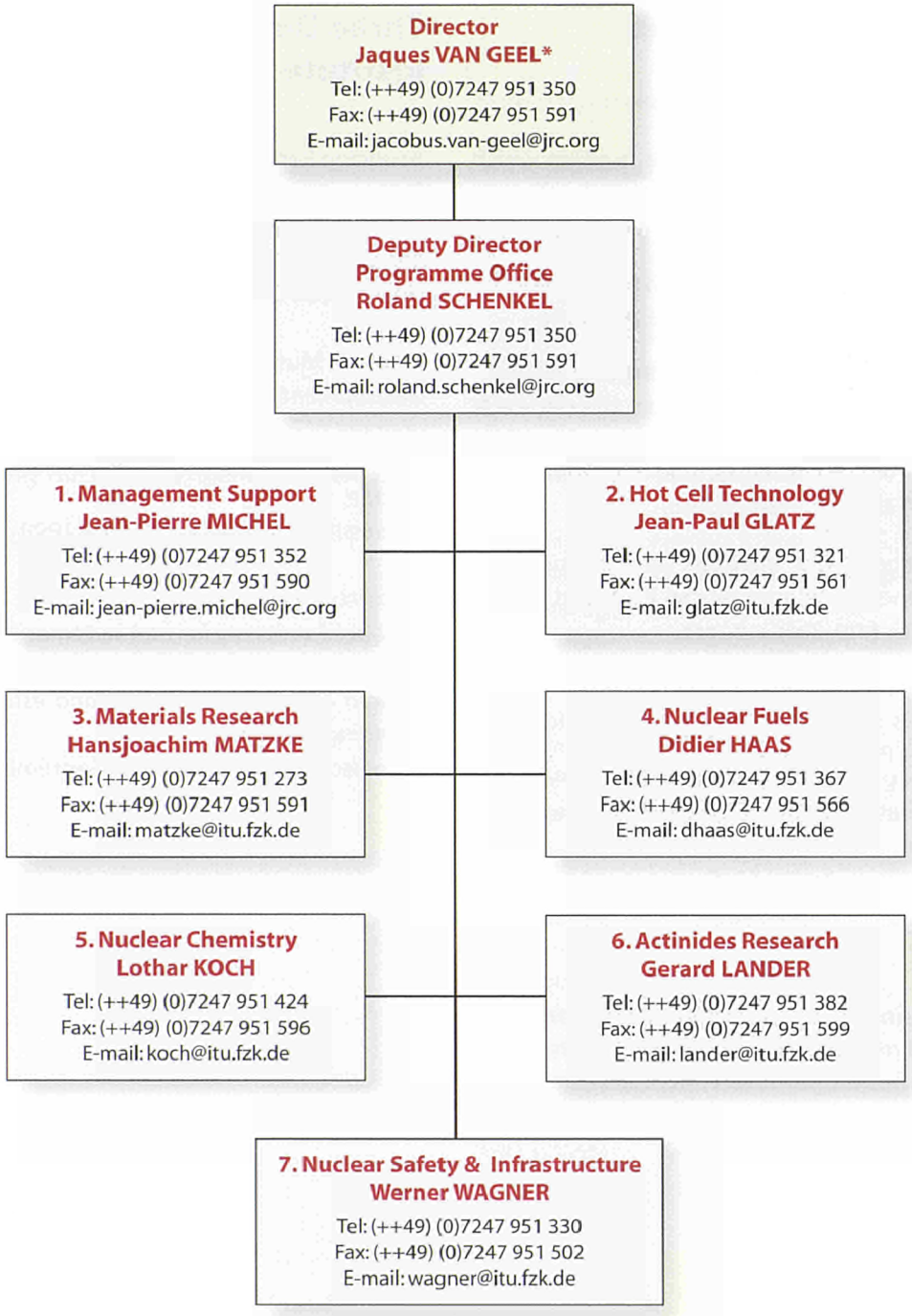

** until 31.1.2000, since 1.2.2000 Roland Schenkel*

February 2000

Publications and Patents: Overview

Informing scientific circles and customers

In Annex I of part B a list of 56 publications is given which have appeared in refereed journals together with information on 96 contributions to various conferences.

In addition 48 technical reports have been issued to our different customers under various competitive activities.

Bibliograpical data along with abstracts of previous publications from the Institute can be retrieved from the database "Publications" of the Community Research and Development Information Service (CORDIS) located in Luxembourg: *http://www.cordis.lu/EN_PUBLI_search.html*

More information about the Institute for Transuranium Elements (ITU) and the JRC in general can be found on the Web server of the JRC: *http://www.jrc.org.*

ITU's previous annual reports 1995-1998 (in PDF format) are also available on this site under the header 'Publications' (More information → Publications).

More detailed information on the Institute at: *http://itumagill.fzk.de*

Three Doctoral grantees from the Institute have obtained their PhD

Asunción Fernández Carretero
Preparación de matrices inertes y su infiltración con materiales radioactivos para la fabricación de blancos para la transmutación e incineración de actínidos.
Universidad Complutense de Madrid, Madrid, ES, 1999

Manuela Musella
Development and test of a method for the simultaneous measurement of heat capacity and thermal diffusivity by laser-flash technique at very high temperatures. Application to uranium dioxide.
University of Warwick, UK, June 1999

Heinrich Ziegler
Advanced concepts for task automation in nuclear extraction chemistry. A contribution to the optimization of automated column extraction chemistry and establishment of a corresponding database.
Technische Universität Wien, September 1999

Patents

During 1999, the Institute has submitted 4 patent proposals; 3 patents have been deposited (first application) and 5 patents have been granted.

First Application (with priority data)

Haas D.; Somers J.
A Method for tailoring the density of nuclear fuel pellets
18/01/1999 99100387.2 EP

Magill J., Peerani P.
A neutron amplifier assembly
20/04/1999 99107327.1 EP

Charollais F.; Somers J.; Fourcaudot S., Fuchs C.; Haas D.
Method for producing nuclear fuel pellets of the MOX type
06/09/1999 99116886.5 EP

Patents granted

van Geel J.N.C.; Koch L.W.; Fuger J.
Verfahren zur Erzeugung von Actinium-225
03/07/1995 88636 LU (Priority)
24/03/1999 0752709 EP

van Geel J.N.C.; Koch L.W.; Fuger J.
Verfahren zur Erzeugung von Aktinium-225 und Wismut-213
23/02/1990 7684 LU (Priority)
23/07/1999 2955884 WO JP

van Geel J.N.C., Peerani P.; Nicolaou G.; Matzke Hj; Magill J.
A method for the destruction of plutonium by irradiation in a light water reactor
04/07/1995 95110397.7 EP (Priority)
12/10/1999 5966418 WO US

Nicolaou G.; Koch L.; Abbas K.
A monitor for measuring both the gamma spectrum and neutrons emitted by an object, such as spent nuclear fuel
15/10/1996 96116506.5 EP (Priority)
03/11/1999 0888621 EP WO/B

van Geel J.N.C.; Koch L.W.; Fuger J.
Verfahren zur Erzeugung von Actinium-225 und Wismut-213 durch Bestrahlung von Radium-226 mit hochenergetischen Gammaquanten
01/07/1995 88637 LU (Priority)
10/11/1999 0752710 EP

Information Dissemination

Tapping ITU expertise

ITU continues to widen its circle of contacts and to search for new target groups by offering its expertise in the fields of nuclear technology and actinide research. Around 600 visitors came to the Institute for one or several days, for discussions, workshops, and to participate in courses or tour the laboratories.

During these visits, representatives of

- Commission services could inform themselves of ITU competence and reliability in the nuclear field which could be of benefit to their particular policy efforts and that sound technical assessments on pertinent issues of a European dimension can be supplied "on call" if and when needed.
- Member State authorities and international organisations could satisfy themselves of ITU's impartial scientific and technical support.
- national research centres, universities and industry could get an impression of the potential for networking with ITU, using its nuclear safety relevant databases, know-how and facilities, training opportunities for the next generation of scientists and, seconding specialists to the Institute's user facilities for specific tasks.

The network of contacts now spans Europe, Eastern countries such as Bulgaria, the Czech Republic, Hungary, Russia and members of the Community of Independent States, the U.S., Argentina and Brazil, Japan and, most recently, Korea.

The main nuclear topics dealt with were: waste management, safety of fuels, safeguarding nuclear material, detecting illicit trafficking and discharges in the environment, and also alpha-immunotherapy – a new approach to treating cancer. Basic Actinide Research results were presented to expert circles in international scientific conferences and journals. (see Annex I of this report)

Some major ITU conferences and courses:

- 'Technical collaboration on accounting and control of nuclear materials between the Russian Federation and the JRC', Joint Steering Committee Minatom – Gosatomnadzor – JRC meeting (January)
- 'Counteracting non-authorised transfer of nuclear material' (January, April, July, October)
- 'On Site Laboratory operation' (April)
- ISO Working Groups workshops including MOX group and plenary session (June/July)
- 'Hot Laboratories and Remote Handling' (October)
- 'High performance trace analysis and environmental sampling techniques' (November).

ITU presented itself at the JRC stand during the launch of the 5th Framework Programme in Essen. It also presented its activities under the new programme to research partners, authorities and Commission services during the international seminar "S&T Support to European Policies – Towards a New Partnership" at Ispra, where delegates from the Central and Eastern European Countries countries were invited.

Information dispatched on the inauguration of the first On-Site Laboratory, designed, developed and installed by ITU for a more efficient control of nuclear material, caught the attention of the media. The event at BNFL's reprocessing plant at Sellafield received good and fair coverage in general and triggered interest with the local branch of national television.

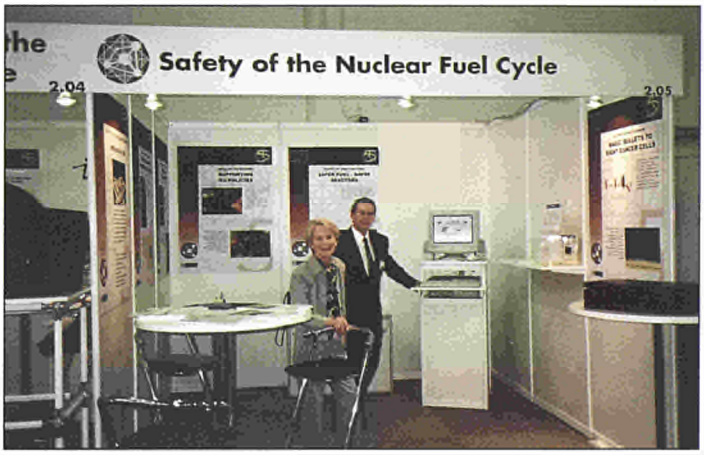

Offering information at an ITU stand during the launch of the 5th Framework Programme in Essen : ITU co-workers Ursula Huber and David Halton.

Presenting latest scientific findings to guests and colleagues: Vincenzo Rondinella from ITU.

Who says nuclear engineering is a man's world? Students from Delft University with their Professor Jacques van Geel (at left) touring ITU labs.

Creating acceptance

ITU's research and support activities are considered useful by Commission services, Member States authorities, international organisations, and academic circles, alike. The general public, however, remains a challenge. ITU tries to demonstrate its usefulness when it comes to, e.g., solving questions of nuclear waste treatment and disposal, detecting clandestine nuclear activities, or monitoring radioactive pollution of the environment. Again, national television reported briefly on such activities.

Arousing interest and deepening insight among the next generation of scientists remains a special ITU concern. Groups of students were invited for tours of the laboratories and discussions.

Local authorities were invited likewise to form an opinion on the activities, get a feeling for the multinational working atmosphere, fathom fields for co-operation, and last but not least appreciate the economic impact of the European institution and its officials on the local economy, mainly small and medium-sized businesses.

In-house transparency through information

Only well informed co-workers can be expected to make a contribution to innovation, be it in the form of new ideas, processes, or products. In addition to traditional scientific seminars a series of 19 lectures were held for co-workers in the framework of "Education Permanente". Topics covered: the role of the JRC in the 5th Framework Programme, the nuclear fuel cycle, non-proliferation, large ITU projects, etc., and lecture notes were distributed. These activities will be continued in 2000.

On their way to the sophisticated laboratories under the guidance of ITU Director Prof. Jacques van Geel (left): Mayor of Karlsruhe Heinz Fenrich (middle) and Deputy Mayor of Karlsruhe Dr. Elmar Kolb (front row, right), Dr. Roland Schenkel of ITU, Dr. Dirk Radloff of Forschungszentrum Karlsruhe, Dr. Peter Fritz, new board member of Forschungszentrum Karlsruhe (second row from left)

ACTIVITIES IN PROGRESS

PART B

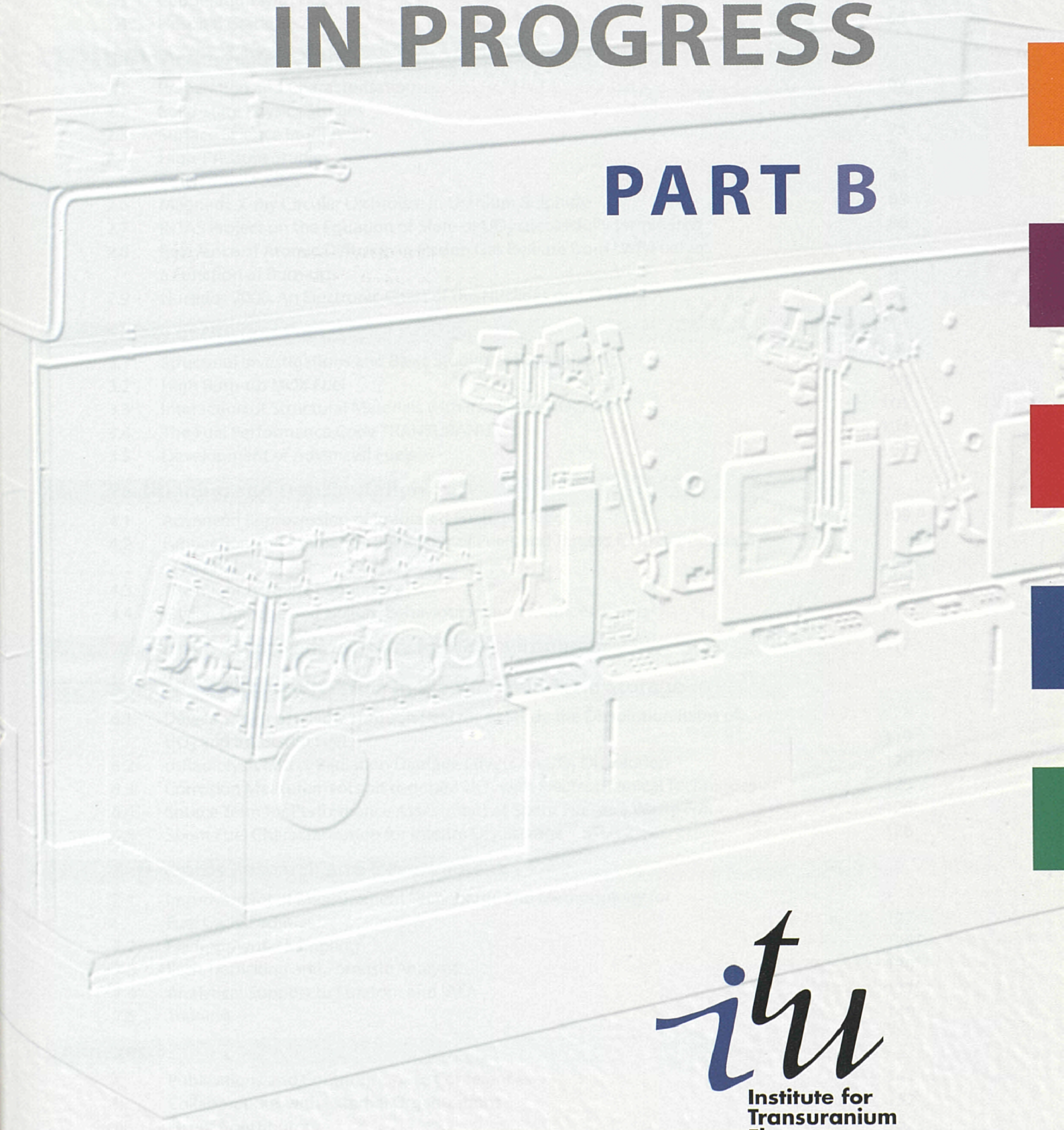

Institute for Transuranium Elements

B - Activities in Progress

1. Alpha-Immunotherapy

Alpha-immunotherapy uses the high selectivity of dedicated monoclonal antibodies (mAb) or peptides, that are linked to an alpha emitting isotope through a bifunctional chelator for the selective irradiation of cancer cells. ITU's role in developing alpha immunotherapy ranges from the production of ^{213}Bi-generators for ongoing trials, to co-operation with hospitals and other institutes on: chelates, large scale isotope production for pre- and clinical testing, and *in vitro* and *in vivo* testing for new biomolecules for alpha immunotherapy.

1.1 Target Production for Irradiating ^{226}Ra in a Cyclotron, to produce ^{225}Ac by a (p,2n) Reaction

Based both on the experience achieved in small scale irradiations of ^{226}Ra in the cyclotron (up to 5 mCi of ^{226}Ra) [1,2] and the associated evaluation and calculations, it was expected that the irradiation of 30 mg (mCi) ^{226}Ra, under properly adjusted irradiation conditions, would result in the production of about 30 mCi ^{225}Ac.

The evaluation of the irradiated target of 30 mCi ^{226}Ra showed however an ^{225}Ac production efficiency of only 11% (i.e. 3,3 mCi). It was diagnosed that the main reason for the lower efficiency was the sub-optimal target fabrication method. It is not straightforward to distribute only 30 mg ^{226}Ra (as 39,2 mg $RaCl_2$) homogeneously on a 2 cm^2 surface.

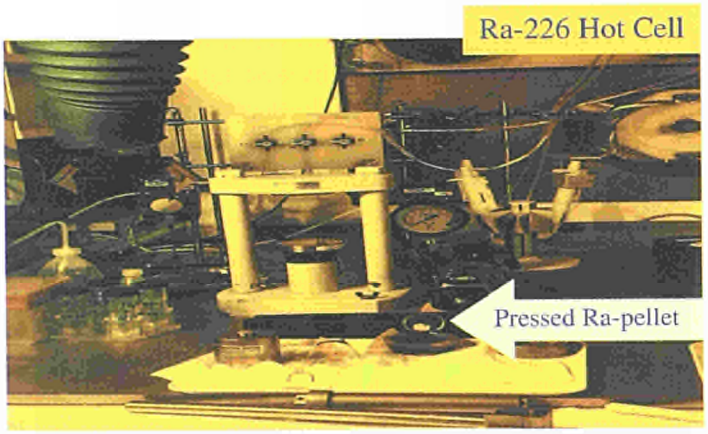

Fig. 1.1 Radium-226 target production in the hot cell.

Therefore a new target fabrication method was developed and a new facility was set up, in order to prepare for larger scale irradiations (up to 500 mg of $^{226}RaCl_2$). (see Fig. 1.1).

The 30 mCi ^{226}Ra is added to about 300 mg $BaCl_2$ to simulate the future larger amount of ^{226}Ra. $BaCl_2$ is used because its chemical and physical properties are very close to those of $RaCl_2$. Both components are mixed and heated, evaporated, and dried at 450 °C (to remove the crystal water) and pressed into a pellet (thickness 7 mm, radius 0,8 cm). This pellet is welded into a leaktight Ag envelope. In a similar manner, in the future, the larger targets of $RaCl_2$ will be produced, without diluent.

The irradation of this newly fabricated target will be performed at the beginning of the year 2000.

References:

[1] L. Koch, J. Fuger , J. van Geel, "Verfahren zur Erzeugung von ^{225}Ac (durch Bestrahlung von ^{226}Ra mit Protonen)", Patent No EP 0752709B1, granted on 24.3.1999 in AT, BE, CH, DE, DK, ES, FI, FR, GB, GR, IE, IT, LI, LU, MC, NL, PT, SE.

[2] C. Apostolidis, W. Janssens, L. Koch, J. Mc Ginley, R. Molinet, M. Ougier, J. Van Geel, J. Möllenbeck, H. Schweickert, "Method for producing ^{225}Ac by irradiation of ^{226}Ra with protons", Patent filed under Provisional No 98109983.1 on 2.6.1998 for AT, BE, CH, CY, DE, DK, ES, FI, FR, GB, GR, IE, IT, LI, LU, MC, NL, PT, SE.1. : Patent WO9963550, published 9.12.1999.

1.2 New Bifunctional Chelators

With the collaboration of INSERM in Nantes and Kantonsspital Basel, Radiological Center, new bifunctional chelates for ^{213}Bi and ^{225}Ac have been developed. ^{225}Ac work is devoted to the synthesis of macrocyclic chelators to stabilize $^{225}Ac^{3+}$ under physiological conditions and coupling it to biomolecules. A good candidate appears to be 1,4,7,10,13,16-hexaazacyclooctadecane, 1,4,7,10,13,16-hexaacetic acid (HEHA), which was synthesized as a monofunctional version using a new and elegant synthetic route. Recently, the chelate has been also synthesized in a bifunctional version of HEHA by modification of the carbon backbone. The preliminary in vitro tests with the monofunctional version have been promising. The final *in vitro* and *in vivo* testing is going to start during year 2000.

For bifunctional chelators for ^{213}Bi two strategies have been followed so far:

a) Transcyclohexyldiamine based 13-membered tetraazatetraacetic acid derivatives; the first step in the synthesis was to make corresponding tetraamines by peptide synthetic methods followed by carbonyl group reduction. Two such precursors were successfully synthesized.

b) Trans-cyclohexyl-DTPA based open chain chelators; like above a strategy has been chosen to form preorganised bifunctional chelators. The starting material was again trans-cyclohexyldiamine which was monoprotected with BOC and monoalkylated with bromoethylamine-N,N-diacetic acid-tbutyl-diester. In the following step the secondary amine was then alkylated with α-bromo-succinic acid-1-tert-butylester-4-benzylester. The synthesis was successful up to this step and will be followed in the future.

1.3 Cooperation with Hospitals

The phase-I study at **Memorial Sloan-Kettering Cancer Center** (MSKCC), New York, using the HuM195 antibody labeled with ^{213}Bi has now been completed. The highest tolerated dose for the treatment of relapsed or refractory of myeloid leukemia has not been reached even with dose level 50 MBq/kg. The main results of the phase-I study are:

1. HuM195-CHXA-DTPA-bismuth-213 construct is stable and safe.
2. The absorbed dose ratio between marrow, liver and spleen volumes and whole body for ^{213}Bi-HuM195 is 1000-fold greater than that commonly observed with β^--emitting radionuclides used for radioimmunotherapy.

Based on these encouraging results, the Phase-II study with ^{213}Bi-HuM195 construct is going to be started during the year 2000 [1].

In the **"Abteilung Nuclearmedizin der Georg-August-Universität Göttingen"** new peptides for alpha therapy are studied. CCK-B receptors are expressed in high amounts in medullary thyroid and small cell lung cancer. However, they have been demonstrated on a variety of other cancers, such as some ovarian tumors, astrocytomas, colon, stomach, or pancreatic tumors as well. Medullary thyroid and small cell lung cancer appeared as very attractive candidates for proof-of-principle of alpha therapy, since both stand at opposite ends of the radiosensitivity spectrum of solid tumors, colorectal cancer being somewhere between them. The same holds true for the incidence, social medical importance, and frequency of these cancer types. On the other hand, with the exception of the stomach mucosa, the physiological CCK-B receptor expression is rather low in peripheral normal organs.

A variety of peptides, all bearing the CCK-receptor binding, were tested in order to develop an optimal ligand which unites in itself both high affinity to and selectivity for the CCK-B receptor. Also a novel DTPA-based chelator DTPA-*D*-Glu has been developed which combines the advantages of DTPA and DOTA without sharing the respective disadvantages. DTPA-*D*-Glu showed improved metabolic stability for a variety of radiometals, such as β^-- (^{90}Y, ^{153}Sm), Auger/conversion electron- (^{111}In, ^{140}Nd), or α-emitters (^{213}Bi/^{213}Po) [2]. One of the most promising peptide in the respect of improved metabolic and increased radiometal chelation stability was the minigastrin derivative: DTPA^0-[*D*-Glu^1]-Glu$_5$-Ala-Tyr-Gly-Trp-Met-Asp-PheNH$_2$ and it was chosen as carrier for all subsequent experiments.

The aim of the subsequent work was to compare the toxicity and anti-tumor efficacy of these peptides, labeled with high linear-energy-transfer (LET) emitters, e.g., Auger/conversion electron- or α-emitters, as compared to conventional low-LET β-emitters [2]. The minigastrin derivative had shown high affinity to and selectivity for the CCK-B receptor. It rapidly internalizes after receptor binding. Biodistribution studies were performed in nude mice bearing subcutaneous TT medullary thyroid cancer xenografts. For therapy, groups of mice were injected with the various radiolabeled peptides, whereas controls were left untreated or were given equal amounts of unlabeled peptide. The maximum tolerated dose (MTD) of each agent was determined. Myelo-, second organ (e.g. renal) toxicity and tumor growth were monitored at weekly intervals. In accordance with kidney uptake values as high as ≥ 30% of the injected dose per gram (ID/g), the kidney was the first dose-limiting organ, regardless of the label used. With all β- and α-emitters, renal doses of ≥ 90 Gy led to acute, ≥ 60 Gy to chronic radiation nephropathy. However, with ^{111}In, renal doses approximately twice these thresholds were tolerated. All high-LET (i.e., Auger electron and α-emitters were ~2-3-fold more therapeutically effective than the conventionally β-emitter labeled conjugates. Whereas low-LET emitters merely led to growth retardation, permanent cures were observed with

Auger electron and α emitters at their MTDs. We concluded that high-LET (Auger- and α-)emitters are therapeutically more effective than conventional β-emitters. Surprisingly, maximum tolerated doses were very similar between α- and β-, but higher with the Auger-emitters, which may be due to their short path length, selectively irradiating the renal tubulus cells, but sparing the much more radiosensitive interstitial tissues of the kidney [2-4].

The aim of a pilot clinical study was to investigate the clinical role in the staging of metastatic medullary thyroid carcinoma (MTC) and to obtain human biodistribution and dosimetry data. Thirty-five patients with MTC were studied using a ^{111}In-labeled DTPA-derivative of minigastrinno. Physiological uptake was observed in any other organ, such as the liver or spleen. All tumor manifestations known from conventional imaging were visualized as early as 1 hour post injection (h. p. i.), with increasing tumor-to-background ratios over time; at least one lesion was detected in 15/16 patients with occult disease. Among them were local recurrences, lymph node, pulmonary, hepatic, splenic and bone metastases.
Summarizing, these data suggest that CCK-B receptor ligands are a promising new class of receptor binding peptides for the staging and treatment of MTC. High-LET emitters, such as alpha or Auger electron emitters seem to have clear therapeutic advantages over the conventionally used low-LET beta emitters.

Under the Commission's "Innovation" program, a project (TNHLARIT IN30848I) in collaboration with the **university hospitals of Heidelberg, Ghent, Hasselt and Deutsches Krebsforschungszentrum Heidelberg** has been continued. Studies of specific and unspecific cytotoxicity of ^{213}Bi labeled anti-CD19 and -CD20 antibodies were carried out. Dr. M. Brechbiel from the National Institute of Health, USA has provided new bifunctional chelate CHXA"-DTPA for our studies. Biodistribution studies with anti-CD20-CHXA"-DTPA antibodies coupled with $^{205/206}$Bi were shown to result in similar biodistributions than other published radiobismuth labeled antibody-constructs with the same chelators. The conclusion, that there is no extra bismuth uptake on the kidneys during first hours, could be confirmed using ^{111}In labelled antibody constructs. The maximum tolerated dose in normal mice was studied after intravenous injections of escalated activities of ^{213}Bi-labeled anti-CD-20 antibody (2.9 to 13.1 MBq). The preliminary results obtained in 5 to 22 mice per each activity level showed a high toxicity for the three highest activity levels (9.5 MBq to 13.1 MBq) with 70-100% mortality after three weeks. At the 6.5 MBq activity level 25% deaths were observed whereas no death was observed with the two lowest activity levels (2.9 MBq and 4.9 MBq). The hematological toxicity data and pathological results are not yet available. Several hundred milligrams CHXA"-DTPA chelated antibodies were produced for clinical Phase trials, which are planned to start during year 2000.

The tumor binding and therapeutic efficiency of ^{213}Bi labeled specific monoclonal antibody against E-Cadherin mutation was studied *in vitro* and *in vivo* in a human intraperitoneal (i.p.) gastric cancer model with the **Nuclearmedizinische Klinik und Poliklinik der Technischen Universität München**. *In vitro* experiments showed approximately one log specific cell killing of the ^{213}Bi labelled 6H8-antibody. In vitro experiments were investigated: biokinetics, tumor binding and therapeutic efficacy of a ^{213}Bi labelled 6H8. After i.p. injection of ^{213}Bi labelled 6H8-nAb into mice bearing tumor cells biokinetics and tumor binding in i.p. tumor nodules were determined. These small tumor nodules in the intraperitoneal cavity bound 62% injected dose/g tumor within 1 h p.i. In tumor nodules expressing wild-type E-Cadherin the uptake was less than 6% injected dose/g. The therapeutic efficacy was evaluated by determination of tumor and ascites development depending on time after i.p. injection of 22.2 MBq ^{213}Bi-6H8 in comparison to untreated animals. 96% of the untreated animals developed large tumor masses and/or ascites within 6-8 weeks after tumor cell inoculation, whereas only 43% of the animals treated with 22.2 MBq of ^{213}Bi labelled antibody showed tumor development within 12 weeks after tumor cell inoculation. 57 % of the treated animals are still alive with no sign of tumor 20 weeks after tumor cell injection. The results show that the ^{213}Bi coupled to a mutation specific antibody binds selectively to tumor tissue or tumor cell clusters expressing the mutated E-Cadherin and therefore has a high potential for radioimmunotherapy of disseminated tumor growth after locoregional administration.

In the two projects of CSA 96202/96P04 and CSA 96114/96P03 carried out together with **INSERM / SUBATECH in Nantes** have been determined the optimal conditions for radio-induced cell death in multiple myeloma (MM) cell lines targeting with ^{213}Bi-labelled BB4 antibody within the scope of potential use for ex vivo bone marrow purging [5]. Complementary studies, using fresh bone marrow sample from patients, showed a high non-specific cell death rate when the cell concentration was high, whereas cell death decreased with a dilution.

The same study has been performed with another antibody, MA5 (anti-MUC 1 antigen), which is an alternative candidate for clinical alpha-immunotherapy study. The same labelling conditions have been validated with an efficient targeting of MM cells.

The aim of the study of analysis of biological mechanisms involved in alpha particle irradiation was to compare the effects of β^- irradiation from ^{131}I or ^{90}Y-labeled antibodies (currently used in radioimmunotherapy clinical studies) with those from an irradiation from ^{213}Bi-labeled antibodies. It has been demonstrated first that a much more efficient cell killing effect is present with alpha than with beta particles, and secondly that a G2M cell cycle arrest is induced by alpha and not by beta particles. This G2M arrest was correlated with the cell death rate in contrast with the accepted statement that this arrest was associated with the cell repair process.

Within the scope of future preclinical alpha-immunotherapy in mice bearing human carcinoma, the maximum tolerated dose in normal mice has been studied after intravenous injections of escalated activities of ^{213}Bi-labelled anti- carcinoembryonic antigen antibody (1.85 to 14.8 MBq). The preliminary results obtained in 5 mice per each activity level showed a high toxicity for the highest activity (14.8 MBq) with 100% mortality after 15 days. With the 7.4 MBq activity level 2 / 5 deaths were observed whereas no death was observed with the lowest activity level. In the three groups, high hematological toxicity was seen and was transient with the lowest level. ^{213}Bi toxicity in this mouse animal model was resulting similar toxicity than in studies of Heidelberg with bismuth-213 labelled anti-CD-20 antibody in healthy mice.

Targeted alpha particle therapy has now passed the initial proof of principle, the tests have successfully demonstrated that it is feasible to manufacture and reliably deliver monoclonal antibodies radiolabeled with alpha emitting atoms to human cancer cells in patients. Based on ongoing pre-clinical trials it is expected rapid expansion of this approach into a variety of other tumor types and possibly non-malignant conditions. Areas for rapid growth will include those tumor types for which established antigen antibody systems exist. This includes antibodies to lymphomas, prostate cancer, and possibly breast cancer and colon cancer. In addition, the use of alpha particles to kill virus-infected cells, such as HIV infected cells, may also be tested in humans. Significant obstacles to the widespread use of alpha particle therapy, such as the limited supply of isotope or inadequate chelates, appear to be largely overcome at this point. Continued efforts at producing large quantities of low-cost isotope will be a key to the most rapid expansion of this therapeutic modality [6].

1.4 Hospital Grade ^{213}Bi

During the reporting period hospital grade ^{213}Bi was produced and carefully separated at ITU for clinical studies. For biodistribution studies $^{205/206}Bi$ nuclides were used because of their longer half lives. The hospitals that were provided with such material are listed in Tab. 1.1.

Tab. 1.1 Overview of the ongoing trials and number of $^{225}Ac/^{213}Bi$ generators provided by ITU in 1999

Partner	Cancer type	mAb or peptide	$^{225}Ac/^{213}Bi$ generators
Memorial Sloan-Kettering Cancer Center, New York (USA)	Acute myelogious leukaemia (AML) Prostate cancer	HuM195 J591	2
INSERM, Nantes (F)	Multiple myeloma	B-B4, MA5	2
University of Heidelberg (D)	Non-Hodgkin's lymphoma (NHL)	CD-19, CD-20	1 + 2*
Clinic Hasselt, Univ. of Gent (B)	Non-Hodgkin's lymphoma (NHL)	CD-19, CD-20	-
University of Göttingen (D)	Colon cancer	CO17-IA	5
Kantonsspital Basel (CH)	Low grade glioma	somatostatin	2
Universitätsklinik München (D)	Stomach cancer	6H8	8

* $^{205/206}Bi$ for biodistribution studies

References:

[1] Sgouros G.; Ballangrund Å.M.; Jurcic J.G.; McDevitt M.R.; Humm J.L.; Erdi Y.E.; Mehta B.M.; Finn R.D.; Larson S.M.; Scheinberg D.A.; Pharmacokinetics and dosimetry of an α-particle emitter labeled antibody: ^{213}Bi-HUM195 (anti-CD33) in patients with leukemia.; Journal of Nuclear Medicine 40 (1999) 1935-1946.

[2] Behr T.M.; Béhé M.; Stabin M.G.; Angerstein C.; Mach R.; Hagemann L.; Apostolidis C.; Molinet R.; Koch L.; Rösch F.; Becker W. Radiopeptide therapy with cholecystokinin-B/gastrin receptor ligands: dose-limiting toxicity and therapeutic efficacy of Auger/conversion electron (^{111}In, ^{140}Nd) versus alpha (^{213}Bi) or conventional beta (^{90}Y, ^{153}Sm) emitters. Eur. J. Nucl. Med. 26 (1999), 1212.

[3] Behr T.M.; Sgouros G.; Stabin M.G.; Béhé M.; Angerstein C.; Blumenthal R.D.; Apostolidis C.; Molinet R.; Shareky R.M.; Koch L.; Goldenberg D.M.; Becker W. Studies on the red marrow dosimetry in radioimmuno-therapy: an experimental investigation of factors influencing the radiation-induced myelotoxicity in therapy with β-, Auger/Conversion eelectron-, or α-emitters. Clin. Cancer Res. 5 (1999), 3031-3043.

[4] Behr T.M.; Béhé M.; Stabin M.G.; Wehrmann E.; Apostolidis C.; Molinet R.; Strutz F.; Fayyazi A.; Wieland E.; Gratz S.; Koch L.; Goldenberg D.M.; Becker W.; High-linear energy transfer (LET) α *versus* low-LET β emitters in radioimmunotehrapy of solid tumors: therapeutic efficacy and dose-limiting toxicity of ^{213}Bi- *versus* ^{90}Y-labeled CO17-1A Fab' fragments in a human colonic cancer model. Cancer Res. 59 (1999), 2635-2643.

[5] Couturier O.; Faivre-Chauvet A.; Filippovich I.V.; Thedréz P.; Saï-Maurel C.; Bardiés M.; Mishra A.K.; Gauvrit M.; Blain G.; Apostolidis C.; Molinet R.; Abbe J.C.; Bateille R.; Wijdenes J.; Chatal J.F.; Cherel M.; Validation of ^{213}Bi-alpha radioimmunotherapy for multiple myeloma. Clinical Cancer Research 5 (10 Suppl.) (Oct 1999) 3165s-3170s.

[6] Scheinberg D.A.: Personal communication.

Contact (1.1-1.4): Christos Apostolidis
tel.: +49 7247 951 389 • fax: +49 7247 951 591
apostolidis@itu.fzk.de

2. Basic Actinide Research

Introduction

This project has as its main goal the understanding of the physics and chemistry of Actinide Systems. Our level of knowledge of actinide metals and compounds is far inferior to that of the rest of the periodic table, mainly because of the difficulty of handling transuranium materials, but also because of the inherent difficulty of understanding the behaviour of the 5f electrons. Their spatial extent and tendency to interact with electrons on ligand sites give actinide materials a complexity unique in the periodic table. Experiments and theory are performed with a view to improved understanding rather than applications. The long-term impact may be viewed in terms of a database for fuels development, for the treatment of waste, and as a contribution to our knowledge of materials in general.

First and foremost in our tasks is the preparation of materials, both in polycrystalline and single crystal form. A second major task is to develop measurement capabilities that can be used both to characterise the material and reveal interesting properties. Since many laboratories are now unable to work with transuranium elements (and sometimes not even with uranium), we have undertaken to construct a "User's laboratory" in Karlsruhe. Interested staff from universities and other institutes come to ITU and use these facilities. In particular, this last year we had a strong collaboration with scientists from Charles University, Prague.

Following the characterisation and initial measurements, usually at ITU, the further understanding of the basic properties often requires the use of other measuring techniques that are available only at large facilities (e.g. neutrons, synchrotron X-rays, and muons) or to perform specialised measurements at other laboratories. In most cases the samples must then leave ITU, and for this aspect we have developed a large number of different capsules. Encapsulation and transportation are then arranged by staff at ITU.

Another important aspect of the work is the training of students and postdoctoral candidates, and we have ~10 attached to the group at any one time. The students, in particular, are cement bonds between our work and that in universities, and help to sustain and spread the knowledge of actinide science. The progress of our work is documented in papers in the open literature, conference reports, seminars, and review chapters.

2.1 Preparation and Characterisation

The main effort of our programme is on the synthesis of new actinide compounds for solid state physics studies for both internal projects and collaborations with external organisations. This activity includes the preparation, characterisation and encapsulation of samples directly driven by "customers" requests for specified types of compounds, or in more systematic investigations of new phases. Our facilities permit the preparation of transuranium systems in various states from amorphous to single crystalline samples.

2.1.1 Preparation and characterisation of $Pu_{1-x}Am_x$ solid solutions

In the pure metals the transition from itinerant to localised 5f electrons occurs between Pu and Am, so that there is a special interest in alloys of these metals.

From a structural point of view, the ageing of Pu produces non-negligible amounts of Am which produces Pu-Am alloys. Samples of solid solutions offer the opportunity to study the effect of ageing on the properties of these materials.

Samples with various concentrations of Am were prepared by arc melting pure metals. For the investigation planned (electrical resistance, mechanical properties, ...) a special geometry of the samples was required. We prepared then "square" rods of 2x2 mm cross section and several cm length, and a special casting technique had to be developed. Fig. 2.1 shows a resulting rod.

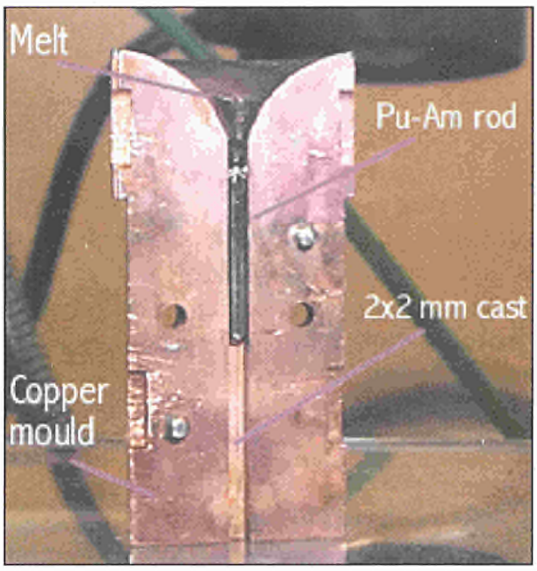

Fig. 2.1 Pu-Am rod obtained by direct arc melting casting.

The samples obtained were characterised by X-ray diffraction on powders. Although at ambient laboratory conditions metallic plutonium has a monoclinic phase and americium a hexagonal one, the solid solutions with low Am content are stabilised in a fcc cubic phase isostructural with δ-Pu and β-Am.

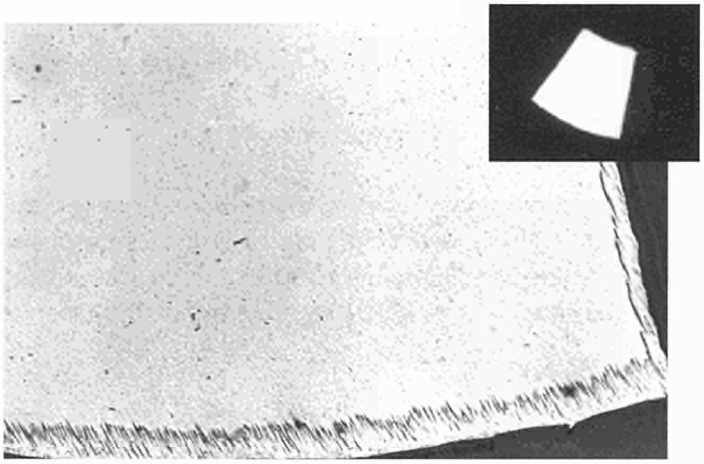

Fig. 2.2 Micrograph of a $Pu_{0.92}Am_{0.08}$ rod sample as cast. One can notice the difference of structure on the edges of the sample due to the high cooling rate. The autoradiography is presented in insert and shows the homogeneous distribution of Am in the sample.

Micrograph and microprobe analyses were also performed on the samples to ensure of their homogeneity and composition. An example of micrograph is given in Fig. 2.2.

Further investigations on these samples are under progress in collaboration with external organisations.

2.1.2 Chemical transport reaction crystal growth of mixed oxides

As presented in the highlights, single crystals of mixed oxides were grown by chemical transport reaction. This method, widely used to grow crystals of large number of refractory oxides, was successfully applied with $TeCl_4$ some years ago to grow pure UO_2 and NpO_2 and the process previously described in detail [1]. This technique, briefly illustrated in Fig. 2.3, was only recently applied to grow mixed oxides due to the increase of interest in these materials.

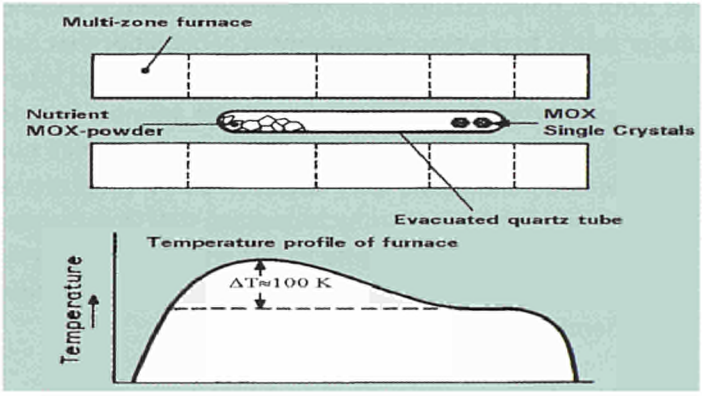

Fig. 2.3 Experimental set-up for the growth of actinide mixed oxide single crystals.

Well-formed single crystals could be obtained (see highlights) and characterised by X-ray powder diffraction (crushed single crystals) and 4-circle diffraction to ensure on the homogeneity and determine the lattice parameters. Systems studied and their lattice parameters are given in Tab. 2.1.

Tab. 2.1 Mixed oxides prepared and their lattice parameters ($^{\nabla}$ determined on single crystal, $^{\otimes}$ refined by Rietveld on powder).

Sample	Lattice parameter (pm)
$(U_{0.55}Np_{0.45})O_2$	544.52 $^{\nabla}$
$(U_{0.75}Np_{0.25})O_2$	546.09 $^{\nabla}$
$(U_{0.50}Pu_{0.50})O_2$	
Sample (1)	543.58 $^{\otimes}$
Sample (2)	543.70 $^{\otimes}$
$(U_{0.80}Pu_{0.20})O_2$	545.78 $^{\otimes}$
$(U_{0.75}Pu_{0.23}Am_{0.02})O_2$	545.63 $^{\otimes}$
$(U_{0.96}Pu0_{.02}Am_{0.02})O_2$	547.22 $^{\otimes}$
$(U_{0.75}Pu_{0.23}Np_{0.02})O_2$	545.63 $^{\otimes}$
PuO_2	540.30 $^{\otimes}$
UO_2	547.25 $^{\otimes}$

2.1.3 Investigation of Np-X (X = Si, Ge) binary phases

Intermetallic compounds R-T-X, where R is either a rare-earth or an actinide, T a transition metal and X a metalloid element have been intensively studied during the past twenty years. Many new compounds with different compositions and crystallising with distinct structure types have been discovered. Particular interest has been devoted to special ternary family of compositions such as RT_2X_2, R_2T_2X or $R_2T_3X_4$. As a result of the intensive experimental and theoretical investigations it was established that their electronic properties are mainly governed by the strength of the f-(spd) hybridisation, i.e. the interaction of the f electrons with the conduction electrons. However many conflicting results were reported on the same compound due to the fact that these physical properties are sensitive to history of the sample like heat treatment, homogeneity or presence of impurities. To establish the intrinsic physical properties, the first step is to determine their relation with the neighbouring phases, and to evaluate their homogeneity range. As a contribution to this subject the correct determination of the binary phase diagram itself is a prerequisite, and recently, binary uranium phase diagram, like U-Si [2], U-Ge [3] and U-Sn [4] were reported, showing interesting properties ranging from paramagnetism, long range magnetic order and superconductivity. Taking account of these new results, a look in the literature show that the corresponding binary phase diagram with neptunium and plutonium are not well characterised. Therefore we have started to investigate the corresponding binary phase diagram, and the preliminary crystallographic results are shown in Tab. 2.2.

Tab. 2.2 Np-Si and Np-Ge binary phases.

Compound	Structure Type	Space Group	a (pm)	c (pm)
$NpSi_3$	$AuCu_3$	Pm3m		
$NpSi_{1.88}$	$ThSi_2$	$I4_1/amd$	397.0	1370.0
Np_3Si_5	AlB_2	P6/mmm	384.46	408.93
Np_3Si_2	U_3Si_2	P4/mbm	742.5	393.0
$NpGe_3$	$AuCu_3$	Pm3m	421.4	
Np_3Ge_5	$ThSi_2$	$I4_1/amd$	408.06	1390.96
Np_3Ge_5	AlB_2	P6/mmm	396.6	416.8
NpGe	USi	I4/mmm	1089.64	2538.70
Np_5Ge_3	W_5Si_3	I4/mcm	1148.4(2)	554.7(1)
Np_3Ge	$AuCu_3$	Pm3m		

The new phases, not reported in the literature, are in italic. The lattice parameters of $NpSi_3$ and Np_3Ge were not reported.

2.1.4 Encapsulation for Collaborative Studies

Compounds encapsulated for various physical properties measurements performed in house or in external institutions in collaborative studies are listed in Tab. 2.3.

References

[1] TUSR 25, ITU-Progress Report Jan-Jun. 1978, EUR 7459 EN, (1978) p. 86-88

[2] K. Remschnig, T. LeBihan, H. Noël, P. Rogl, Journal of Solid State Chemistry 97 (1992) 391

[3] P. Boulet, A. Daoudi, M. Potel, H. Noël, G.M. Gross, G. André, F. Bourrée, Journal of Alloys and Compounds 247 (1997) 104

[4] P. Boulet and H. Noël, Solid State Communications 107, n°3 (1998) 135

Contact (2.1): Franck Wastin • tel.: +49 7247 951 387
fax: +49 7247 951 599 • wastin@itu.fzk.de

Tab. 2.3 Samples prepared, characterised and encapsulated in 1999 for the indicated measurements.

Measurements	Laboratories	Compounds	Form
Resistivity Magneto-Resistance	ITU-Karlsruhe	$Np_2Tc_3Si_4$, $NpNi_2B_2C$, $(U_{0.5}Np_{0.5})_2Rh_2Sn$, $(U_{0.75}Np_{0.25})_2Rh_2Sn$, $(U_{0.25}Np_{0.75})_2Rh_2Sn$, $U_{0.95}Np_{0.05}Ru_2Si_2$, $Np_2Tc_3Ge_4$, $Np_2Nb_3Ge_4$	AcM
Mössbauer Spectroscopy	ITU-Karlsruhe	$Np(As_{0.8}Se_{0.2})$, $(Np_{0.9}U_{0.1})_4Ru_7Ge_6$, Np_2Ir_2In, $(U_{0.1}Np_{0.9})Ni_2Al_3$, $(U_{0.55}Np_{0.45})O_2$, $(U_{0.75}Np_{0.25})O_2$ Np_3Si_5, $(U_{0.25}Np_{0.75})_2Rh_2Sn$, $(U_{0.5}Np_{0.5})_2Rh_2Sn$ $(U_{0.75}Np_{0.25})_2Rh_2Sn$, Np_3Ge_5, $(U_{0.96}Pu_{0.02}Am_{0.02})O_2$	AcM & G-SC
Neutron Scattering	ILL-Grenoble Argonne Nat. Lab.	UCu_5Al, U_2Ni_2Sn, U_2Pt_2Sn, UPtGe ThO_2, $U_{0.4}Th_{0.6}O_2$	SC P
Magnetisation	ITU-Karlsruhe	$Np_2Tc_3Si_4$, $Np_2Mo_3Si_4$, $Np_2Tc_3Ge_4$	AcM
Magnetic X-ray Scattering	ESRF-Grenoble BNL-Brookaven	UPtGe, U_2Ni_2In, UGa_3, UNi_2Al_3 $^{242}PuSb$, $Pu_xY_{1-x}Sb$ (x= 0.4, 0.6), $Pu_xU_{1-x}Sb$ (x= 0.25, 0.5, 0.75)	SC SC
High-Pressure X-ray Diffraction	ITU-Karlsruhe	$ThMn_2$, $ThAl_2$	P
High-Pressure Resistivity	ITU-Karlsruhe	PuSe	SC
XPS-UPS	ITU-Karlsruhe	PuSe, PuS	SC

AcM = arc melting SC = single crystal P = powders, polycrystalline sample G-SC = grinding single crystals

2.2 Solid-state Physics Studies

Since many laboratories are now unable to work with transuranium elements (and sometimes not even with uranium), we have undertaken to develop in-house facilities for solid-state studies on transuranium compounds. These facilities are open to external users in the frame of a "User's laboratory". This complements also the efforts of preparation and characterisation in allowing a first estimation of bulk physical properties of new materials. Mainly Mössbauer spectroscopy experiments, transport (resistivity) and magnetic measurements at cryogenic or elevated temperatures (from 1.5 K to 800 K) are performed.

Some of the results obtained in 1999 are described in the following sections.

2.2.1 Magnetic Studies

The investigation of the magnetic properties of $Pu_xU_{1-x}Sb$ single crystals, started in 1998 [1], continued in 1999 with the study of new compositions and the development of SQUID-measurements at elevated temperatures.

We investigated the magnetisation and magnetic susceptibility of single crystals of the pseudobinary system $Pu_xU_{1-x}Sb$ with x = 0.25, 0.50 and 0.75 at low temperatures with a commercial SQUID magnetometer. In the samples with low plutonium concentration the antiferromagnetism already known from USb remains stable. However, in the case of $Pu_{0.75}U_{0.25}Sb$ another phase transition is present at 55 K.

The paramagnetic susceptibility follows the Curie-Weiss law. The average effective magnetic moment changes almost

linearly with concentration between the values for USb and PuSb. To measure the susceptibility up to 800 K we developed sample holders and studied their magnetism. The sample holders consist of two quartz rods within a tube with an inner diameter of 2 mm. The samples can be put between the two rods and the sample space can be evacuated, Fig. 2.4.

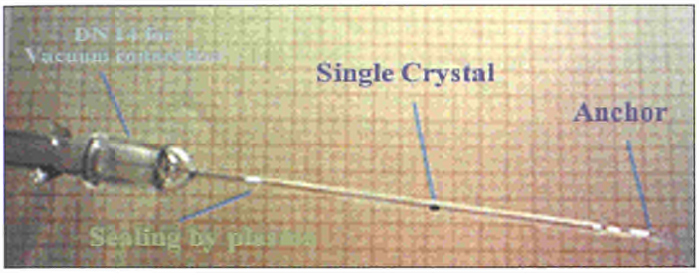

Fig. 2.4 Sample holder for high temperature susceptibility studies on radioactive compounds.

2.2.2 Mössbauer Studies

Using the ^{237}Np we investigated a number of interesting actinide compounds. There are mainly two ways to classify our results: "Horizontally", if one considers the kind of compounds and the family it belongs to – NpX, Np_2T_2X, $Np_4T_7X_6$, $Np_2T_3X_4$ – and "vertically", if one considers the stage of investigations - preliminary measurements, intensive studies or complementary experiments. In this paragraph we will deal with the "horizontal" classification and briefly review the main compounds studied in 1999 (results are summarised in Tab. 2.4). In the next paragraph, the "vertical" approach has been chosen with the example of the $Np_2T_3X_4$ series, first investigated last year and further early this year by Mössbauer spectroscopy and then completed with magnetisation and resistivity measurements.

– Np_2Ir_2In

In the frame of the general investigation of magnetic and electronic properties of the large isostructural An_2T_2X (An=U,Np,Pu,Am;T=transition metal;X=In,Sn) family which allows in particular the observation of general trends, and the comparison of similar systems containing different actinide elements, we measured Np_2Ir_2In in order to complete the systematic Mössbauer study of so far available Np_2T_2X compounds [2]. It is worth mentioning that the fitting of the 4.2 K spectrum requires 5 distinct Np sites.

- $(Np_xU_{1-x})_4Ru_7Ge_6$ (x=0.995, 0.95, 0.9)

We have undertaken Mössbauer measurements in these solid solutions in order to tune the competing RKKY and Kondo interactions and investigate the intermediate systems between the ferromagnetic Kondo lattice URu_7Ge_6 ($T_C \approx 12K$) and the possibly heavy fermion $Np_4Ru_7Ge_6$ which does not order magnetically but is close to a magnetic instability [3]. Other values of x will also be investigated.

Tab. 2.4 Local magnetic moment μ_{Np}, isomer shift δ_{IS}, quadrupolar interaction parameter e^2qQ, line width W, relative intensity $I_{relative}$, magnetic ordering temperature T_{ord} and asymmetry parameter at 4.2 K and above T_{ord}, for Np_2T_2X, NpX, $Np_4T_7X_6$ and NpT_2X_3 compounds and solid solutions investigated by Mössbauer spectroscopy. Isomer shifts are given relative to the standard absorber $NpAl_2$. (a) Only 4.2 K Mössbauer investigations were required in this collaborative measurement. (b) No ordering occurs in these compounds, then the values given for $T > T_{ord}$ are those obtained at 100 K.

	T = 4.2K					T_{ord}	T > T_{ord}				
Compound	μ_{Np} (μ_B)	δ_{IS} (mm/s)	e^2qQ (mm/s)	W (mm/s)	$I_{relative}$	(K)	δ_{IS} (mm/s)	e^2qQ (mm/s)	W (mm/s)	$I_{relative}$	η
Np_2Ir_2In	0.93(1) 0.81(1) 0.68(1) 0.56(2) 0.30(2)	−15.0(1)	+10(2) +6(1) −7(1) −25(4) −28(7)	5.3(2)	18% 37% 34% 6% 5%	30	−14.5(1)	31.6(2)	3.6(2)	100%	0.49(5)
$NpAs_{0.8}Se_{0.2}$	2.51(1)	17.8(8)	−30(1)	4.9(2)	100%	(a)	(a)	(a)	(a)	(a)	0
$(Np_{0.995}U_{0.005})_4Ru_7Ge_6$	0	-8.4(4)	70.4.(3)	2.7(2)	100%	(b)	−8.3(4)	69.7(3)	2.8(2)	100%	0
$(Np_{0.95}U_{0.05})_4Ru_7Ge_6$	0	-8.5(4)	70.6.(3)	2.6(2)	100%	(b)	−8.2(4)	69.6(3)	2.7(2)	100%	0
$(Np_{0.9}U_{0.1})_4Ru_7Ge_6$	0	-8.3(4)	70.1.(3)	2.7(2)	100%	(b)	−8.3(4)	69.3(3)	2.8(2)	100%	0
$Np_{0.9}U_{0.1}Ni_2Al_3$	1.20(2) 0.90(2) 0.44(2)	0.9(3)	35.7(4)	9.1(3)	39% 41% 20%	18	−0.2(2)	37.8(2)	3.1(1)	100%	0

2.2.3 Electronic and magnetic properties of $Np_2T_3X_4$ compounds

We report here on the first electronic and magnetic measurements in the $Np_2T_3X_4$ series. Three compounds of this series, $Np_2Mo_3Si_4$, $Np_2Tc_3Si_4$ and $Np_2Tc_3Ge_4$, were investigated by Mössbauer spectroscopy using the ^{237}Np resonance. $Np_2Mo_3Si_4$ crystallises in the monoclinic $U_2Mo_3Si_4$-type structure (space group $P2_1/c$), $Np_2Tc_3Si_4$ in the $Np_2Tc_3Si_4$-type structure (space group $P2_1/c$) and $Np_2Tc_3Ge_4$ in the orthorhombic $Np_2Tc_3Ge_4$-type structure (space group Pbcn) . These structures are very similar to each other and it is worth noticing that there is only one crystallographic Np site with almost the same environment in all cases [4].

Mössbauer investigations as reported last year, show ordering temperatures of 47 K and 19 K for $Np_2Mo_3Si_4$ and $Np_2Tc_3Si_4$, respectively, and a rather complex situation for $Np_2Tc_3Ge_4$, with possible ordering around 15 K.

These results were confirmed by resistivity measurements which show for $Np_2Mo_3Si_4$ the occurrence of magnetic ordering around 39 K and for $Np_2Tc_3Ge_4$ display a broad maximum around 30K and a slight slope break around 15 K, corresponding to the ordering temperature deduced from Mössbauer measurements.
The study of these compounds was complemented by magnetic measurements with our SQUID apparatus. $Np_2Mo_3Si_4$ shows a ferrimagnetic transition at $T_C \approx 38$ K in agreement with the resistivity data and an antiferromagnetic-like transition at $T_N \approx 47$ K – i.e. the temperature at which the onset of magnetic ordering is observed in Mössbauer spectra. The moment saturates around 0.42 μ_B in magnetisation curves and a modified Curie-Weiss fit of the susceptibility yields $\theta_p \approx 30$ K, $\mu_{eff} \approx 2.81$ μ_B and $\chi_0 \approx 0.00112$ emu/mole.

$Np_2Tc_3Si_4$ exhibits an antiferromagnetic-like transition at $T_N \approx 19$ K, remaining antiferromagnetic up to 7 T. The Curie-Weiss parameters are $\theta_p \approx -60$ K, $\mu_{eff} \approx 2.51$ μ_B and $\chi_0 \approx 0.00127$ emu/mole.

No occurrence of magnetic order could be inferred from the magnetisation and susceptibility behaviour of $Np_2Tc_3Ge_4$, which may be explained by the fact that the ordered contribution observed in the Mössbauer spectra of this compound is dominantly paramagnetic. The modified Curie-Weiss fit yields $\theta_p \approx -80$ K, $\mu_{eff} \approx 2.88$ μ_B and $\chi_0 \approx 0.00168$ emu/mole.

It should also be mentioned that the very high sensitivity of the SQUID measurements allowed the identification of minor impurities phases observed on the susceptibility plots at low field (see (a) and (b) on Fig. 2.5) not seen by other techniques but they do not complicate the interpretation of the data.
As a conclusion, $Np_2Mo_3Si_4$, $Np_2Tc_3Si_4$ and $Np_2Tc_3Ge_4$ exhibit interesting magnetic properties. From Mössbauer experiments, it is inferred that all three compounds of this new-investigated series order into modulated magnetic structures with a surprising dominant zero field component in $Np_2Tc_3Ge_4$. The resistivity and magnetisation measurements suggest the occurrence of two magnetic phase transitions in $Np_2Mo_3Si_4$ and one in $Np_2Tc_3Si_4$ but no clear hint of intrinsic ordering in $Np_2Tc_3Ge_4$. For this last compound, further studies are in progress to elucidate this apparent contradiction.

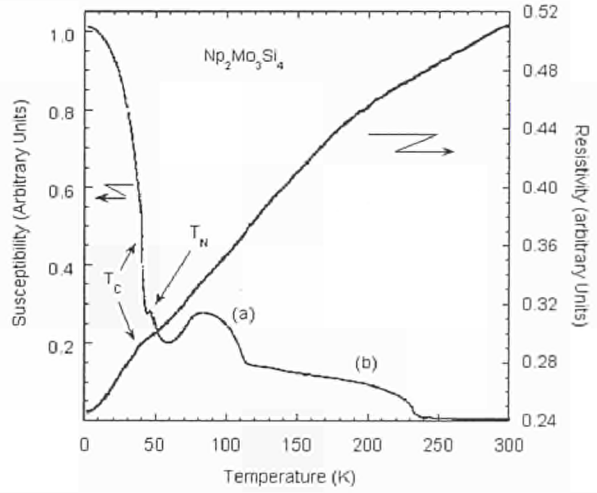

Fig. 2.5 Magnetic susceptibility and resistivity of $Np_2Mo_3Si_4$. Antiferromagnetic (T_N and ferrimagnetic T_C) ordering temperatures are shown. The (a) and (b) contributions are due to impurities ordering at higher temperatures.

References

[1] TUAR-98, p 52
[2] L.C.J. Pereira, F. Wastin, J.M. Winand, B. Kanellakopoulos, J. Rebizant, J.C. Spirlet, M. Almeida, J. Solid State Chem. 134 (1997) 138
[3] C. Jeandey, J.P. Sanchez, J.L. Oddou, J. Rebizant, J.C. Spirlet, F. Wastin, J. Phys.: Condens. Matter 8 (1996) 4259-4268
[4] F. Wastin, J. Rebizant, J.P. Sanchez, A. Blaise, J. Goffart, J.C. Spirlet, C.T. Walker, J. Fuger, J. Alloys Comp. 210 (1994) 83-89

Contact (2.2): Jean Rebizant • tel.: +49 7247 951 228
fax: +49 7247 951 599 • rebizant@itu.fzk.de

2.3 Surface Science Studies

The main issue of actinide surface science is to investigate the electronic structure and surface reactivity of actinides and, on a broader scale, nuclear systems. In the study of the electronic structure we concentrate on the behaviour of the 5f states in highly correlated systems, and their extent of localisation. Also the role of surface and interfaces in 5f delocalisation is addressed. Assessment of the reactivity of actinide surfaces is particularly important, because the surface is the contact between the solid and the environment, and critical properties of nuclear systems such as their resistance to corrosion directly depend on surface reactions. In this context we have to consider that nuclear systems are generally very complex, inaccessible to mechanistic studies, while any long term prediction of chemical behaviour should be based on an understanding of the reactions involved. To bridge the gap between simple model and complex real world systems, thin film techniques are especially well suited, because they allow us to produce well characterised systems of varying complexity.

In 1999 we deposited thin films of PuSb, UGa_2 and UGa_3 and studied their surface composition and electronic structure. Also thin films of UO_2 were deposited and their surface reactivity was assessed by electrochemical methods. First attempts to dope Cs into UO_2 were successful. Finally, we used reactive sputtering to produce films of U nitride (UN) and oxynitrides, and studied their chemical reactivity by adsorption studies.

2.3.1 Study of the electronic structure of thin films of PuSb

This work complements the previous study of PuSe [1]. Although PuSe and PuSb belong to a family of NaCl type PuX compounds (X = Chalcogenide or Pnictide), they differ in many of their physical properties. The magnetic properties of PuSb point to a localised 5f state, weakly hybridised to conduction band states. For PuSe, on the other hand, the high electronic specific heat points to a high density of (quasiparticle) states (DOS) at the Fermi-level, and photoemission confirms this [1]. Our goal was to study the contrast between the two by photoemission [2].

Fig. 2.6 shows the 4f core-level spectra of PuSe and PuSb compared to data obtained on bulk α-Pu. The positions of the $4f_{5/2}$ and $4f_{7/2}$ correspond to the final state with the 4f photohole screened by 5f electrons (so-called good screening), implying thus their itinerancy [3]. The satellites on the high binding energy (BE) side correspond to the final state with the 4f photohole screened by non-f conduction band electrons (poor screening). In case of 5f localisation, this is the only screening channel. Relatively weak poorly screened satellites in α-Pu reflect a situation found, for example, in most U intermetallic compounds with undoubtedly band-like character of the 5f electrons states, and is for α-Pu fully corroborated by electronic structure calculations. PuSe shows an increase of the poorly screened peak, while in PuSb it replaces completely the well screened feature. This indicates the transition of the 5f states from delocalised (α-Pu) to localised (PuSb) behaviour.

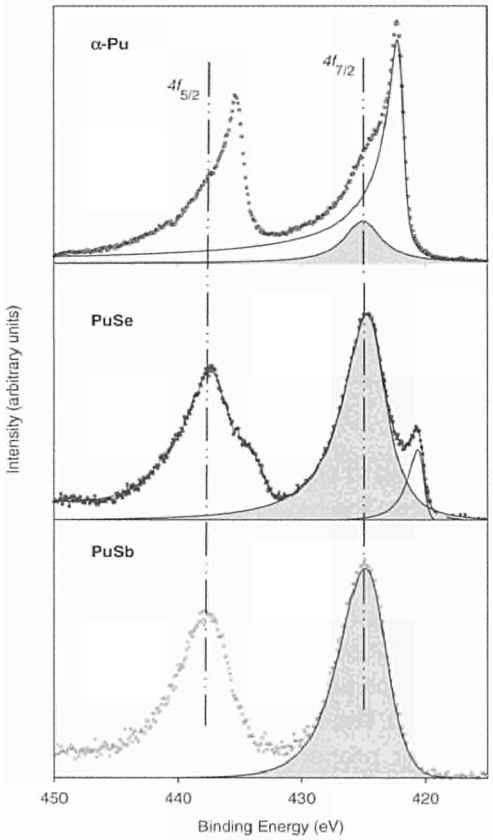

Fig. 2.6 Pu4f spectra of α-Pu, PuSe and PuSb.

Fig. 2.7 compares valence band spectra of α-Pu, PuSe and PuSb. Hell spectra of α-Pu show a maximum at the Fermi-level, also found in the valence band spectra of the other early actinide pure elements (U and Np). It is attributed to the band-like response of delocalised 5f states. In PuSe there is still a maximum at the Fermi-level, but additional 5f features appear at high BE. A temperature dependent study showed [4], that the three-peaks at low BE (including the

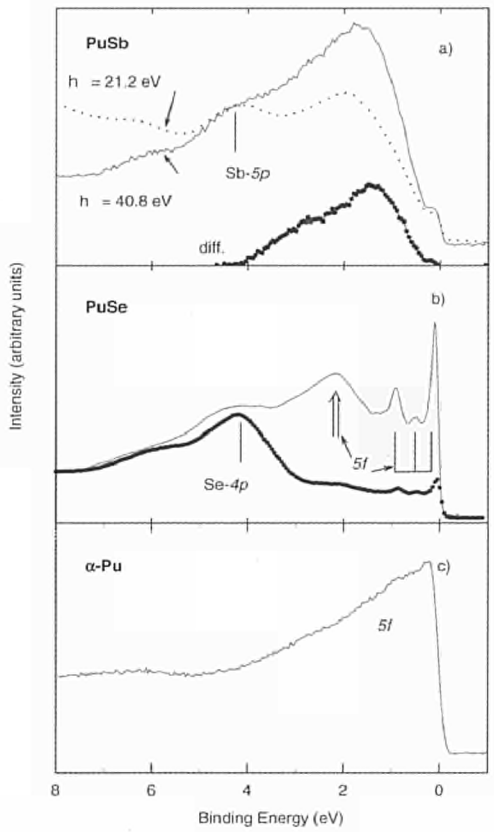

Fig. 2.7 Hell Valence Band spectra of α-Pu, PuSe and PuSb.

peak at E_F), belong to one same final state, attributed the delocalised 5f states. The broad peak at 2 eV BE is attributed to the localised 5f peak. Valence band spectra are thus interpreted along the same lines as the core level data, i.e. there is a well (f) screened response at low BE, and a poorly (non-f) screened response at high BE. In PuSb, the three peak structure is completely missing and the intensity at E_F is strongly reduced. The remaining intensity is in agreement with the metallic properties of PuSb and should be attributed, at least partially, to Pu-6d states.

Both core-level and valence-level spectroscopies show a transition from delocalised to localised 5f behaviour, when going from α-Pu to PuSe and PuSb. In general the valence band spectra show a more intense well screened peak, than the core level, pointing to a more delocalised 5f response. This may be understood when considering that a photohole in the core-level is more strongly felt by the valence electrons, than a hole in the valence band, and the stronger local potential should result in a more pronounced 5f localisation. Thus final state localisation effects should be more pronounced for core-level lines.

2.3.2 Deposition of thin films of UO_2 and study of their electrochemistry in contact with water

The motivation for this work is the assessment of the long term storage behaviour of nuclear waste in contact with ground water. In many cases the waste consists of a UO_2 matrix, loaded with various fission products, and an understanding of the dissolution mechanisms is important. For this we simulate the waste by UO_2 films with varying degree of complexity, whose dissolution behaviour is studied by electrochemistry. We started with the simplest possible system, i.e. pure UO_2. UO_2 films have been prepared by reactive sputter deposition, and their electrochemical properties are compared to pure bulk single crystals. In future work, UO_2 films containing fission products will be prepared and studied electrochemically.

In a first step, we determined the conditions for preparation of stoichiometric UO_2 films. We studied the oxygen composition of the films and the oxidation state of U as a function of the oxygen pressure during the deposition process. Fig.

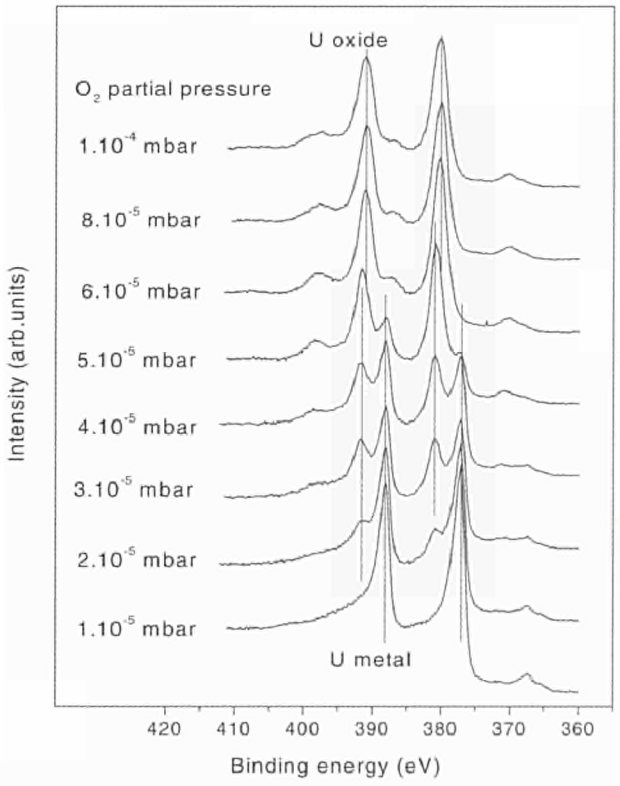

Fig. 2.8 U4f spectra of U films deposited at increasing O_2 partial pressures.

2.8 shows U4f spectra of U-O films, deposited at different O_2 partial pressures. With increasing O_2 pressure, the U metal lines are replaced by UO_2 oxide lines, identified by their characteristic higher binding energies. As long as U metal is present, only substoichiometric UO_{2-x} is formed. When the metal disappears (at 6 10^{-5} Torr O_2), the UO_{2-x} is further oxidised to UO_{2+x}, as shown by a slight shift of the oxide line to lower binding energy. When deposited as pure U-O films, hyperstoichiometric UO_{2+x} ($x \cong 0.1$) is the highest possible oxidation state we can reach under ultra high vacuum conditions. This changes drastically when the oxide films are doped with Cs: oxidation states up to U^{6+}, corresponding to UO_3, have been observed in a first set of experiments. This would have a strong influence on the dissolution behaviour of the U oxide, and will be investigated in detail in the near future.

In the electrochemistry experiments the films are exposed to water solutions characteristic of the various ground water systems. pH, carbonate and chloride concentrations, etc. are varied and their influence on the dissolution process is assessed. First studies of thin UO_2 films were done by electrochemical impedance spectroscopy (EIS). The immersed sample is brought to a positive electrical potential which favours oxidative dissolution of the surface layers. The dissolution process is measured by superimposing a small ac potential and measuring the ac current, i.e. the impedance of the system. This gives information on the dissolution reaction and the diffusion of surface species into solution [5]. Fig. 2.9 shows the impedance spectra (imaginary versus real part) of a UO_2 thin film electrode in KCl 0.1M at various pH values.

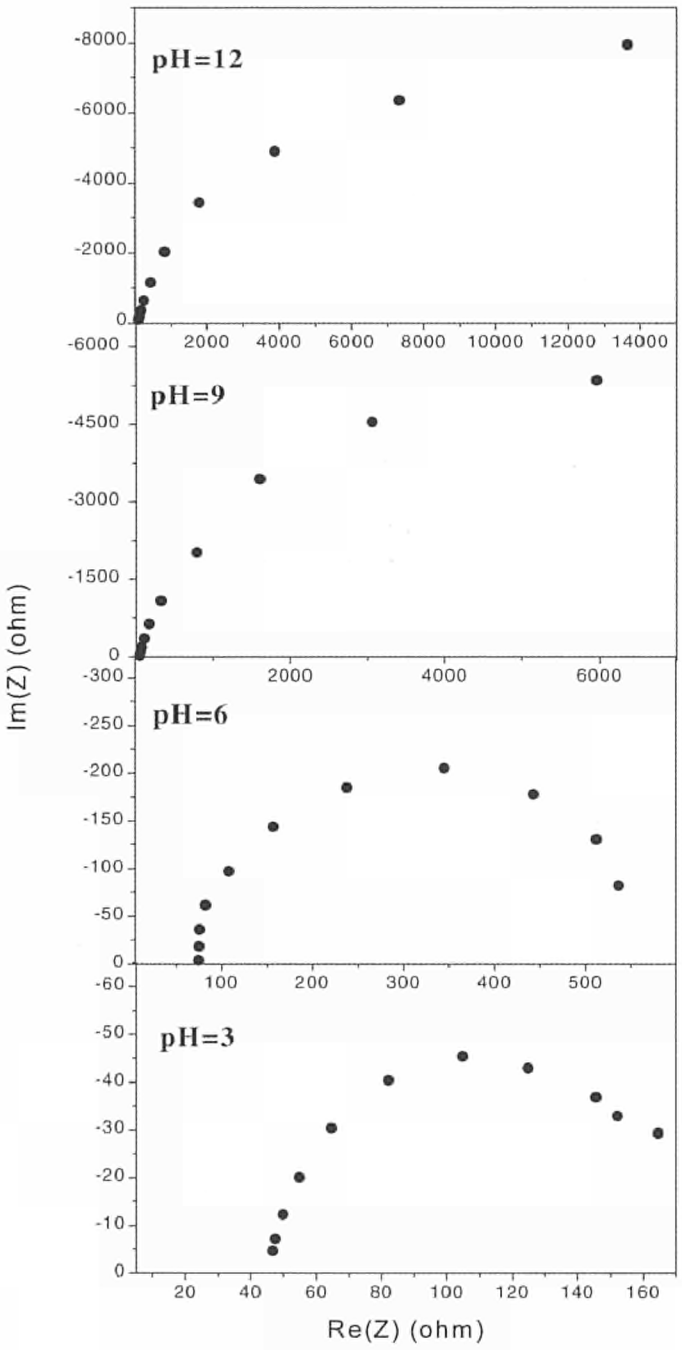

Fig. 2.9 Electrochemical Impedance Spectra of UO_2 films at different pH values. The curves form semicircles, whose diameters directly depend on the charge transfer resistance, i.e. the rate of the anodic oxidation reaction. A lower diameter corresponds to a higher dissolution rate. This takes place as the solutions become more acidic, which is in agreement with the dissolution studies of UO_2 pellets [6].

2.3.3 Study of thin films of UN

Studies of thin films of UN are motivated by the interesting electronic structure of the various nitrides and oxynitrides, and by their possible use as advanced fuels. Previous studies in literature, performed on bulk UN compounds, were only partly successful and reliable in describing formation of UN and its reactivity towards oxygen. In particular, preparation of clean stoichiometric UN surfaces was difficult. We used reactive sputtering of metallic U, in presence of a partial pressure of N_2, to produce thin films of UN_x. Our films were superior in purity to the bulk samples. We then exposed these films to O_2 and studied the formation of the different oxides and nitrides during the reaction.

First we studied the formation of UN at room temperature as a function of N_2 partial pressure (Fig. 2.10), similar to the UO_2 films discussed above. Formation of a nitride is shown by the growth of the N1s lines, and by the replacement of the U4f lines of metallic uranium by lines at higher BE. The ratio of the N1s/U4f intensities saturates between 5 10^{-5} Torr and 5 10^{-4} Torr, and stays constant over two orders of magnitude, which is an indication for the formation of a stable compound. Quantitative analysis of the ratio indicates formation of $UN_{0.99\pm0.05}$.

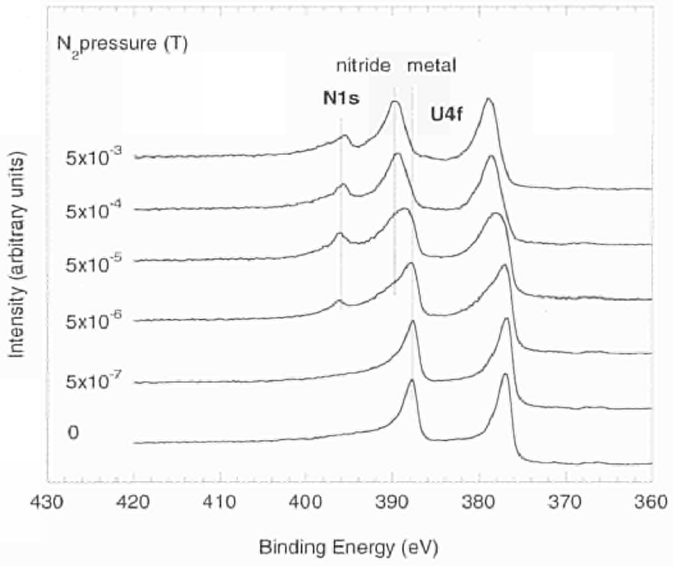

Fig. 2.10 U4f spectra of U films deposited at increasing N_2 partial pressures.

However this stability of UN seems to be closely related to the deposition temperature. Films deposited at higher temperature (573 K) show a significantly increased nitrogen content when compared to the films deposited at room temperature. This is seen in Fig. 2.11 by the growth of the N1s intensity, and by the shift of the U4f to higher binding energy, both pointing to the formation of a higher nitrides, probably U_2N_3. All nitride films showed a high reactivity towards oxygen, which also explains the difficulties in preparing clean UN bulk compound surfaces. We found indications that the early oxidation, even at room temperature, does not proceed via formation of UO_2 but rather a UO surface species. This would correspond to the formation of a surface oxycarbide UO_xN_y, which should still have metallic properties. Valence band studies are planned for next year to study this in more detail.

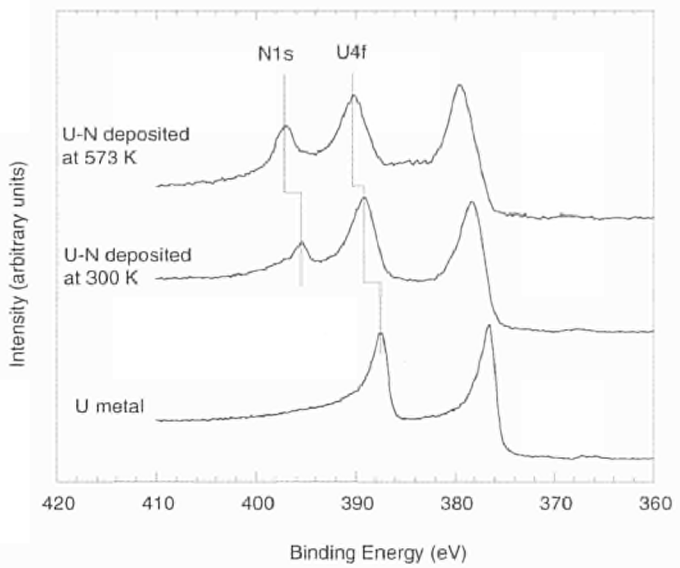

Fig. 2.11 U4f spectra of U-N films deposited at 300 and 473 K are compared to a U film.

References

[1] TUAR-98, p. 53

[2] T. Gouder, F. Wastin, J. Rebizant, L. Havela, Phys. Rev. Letts. 84 (2000), 3378

[3] Y. Baer, in 'Handbook on the Physics and Chemistry of Rare Earths', eds. A.J. Freeman and G.H. Lander, North-Holland, Amsterdam, Vol. 1 (1984) p. 271

[4] T. Gouder, L. Havela, F. Wastin, Journées des Actinides 99, Luso, Portugal

[5] G. Marx, J. Engelhardt, F: Feldmaier, M. Laske, Radiochimica Acta 74 (1996) 181-184

[6] D.W. Shoesmith, S. Sunder, AECL Report 10488, Pinawa, Canada (1991)

Contact (2.3): Thomas Gouder • tel.: +49 7247 951 243
fax: +49 7247 951 599 • gouder@itu.fzk.de

2.4 High-Pressure Studies

2.4.1 High-pressure resistivity study on the Pu monochalcogenides

Last year, we reported on a high-pressure resistivity study on PuTe up to 24.3 GPa (TUAR-98, p. 14-15). This study revealed striking features in the transport properties of both

the NaCl (low-pressure) and CsCl (high-pressure) structural phases. This year we performed a careful measurement of the low-temperature resistivity of PuTe up to around 10 GPa. This allowed us to propose a model for the temperature variation of the resistivity in the NaCl phase. We also present preliminary results on PuS for which there is no structural transition.

In Fig. 2.12, we show the temperature variation of the resistance R of PuS up to 9.5 GPa. At 0.56 GPa, the temperature variation of R agrees well with the ambient pressure result [1]. With the application of pressure, we observe an anomalous enhancement of the low-temperature resistance. This feature is very similar to the behaviour that we previously observed in PuTe [2] (see inset of Fig. 2.12). The temperature variation of R in the Pu monochalcogenides suggests an activated behaviour i.e. the existence of a gap in the density of states causing the resistivity to increase at low temperature. Under pressure, conduction and valence bands normally broaden, which should thereby decrease any semiconducting gap. The opposite behaviour observed in PuTe and PuS suggests that the low-temperature upturn may have another origin.

To extract the low-temperature activation energy from our data we propose the following model where the low-temperature conductivity σ is composed of 2 contributions

$$\rho_{BT}^{-1} = \sigma_{BT} = \sigma_{0BT} + \sigma_{VRH} = \sigma_{0BT} + \sigma_{1BT} \times exp - \left(\frac{T_0}{T}\right)^{1/4}$$

σ_0 is temperature independent and accounts for the small density of states predicted by the semimetal description and the γ value [3,4]. σ_{VRH} is the Mott's variable-range hopping term. In our model, we suggest that the conductivity at low-temperature is caused by hopping conduction between localised impurity states and mediated by phonons. Mott first addressed this mechanism for non-interacting electrons in glasses containing transition metal ions [5]. We can well fit our data to this law over a broad temperature range (1.5-100 K) (Fig. 2.13). The pressure dependence of T_0 is shown in the inset of Fig. 2.13 as well as for PuS for which we used the same model. In PuTe, k_BT_0 increases from 22 meV up to 110 meV at 5 GPa and is nearly constant up to 10.7 GPa. In the discussion of the variation of T_0 we have to take into account two parameters which are the density of states and the localisation length of the impurities.
In PuS, T_0 is rather constant (10 meV) and tends to decrease. At 9.5 GPa, this description is no longer valid for this compound.

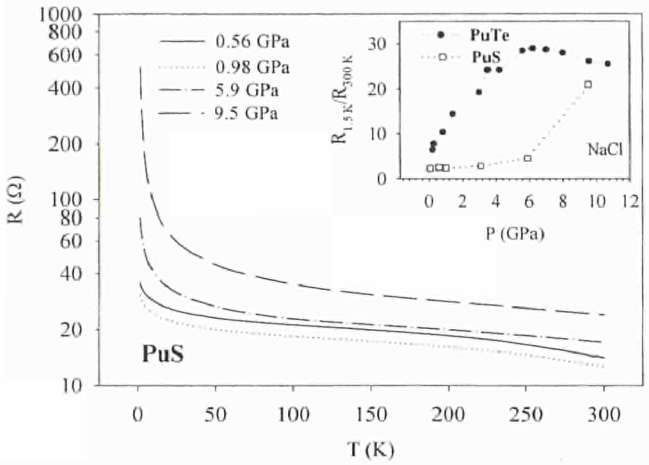

Fig. 2.12 Temperature variation of the resistance R of PuS between 1.5 K and 300 K up to 9.5 GPa. The inset shows the normalised resistance $R_{1.5K}/R3_{00K}$ for PuS and PuTe.

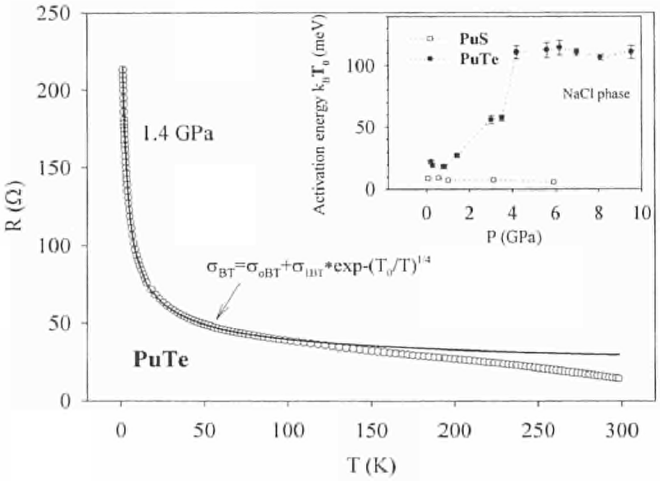

Fig. 2.13 Variable Range Hopping fit between 1.5 K and 100 K for PuTe. The inset shows the extracted activation energy T_0 for PuS and PuTe.

References

[1] J.M. Fournier, E. Pleska, J. Chiapusio, J. Rossat-Mignot, J. Rebizant, J.C. Spirlet, O. Vogt, Physica 163B (1990) 493-495.
E. Pleska, PhD Thesis, Université de Grenoble (1990)

[2] V. Ichas, J. Rebizant, J.C. Spirlet, J.C. Griveau (to be published)

[3] P.M. Oppeneer, T. Kraft, M.S.S. Brooks, to be published in Phys. Rev. B

[4] G.R. Stewart, R.G. Haire, J.C. Spirlet, J. Rebizant, J. Alloys and Comp. 177 (1991) 167

[5] N.F. Mott, J. Non-Cryst. Solids 1 (1968) 1

2.4.2 Structural studies under pressure

2.4.2.1 US, $U_{0.4}La_{0.6}S$, LaS

These compounds form part of our detailed investigation into the properties of the US/LaS phase diagram. We have performed a number of experiments using helium, argon and silicone oil as the pressure transmitting media at the ID30 high-pressure beamline of the ESRF synchrotron in Grenoble France. The pure LaS sample has not been studied under pressure before and shows two phase transitions from the initial fcc (B1) to a rhombohedral distorted structure at around 4 GPa and eventually to a bcc (B2) phase at between 25 and 28 GPa. The transition to the B2 phase was accompanied by a 9.5% volume decrease. The $U_{0.4}La_{0.6}S$ compound showed the same sequence of phase transitions as LaS with the B2 phase appearing sluggishly between 33 and 45 GPa. The volume decrease was also identical to that of LaS at 9.5%. Experiments were also performed on pure US using He as the pressure transmitting medium as well as in a Cornell type megabar cell to understand the exact nature of the rhombohedral distortion and to identify a possible very high pressure phase transition. These experiments showed that the distortion is much more pronounced for US than for LaS but also depends strongly on the non-hydrostatic stresses related to the choice of pressure transmitting medium. A phase transition was identified for US at above 80 GPa but the structure of this phase has yet to be resolved.

A partial summary of the results on these samples can be seen in the pressure-volume diagram shown in Fig. 2.14.

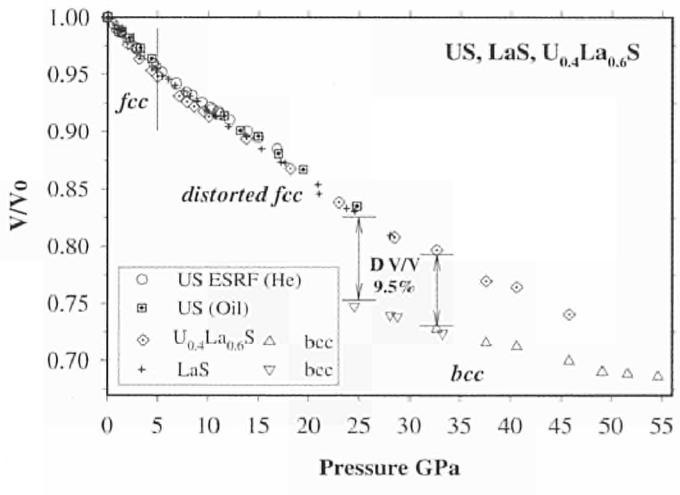

Fig. 2.14 Relative volume vs pressure of US, $U_{0.4}La_{0.6}S$ and LaS.

2.4.2.2 Structures of UMn_2 and $ThMn_2$

Under ambient conditions UMn_2 is characterised by the cubic Laves-type structure ($MgCu_2$-type), but it is also known for an orthorhombic distortion of this high-symmetry struc-

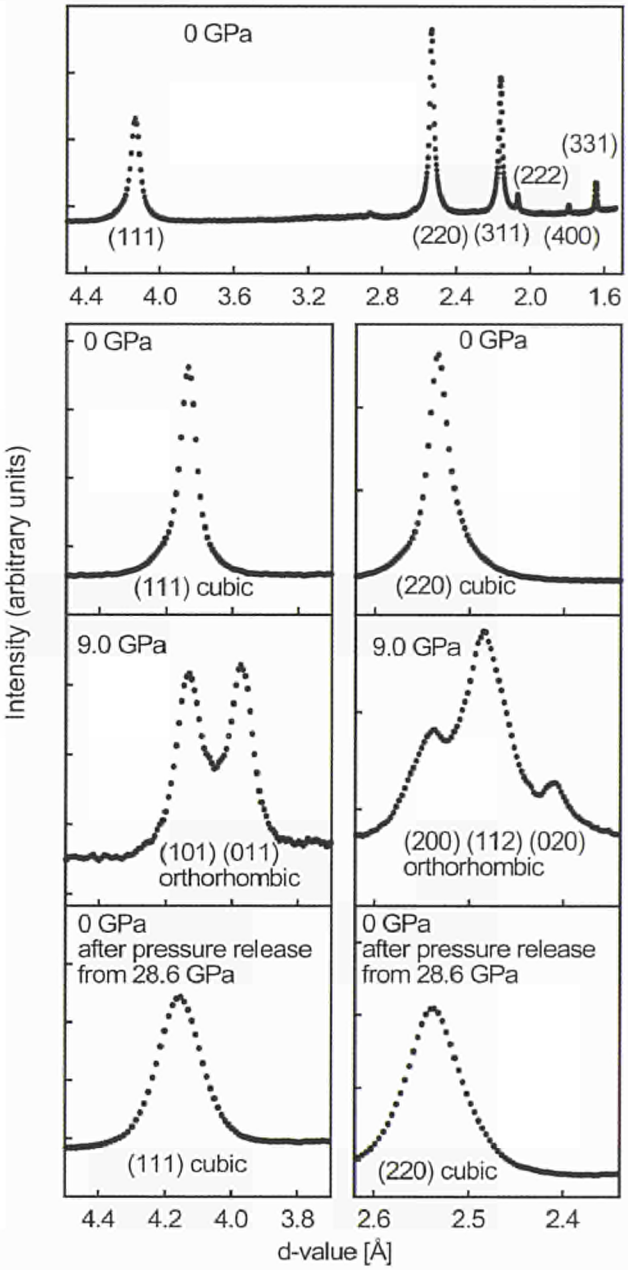

Fig. 2.15 In the upper part of the figure the X-ray diffraction pattern of UMn_2 at 0 GPa before application of pressure is shown. The lower part shows the splitting of the (111) and (220) cubic lines at 9 GPa and the recovery of the cubic structure after pressure release. The indices of the lines at 9 GPa correspond to the orthorhombic description of the distorted cubic cell.

ture below 230 K, which is not associated with magnetic ordering [1]. We performed high pressure X-ray diffraction experiments in order to re-investigate the pressure-induced structural transition occurring above about 3 GPa, which we observed last year at HASYLAB (TUAR-98, p. 58). The experiments were performed at the high-pressure beamline ID30 at the European Synchrotron Radiation Facility ESRF (Grenoble, France) with an angle dispersive detector system, using a Syassen-Holzapfel-type diamond anvil cell.

In order to improve the resolution of the line splitting, we used nitrogen as the pressure transmitting medium, which remains more hydrostatic at high pressures. Fig. 2.15 shows the integrated X-ray pattern and selected reflections at different pressures. As can clearly be seen the (111) cubic reflection is split into two peaks, and the (220) into three peaks, at 9 GPa. This kind of splitting can be explained by assuming an orthorhombic distortion, i.e. a distortion along a face diagonal of the cubic cell, which is qualitatively the same as the above mentioned low-temperature distortion. The pressure vs. volume curve obtained from the HASYLAB data below the transition point and from the new ESRF data is shown in Fig. 2.16. As can be seen there is a normal compression curve with a bulk modulus $K_0 = 149 \pm 7$ GPa and a pressure derivative $K_0' = 2.5 \pm 0.6$.

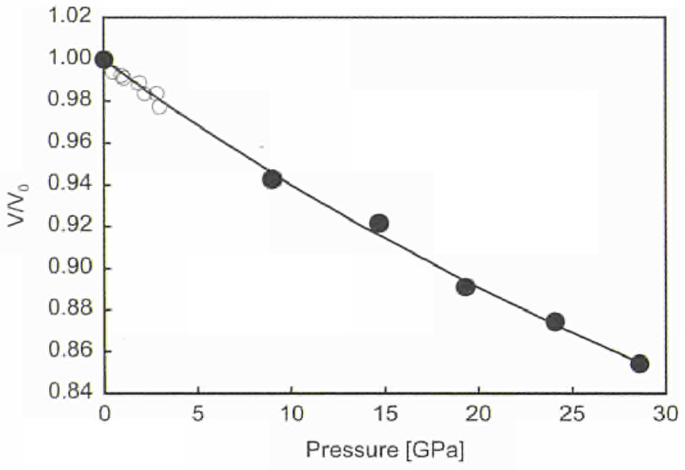

Fig. 2.16 The relative volume of UMn_2 is shown as a function of the applied pressure. The full symbols denote the values obtained from the ESRF experiment with nitrogen as pressure transmitting medium, the open symbols denote the values obtained at HASYLAB with silicone oil and an 4:1 methanol-ethanol mixture as pressure transmitting media. The line represents the fit of the Murnaghan EOS to the experimental data.

$ThMn_2$ has been investigated in order to find a possible pressure-induced change of the C14-type crystal structure (hexagonal Laves phase). The experiments were performed at the ESRF with silicone oil as the pressure transmitting medium, all other experimental details are the same as for UMn_2. Fig. 2.17 shows the pressure dependence of the c/a ratio and of the relative volume. The bulk modulus K_0 is 66 ± 2 GPa and its first pressure-derivative K_0' is 6.2 ± 0.2, which indicates a relatively high compressibility, as compared to UMn_2. In contrast to UMn_2 the symmetry of the structure does not change up to pressures of more than 50 GPa, but there is a pronounced change of the c/a ratio at low pressures, from about 1.629 at 0 GPa to 1.620 at 10 GPa.

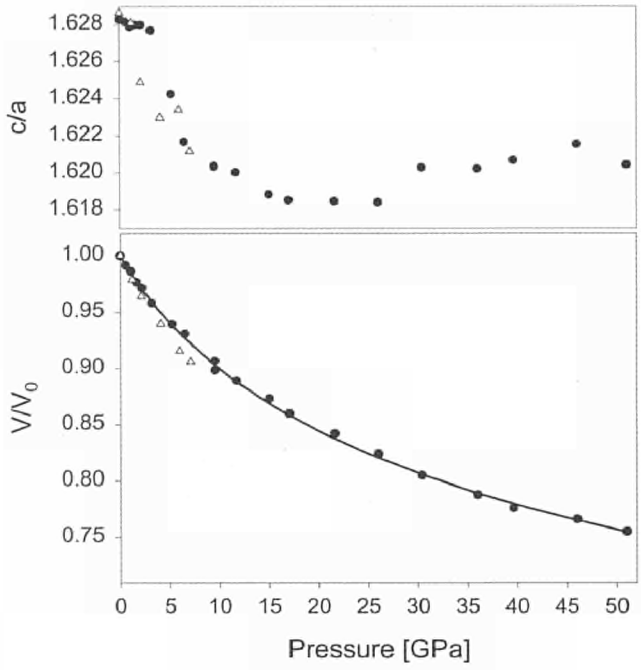

Fig. 2.17 The c/a ratio and the relative volume of $ThMn_2$ are shown as a function of the applied pressure. The different symbols denote the results of different runs. The line represents the fit of the Murnaghan EOS to the experimental data.

Reference

[1] A.C. Lawson, Allen C. Larson, R.B. von Dreele, A.T. Ortiz, J.L. Smith, Journal of the Less-Common Metals 132 (1987) 229-235

2.4.2.3 Optical reflectivity under pressure

As a complementary measurement to those reported on the structures under pressure, we are now measuring the optical properties of certain compounds.

The measurements have been performed in a Syassen-Holzapfel Diamond Anvil Cell (DAC) with optical diamonds up to 40 GPa.

As shown in Fig. 2.18 for the uranium monochalcogenides at low pressures a peak around 1 eV and a shoulder around 3 eV can be observed that agrees with UHV-spectra [1]. LaS shows a peak at 1.5 eV and a shoulder at 2.5 eV.

With increasing pressures all the compounds show an increasing intensity for the second peak.

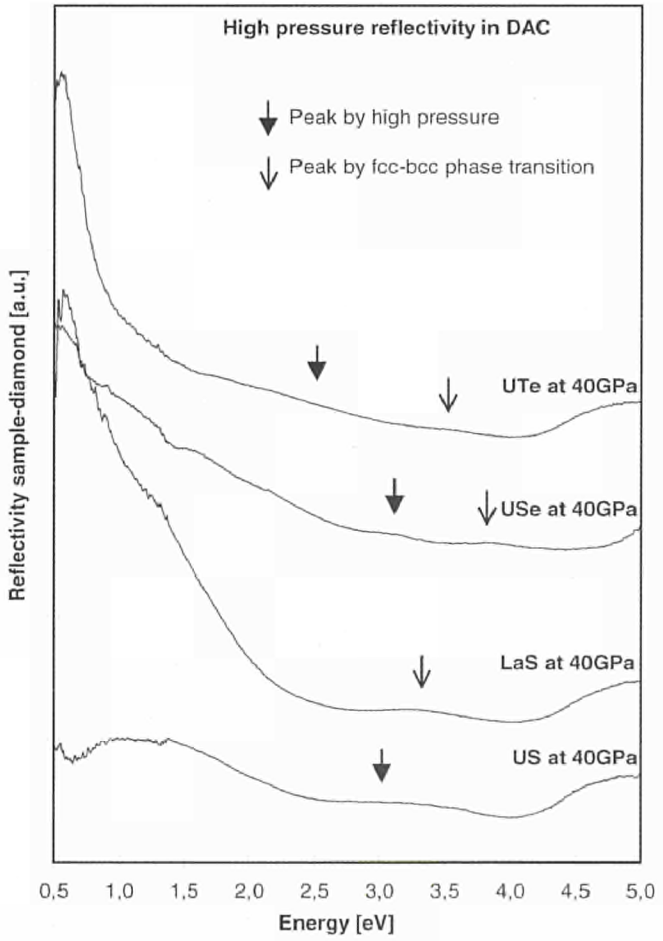

Fig. 2.18 High-pressure reflectivity of US, LaS, USe and UTe at 40 GPa in DAC. Full arrows show increasing intensity with pressure, open arrows show new peaks induced by phase transition.

For those compounds that have a crystal phase transition (USe at 31 GPa, UTe at 10 GPa and LaS at 24 GPa) this second peak splits into two and a dramatical increase in the metallic-like behaviour can be observed by the increasing reflectivity in the low energy range.

Reference

[1] J. Schoenes, in 'Handbook on the Physics and Chemistry of the Actinides', eds. A. J. Freeman and G.H. Lander, North-Holland, Amsterdam, Vol. 1 (1984) p. 365

Contact (2.4): Steve Heathman • tel.: +49 7247 951 277
fax: +49 7247 951 599 • heathman@itu.fzk.de

2.5 Scattering Studies

A number of neutron experiments have been performed this year at the Institut Laue-Langevin (ILL, Grenoble) and at Risø National Laboratory in Denmark. New efforts, initially at Risø, concern the discovery of a magnetic response in UBe_{13}, the one heavy-fermion superconductor that up to now has seemed devoid of any sign of magnetism. Progress was also made on the characterisation of the of the (U,La)S system, in which theory has made a number of predictions. The use of polarisation analysis continued with experiments on UNi_2Al_3 and UO_2. Experiments at the ILL were performed on Np(As,Se) and (Pu,U)Sb crystals in collaboration with outside users. In this report we present work on UGa_3 single crystals.

X-ray magnetic scattering investigations have continued at both Brookhaven Nat. Lab., USA and at the European Synchrotron Radiation Facility (ESRF) in Grenoble. Experiments at ESRF on the $(Np_xU_{1-x})Ru_2Si_2$ series were completed in 1999, and an initial effort on NpO_2. This is briefly mentioned in the highlight. Here we describe work on UGa_3 and on the mixed samples (Pu,U)Sb.

2.5.1 Neutron scattering from itinerant UGa_3

Magnetic moments in solids arise from two possible sources. First, the unpaired electron spins create a spin moment, μ_S, and then the motion of their charges around the nucleus induces a current resulting in an orbital moment, μ_L. Models for cooperative magnetism in metallic systems start from one of two relatively well understood hypotheses. The 3*d* transition metals and their compounds (Fe, Ni, & Co) are

itinerant systems that are best described with a band-electron approach and the orbital moment is almost always quenched, i.e. $\langle \mu_L \rangle \sim 0$. In the 4*f* series (lanthanides) the unpaired 4*f* electrons are well localised, the spin-orbit interaction is large, and the crystal field is small. This results in localised magnetism and large orbital moments. The actinides (5*f* electrons), and some cerium compounds, prove difficult to fit into these schemes, and much effort has been expended in developing models for the actinides that test our fundamental understanding of magnetism. The difficulty is that the spin-orbit interaction is large in the actinides, but many aspects of their magnetism can be described by band models. Of particular interest is the theoretical prediction that certain actinide systems with 5*f* electrons may best be described as itinerant, but, at the same time, a large orbital moment exists [1].

We have also performed neutron inelastic scattering (at both LLB – Saclay and ILL) experiments on single crystals of UGa_3. These experiments established an inelastic response, with a gap of about 6 meV. Most puzzling is that this excitation, despite its relatively steep dispersion, exists over only a small part of the magnetic zone and thus cannot be classed as a spin wave. Working with a cold-source triple axis (IN14) we find an additional low-energy response. Fig. 2.19 shows this at $\mathbf{Q_o}$ as function of temperature (a) and as a function of wavevector at 15 K (b). As with the inelastic part of the spectrum, the quasielastic part dies away rapidly away from the zone centre. The solid lines in Fig. 2.19 are deduced from a parametric model we have developed previously for UPd_2Al_3 [2] and consists of two modes, one with its pole at E = 0 (quasielastic) and one with its pole at a finite energy. The two modes are coupled in a mean-field approximation to yield a total susceptibility.

The temperature dependence at $\mathbf{Q_o}$ is given in the colour plot, Fig. 2.20. This shows, for T < 35 K, the clear resolution of two features in the excitation spectra. The distinct gap between the quasielastic and inelastic modes washes out as the temperature is raised. The two component spectrum of UGa_3 may be associated with the propagating (inelastic) and over-damped (quasielastic) part of the 5*f*-conduction band response. The finite energy gap in the propagating part of the response (Fig. 2.20), which in part may be attributed to the spin-orbit interaction, decreases together with the staggered spin polarisation on approaching T_N. However, even above T_N (in fact up to at least 2 T_N) there are still strong quasielastic correlations of the dynamic magnetic response around the incipient antiferromagnetic wave vector. The Fermionic part of the spectral weight may be associated

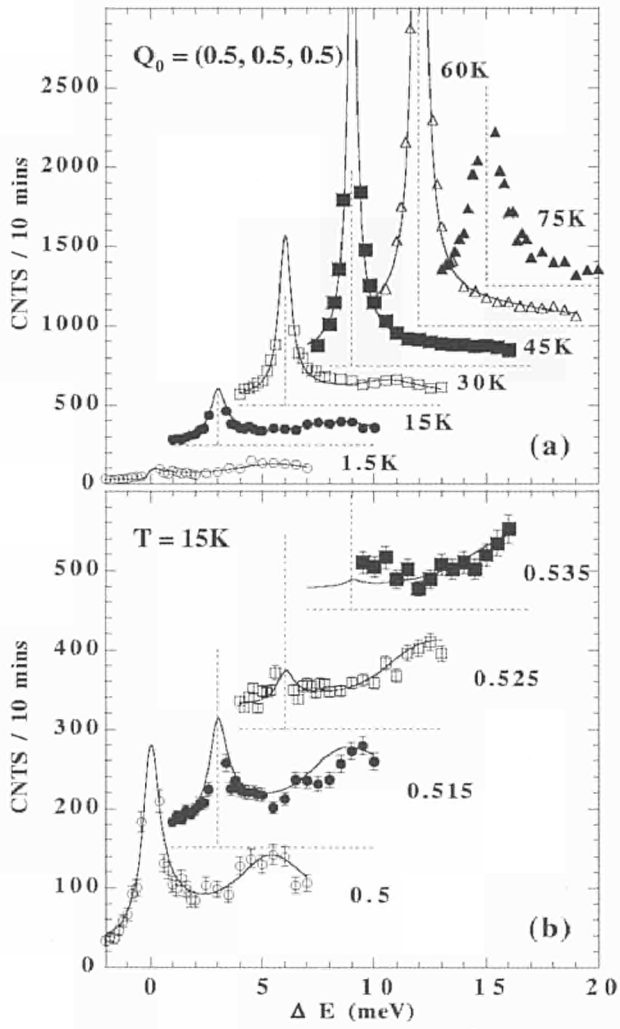

Fig. 2.19 (a) Temperature dependence of the scattering at the antiferromagnetic wavevector $\mathbf{Q_o} = \left(\frac{1}{2}\frac{1}{2}\frac{1}{2}\right)$
(b) $\mathbf{Q}$*-dependence of the scattering in the [111] direction at T = 15 K.*
Note the displaced axes in both panels. The solid lines are fits to the interacting two component model as described in the text, and more fully in Ref. [2].

with excitations across the quasiparticle Fermi surface, thus confirming the itinerant nature of the 5*f* states in UGa_3. Taking this response to have the similar topology as derived in the one particle calculations [3], it appears that the "rugby ball" surface near the magnetic zone centre may play a predominant role – the strong curvature would suppress the low energy excitations for wave vectors substantially different from $\mathbf{Q_o}$. The weak temperature dependence of the spatial extent of the quasielastic scattering may likewise be rationalised ($T << T_{Fermi}$).

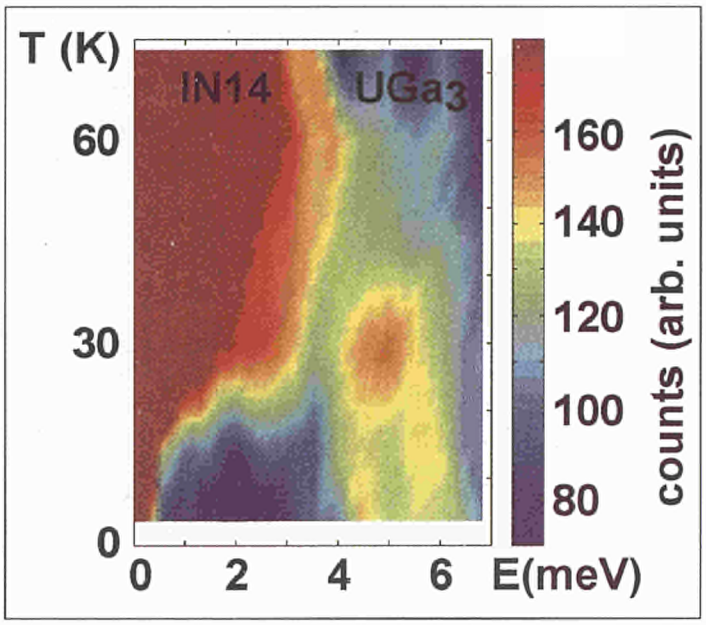

Fig. 2.20 Colour representation of the scattering in UGa_3 at $\mathbf{Q_o}$ as a function of T and as measured on IN14. Note that distinct inelastic feature disappears around 40 K, and the response is then dominated by the quasielastic component. (T_N = 67 K.)

2.5.2 Synchrotron magnetic scattering

We first reported unsuccessful efforts to find magnetic scattering from samples containing Pu in 1995 and 1996 [4]. After discussion with a number of chemists we suspected that gas released as a result of radiolysis of the epoxy used to stick the crystals to the copper base might be the cause of the surface degradation. The latter was confirmed when the samples were returned from Brookhaven and their surface examined optically. To avoid this problem a new sample mounting procedure was used in which the samples were welded with indium to the holder. These samples were then sent to Brookhaven and magnetic scattering from a sample of PuSb was observed in March 1999. We show in Fig. 2.21 the intensity as a function of incident photon energy scattered from the ordered antiferromagnet $(U_{0.25}Pu_{0.75})Sb$. These data show that, as expected, *both* Pu and U atoms carry magnetic moments. What appears quite new in this experiment is the additional feature on the high-energy side of the Pu M_5 resonance. Such an effect has not been observed so far in any U or Np compounds. It is almost 12 eV above the M5 position, and this is too large an energy difference for the structure to be associated with the intermediate-state multiplets. Further experiments are planned for early 2000 to examine another Pu-containing compound. Unusual effects are also observed in the synchrotron data from $(U_{0.25}Pu_{0.75})Sb$ as a function of temperature. Neutron experiments are being used to study the phase diagram so that the details revealed by x-rays can be properly interpreted. As described above the resonant x-ray magnetic scattering (RXMS) technique at synchrotron sources has been applied to a wide variety of elements throughout the periodic table, but in almost all cases these elements have been *magnetic*. In the few cases in which non-magnetic elements have been examined the signals have been small and compatible with a small induced signal at the non-magnetic element.
However, recent experiments at the ESRF have found surprisingly large signals at energies associated with non-magnetic elements in uranium compounds. These signals have been found in both x-ray magnetic circular dichroism (XMCD) and in scattering. The XMCD signals were first found at the sulphur K edge in the ferromagnet US, and subsequently at the Ga K edge in UGa_2, also a ferromagnet [5].

Scattering experiments were first performed on single crystals of UGa_3. As discussed above in this Annual report UGa_3 is an antiferromagnetic material (T_N = 67 K with a moment of ~ 0.6 μ_B on the U site) and initial experiments were per-

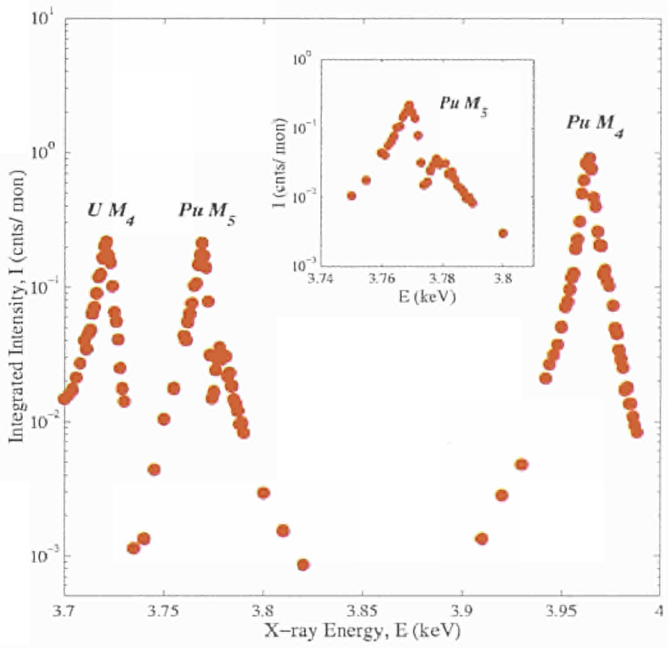

Fig. 2.21 Intensity of the 1st-order antiferromagnetic Bragg peak from a sample of $(U_{0.25}Pu_{0.75})Sb$ as a function of incident photon energy. The individual resonant energies are marked. Note the extra small peak on the high-energy side of the Pu M_5 peak.

formed on the large M edge resonances of U (3.55 and 3.78 keV). The photon energy was then tuned to the K edge of Ga (10.37 keV). A very large (by a factor of ~1000) enhancement of the small non-resonant magnetic scattering intensity was observed. This is demonstrated by plotting the integrated intensity as a function of incident photon energy in Fig. 2.22a. The energy width is ~ 4 eV, close to the expected core-hole lifetime of the intermediate state. Superposed on this is the fluorescence spectra measured in the same experiment. The position of the peak in energy strongly suggests that the resonance is dipole in nature, i.e. involves the 4*p* electron states of Ga. The signal has a periodicity identical to that of the uranium magnetic structure, is long range in real space, and disappears above T_N. Fig. 2.22b shows the intensity as a function of position in reciprocal space. The signal is present only in the $\sigma \rightarrow \pi$ channel with σ incident polarization from the synchrotron, again consistent with a dipole transition. Similar effects were observed in UAs when photons were tuned to the K edge of arsenic. In these experiments at the K-edges enhancements of the scattering as compared to the non-resonant signal from the uranium moment exceed factors of 1000, which is much greater than found in even *magnetic* 3*d* elements.

In all experiments reported here the signal does not arise from a simple dipole situated at the non-magnetic element – its size would have to be so large that it would have been seen easily by neutron scattering. The effect is undoubtedly more subtle than that, involving the hybridisation of the *p* with the uranium 5*f* states. Theory continues to address the underlying physics, but the experiments open new perspectives using resonant effects, which will certainly be the subject of future efforts.

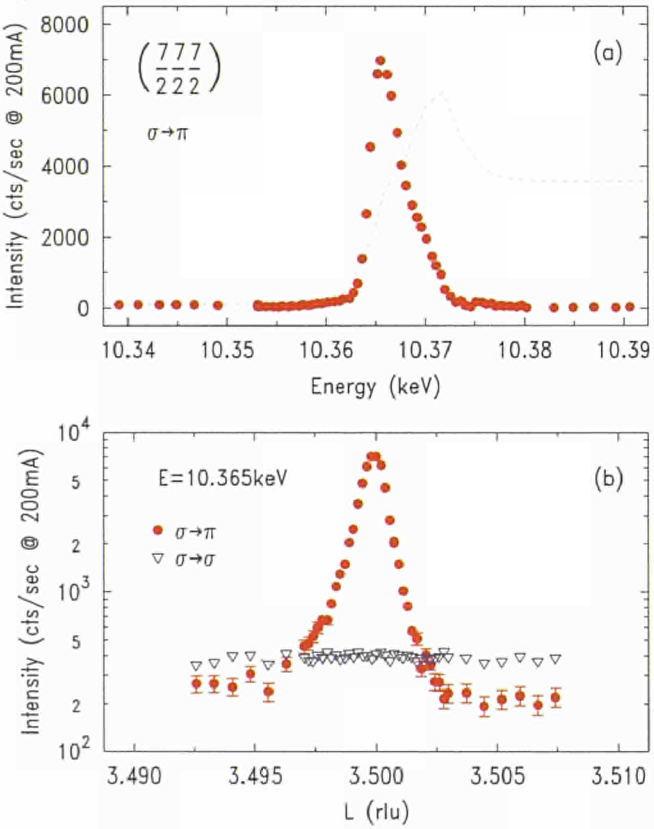

Fig. 2.22 Resonant intensity associated with Ga K edge in the antiferromagnet UGa_3.

(a) Data points are integrated intensity as a function of incident photon energy. The dashed curve superposed is the fluorescence.

(b) Intensity at a photon energy of 10.365 keV for the antiferromagnetic Bragg reflection as a function of the longitudinal wavevector [ξξξ], where these are coordinates in reciprocal space. The peaks occur at exactly the same positions as those from the uranium moments, and their narrow width (in q-space) indicates long-range real space correlations. The higher background in the $\sigma \rightarrow \sigma$ channel comes from the fluorescence.

References

[1] M.S.S. Brooks and P.J. Kelly, Phys. Rev. Lett. 51 (1983) 1708

[2] N. Bernhoeft et al., Phys. Rev. Letters 81 (1998) 4244; Physica B 259-261 (1999) 614

[3] A.L. Cornelius et al., Phys. Rev. B 59 (1999) 14473

[4] D.G. Mannix et al., Physica B 262 (1999) 125

[5] A. Rogalev et al. (to be published)

Contact (2.5): Gerard Lander • tel.: +49 7247 951 382 • fax: +49 7247 951 599 • lander@itu.fzk.de

2.6 Magnetic X-ray Circular Dichroism in Uranium Sulphide

Interest in the integrated x-ray magnetic circular dichroism (XMCD) signals at the $M_{4,5}$ edges of uranium compounds is partially due to the existence of sum rules [1] which relate the integrated XMCD to the spin and orbital magnetic moments of these compounds. However recent experiments [2] have shown that the application of the sum rules to uranium compounds is ambiguous since they involve the expectation value of the dipole operator, $\langle T_z \rangle$, which has not been measured. For lighter elements, where spin-orbit interaction is small, $\langle T_z \rangle$ is small and may safely be neglected - as demonstrated with calculations of $\langle T_z \rangle$ for Fe, Co and Ni.

In order to resolve the ambiguities in experiments calculations have been made of the XMCD, orbital and spin magnetic moments, and $<T_z>$ for uranium sulphide *ab initio*. Although the evaluation of these quantities is complex almost perfect consistency is found between the computed values and measurements. Firstly calculations show that the integrated magnetic linear dichroism can be neglected, as was assumed in the analysis of the experiments. Secondly the calculated integrated XMCD at each edge vanishes if the spin is set to zero (the paramagnetic case). Thirdly the calculated sum of the integrated XMCD at the M_4 edge cancels the integrated XMCD at the M_5 edge and the orbital magnetic moment vanishes when the spin-orbit interaction is set to zero, as required by the sum rules. Finally we computed $<T_z> = 0.26$, an orbital moment of 3.2 μ_B, a spin moment of −1.63 μ_B and a total moment of 1.57 μ_B from both the ground state and the integrated XMCD. These values are also in excellent agreement with the results of elastic neutron scattering experiments [3].

References

[1] B.T. Thole et al., Phys. Rev. Lett. 68 (1992) 1943
[2] S.P. Collins et al., J. Phys. Condens. Matter 7 (1995) 9325
[3] F.A. Wedgwood, J.Phys.C5 (1972) 2427

Contact (2.6): Michael S.S. Brooks • tel.: +49 7247 951 476 fax: +49 7247 951 599 • brooks@itu.fzk.de

2.7 INTAS Project on the Equation of State of UO_2 successfully terminated

An international Project supported by the International Association for the Promotion of Co-operation with Scientists from the Independent States of the Former Soviet Union (INTAS) was started in 1994 under the co-ordination of ITU with the intent of constructing an Equation of State (EOS) for liquid and gaseous UO_2, which fully reproduces the consolidated thermodynamic database of this compound, and further, provides trustworthy extrapolations up to the critical point.

The equation of state of fluid UO_2 was first needed in the analysis of hypothetical reactor accidents where temperatures are expected, at which the vapour pressure of the fuel is sufficiently high to produce liquid mass displacements. In the last decade, however, increasing attention was directed on the effects of the atmospheric environment on the vaporisation rate of the molten fuel. In this context, empirical thermodynamic properties of urania at high temperatures are presently restricted to the near-stoichiometric or congruent-vaporisation compositions. Therefore, the new equation of state was devised for applications encompassing hypo- and hyperstoichiometric compositions under both equilibrium and non-equilibrium conditions over a broad temperature range.

The typical example of hypothetical accident, where extremely high temperatures can be achieved, is a reactivity-initiated accident in a Liquid Metal Fast Breeder Reactor (LMFBR), e.g. a supercritical excursion, caused by a loss of liquid-metal coolant. In such an excursion, the release of energy is so rapid that the action of the fuel vapour pressure can result in the *explosive disassembly* of the molten core.

The connection between pressure and temperature is provided by the thermodynamic equation of state, $p(T,V)$, in which the volume, V, of the system enters; however, like the internal energy, U, the volume is not fixed by the *thermal* Equation of State, but requires, instead, a *caloric EOS*, such as is afforded, for example, by the heat capacity at constant volume, $C_v(T)$. It is thus this equation which provides the essential link between the *nuclear aspects* of a supercritical excursion and the *dynamic response* of the molten core; for a given density, $T(U,V)$ controls the nuclear cross-sections via the Doppler coefficient, whilst $p(U,V)$ controls the time-dependence of the fuel-mass geometry *via* hydrodynamics. The reliability of reactor safety analyses is thus contingent on the accuracy to which the *EOS* of the UO_2 is known – in particular, in the liquid-vapour coexistence region which extends to the Critical Point – a most important invariant point on the phase diagram of any material.

Despite considerable effort over the past 30 years, the phase diagram of the U-O system in the vicinity of UO_2 was still very incomplete in 1993, when the project was started, due primarily to three features – *(i) the very high melting temperature* (~ 3100 K), which, until the advent of rapid, laser heating techniques, not only restricted the acquisition of experimental data, but also posed problems for the containment of the sample, with the attendant possibility of sample contamination, *(ii) the rather wide range of stoichiometries* over which Urania, ($UO_{2\pm x}$) can exist as a single phase system, and the related problem of controlling the stoichiometry of any *given* sample throughout the course of an experiment, and *(iii)* the possible non-congruency of the melting and vaporisation of the material under conditions of thermodynamic equilibrium.

Given, however, the recent advances both in high temperature experimental technology and in the theoretical understanding of binary systems of variable composition, the possibility of further progress presented itself - involving not only further refinements, but also, more importantly, the possibility of exploring hitherto experimentally inaccessible regions of the phase diagram. With this prospect to hand, the present *INTAS* Project was conceived as an integrated programme of experimental and theoretical work, in which the best 'State of Art' equipment and expertise would be brought to bear on this fundamentally important problem of over 30 years standing.

To date, the objective of the Project has been achieved: a new equation of state of UO_2 has been constructed on adequate physical fundaments, which make it possible to predict the thermodynamic properties of the system under the most general environmental conditions.

Results

A so-called "Chemical Plasma Model" approach was used for the theoretical description of liquid urania. This model describes, in a unified formalism, a *multi-component mixture* of chemically reactive, strongly interacting neutral and charged molecules and atoms (see Tab. 2.5). Their interaction parameters were first expressed theoretically, and then "calibrated" to reproduce sufficiently well established properties of molten $UO_{2.00}$ at the melting point.

Tab. 2.5 Salient features of the INTAS-Equation of State of UO_2.

TYPE OF "ANSATZ" - Quasi-chemical representation of both liquid and gaseous phases -
MODEL ELEMENTS – (Gaseous and Liquid Phases) ***Neutrals:*** $UO + UO_2 + UO_3 + U + O + O_2$ ***Ions:*** $UO_2^{(+)} + UO^{(+)} + U^{(+)} + UO_3^{(-)} + UO_2^{(-)} + O^{(-)} + e^{(-)}$
INTERACTIONS R – Intensive Short-Range Repulsion C – Coulomb Interaction between Charged Particles A – Short-Range Attraction between all Particles
FORMULATION OF THE INTERACTIONS R – Hard-Sphere Mixture with varying diameters (*) C – Mean Spherical Approximation (MSA) (*) A – Thermodynamic Perturbation Theory (TPT – σ,ε) (*) { $\sigma = \sigma(T)$ and $\varepsilon = \varepsilon(T)$ } (*) – *Modified for mixtures*

Comparing the predicted equilibrium vapour pressure with the literature data provided a first validation of the model up to temperatures of the order of 5500 K. A further, positive result is the good agreement of the predicted heat capacity (Fig. 2.23) with the experimental values of Ronchi *et al.* [1], which extend up to 8000 K.

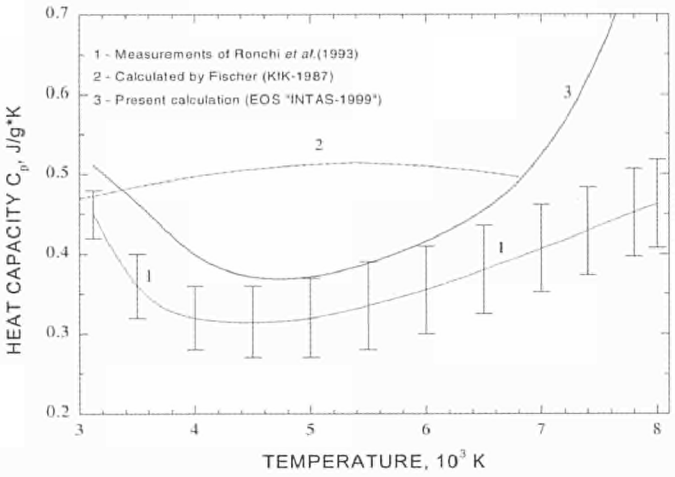

Fig. 2.23 The heat capacity of liquid UO_2 predicted by the INTAS model compared to experimental results of ITU. The results of the Equation of State of Fischer, KfK [2] are also plotted.

Up to now, none of the existing liquid UO_2 models was able to correctly reproduce the observed dependence of C_p on temperature. The calculations were finally extrapolated to the high-pressure and high-temperature region ($p \leq 10$ GPa, $T \leq 20000$ K).

A relevant result is the unusual structure of the gas-liquid phase transition boundary (Figs. 2.24 and 2.25), which exhibits a *striking difference* with respect to that of ordinary liquids. This feature is caused by the *non-congruency* of the coexisting phases in $UO_{2\pm x}$. Both the total vapour pressure and the degree of oxygen enrichment of the vapour phase strongly depend on the evaporation regime. Two distinct pressure-temperature functions $p=p(T)$ were, therefore, calculated (Fig. 2.24), corresponding to the limiting cases of: *a) boiling*, i.e. *slow* evaporation under "global equilibrium conditions", and *b) saturation*, i.e. *fast*, non-equilibrium evaporation (the so-called "forced-congruent mode").
A characteristic feature of non-congruent vaporisation in $UO_{2\pm x}$ is the production of a very high maximal vapour pressure ($p_{max} \sim 1$ GPa) as well as a substantial oxygen enrichment of the vapour phase over boiling UO_2 ($(O/U)_{max} \sim 7$), as

shown in Figs. 2.24 and 2.25. The implicit correlation of the total vapour pressure with the effective oxygen chemical potential is obviously of great importance for a correct prediction of the fuel vaporisation rate in a real reactor-accident scenario.

The critical point of *truly non-congruent* phase transition in UO_2 was also calculated. This point *essentially differs* from that defined for a gas-liquid phase transition in *simple liquids;* in particular, we have here $(\partial p/\partial V)_c \sim (p/V) \neq 0$. The predicted critical parameters are:

$T_c \approx 10120$ K, $p_c \approx 965$ MPa, $\rho_c \approx 2.61$ gcm^{-3}

There is no doubt that the new model represents a substantial progress with respect to those used in the past. First, because of its better reproduction of new, recently discovered, empirical data of the liquid (in particular the heat capacity), secondly because of its inherent features, which provide a superior description of very important properties. In this context, the following topics should be mentioned:

- Satisfactory accounting for the twofold character - ionic/covalent - of the examined material: though the chosen formalism is necessarily based on idealisation of the constituents, its thermodynamic justification is based on rigorously demonstrated theorems.

- Transparent calibration procedure: the model contains a number of physical parameters, which are taken from reliable experimental measurements. Tuning was therefore restricted to a few unknown parameters (whose physical meaning is, however, clear), which may be experimentally measured in the future.

- The EOS extends over a broad composition range of $UO_{2\pm x}$: it is known that deviations from O/U=2 produces dramatic effects in the high temperature solid. Extension of the stoichiometry dependence to the liquid EOS represents a substantial progress, especially in view of reactor-safety engineering applications.

- The concept of thermodynamic criticality in the presence of variable stoichiometry, entailing non-congruency of vaporisation, was re-defined on a more general basis. The related considerations are valid, independently of the presently assessed values of the critical temperature, pressure and density – whereby the first two are markedly higher than those assumed up to now.

A detailed monograph on this subject is in preparation.

References

[1] C. Ronchi, J.-P. Hiernaut, R. Selfslag, G.J. Hyland, Laboratory measurement of the heat capacity of urania up to 8000 K, Nucl. Sci. Eng. 113 (1993) 1-19

[2] E.A. Fischer, Evaluation of the urania equation of state based on recent vapour pressure measurements, Report KfK-4084, 1987

[3] D.W. Green, L. Leibowitz, Vapor pressures and vapor compositions in equilibrium with hypostoichiometric uranium dioxide at high temperatures, J. Nucl. Mater. 105(2/3) (1982) 184-195

Contact (2.7): Claudio Ronchi • tel.: +49 7247 951 402
fax: +49 7247 951 591 • ronchi@itu.fzk.de

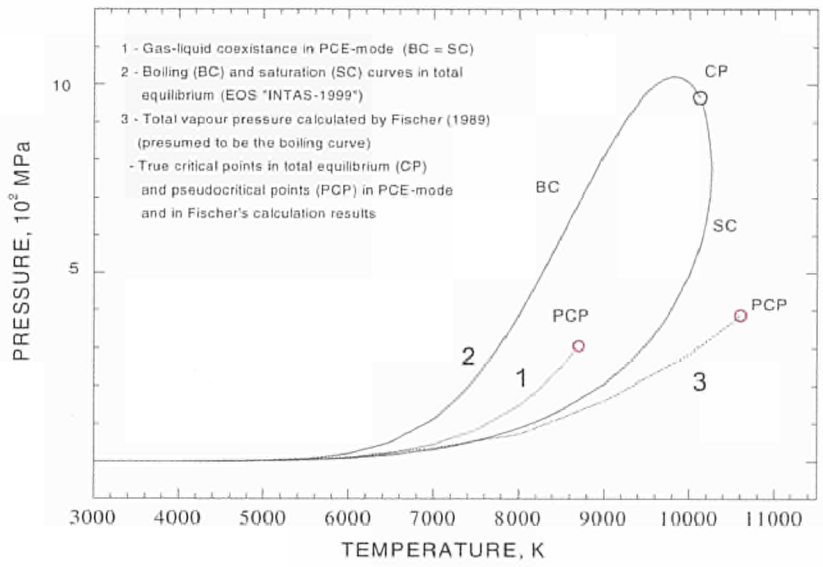

Fig. 2.24
Plot of the p(T) diagram corresponding to partial-congruent evaporation mode (PCE) and to the distinct boiling and saturation modes (respectively, BC and SC). The "banana" shaped curve is typical for non-congruent vaporising systems. Curve 3, predicted by Fischer's model [2], follows the INTAS saturation curve for T = 7000 K, whilst at higher temperatures a large discrepancy is found.

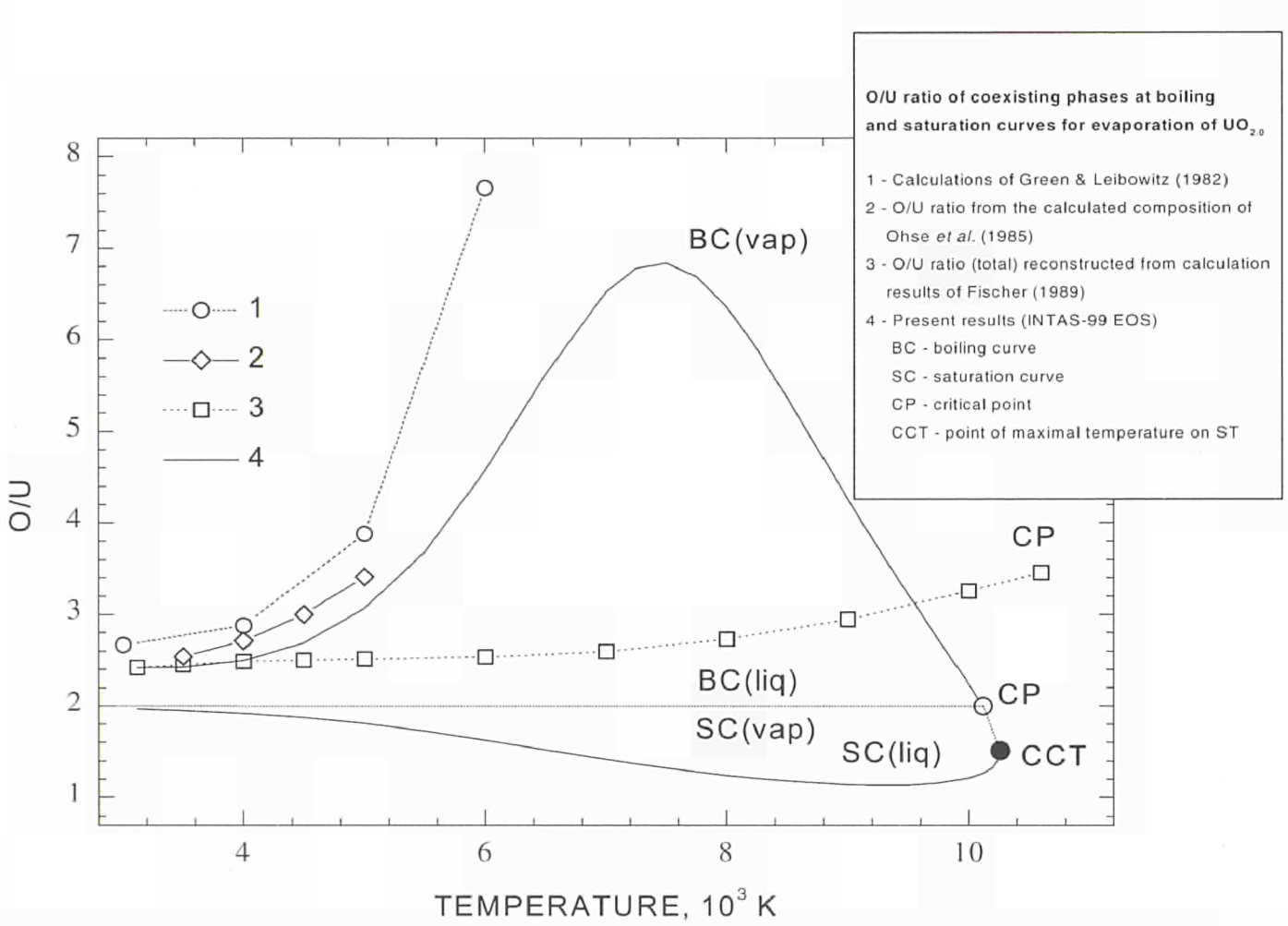

Fig. 2.25 Stoichiometry of the vapour over liquid $UO_{2.00}$. One can see that under boiling conditions the vapour is very rich in oxygen, in agreement with the Green & Leibowitz model [3]. Note that the INTAS model correctly predicts that O/U=2 at the critical point, CP. This is not the case for Fischer's model [2] (curve 3).

2.8 Relevance of Atomic Diffusion in Fission Gas Release from LWR fuel as a Function of Burnup

One of the great concerns in operating LWR fuel at very high burn-ups is the enhancement of fission gas release, which deteriorates the fuel/cladding gap conductance, in large part sustained by the high thermal conductivity of the pure helium filling the pressurised rod. Since fission gas is effectively insoluble in UO_2, release is primarily the result of an in-solid diffusion process. Collisions with fission fragments and long residence times in reactor, favours athermal diffusion. However, accumulation of fission damage and fission products does finally affect the state of gas-in-solid and, hence, its intrinsic mobility, causing consequences which are not yet fully understood.

In the last few years, a number of irradiated UO_2 fuel samples at various burnups have been submitted to accurate fission-gas release tests in the ITU Knudsen-cell facility. Release of fission gas was measured in vacuo, together with effusion of less volatile fission products, by a mass spectrometer placed at a distance of a few centimetres from the heated sample. Almost all fission fragments were detected, in conjunction with the uranium and actinide-bearing species. Isochronal annealing tests were performed up to temperatures at which substantial fuel vaporisation occurs, and were terminated by complete vaporisation of the sample. The analysis of the results was performed based on a sufficiently

realistic model [1] which describes release in terms of a combined diffusion/trapping mechanism.

Three thermally activated release stages can be identified: *i)* diffusion along extended defects (grain boundaries or dislocation networks), *ii)* volume diffusion in the intragranular range, and *iii)* gas in bubble release - in this case due to progressive sublimation of the sample. The analysis of the empirical fractional release curves provides for each stage both the enthalpy of diffusion and the corresponding pre-exponential entropy factor. In the case of atomic diffusion this latter is a function of the competing sink strengths (respectively of the intragranular bubbles and of the vented pore network). Fig. 2.26 shows a typical curve obtained from the model.

The function, Z, plotted is the logarithm of the fractional rate of change of the gas retained. Independently of the annealing history, this function has the property of manifesting the various release stages as quasi-linear segments.

The examined samples were taken from different LWR fuel rods, and extracted from pellet regions whose irradiation temperature was sufficiently low to prevent important in pile release. At low and moderately high burnups, the fission gas was dynamically dissolved or finely dispersed or in the form of small intragranular bubbles (with sizes of the order of 10 nm and concentrations of 10^{17} cm^{-3}). At very high burn-ups, the samples exhibit the typical RIM re-structuring with formation of sub-grains of size of less than one micron, on whose boundaries larger bubbles are formed. Fig. 2.27 shows the release curves at two different burnups.

The measured parameters of the three different stages are reported in Tab. 2.6.

Release stage I, involving gas migrated to the grain boundaries during irradiation, is limited to less than 7% at low burnups, and does not exceed 15% at 100 GWd/t. As for stage II, where release is described as controlled by volume diffusion, an evident shift of the onset of release towards lower temperatures is observed with the increasing of burnup. Inspection of the dependence of the release rate on temperature indicates that the process is reasonably described by single-energy thermally activated atomic jumps. The diffusion enthalpy decreases continuously from approximately 106 kcal/mole at 25 GWd/t burnup down to less than 70 kcal/mole at 95 GWd/t. The high value, confirmed by previous measurements [2], is near to that of diffusion of vacancy-stabilised rare gas in fresh UO_2. The decrease of the diffusion enthalpy of circa 30 kcal/mole is here certainly significant, although in the literature the data range from 120 to 70 kcal/mole. The effect is very likely due to defects in the lattice associated to chemical impurities, whose presence tends to reduce the formation energy of cation vacancies. This would explain, at least qualitatively, the effect of burn up on the diffusion enthalpy of highly stabilised gas-in-solid.

The second relevant aspect is the increase with burnup of the gas amount (absolute as well as fractional) reaching the fuel free surfaces without precipitating into the densely dispersed intragranular bubbles. In fact, this fraction increases from 25% up to 83% in the explored burnup range.

Tab. 2.6 Fission gas (*) release after isochronal annealing of irradiated UO_2.

		STAGE I	STAGE II		STAGE III
Structure	Burnup (MWd/ton)	% released (²) of initial grain boundary gas	% released from volume diffusion	Enthalpy (kcal/mole)	% released via sample vaporisation after trapping in bubbles
Normal	25000	5-7	25	106.7	68-70
Normal	35000	5-7	51	97.5	39-42
Normal	55000	6-8	58	83.2	30-32
Normal	65000	7-8	61	88.0	25-29
RIM	80000	9-10	76	70.0	9-14
RIM	95000	12-15	83	68.5	1-5

(*) : The values in the Table represent the measured average for the isotopes: ^{84}Kr, ^{85}Kr, ^{86}Kr, ^{131}Xe, ^{132}Xe, ^{134}Xe, ^{136}Xe.
(²) : In percent of the retained gas (that is almost equal to the burnup inventory)

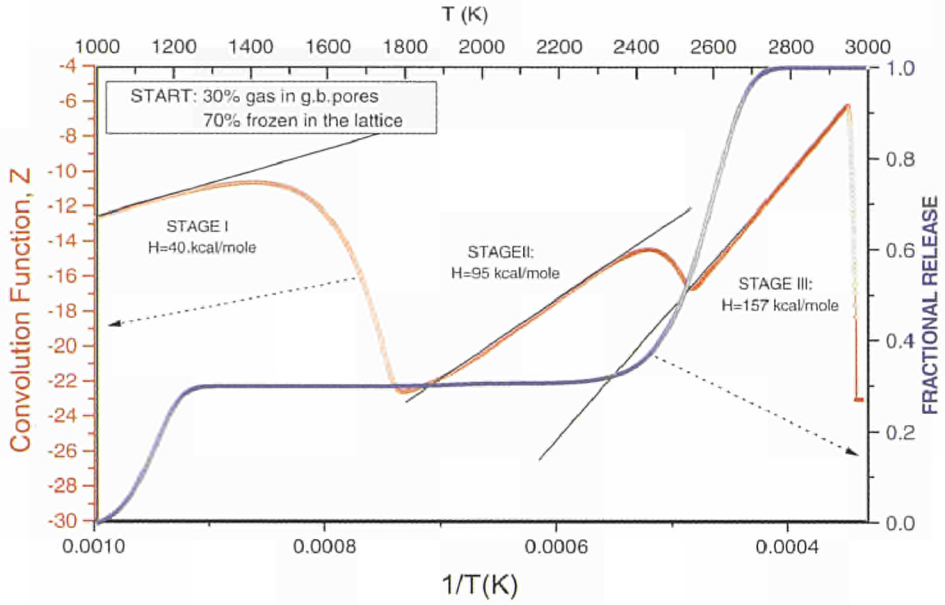

Fig. 2.26
Model prediction of release for a typical Knudsen vaporisation experiment. The initial conditions correspond to a fission gas repartition at end-of-life of 30% on the grain boundaries and 70% frozen from dynamical solution during irradiation.

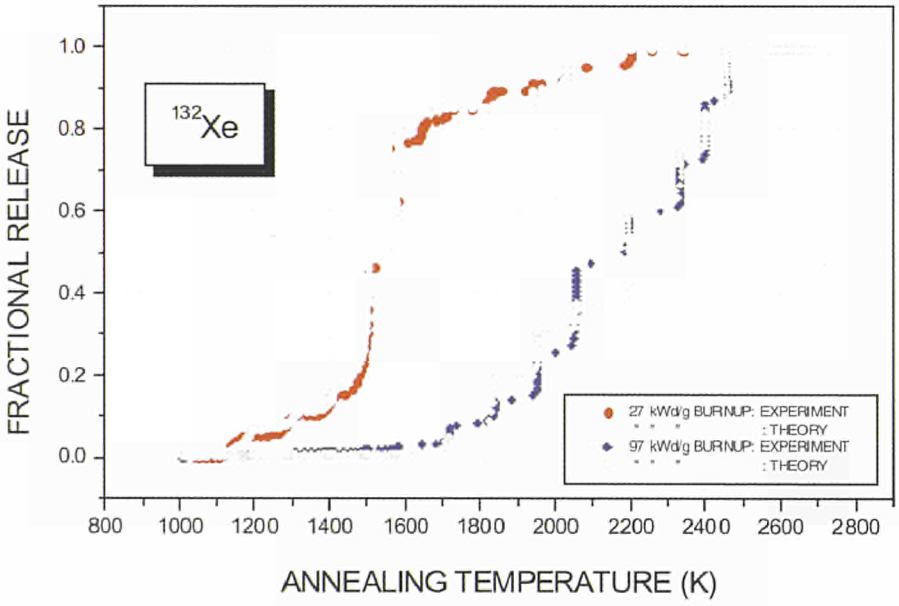

Fig. 2.27
Fractional release of a Xenon isotope from UO_2 irradiated at low and high burnup, as a function of temperature.

Analysis of the fraction of gas precipitated during random diffusion in a heterogeneous medium shows that this is proportional to the relative sink strength of the intragranular bubbles, k_{sc}, compared to that of the vented sinks, k_{gb}, (internal free surfaces and open pores) [3]. The intragranular bubble sink strength is proportional to the size of the bubbles and to their concentration, as well as to a bias term, L, which depends on the stress field around the bubble surface and on the vacancy availability in the lattice [2]. The sink strength of the vented sinks has a more complex expression. Hence, for simple thermal annealing conditions, the ratio of the gas amount arriving to the vented sinks to that trapped in the bubbles, in a first approximation, is *independent* of the mobility of the gas. At sufficiently large bubble concentrations, if α is the cell size of the vented-pore network, the approximate relation holds:

$$k_{gb} \cong (6L\, k_{sc}/\alpha)^{1/2} \text{ where}$$

$$R = k_{gb}/(L\, k_{sc}) = (6/L\, k_{sc}\, \alpha)^{1/2} \begin{cases} \cong 0.36 \text{ at 25 GWd/t} \\ \approx 40 \text{ at 95 GWd/t} \end{cases}$$

In fact, the release-to-precipitation rate increases by *two* orders of magnitudes from low to high burnup; hence, according to the equation above the product $L\ k_{sc}\ \alpha$ should decrease by *four* orders of magnitude. We know that the cell size α in the RIM structure is much smaller than the initial sintered grains, however not so that it can explain such a large factor. On the other hand, bubble concentration and size certainly do not decrease with increasing burnup. Furthermore, high values of fraction R are observed even at medium burnups, where the RIM structure is not yet formed.

Finally, the only factor that can be responsible for the large increase of R is then the bias term L. This factor represents a fundamental condition for gas precipitation, i.e. that gas precipitates into intragranular bubbles at the rate predicted by a random collision model *only* in the case where vacancies are sufficiently available to keep the bubble close to elastic equilibrium with the capillary forces: otherwise, a compressive stress field around the bubble is created, which delays precipitation, with respect to other sinks (e.g. extended defects) where vacancy availability is higher.

From the reported results, one must conclude that the effective number of free vacancies per gas atoms frozen in the lattice decreases with burnup. Very likely, at high burnup most of the vacancies created are captured by permanent defects dispersed in the lattice, so that a sort of hardening of the matrix is produced. Consequently, gas swelling occurs only through growth of pores on extended defects, which act as structural sources of vacancies.

References

[1] F. Capone, J. P. Hiernaut, M. Martellenghi, C. Ronchi, Nucl. Sci. Eng. 124 (1996) 436-454
[2] C. Ronchi, I. Sakellaridis, Nucl. Sci. Eng. 95 (1987) 282-295
[3] C. Ronchi, J. Nucl. Mater. 148 (1987) 316-323

Contact (2.8): Claudio Ronchi • tel.: +49 7247 951 402 • fax: +49 7247 951 591 • ronchi@itu.fzk.de

2.9 Nuclides 2000: An Electronic Chart of the Nuclides on CD-ROM

The first edition of *Nuclides 2000* was successfully completed in June 1999. This is a commercial multimedia product consisting of a CD-ROM and an 82 page User Guide. Apart from providing basic nuclear data on over 2600 nuclides, the user can solve decay equations with a mouse "click". The package has been designed to be extremely user friendly and to appeal to both non-experts and experts alike. Nuclides 2000 has its own website at:

http://itumagill.fzk.de/nuclides_2000/

where the latest information on the product can be found together with further information, frequently asked questions (FAQs), Case Studies, ordering information etc. In the first six months on the market, we have over 200 registered users.

From the mainstream nuclear area customers include:
LANL, BNL, ORNL, LBL, GA, FZK, FZJ, FZ Rossendorf, EnBW, GRS, GSI, EDF, CEA, CNRS, ESRF, COGEMA, CERCA, CRIEPI, NOK, ENEA, Empr. Agrupados, CIEMAT, SCK-CEN, NRG, IAEA, UKAEA, PSI, VTT, Hungarian AEA, Studsvik Nuclear, ABB Atom, AEC, BARC.

From the field of medicine & medical isotopes:
Deutsches Krebsforschungszentrum, CIS Bio-international, MDS/Nordion, Mallinkrodt, Zentralklinik Bad Berka, Glostrup Hospital, The Royal Marsden NHS, etc.

Others organisations include:
The universities of Liège, Glasgow, Tohoku, Madrid, Hamburg, West of England, Bialystok, Institute Jozef Stefan, and Ohio State. Also Defence Research Establishment, Nuclear Cargo + Service GmbH, The Andriey Soltan Institute for Nuclear Studies, National Radiological Protection Board, Bundesamt für Strahlenschutz Institut für Strahlenschutz, GSF Forschungszentrum für Umwelt und Gesundheit, Neuherberg, SEIKO EG&G.

At present we are involved in the marketing of the product through the Nuclides 2000 website, information brochures, product announcements in magazines, product reviews in specialist journals, presentation at conferences, etc. Existing customers have been asked for feedback on the product through a questionnaire. An initial poll indicates customer

satisfaction and a strong interest in further development of the product. On this basis, a new edition is planned for the end of 2000. In this new edition, based on user feedback, the main new features will be

- the inclusion of averaged cross section data, and
- the possibility to do shielding calculations.

Other features, which are being considered, include

- a "wizard" for generating charts. This will allow the user to generate colour charts based on the property of choice (e.g. radiotoxicity)
- virtual nuclides. At present calculations can be made with only a single nuclide. This facility will allow calculations with an nuclide inventory
- nuclear reaction Q-values. This gives the user the possibility to investigate a variety of neutral and charged particles reactions. This powerful and flexible module will give information on whether particular reactions are exo- or endothermic, threshold energies, and allow the user to investigate unusual decay modes (e.g. heavy ion radioactivity)
- information on fission products and yield data

Contact (2.9): Joseph Magill • tel.: +49 7247 951 366
fax: +49 7247 951 591 • magill@itu.fzk.de

Fig. 2.28 Nuclides 2000 Home Page

3. Safety of Nuclear Fuel

3.1 Structural Investigations and Basic Studies at High Burn-up

3.1.1 Installation of two new microscopes in the hot cell facility

In the course of 1999 the equipment for the microscopic examination of irradiated nuclear materials in the hot cell laboratory has been renewed. The capabilities and performance of both electron and optical microscopy could thus be considerably improved.

Scanning Electron Microscope

In the early eighties a JEOL 35C scanning electron microscope (SEM) was installed in the hot cell facility at ITU. The microscope was especially adapted to analyze highly irradiated nuclear materials [1].

After nearly twenty years of service its performance had greatly deteriorated and therefore its replacement was necessary.

After decontamination of the existing beta-gamma glove box facility, a new JEOL JSM 6400 scanning microscope has been installed (see Fig. 3.1). This microscope operates at a variable accelerating voltage from 0.2 to 5 kV (100 V steps) and from 5 to 40 kV (1 kV steps). It is equipped with a shielded secondary electron detector for the examination of highly radioactive materials. It is used for surface characterization and its resolution varies according to the radiation level of the samples: for highly irradiated fuel pellets it is in the order of 20 nm and for non-irradiated materials it is in the order of 5 nm.

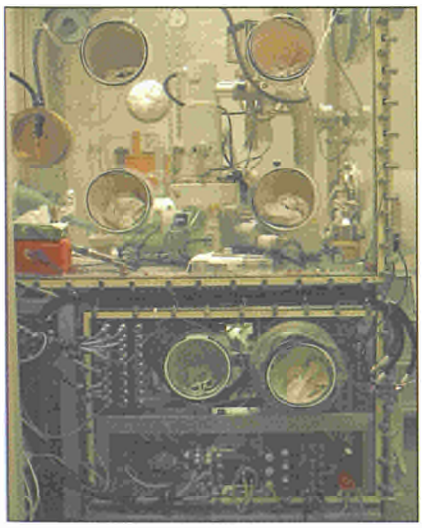

Fig. 3.1
View of the JSM 6400 microscope in the SEM beta-gamma facility of the Hot Cell Technology department, showing the glove box containing the column and specimen chamber (upper part) and the vacuum system with a turbo molecular pump (lower part).

Fig. 3.2 Telatom III optical microscope equipped with the Leica-QWin image analysis system in a beta-gamma hot cell facility.

In the year 2000 the instrument will be equipped with a Peltier cooled detector for energy dispersive X-ray analysis (EDX).

Optical microscope

The installation of a shielded remote-controlled optical microscope, Telatom III (Reichert-Leica) was completed. The lead shielded (15-25 cm wall thickness) beta-gamma -glove box shown in Fig. 3.2, is especially conceived for highly irradiated nuclear materials, mainly nuclear fuels. The optical microscope is equipped with a radiation resistant set of objective lenses, a Vickers micro-hardness testing device and the most recent version of a Leica-QWin, image analysis system. The transfer and displacement of the samples in the glove box is done by means of a computer controlled robotics system. Up to ten metallographic samples can be stored in the microscope compartment at any one time. They are transferred from the neighbouring cell, where they are polished, by means of a " La Calhène" connecting channel.

Reference:

[1] M. Coquerelle, P. Knappik, J-C. Perrier, J. Physique 45 (C2) (1984) 84

Contact (3.1.1): Achilleas Stalios • tel.: +49 7247 951 376 • fax: +49 7247 951 561 • stalios@itu.fzk.de

3.1.2 Performance of commercial PWR fuel rods at high burn-up

Since 1993 the Institute and Siemens-KWU have been co-operating in the study of the performance of high burn-up PWR fuel. The focus of the work is on fission gas release and swelling behaviour of the fuel and the contribution made by the high burn-up structure [1] to these quantities. In 1999, as part of this research co-operation, a fuel rod with an unusually high average burn-up of 98 MWd/kgU was examined at the Institute. It was seen that fuel microstructure changes in a continuous manner up to a pellet burn-up of at least 102 MWd/kgU. This finding is important because it means that existing computer codes can be used to predict fuel rod behaviour at ultra-high burn-up. Most significantly, no burn-up limiting phenomena were encountered. The fractional fission gas release determined by rod puncturing was about 28% at 100 MWd/kgU. (It is normally less than 10% at 50 MWd/kgU.) It was concluded that a large fraction of the gas released came from the inner regions of the pellet between the fuel centre and $r/r_o = 0.7$. In the outer regions of the pellet the high burn-up structure penetrates progressively deeper into the fuel with burn-up, and at 102 MWd/kgU, the highest burn-up seen, it extended over a distance of 1.15 mm to about $r/r_o = 0.75$. Above a pellet burn-up of about 70 MWd/kgU, the presence of the high burn-up structure leads to a change in the fuel swelling rate from the standard value of 1% per 10 MWd/kgU to 1.5% per 10 MWd/kgU (see Fig. 3.3).

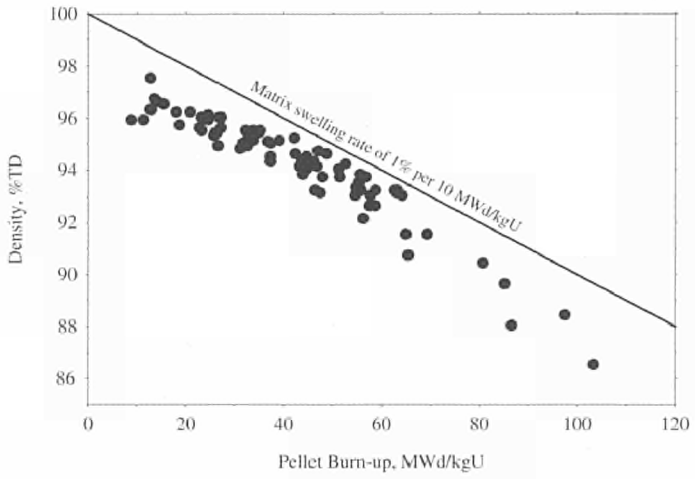

Fig. 3.3 Decrease in the density of PWR fuel with increase in pellet burn-up (after Manzel and Walker, ref. [2]). The solid line shows the density change resulting from a matrix swelling rate of 1% per 10 MWd/kgU (the standard value). Above 70 MWd/kgU, the widespread formation of the high burn-up structure in the outer region of the fuel causes the swelling rate to increase to 1.5% per 10 MWd/kgU. This is detected as a change in the rate at which the fuel density decreases with burn-up.

Electron probe microanalysis revealed that the concentration of the fission gas xenon in the recrystallised grains of the high burn-up structure did not increase with burn-up, but remained at a low level over the whole range of burn-up studied. In fuel pellets with burn-up greater than 80 MWd/kgU, it was observed that within a 100 µm of the fuel surface the gas pores of the high burn-up structure experienced enhanced growth (Fig. 3.4). At present, this growth is assumed to occur because there is a large reservoir of vacancies at the pellet rim where the fission density is two to three times higher than in the body of the fuel. At a pellet burn-up of 102 MWd/kgU, the growth of the gas pores at the pellet rim, where the burn-up was greater than 200 MWd/kgU, was apparently accompanied by the release of fission product caesium from the pellet.

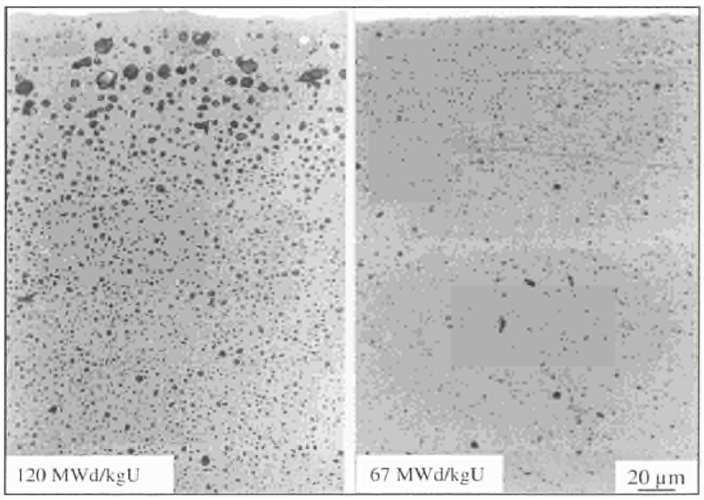

Fig. 3.4 Photomicrograghs showing the high burn-up structure at the surface PWR fuel pellets irradiated to a burn-up of 67 and 102 MWd/kgU. The gas pores have grown markedly in size with increased in burn-up.

References

[1] C.T. Walker, J. Nucl. Mater. 275 (1999) 56.

[2] R. Manzel, C.T. Walker, Proc. ANS International. Topical Meeting. on Light Water Fuel Performance, Park City, Utah, USA, 9-13 April 2000, p. 604

Contact (3.1.2): Clive Walker• tel.: +49 7247 951 477 • fax: +49 7247 951 591 • clive.walker@itu.fzk.de

3.1.3 Analysis of the corrosion properties of zircaloy cladding in LWR reactors (Siemens-KWU)

The different types of particles in an unirradiated cladding sample KWU 702-01, have been analysed to obtain a better understanding of their influence on the corrosion behaviour. This was a very extensive analysis involving the measurement of 1000 FeCr-rich (Laves phase) and FeNi-rich (Zintl phase) particles by TEM. In addition to this measurements have been made on larger FeNi-rich particles using SEM on a lightly etched surface of the cladding since many of the larger particles were lost in the electropolishing process and could not be seen by TEM.

For the first time the particles were also distinguished by their morphologies in cases where they were too small for EDX analysis. This enabled the full size range from 20 nm to 0.5 µm to be covered.

These results constitute a database with which the results on two specimens of cladding from high burn-up fuel rods are being compared.

Fig. 3.5 shows an example of a transmission electron micrograph of this material demonstrating the typical morphologies of the two types of particle.

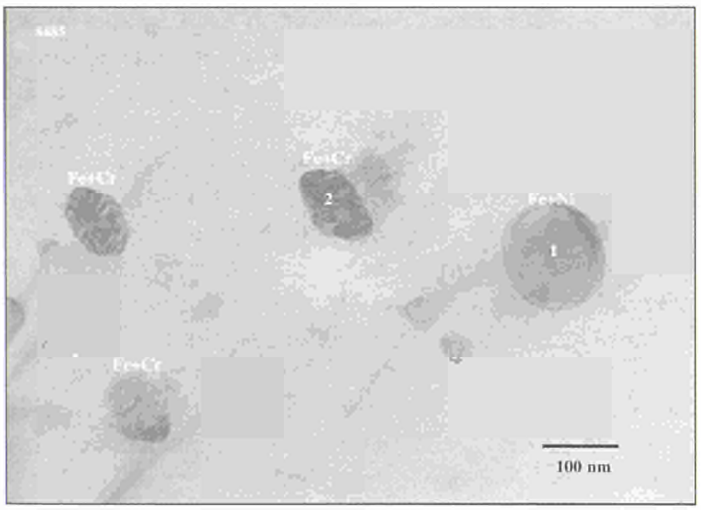

Fig. 3.5 Transmission electron micrograph of the unirradiated cladding reference sample KWU 702-01 showing the characteristic morphological differences between the FeCr-rich and FeNi-rich intermetallic particles. This enabled a type distinction to be made in cases where EDX analysis was not possible.

Contact (3.1.3): Ian Ray • tel.: +49 7247 951 378
fax: +49 7247 951 591 • ray@itu.fzk.de

3.1.4 Post-irradiation examination of pressurised and boiling water reactor fuel rods.

In the framework of the contract with Siemens AG-Bereich Energieerzeugung (KWU), non-destructive and destructive examinations of power reactor fuel rods were carried out. The work performed and described in the previous annual reports [1] has continued and a list of the types and number of examinations carried out on different fuel rods in 1999 is given in Tab. 3.1.

Tab. 3.1 Type and number of examinations performed on PWR and BWR fuel and cladding during 1999.

TYPE OF EXAMINATION	PERFORMED
Visual examination	4
Defects (cladding)	3
Gamma scanning	4
Fission gas analysis	5
Free volume determination	5
Metallography	14
Ceramography	1
Burn-up determination	1
EPMA	1
TEM	2
Re-fabrication	5
Creep test	2
Glow discharge	2
Chemical analysis	2
Creep (long term)	1
TOTAL:	52

In 1999 five fuel rods from a commercial PWR were transferred to our hot cells. The goal of the examinations was the study of the dimensional stability and oxidation behaviour of advanced cladding materials. In addition, 8 segments were re-fabricated and sent to the High Flux Reactor in Petten to examine their behaviour under Loss of Coolant Accident (ramp) conditions.

A new type of test was developed to examine the mechanical properties of high burnup fuel rods under intermediate storage conditions. It will enable the determination of the long-term creep properties of irradiated fuel rods. Cladding

material from pressurised and boiling water reactor fuel rods will be examined in a two year programme.

13 capsules containing fuel rods segments were shipped back to the pool of the reactor in which they had been irradiated.

Reference:

[1] EUR 14493 (TUAR-91), p. 199; EUR 15154 (TUAR-92), p. 199; EUR 15741 (TUAR-93), p. 227; EUR 16152 (TUAR-94), p. 205; EUR 16368 (TUAR-95), p. 199; EUR 17296 (TUAR-96), p. 127; EUR 17746 (TUAR-97), p. 74; EUR 18715 (TUAR-98), p. 74.

Contact (3.1.4):
Enrique H. Toscano • tel.: +49 7247 951 409
fax: +49 7247 951 591 • toscano@itu.fzk.de

3.1.5 The RIM effect irradiation

The PIE investigations for the International High Burnup Rim Project, HBRP, were continued and are near to being concluded. The aim of this project is to study the threshold values of burnup bu, temperature T, pressure p and type of fuel for the formation of the rim structure [1,2]. The project is managed by the Central Research Institute of Electric Power Industry, CRIEPI, and is sponsored by 23 different organisations.
Ceramography, scanning and transmission electron microscopy, XRD analyses, density and oxygen potential measurements, Knudsen cell effusion and hot cell annealing tests as well as thermal diffusivity measurements were all performed on a larger number of fuel disks with selected values of bu, T and p. The work will be concluded in the year 2000.

References

[1] M. Kinoshita, S. Kitajima, T. Kameyama, T. Matsumura, E. Kolstad, Hj. Matzke, ANS Int. Topical Meeting on LWR Fuel Performance: "Going Beyond Current Burnup Limits", Portland, March 2-6, 1997, Proceedings ANS (1997) p. 530

[2] T. Sonoda, Hj. Matzke and M. Kinoshita: „High Burnup Rim Project: Threshold Burnup of Rim Structure Formation", Enlarged Halden Project Meeting, Loen, May 1999, Proc. Paper F 1.1

Contact (3.1.5):
Hansjoachim Matzke • tel.: +49 7247 951 273
fax: +49 7247 951 591 • matzke@itu.fzk.de

3.2 High Burn-up MOX Fuel

3.2.1 Introduction of large-area quantitative X-ray mapping in electron probe microanalysis

The reporting period saw the introduction of a new electron probe microanalysis technique: large-area, false-colour, quantitative X-ray mapping. The technique, which reveals the variation in concentration of a given element in a selected area, has been successfully employed to assess the homogeneity of BNFL's SBR MOX fuel after irradiation, and the homogeneity of MIMAS MOX fuel prepared at the Institute by three different fabrication routes. The technique has been found to be greatly superior to X-ray line profiling which is used for the same purpose, but can only provide information in one dimension. The technique also has the advantage that, in addition to supplying quantitative data on the distribution of an element, information on the size, morphology and volume fraction of the different phases present can be obtained through image processing.
The greatest challenge in making a large area (≥ 1 mm^2) X-ray map is to obtain a high resolution image. This was achieved by producing a collage of X-ray maps acquired using classical conditions; magnification X 400, spatial resolution 256 x 256 pixels, and each covering an area measuring roughly 250 x 250 µm. The individual maps are converted to quantitative images using a standard and by applying background and matrix corrections to the measured X-ray count in each picture element (pixel). The matrix correction was made using the Himax® software package and the Xmas® program from SAMx. The background correction, although acknowledged to be an important step, was not performed because its usefulness is limited for elements of high concentration. The composite area picture was produced using the "Multiple Image Alignment" function of the AnalySIS® image processing software. A compositional map for Pu in a MIMAS MOX fuel pellet is shown in Fig. 3.6.

Fig. 3.7 shows histograms for the distribution of the Pu concentration in the pellet by area fraction and cumulative area fraction.

3.2.2 Post-irradiation examination of BNFL's first commercially irradiated SBR MOX fuel

British Nuclear Fuels (BNFL) has entrusted the Institute with the detailed non-destructive and destructive examinations of seven fuel rods with average burn-ups of 33 GWd/tM

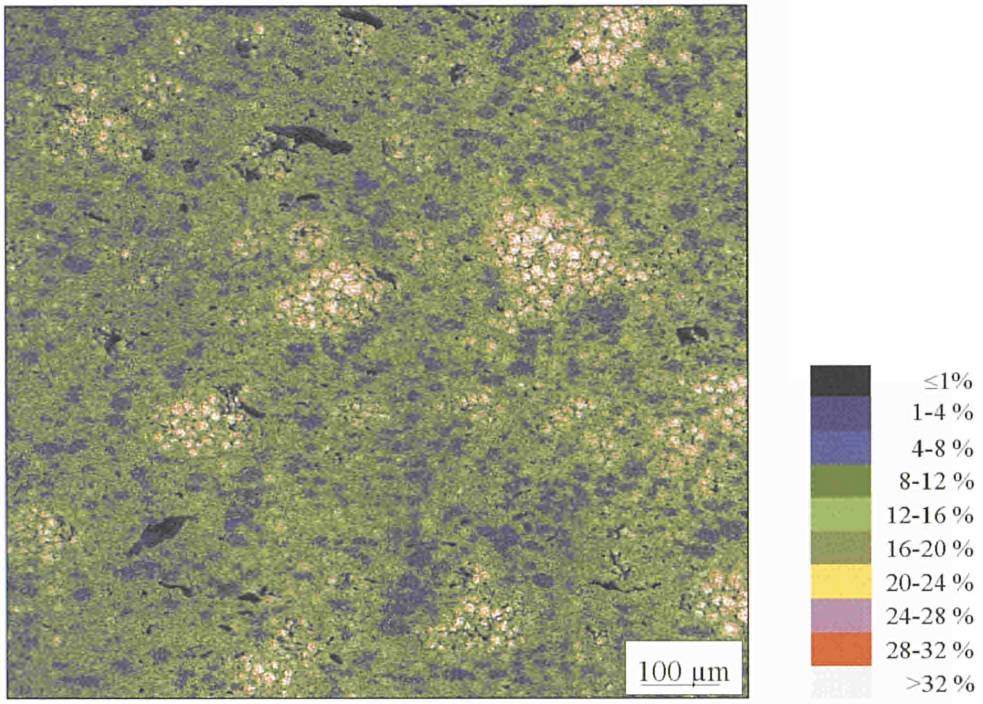

Fig. 3.6 False colour quantitative X-ray map for the distribution of Pu in a (U,Pu)O_2 MOX fuel fabricated by the MIMAS process at the Institute. The local Pu concentration varies from less than 4 wt% to up to 60 wt%. Resolution 950 x 920 pixels. Total dwell time 14.5 hrs

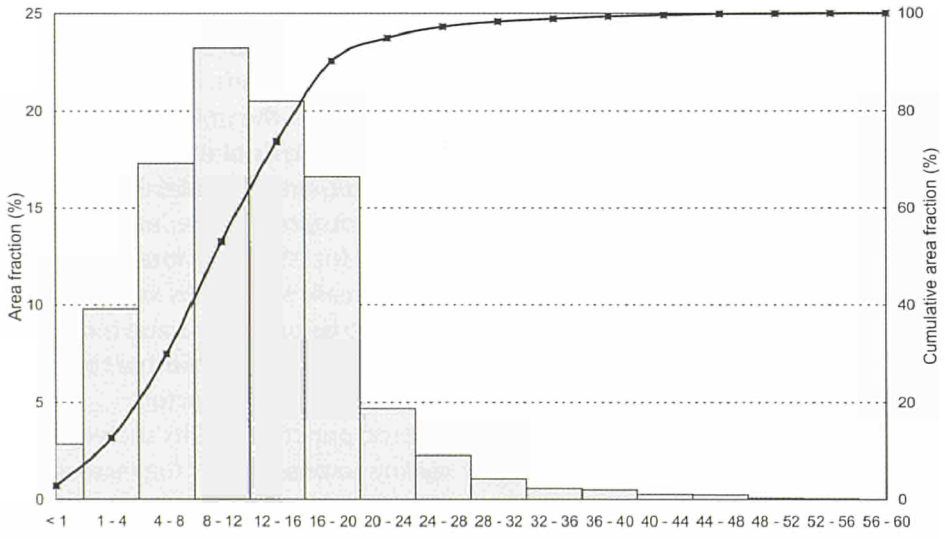

Fig. 3.7 Histograms for the distribution of Pu in a (U,Pu)O_2 MOX fuel fabricated by the MIMAS process as revealed by imaging processing of the quantitative X-ray map in Fig. 3.6. Areas containing 10-14 wt% Pu constitute about 23% of the fuel. Specified Pu concentration 12 wt%.

(where M = heavy metal). In 1999 the non-destructive examination of these rods was completed. A wide range of examinations were performed including:

- Visual examination and rod length measurement
- Cladding oxide thickness measurements and defect testing by eddy current
- Fuel rod diameter profilometry at high resolution
- Gross and isotopic gamma-scanning
- Rod puncture to determine the percentage of fission gas release and the isotopic composition of the gas; the internal rod pressure and the free volume reduction.

It was confirmed that the performance of the fuel rods had been very good with significant margins to the design limits. No clad defects were detected by the visual examinations and eddy current testing. Eddy current measurements revealed that the thickness of the oxide layer on the outer cladding surface was 30 µm or less in all cases. Over most of the rod length the oxide thickness was well below 20 µm. Profilometry showed creep-down of the cladding along most of the rod length and creep reversal due to fission product swelling (see Fig. 3.8). The increase in fuel rod length during irradiation was in line with what would be expected for UO_2 rods at a burn-up of 35 GWd/tM.

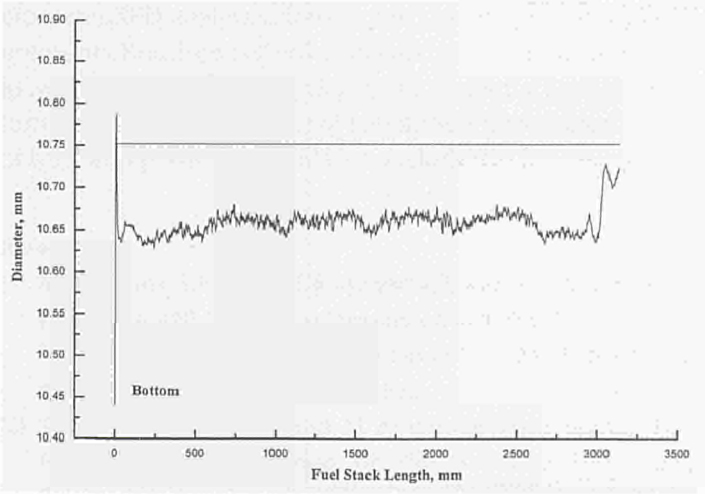

Fig. 3.8 An example of a diameter profile from one of the SBR MOX fuel rods. Clad creep-down has occurred along the entire length of the rod. The profile shows evidence of fuel-clad contact and creep reversal due to fuel swelling.

The gross gamma-scans displayed a generally flat burn-up profile with local intensity reductions at the spacer grids and a steep fall off in gamma-activity at the ends of the rods (see Fig. 3.9).

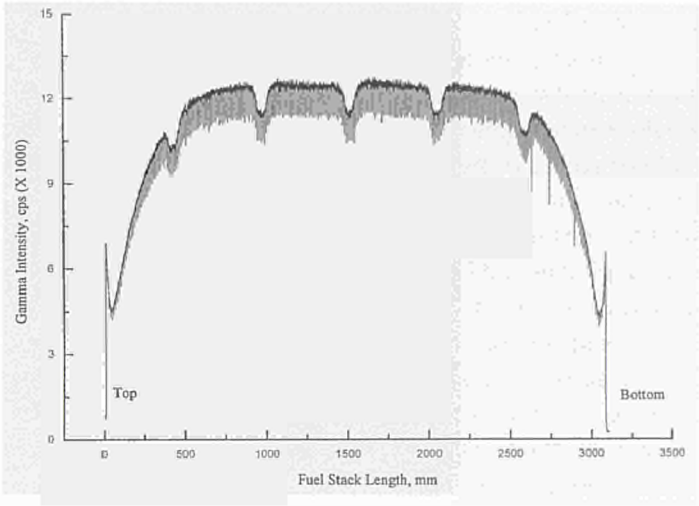

Fig. 3.9 Typical gross gamma-scan from one of the SBR MOX fuel rods. The effect of the spacer grids in lowering the burn-up is clearly seen. The pellet-pellet interfaces are fully resolved indicating that little axial migration of fission product caesium as occurred and that dimple filling due to fuel creep was also limited.

The isotopic gamma-scans present a similar picture to the gross gamma-scans. Most importantly, there is little if any evidence for the migration of fission product caesium. Detailed analysis of the gross gamma-scans using the computer program "Gamble", which was specifically developed for this purpose at the Institute, revealed that in all seven rods the fuel stack was intact with no large inter-pellet gaps. The increase in the fuel stack length was also determined from the gamma scans and indicates that the fuel swelling rate is similar to that of other types of MOX fuel irradiated in commercial power reactors.

The rod puncture results showed that clad creep-down was mainly responsible for the increase in the rod internal pressure during irradiation and that fission gas release was low (<0.6% in six of the rods). In the one rod to show any significant thermal release (1.1%), the temperature at the fuel centre had just exceeded the Vitanza threshold [1] at the end of life. This suggests that the mechanisms of gas release are similar to those operating in UO_2 fuel.

A detailed account of the non-destructive examination results was given at the IAEA International Symposium on MOX Fuel Cycle Technologies in Vienna in 1999 [2] and a further report which included the results of optical ceramography and electron probe microanalysis was made at the ANS International Topical Meeting on LWR Fuel Performance in the USA in April this year [3].

References

[1] C. Vitanza, E. Kolstad, U. Graziani, in Proc. ANS Topical Meeting on Light Water Reactor Fuel Performance, Portland, USA, 1979, p.366.

[2] P. Cook, I. Palmer, R. Stratton, C.T. Walker, in Proc. IAEA Internat. Symposium on MOX Fuel Cycle Technologies in Medium and Long-Term Deployment, Vienna Austria, 17-22 May 1999, paper IAEA-SM-358/16, in press.

[3] P. Cook, R. Stratton, C.T. Walker, in Proc. ANS Topical Meeting on Light Water Reactor Fuel Performance, Park City, USA, 9-13 April 2000, p. 653.

Contact (3.2): Clive Walker • tel.: +49 7247 951 477
fax: +49 7247 951 509 • clive.walker@itu.fzk.de

3.3 Interaction of Structural Materials with Irradiated UO_2 Fuel

3.3.1 Corium interaction thermochemistry project (CIT)

In the previous annual report (TUAR '98, p. 78-79) the experiments carried out with 3 mm high, cladded, irradiated UO_2 fuel segments and 3 mm high, cladded non-irradiated UO_2 segments at 2000 °C under inert atmospheres for 25s to 190s were reported. The irradiated UO_2 was BR3 fuel with 53 GWd/tU burn-up. This year's report will outline the results of optical phase analysis and microprobe analysis of the melts used to assess the kinetics of the irradiated UO_2 dissolution by zircaloy dissolution

The irradiated fuel melt (see Fig. 3.10) showed two main phases: an U-rich ceramic phase and a Zircaloy-rich metallic phase. These corresponded to compositions of 77 w/o U and 12 w/o Zr ($(U_{0.73}Zr_{0.27})O_2$) for the ceramic phase and 8 w/o U and 91 w/o Zr ($Zr_{0.97}U_{0.03}$) for the metallic phase. Additionally some occasional very dense U,Zr phases were noted with 2 w/o Mo.

The fuel showed no penetration by diffusion of Zircaloy. Small metallic spherical precipitates were observed in the heat-treated fuel that contained Tc, Ru, Mo and sometimes Pd (occasional, very fine, metallic precipitates had been observed in the fuel matrix before the test). These were evidently the so-called 5-metal fission product precipitates. These had rapidly grown during the heat treatment at 2000 °C, often forming within the grains. These have often been observed in the Phebus corium [1]. Sometimes they may have continued to exist after dissolution of the fuel, sometimes they have dissolved up and interacted with stainless steel components (especially Ni) to form new intermetallic precipitates.

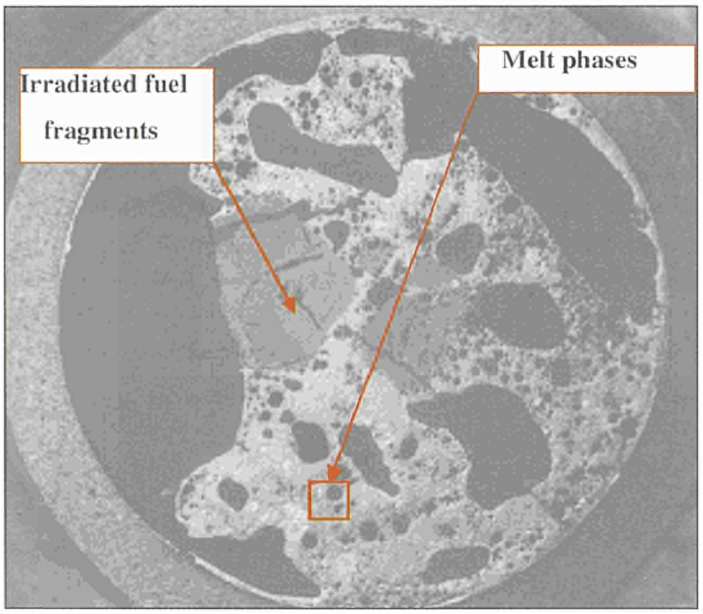

Fig. 3.10 Macro-photograph of an irradiated fuel segment after 190s at 2000 °C under inert Ar atmosphere (5x mag).

The porosity of the CIT fuel is very high (reaching 30%) due to the fission gas bubble formation and its release. The fuel itself fractures into smaller pieces due to cracks and fissures pre-existing in the irradiated state. This compares with larger, slower break-up seen in the corresponding non-irradiated fuel sample (Fig. 3.11). Thus, the faster attack of the irradiated UO_2 compared to the non-irradiated fuel is due to its cracked state and to the fission gas bubble formation forming a larger surface area for fluxing by the liquid Zircaloy.
The phase analysis of the ceramic and metallic phases was combined with the microprobe analysis of the irradiated UO_2 to determine the total U content of the melt. This was compared with the U content in U-Zircaloy melts from non-irradiated UO_2-Zircaloy dissolution experiments performed

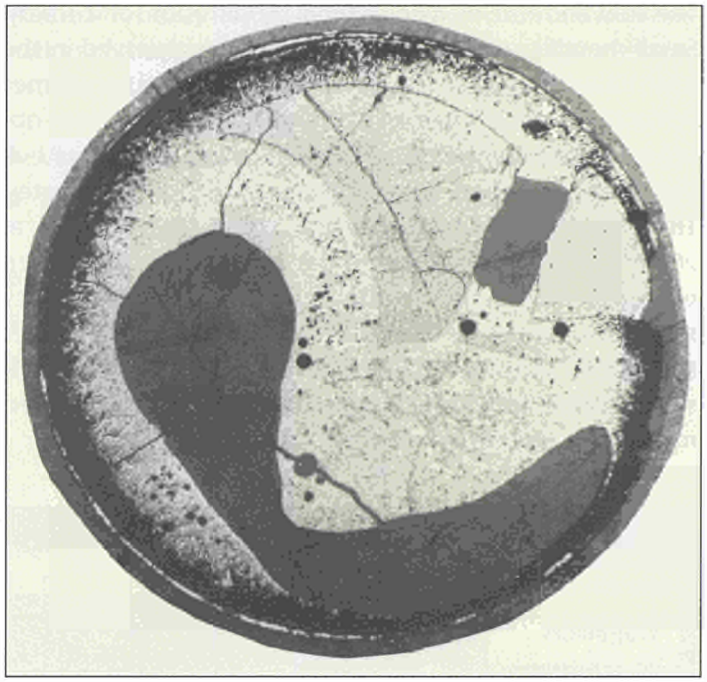

Fig. 3.11 Macro-photograph of a non-irradiated fuel segment after 190s at 2000°C under inert Ar atmosphere (5x mag).

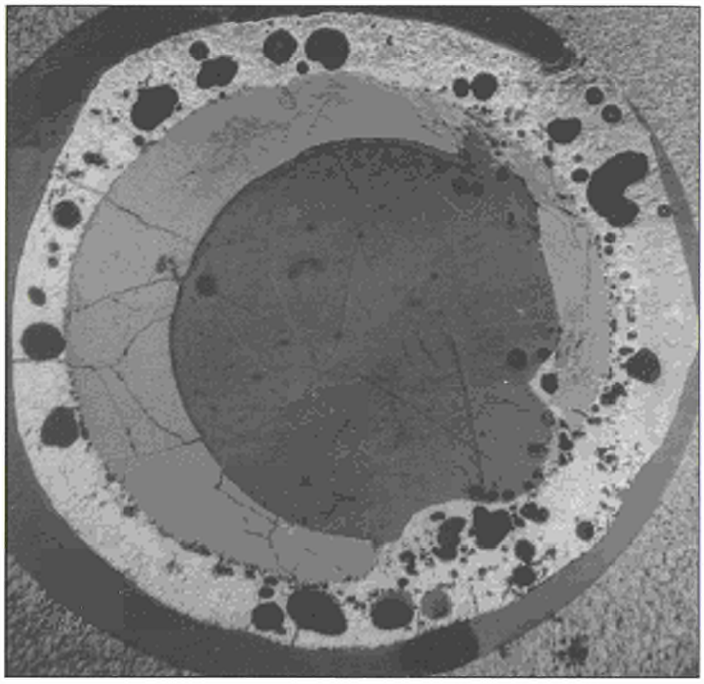

Fig. 3.12 Macrograph of the low temperature irradiated fuel segment after heating for 600 s to 1740 °C under inert He atmosphere. The swelling of the cladding and its interaction with the fuel is clearly evident. (5x mag.)

at 2000-2200 °C by other partners in the project. The U content for irradiated fuel dissolution by Zircaloy melt at 2000 °C appeared to be similar to the U content in Zircaloy melts dissolving non-irradiated fuel at about 2150 °C. This implies that the dissolution rate of irradiated fuel is somewhat higher than that of non-irradiated fuel.

Modelling based on the non-irradiated fuel indicates a rapid initial UO_2 dissolution phase followed by a precipitation phase of a ceramic (U, Zr)O_2 phase in the saturated liquid Zircaloy, during which the UO_2 dissolution is much slower. In contrast, we noted no saturation phase of slowed UO_2 dissolution for the irradiated fuel. However, the testing times may need to be extended to observe this saturation.

A further test at approximately the melting point of Zircaloy (~ 1750 °C) was also carried out with a 3 mm thick segment of the cladded irradiated fuel for 600s under inert (He) atmosphere. It is seen (Fig. 3.12) that the cladding has become considerably thicker (~ 1.1 mm thick instead of approx. 0.64 mm thick) with large bubbles and that it contains two phases: a darker ceramic phase of approx. 8 w/o Zircaloy ($(U_{0.75}Zr_{0.25})O_2$) and a lighter metallic phase of composition 89 w/o Zr and 4 w/o U ($Zr_{0.99}U_{0.01}$).

The swelling may have contributions from the Zircaloy slumping from above, as well as from large bubbles of either fission gas from the fuel (which is also seen to be very porous) or from the hydrides formed in the Zircaloy cladding during the irradiation that exsolve during the heating. As to the smaller bubbles at the fuel/cladding boundary these are almost certainly due to fission gas release. Thus, the interaction between Zircaloy and irradiated fuel appears to commence directly upon zircaloy melting with the formation of the same phases as at 2000 – 2200 °C.

References

[1] P.D.W. Bottomley, S. Bremiér, J.-P. Glatz, C.T. Walker, 6th European Microbeam Analysis Society Workshop, 3-7 May '99, Konstanz, (Mikrochimica Acta, in press)

3.3.2 Phebus FPT1 bundle post-irradiation examination (PIE)

The cutting of the FPT1 bundle into discs, followed by cutting out of selected samples from these discs for optical microscopy and microanalysis, along with the first optical microscopy results, was reported in the previous annual report

(TUAR '98, p. 73-74). The microscopic examination and microprobe analysis of the remaining samples were completed during this year.

The samples examined came from the upper and lower corium pool, the cavity above the pool as well as from severely degraded remnants from the mid-height zone. Microprobe line and spot analyses were performed across the central zone of the corium pool. These indicated that the corium composition was uniform and corresponded to $(U_{0.52}Zr_{0.44}Fe_{0.03}Cr_{0.01})\ O_{2\pm x}$. This represents a melting together of the UO_2 fuel and Zircaloy and its oxidation along with some incorporation of Fe and Cr from the steel and nickel-based structural materials. The oxygen content was difficult to establish but showed no consistent large deviation from stoichiometry. Thus despite a steam atmosphere, there has been no significant oxidation of the fuel to higher, more volatile oxides such as UO_3. No such oxides were observed as separate phases in the corium or elsewhere in the bundle.

Minor amounts of secondary phases were observed at the grain boundaries of the corium. These usually contained Fe, Ni, and Cr from the structural materials, from the cladding or thermocouples, and were usually in the oxide state. Additionally spherical metallic inclusions were observed intragranularly as well as at the grain boundaries of 1-10 μm size, this compares with a size of 1 μm for similar spherical precipitates observed in fuel fragments nearby the corium. Microprobe analyses of the fuel precipitates showed these to contain Pd, Ru and Tc and so these are assumed to be the 5-metal fission products that had precipitated out in the overheated fuel grains before dissolution. Microprobe analyses of the larger corium precipitates revealed them to be Ni-rich but containing Ru, Tc, and Pd. This latter observation indicates that at least some of the 5-metal precipitates have undergone reactions with structural materials in the melt. Moreover, fission and activation products such as Nd, Ce and Pu were also detected in the melt by microprobe analysis-unlike FPT0, where the trace-irradiated fuel did not have them in detectible quantities. Similarly the non-irradiated instrumented fuel rods had no 5-metal precipitates.

Fig. 3.13 Section across a half-melted fuel rod surrounded by corium at the outer edge of the cavity just above the corium pool (+261 mm from bottom of the bundle) (Mag. 6x)

The very high porosity of the irradiated fuel as it is dissolved by the $(U,Zr)O_2$ corium heated to at least 2500 °C has already been commented on in the previous Annual Report TUAR '98 (p. 73-74), as well as its role in accelerating the attack by increasing the surface area for interaction. The cavity above the corium showed semicircular cross-sections of attacked fuel rods with high porosity at their inner edges (Fig. 3.13).

The clearly defined melting edge across the rod indicates a high thermal gradient and thus the corium must have sufficient superheat above its minimum melting temperature (estimated at 2500°C) to rapidly attack UO_2 fuel (even non-irradiated fuel rods). This probably represents the hottest zone of the fuel bundle before it fused and relocated downwards as a corium.

The mid-bundle contained inner fuel rod remnants above the cavity (Fig. 3.14).
These show little corium present. The fuel is porous and fractured and the cladding remnants are completely oxidised and have deformed. The oxide has two layers of columnar grains due to simultaneous inner and outer attack and indicates the cladding had already ruptured to allow steam to oxidise the inner surface of the cladding. No higher oxides of uranium were observed in these fuel fragments. The fuel however, had become very porous reaching well over 50% in some places. Some local liquefaction of the UO_2 fuel was observed which was due to the melted Zircaloy running down the interface. The large metallic inclusions observed within some fuel fragments could be liquefied Zircaloy-Ni-Fe intermetallics that had penetrated the fuel via fissures.

Fig. 3.14 Section through fuel rod remnants and oxidised and deformed cladding fragments at mid- height in the test assembly (+473 mm from bottom of the bundle) (Mag. 5x)

However, liquefaction was not as important in general as at the lower heights, and physical fracturing and collapse of solid materials also contributed to the relocation downward from the bundle mid-height whereas the corium pool is evidently a cumulation point. The remaining structures have evidently undergone substantial degradation in a solid state for long periods at high temperatures since most of the remaining Zircaloy was fully oxidised to ZrO_2.
The remaining measurements are a final microprobe analysis of a fuel fragment at the bundle mid-height, as well as a series of melting point determinations by laser flash pyrometry of the irradiated and non-irradiated fuel from the corium pool and the fuel at mid-height. The corium pool's melting point will also be determined.

Contact (3.3): David Bottomley • tel: +49 7247 951 364 • fax: +49 7247 951 561 • bottomley@itu.fzk.de

3.4 The Fuel Performance Code TRANSURANUS

The TRANSURANUS research network

TRANSURANUS is a computer program for the thermal and mechanical analysis of fuel rods in nuclear reactors which has been developed at the European Institute for Transuranium Elements [1]. It is fully described in the literature and has been outlined in previous Annual Reports. The code is in use in several European organisations, both research and private industry and is under continuous development.

The close collaboration with several groups, especially from Eastern European, continued. Version V1M1J99 of the TRANSURANUS code, has been released to all users together with the pre- and post processors as well as a revised handbook.

Within the IAEA "Third International Seminar on WWER Fuel Performance, Modelling and Experimental Support", 4-8 October 1999, Pamporovo, Bulgaria, the Third TRANSURANUS User's Meeting was held. Approximately 30 participants from 12 countries discussed WWER related problems, the application of the TRANSURANUS-WWER version and its application to safety criteria. The course was supported by the IAEA under the regional technical co-operation program RER 4/019 ("Licensing fuel and modelling codes for VVER reactors").

Specific TRANSURANUS model developments and results

The work on the development of high burn-up models continued. The question raised in the previous annual report

"Where does the increased fission gas come from that is observed at extended burn-up in all reactor irradiations:

1. from the inner hot regions by thermal gas release processes or
2. by an athermal process from the outer cold regions that show the High Burn-up Structure?"

could not yet be answered. From the analysis of WWER-440 irradiations up to a very high burn-up (KOLA-3 data from the

IFPE database) it is concluded that the maximum temperatures at end of life are far below the presently accepted Vitanza threshold. If gas release from the high burn-up structure is assumed in our theoretical fission gas release model, a good agreement between measured and predicted fission gas release is obtained. However, the predicted Xe/Kr ratio is in disagreement with other (but similar) irradiations.

Analysis of the thermal conductivity at high burn-up

In view of its relevance, an extensive review of the degradation of the thermal conductivity with burn-up was per-

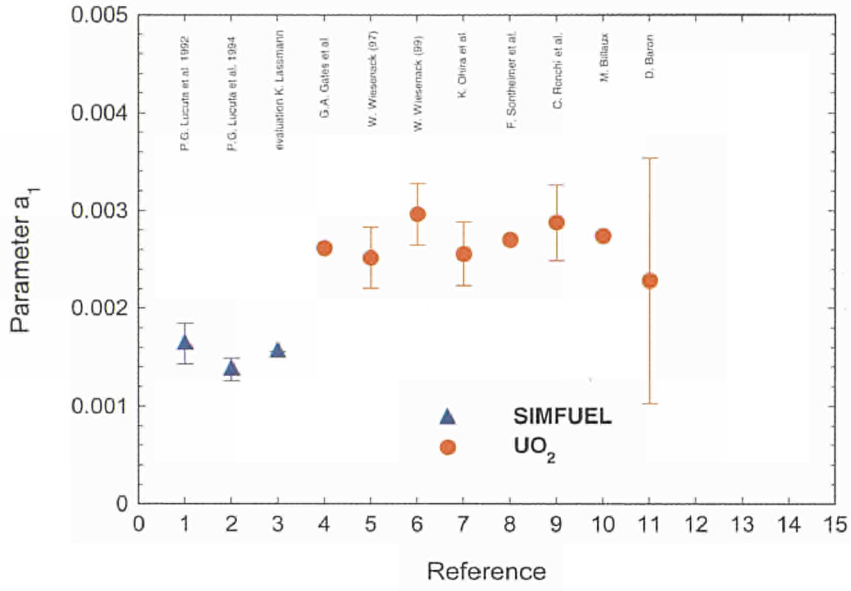

Fig. 3.15 Comparison of the coefficient a_1, that describes the degradation of the thermal conductivity with burn-up, according to various references. As can be seen, Simfuel gives a significantly lower value than irradiated UO_2.

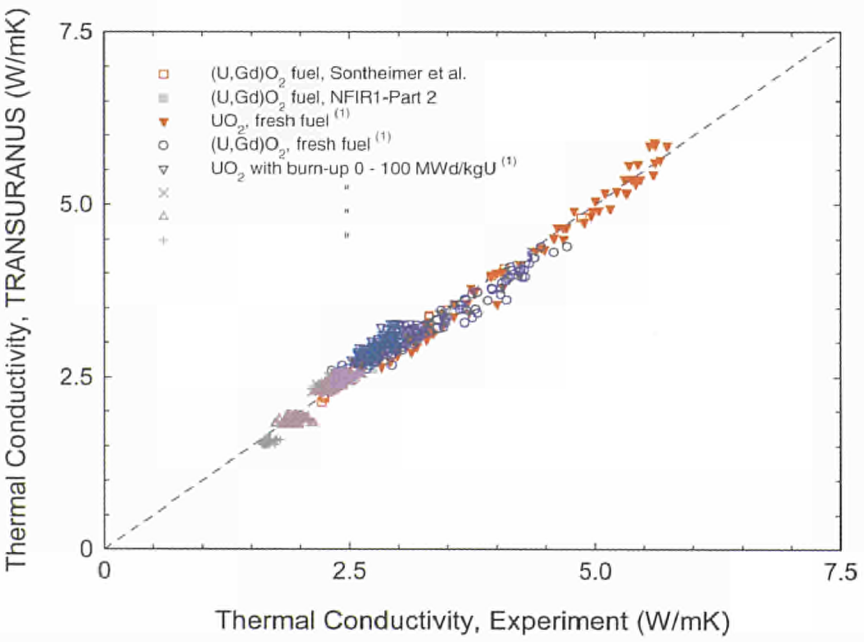

Fig. 3.16 Comparison between measured and evaluated thermal conductivities; (1) indicates the measurements of C. Ronchi and M. Sheindlin.

formed. In order to compare the various correlations from the literature, a conversion to the simplest form of the phonon term

$$\lambda = 1 / (a_0 + a_1 bu + bT)$$

was made, where λ is the thermal conductivity, T the temperature and a_0, a_1 and b are parameters. Fig. 3.15 shows that there is a very consistent picture of the coefficient a_1. In addition, it can be seen that the results from Simfuel measurements gave a significantly lower value, due to the fact that radiation effects such as the formation of bubbles are not accounted for.

Several correlations for the thermal conductivity from the open literature have been incorporated into the TRANSURANUS code. An own correlation, developed from ITU measurements of C. Ronchi and M. Sheindlin, summarizes our present-day knowledge. This correlation includes the effect of gadolinium. Fig. 3.16 shows the good agreement between this correlation and measured data for a wide range of conditions.

Further development of the transient TRANSURANUS version

A simple one-group point kinetics model has been incorporated into the TRANSURANUS code version v1m2j99. Several different numerical techniques to solve the very sensitive feedback between temperature and reactivity have been carefully investigated. Two sample calculations demonstrate the capabilities of the model for a WWER-440 reactor at begin and end of life at full power conditions. The RIA analysed is initiated by the ejection of a rod within 0.15 s. This is a conservative value compared with realistic values that are in the range of 0.5 s. During this time of 0.15 s a reactivity of 0.01 is injected, corresponding to 1.56 $ at BOL and 1.79 $ EOL, respectively. Typical WWER-440 conditions were applied. The emergency scram is assumed to occur after 2 s. As can be seen in Fig. 3.17a and 3.17b, however, the transient is over long before the scram occurs. Details of this investigation are given in Ref. [2].

The main goal of this work is to better analyse the failure propensity under all conditions up to very high burn-up. Clearly, details of the fuel rod such as gap size, burn-up, embrittlement of cladding etc. need to be taken into account.

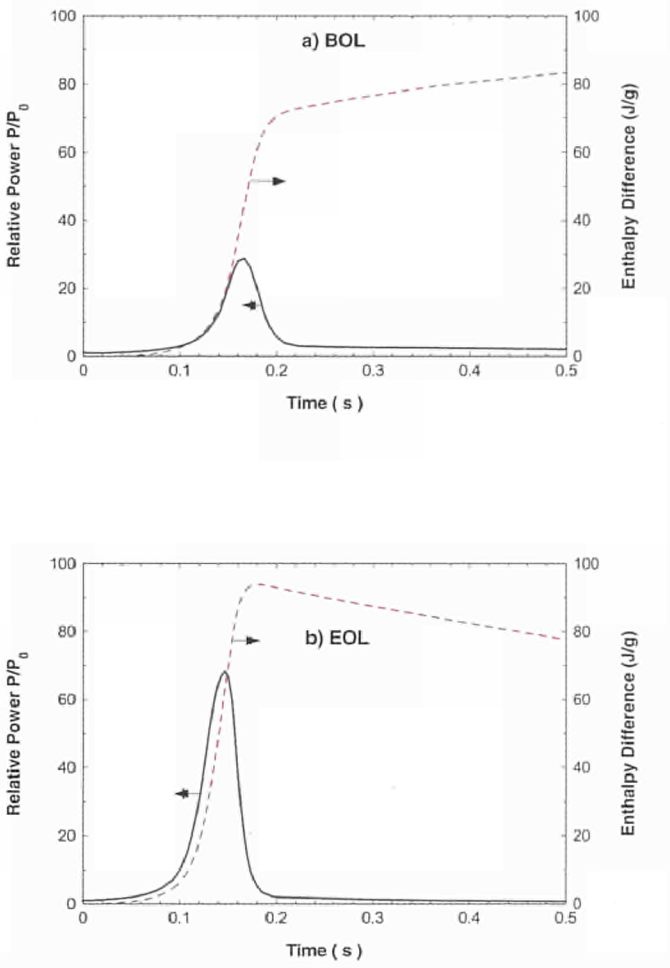

Fig. 3.17 Relative power P/P_0 (full line, left scale) and average enthalpy difference (dashed line, right scale) in the highest rated fuel section during the RIA as calculated by the built-in point kinetics model of the TRANURANUS code; The data refer to WWER-440 conditions followed by a reactivity injection of 0.01.

References

[1] K. Lassmann; Journal of Nuclear Materials 188 (1992) 295-302.

[2] K. Lassmann, J. van de Laar, D. Elenkov, Analysis of RIA accidents for WWER reactors employing the TRANSURANUS code, Paper presented at the "Third International Seminar on WWER Fuel Performance, Modelling and Experimental Support", 4-8 October 1999, Pamporovo, Bulgaria

Contact (3.4): Klaus Laßmann • tel: +49 7247 951 297
fax: +49 7247 951 591 • k.lassmann@itu.fzk.de

3.5 Development of Advanced Fuels

The attainment of high fuel burn-ups is one way by which the economy of the nuclear fuel cycle could be improved. Reactors would require less fuel element recharging and the volume of spent fuel to be conditioned for direct geological disposal or reprocessing would be reduced. In the case of UO_2, such savings must be offset against larger fuel costs due to the higher initial enrichment. For MOX no such additional cost is ensued.

The present burn-up limit in commercial light water reactors, for UO_2 fuel 50-60 MWd/kgHM and for MOX 40-50 MWd/kgHM, is determined by a number of factors. One of these is fission gas release, which is higher in MOX than in UO_2. One possibility considered to improve the retention of fission gases is the fabrication of fuels with larger grains (ca. 50 µm). For UO_2 several such fuels are being irradiated to determine their performance at higher burn-up [1].

In a first step, the sol-gel process provides a means to fabricate homogeneous MOX reference fuel directly. The process involves the preparation of a solution containing Pu and Uranyl Nitrate in the desired composition, which is converted into beads in a droplet to particle conversion step. The resulting particles are dried, calcined and compacted into pellets which are sintered at elevated temperature (ca 1650 °C) under an Ar/H_2 atmosphere. Fig. 3.18 shows a ceramograph of a $(U_{0.85}Pu_{0.15})O_2$ fuel prepared by sintering for 4 hours under a dry Ar/H_2 atmosphere. This fuel has a grain size of ca. 12 µm (Mean Linear Intercept – MLI method without correction).

Larger grains can be obtained by the addition of small quantities of water vapour to the sintering gas and extending the sintering time. In Fig. 3.19 the ceramograph corresponds to the same fuel, but sintered for 24 hours in a humid (P_{H_2}/P_{H_2O} = 33) Ar/H_2 atmosphere. A grain size of 35 µm is obtained. Unlike UO_2 or MOX produced by the sol gel process, industrial MOX fuels produced by powder metallurgy (e.g. MIMAS) exhibit an inhomogeneous distribution of the fissile material in the fuel pellets, as the micronised master blend (with typically 30% Pu) is diluted to the required fissile composition by mixing with UO_2 prior to pelletisation. Thus, higher burn-up fuels probably necessitate homogenisation of the Pu distribution along with increasing the grain size. Addition of mullite ($3Al_2O_3.2SiO_2$) to the diluting UO_2 enhances both effects. Fig. 3.20 shows the ceramographs following UO_2 and $(U,Pu)O_2$ etching of a MIMAS fuel obtained following addition of 1000 ppm of mullite. In contrast to a traditional MIMAS fuel without additives, isolated regions of UO_2 are found dispersed through a $(U,Pu)O_2$ matrix. In addition, the grain size of the $(U,Pu)O_2$ matrix is increased to about 20 µm. A similar result has been obtained without recourse to additives, but when an advanced UO_2 powder is used in the dilution step.

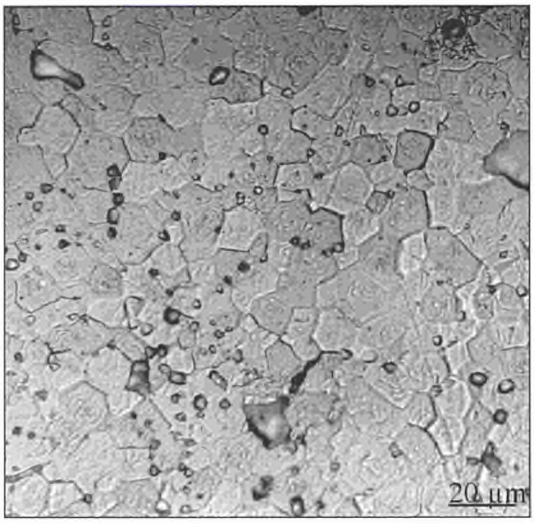

Fig. 3.18 Micrograph of a MOX fuel produced by the sol-gel method following sintering under a dry Ar/H_2 atmosphere for 4 hours.

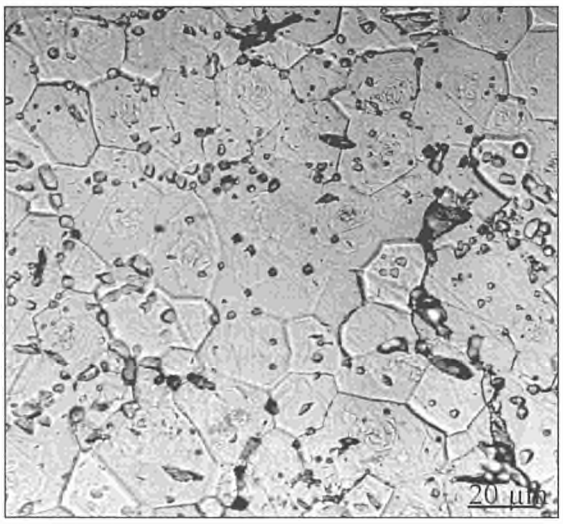

Fig. 3.19 Micrograph of a MOX fuel produced by the sol gel method following sintering under a humid (P_{H_2}/P_{H_2O} = 33) Ar/H_2 atmosphere for 24 hours.

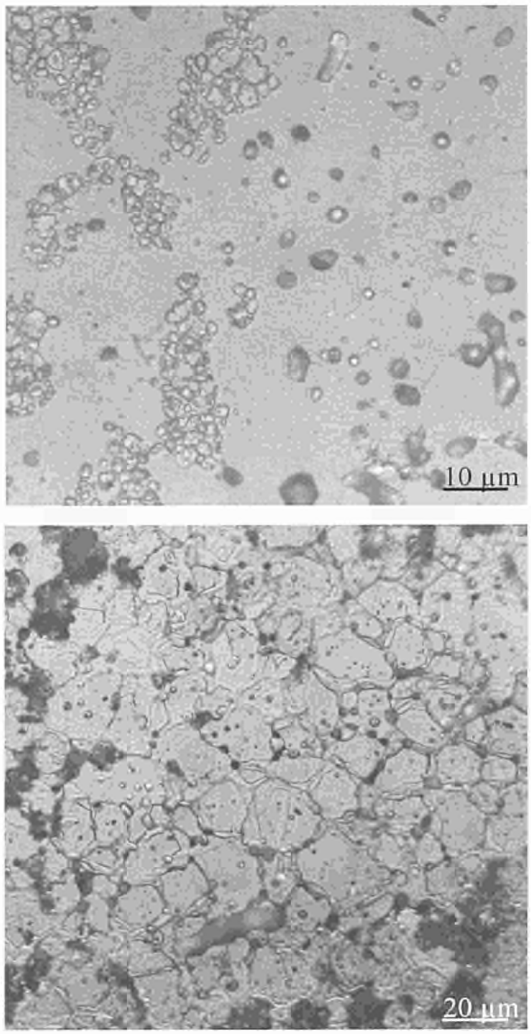

Fig. 3.20 Micrographs of an homogenised MOX fuel produced by the MIMAS process with addition of mullite (1000 ppm) in the diluting UO_2 (UO_2 etching above; $(U,Pu)O_2$ etching below).

Further EPMA investigations are underway to quantify the homogenisation of these fuels. Additional experiments will be performed to understand the phenomena causing the diffusion processes leading to homogenisation so that the process can be optimised for the production of fuels with specific grain sizes, and distributions of the fissile material throughout the fuel.

Reference

[1] M. Hirai, T. Hosokawa, R. Yuda, K. Une, S. Kashibe, K. Nogita, Y. Shirai, H. Harada, T. Kogai, T. Kubo, J.H. Davies, Proceedings of the 1997 International Topical Meeting on LWR Fuel Performance (1997) 490

Contact (3.5): Joseph Somers • tel.: +49 7247 951 359 • fax: +49 7247 951 566 • somers@itu.fzk.de

4 Partitioning and Transmutation

4.1 Advanced Reprocessing of Irradiated Fuels

Two contributions to this chapter can be found in part A:

- Separation of Minor Actinides from Lanthanides (see highlight, p. 26)
- Partitioning Studies at ITU (see review article, p. 39)

4.2 Fabrication and Irradiation Behaviour of Fuels and Targets for Transmutation of Actinides

4.2.1 The EFTTRA-T4 experiment on americium transmutation

The experimental feasibility of transmutation of americium has been studied in the EFTTRA-T4 experiment, a shared-cost action project in the specific programme on Nuclear Fission Safety of the Fourth Framework Programme of the European Union (1994-1998). The EFTTRA-T4 target was produced at ITU by the infiltration technique (see TUAR-96, p. 77 or ref. [1]) and contained about 11 w/o americium dispersed as small particles in a matrix of magnesium aluminate spinel. The target was irradiated in the HFR Petten during 358 full power days. The extent of transmutation of the americium was 96% (with mainly curium and plutonium isotopes being produced), while 28% of the initial americium content was destroyed by fission. Destructive post-irradiation examination of EFTTRA-T4 target was performed at ITU, supplementing the non-destructive examinations of the target performed by NRG in Petten, which had revealed a considerable swelling of the target pellets [2].

Ceramography indicates a significant increase of the porosity of the target pellets due to the formation of gas bubbles (see Fig. 5, review article, p. 43). The major component in the gas bubbles is most likely helium produced by the alpha decay of ^{242}Cm, one of the actinides formed in the transmutation scheme of ^{241}Am (see Fig. 4.1). The overall porosity in the sample after irradiation was about 18%, which is much larger than the mean initial porosity of the unirradiated pellet (3%) but is closely correlated to the extent of swelling deduced from the non-destructive examinations. It is therefore concluded that the accumulation of helium in the target is the major cause for the swelling [2]. This is an intrinsic characteristic of americium transmutation in reactor fuels or targets which should be taken inot account in the optimisation of the target design.

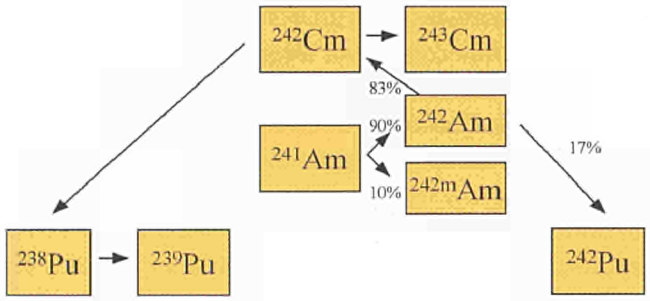

Fig. 4.1 Transmutation scheme for ^{241}Am in a thermal flux. Because of the very short half-life of ^{242}Am ($t_{1/2}$ = 16 h) most of it decays to ^{242}Cm, even though its fission cross section is high (σ_f = 2900 barn). The decay product ^{242}Cm has a low fission cross section (σ_f < 5 barn) and decays with a short half life of 163 days, producing ^{238}Pu and emitting an alpha particle.

4.2.2 New concepts for heterogeneous actinide targets

Homogeneous (solid solutions) and heterogeneous target designs are considered for transmutation of actinides. In a heterogeneous target the actinide phase is dispersed in a non-fissile matrix which is relatively inert against neutron activation. The role of this inert matrix is to act as a support and to improve the thermal and mechanical properties of the target. Presently, most attention is given to oxide matrices, especially magnesium oxide (MgO), stabilised cubic zirconium oxide (ZrO_2) and magnesium aluminate spinel ($MgAl_2O_4$). In the case of americium the dispersed phase could be AmO_{2-x} but this compound has the disadvantage of a high oxygen potential and a high chemical reactivity. To overcome these difficulties the incorporation of americium in a zirconia-based host phase is proposed [3].

In a heterogeneous target the matrix will suffer from the impact of neutrons, alpha decay and fission fragments, which have different effects depending on the energy loss and range of energy deposition. Energetic neutrons cause isolated collision cascades throughout the material. Alpha decay

causes isolated displacements within the range of the alpha particle (20 µm) and a very dense short (25 nm) collision cascade produced by the recoil atom (e.g. ^{238}Pu in the decay of ^{242}Cm) at the site of the decay. Fission products create fission tracks of about 8-10 mm length. The latter effect will dominate the damage to the matrix as it will cause most atomic displacements. This can be minimised, however, by increasing the size of the dispersed phase to about 100-300 µm, as a result of which the damaged volume of the matrix phase is relatively small [2]. A schematic presentation of the design for heterogeneous targets is shown in Fig. 4.2.

As an alternative, a homogeneous target of $(Zr,Y,Am)O_{2-x}$ is being considered. This is simpler to fabricate, but has the disadvantage of a low thermal conductivity. Methods to fabricate both types of targets are being investigated in order to prepare targets for irradiation experiments in HFR Petten and Phénix in Marcoule in which the irradiation behaviour can be tested.

4.2.3 Fabrication of heterogeneous targets

A fabrication process for heterogeneous targets for americium transmutation is being developed now and will be implemented in the Minor Actinide Laboratory in the future. The method is based on aqueous processes to avoid the formation of radioactive dust that can accumulate in the glove boxes. In the test phase, the experiments are performed with cerium as a stand-in for americium.

The first step of the process involves the fabrication of porous spheres of yttria-stabilised zirconium oxide [4] by the external gelation process using a vibrating nozzle disperser to obtain spheres of uniform size (Fig. 4.2). In this process step no radioactive materials are used and it can be realised outside glove boxes. In the second step the spheres are infiltrated with a cerium nitrate solution. The infiltrated spheres are dried and the metal nitrate formed in the pores, is decomposed by thermal treatment. Experiments have shown that up to 35 w/o of cerium can be infiltrated into the spheres. The third step of the process involves the mixing of the infiltrated spheres with the matrix material, followed by pressing and sintering of the pellets. In Fig. 4.2, a ceramography of a target composed of $(Zr,Y,Ce)O_2$ spheres in a magnesium aluminate spinel matrix ($MgAl_2O_4$) is shown. Although the feasibility of this process has been demonstrated in these laboratory experiments, a more homogeneous distribution of the spheres in the matrix has to be pursued.

4.2.4 Fabrication of homogeneous targets

In addition to the heterogeneous targets, a process for the fabrication of homogeneous targets has been developed using again a combination of the sol-gel and infiltration methods. In this process porous spheres of yttria-stabilised zirconium oxide are produced by the external gelation method using the rotating cup atomiser, which yields particles with a size distribution between 20 and 180 µm. Similar to the process for heterogeneous targets, the spheres are in-

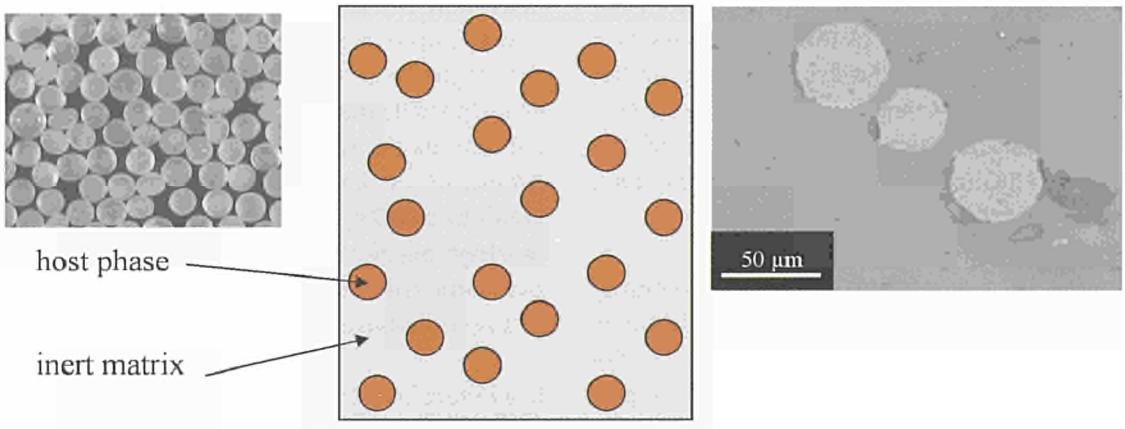

Fig. 4.2 Schematic representation of the "hybrid" fuel concept of a heterogeneous fuel for transmutation of americium. On the right side a ceramography of $(Zr,Y,Ce)O_2$ spheres in $MgAl_2O_4$ as prepared at ITU is shown.

filtrated with the required quantity of cerium and, after thermal treatment, they are compacted into pellets. Pellets have been produced containing about 12 w/o Ce with a density of greater than 94% of the theoretical value. In the next phase, the process will be qualified with plutonium instead of cerium before the first targets containing americium are produced.

References

[1] K. Richter, A. Fernandez, J. Somers, Infiltration of highly radioactive materials: a novel approach to the fabrication of targets for the transmutation and incineration of actinides. J. Nucl. Mat. 249 (1997) 121.

[2] R.J.M. Konings, R. Conrad, G. Dassel, B. Pijlgroms, J. Somers, E. Toscano, The EFTTRA-T4 experiment on americium transmutation. Report EUR 19138 EN, 2000.

[3] N. Chauvin, R.J.M. Konings, Hj. Matzke, Optimisation of inert matrix fuel concepts for americium transmutation. J. Nucl. Mat. 274 (1999) 105.

[4] N. Boucharat, J. Somers, D. Haas, C.T. Walker, Fabrication of macrosphere targets using a combination of sol-gel and powder blending techniques. Proceedings GLOBAL'99.

Contact (4.2.1-4.2.4): Rudy Konings • tel.: +49 7247 951 391 fax: +49 7247 951 566 • konings@itu.fzk.de

4.2.5 Post-irradiation examination of high plutonium content fuels (Trabant 1)

Within the CAPRA (Consommation Accrue de Plutonium dans les RApides) and CADRA (Consommation Accrue des Dechets dans les RApides) programmes, the Institute for Transuranium Elements, the Commissariat à l'Energie Atomique and the Forschungszentrum Karlsruhe are investigating the incineration of Pu and other actinides within the frame of a tri-lateral agreement. The objective of this programme is the optimisation of reactor cores for the incineration of Pu and minor actinides.

In the first experimental programme for the Transmutation and Burning of Actinides in Triox (TRABANT 1), four different high Pu content fuels with annular pellets were irradiated in HFR Petten. The irradiation of the $(U_{0.55}Pu_{0.45})O_{2-x}$ fuel pin and the Ce-Pu fuel pins were halted prematurely due to a failure of the $(U,Pu)O_2$ fuel pin and melting of the $(Ce_{0.56}Pu_{0.44})O_{1.93}$ fuel [1]. The melting of the latter fuel was most likely due to the poor thermal conductivity of the Ce-Pu oxide at low O/M ratios. The cause of the failure of the $(U_{0.55}Pu_{0.45})O_{2-x}$ fuel pin is the subject of debate.

The post-irradiation examinations on the failed pin started in 1998 (TUAR-98, p. 92-94) and were completed in 1999. The fuel pin was sectioned and it was observed that the central channel in the ruptured zone was full of material. This led to the hypothesis that the pin failed due to an excess reactivity caused by the condensation of highly Pu-enriched $(U,Pu)O_2$ in the central void. Hence, detailed EPMA analysis of a metallographic sample from the ruptured zone was carried out to determine the composition of this deposited material. Fig. 4.3 shows the zones analysed by EPMA, and the fuel composition in the different zones (1, 3 and 5) are given in Fig. 4.4.

An increasing Pu content from the centre to the periphery of the fuel was measured with a value substantially below the original 45 w/o in the material which filled the central hole in contrast to the expected higher Pu concentration. Whether the 25-35 w/o Pu concentration in the pellet centre are still sufficient to explain the failure of the pin or whether an excess of tellurium, produced as a consequence of the high linear power at the beginning of the irradiation, was responsible for intergranular corrosion of the cladding needs further investigations. In both cases, however, it is postulated that a burst of fission gas was released into the liquid sodium, leading to inefficient cooling of the cladding which melted as a consequence of this process.

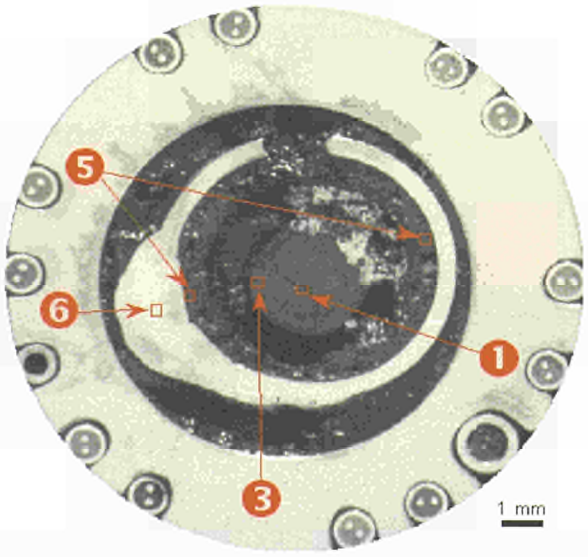

Fig. 4.3 Positions of EPMA in the ruptured zone of pin 1 of Trabant 1.

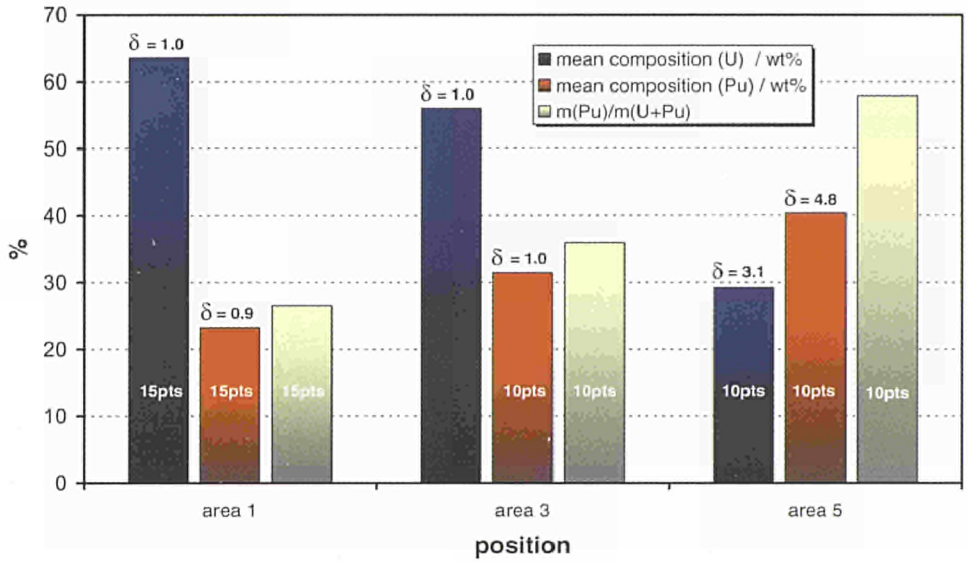

Fig. 4.4 Pu content in the ruptured zone of pin 1 of Trabant 1 from EPMA-point analysis.

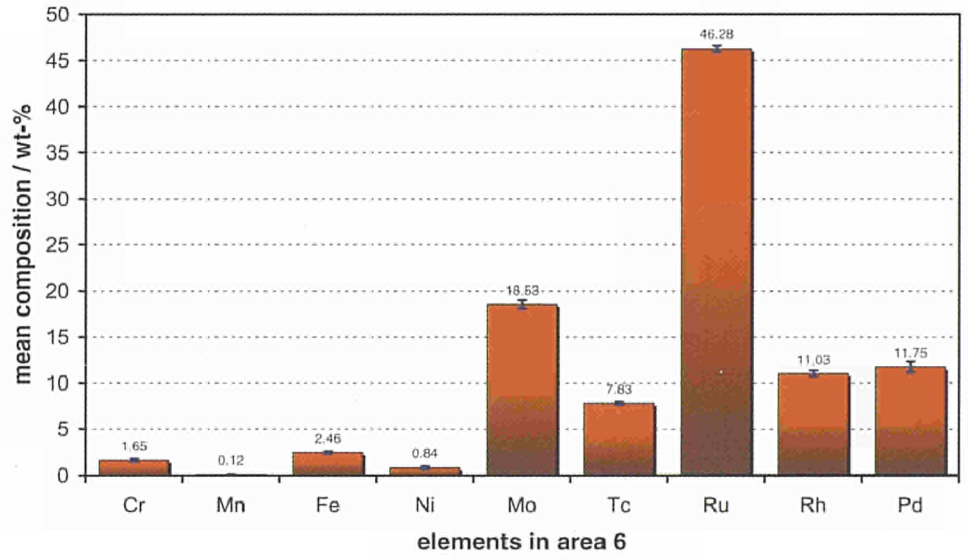

Fig. 4.5 Composition of the solidified melt on the outer surface of the cladding.

The optical microscopy and EPMA of the solidified melt attached the outer surface of the cladding indicated the existence of a fine eutectic structure which would suggest that the material had been exposed to temperatures higher than 1900°C. EPMA revealed that the material contained high amounts of the metallic fission products Ru, Mo, Pd, Rh and Tc (Fig. 4.5). With intact cooling of the pin the temperature at the outer cladding/sodium interface should not have exceeded 600°C, while the temperature at the outer fuel surface would have reached approximately 900°C (in the centre approx. 2500°C).

Reference

[1] J. Somers, J. P. Glatz, D. Haas, D. H. Wegen, D. Planqc, G. Mühling, S. Fourcaudot, C. Fuchs, A. Stalios , Status of the TRABANT Irradiation Experiments,Global 1999, International Conference on Future Nuclear Systems, August 29 - September 3, 1999, Jackson, Wyoming, USA

Contact (4.2.5): Detlef Wegen · tel.: +49 7247 951 364 • fax: +49 7247 561 · detlef.wegen@itu.fzk.de

4.3 The Minor Actinide Laboratory

The Minor Actinide laboratory is a unique facility that is being build to fabricate fuels and targets containing significant quantities of minor actinides such as americium and curium (e.g. 50 g of ^{241}Am). It consists of 10 shielded glove boxes that form a complete fabrication chain in rooms F105 (boxes 1 to 5) and F106 (boxes 6 to 10). The operators of the chain are protected by a steel wall containing up to 5 cm lead to shield the gamma radiation and up to 50 cm water to shield neutron radiation. The processes in the glove boxes are partly automated by the use of robots and remote control, but work is also carried out using telemanipulators.

For 1999 the following achievements can be reported:

- The decommissioning of the existing glove boxes in F105 has been started and is nearing completion. This involved the removal and storage of all radioactive materials and cleaning of the glove boxes prior to their removal.
- The shielded walls in laboratory F106 have been installed (see Fig. 4.6).
- The first two glove boxes (no 6 and 7 hosting the press and the sintering furnace respectively) have been commissioned in the Central Workshop.
- The design of the transfer systems between box 5 in room F105 and box 6 in room F106 as well as the transfer systems between boxes 6, 7 and 8 have been finished and approved. Their construction has been started.

Fig. 4.6 Installation of the protection wall in laboratory room F106.

Completion of the laboratory is now foreseen for 2001, which is a little later than planned. The delay is due to the highly innovative character of the facility, which requires very careful planning and evaluation to achieve the high safety standards for its operation.

Contact (4.3): Rudy Konings • tel.: +49 7247 951 391
fax: +49 7247 951 566 • konings@itu.fzk.de

4.4 Fission Damage and Helium Behaviour in Inert Matrices

Spinel

The work on basic properties [1] of inert matrices, and particularly on their radiation stability against fission products as well as alpha-particles, was pursued.

Spinel single crystals consisting either of bulk specimens (1 cm^2 x 0.3 cm) or of 3 mm diameter pre-thinned TEM disks were irradiated at the TANDEM accelerator at TU München. The irradiations (their conditions are summarised in Tab. 4.1) were performed in vacuum at room temperature with a mean dose rate of 10^9 ions/cm^2.s. The ion-beam current was monitored each 10 min. and the different fluences calculated by integrating these values over the irradiation times. After swelling measurements, i.e. profile measurements using a Hommelwerke T10 G-2 profilometer, the single crystals with the implanted areas were used for preparing cross-sectional TEM specimens. The irradiated crystals were glued on virgin samples and cut transsectionally. Disks of 3 mm thickness were extracted, dimpled and thinned with a double Ar^+- beam of 6 kV (see TUAR-95, p. 71).

Tab. 4.1 Irradiation conditions and main observations of spinel single crystals.

Fluence, ions/cm^2	Specimen type	Swelling, %	TEM observations
10^{11}	TEM foil	–	tracks
10^{13}	TEM foil	–	tracks/no amorphization
5.10^{13}	Bulk	7.25 (11.4)	
5.10^{14}	Bulk	13.5 (22.2)	
5.10^{15}	Bulk	21 (33.1)	amorphization for dE/dx > 6 keV/nm

This technique allowed one to observe the nature of the damage along the path of the fission products in the material and to investigate the influence of the energy loss of the ions. Fig. 4.7 shows some TEM diffraction patterns recorded at different depths of the penetrating ions indicating amorphization up to a depth of about 5 mm based on the original surface.

The corresponding threshold energy loss for amorphization of spinel is 6 keV/nm. Formation of nanocrystals in amorphized spinel due to the electron beam of the microscope has also been observed in these experiments, as shown in the two micrographs in Fig. 4.8. The inset in the left micrograph shows the diffraction pattern revealing the polycrystalline nature of the specimen.

Spinel is very resistant against neutron damage. In contrast, recent work at ITU has shown that it swells significantly under fission product impact (TUAR-97, p. 85 and [2]). The above results prove that this swelling is due to the (unexpected) amorphization. The former swelling values have been recalculated by assuming that only amorphization (i.e. only 2/3 of the irradiated volume) is responsible for the volume changes. These values are reported in parenthesis in table 1 together with the (underestimated) values reported previously (see TUAR-97, p. 85 and [2]).
Work on He behaviour in spinel has been continued [3]. New crystals have been implanted with 100 and 260 keV He-ions to large fluences (up to 1.2x1017 He/cm2). The damage has been monitored using the Rutherford Backscattering technique in the Channeling mode. A small damaged area was

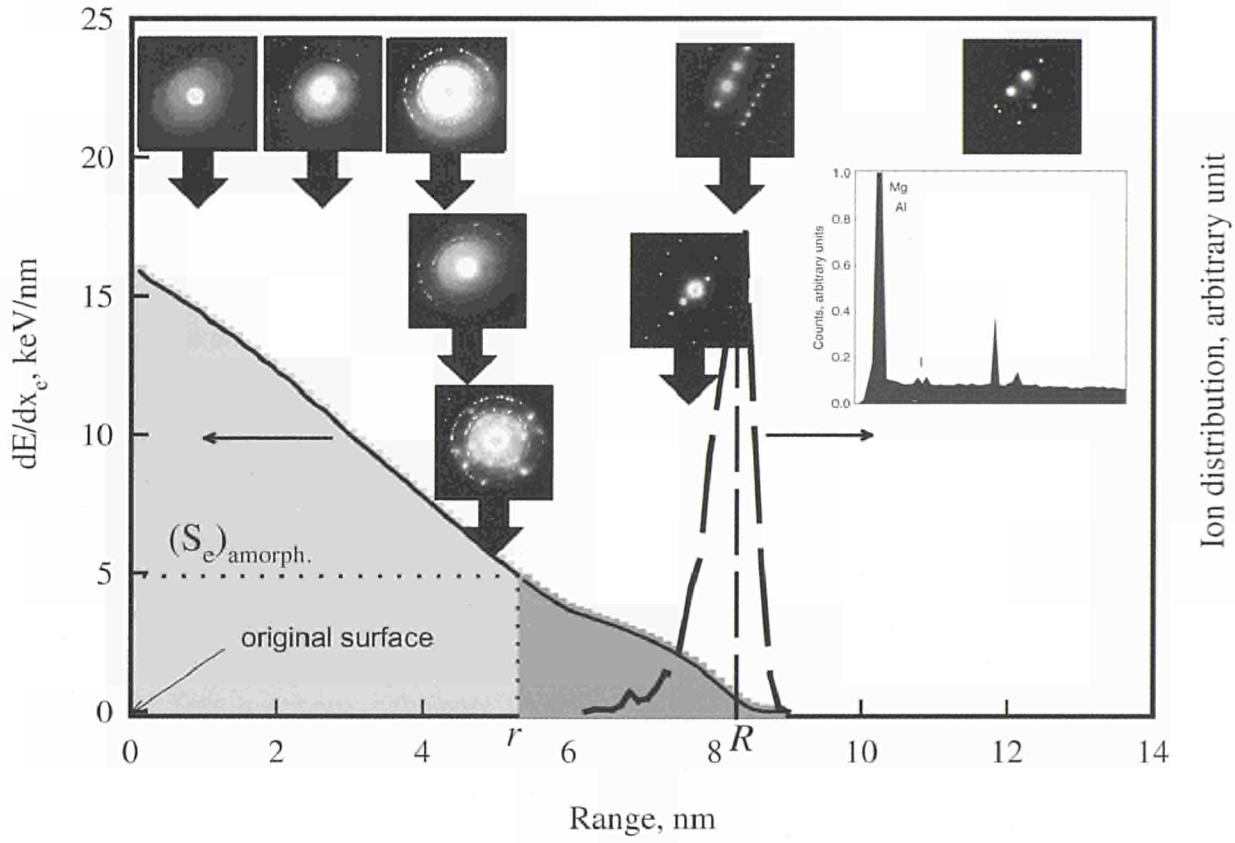

Fig. 4.7 Electronic energy loss (gray area) and distribution (dashed curve) of 70 MeV iodine-ions in $MgAl_2O_4$ calculated using the SRIM2000 code. The energy loss threshold for amorphization ($(S_e)_{amorph.}$) was determined to be around 6 keV/nm corresponding to a penetration depth of the ions of r ~ 5 μm, compared to their range of R = 8.2 μm. An EDX spectrum confirming the implanted iodine location at the end of the ion range is shown as inset. Diffraction patterns taken at different depths of the irradiated layer indicate the amorphous zone (diffuse halo) corresponding to the light gray area while the dark gray area corresponds to the unrestructured crystal. The diffraction patterns with multiple reflections spots (on the originally amorphized layer) indicate the recrystalisation of the previously amorphized spinel due to the electron beam (see also Fig. 4.8).

found at the end of the range of the He-ions (see Fig. 4.9 for penetration depth of the He in spinel). However, no significant damage was found neither on the surface of the implanted specimens nor along the major part of the path of the ions. Spinel was thus shown to be structurally stable against impact of alpha-particles.

Helium release from implanted samples was measured using the Knudsen cell technique (TUAR-98, p. 85, [3]). Fig. 4.10 shows the release and the heating schedule for a spinel single crystal implanted with 100 and 260 keV He-ions to fluences of $5 \cdot 10^{16}$ and $1.2 \cdot 10^{17}$ ions/cm^2 respectively. Release started at 600 °C and was almost complete at around 1400 °C. The release profile seems to indicate diffusion-like processes for He-release as well as burst release processes. Optical microscopy revealed formation of blisters

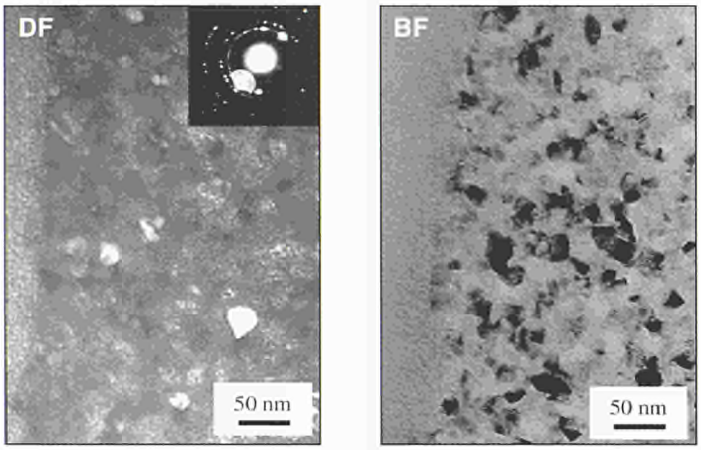

Fig. 4.8 TEM micrographs showing a dark field (left) and a bright field picture (right) of electron-induced recrystallized spinel following amorphization due to irradiation with 5.10^{15} I-ions/cm^2 of 70 MeV energy. The upper left micrograph indicates the diffracted spot used for the dark field image as well as the multiple reflexions indicating the polycrystallinity of the original single crystal.

and of bubbles in the implanted crystal following annealing. On two small areas, spalling of the blisters was observed. On the release curve Fig. 4.10, two pronounced peaks were found at around 1200 °C, attributed to spalling.

Zirconia

Cubic zirconia is known to be radiation resistant (TUAR-98, p. 85 and [4]). Irradiation with 70 MeV iodine-ions did not produce tracks as observed in spinel. Irradiation at higher energies (energy losses) are ongoing to determine the threshold energy loss for track formation. He-release measurements are underway in a similar way as with spinel.

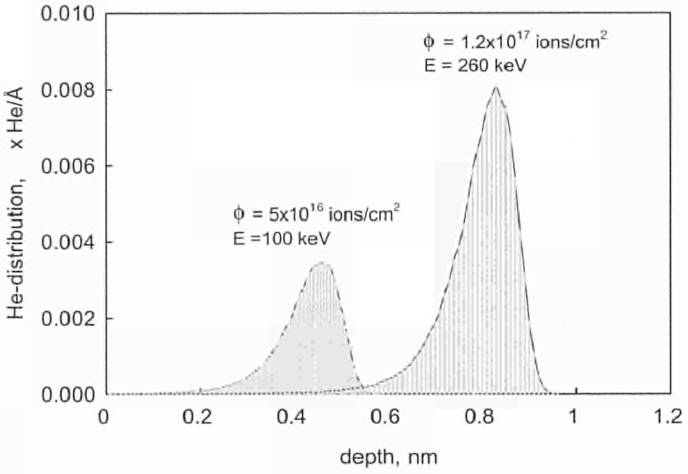

Fig. 4.9 He distribution in spinel for two energies and two fluences (ϕ) calculated with SRIM2000.

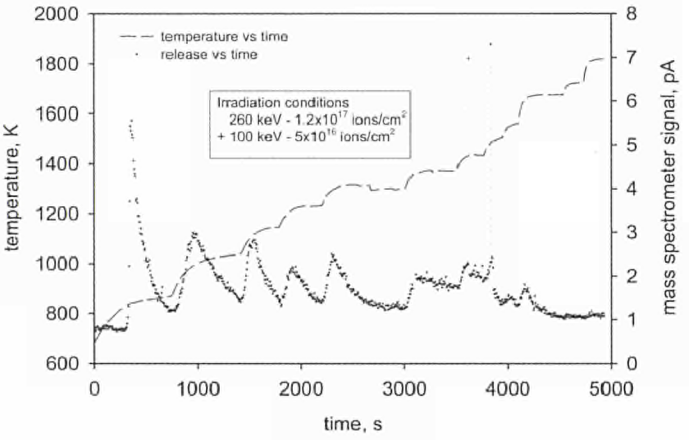

Fig. 4.10 Release of He from a He-irradiated spinel crystal as a function of time. The temperature profile used for the experiment is plotted as a dashed line.

References

[1] Hj. Matzke, V. V. Rondinella and T. Wiss, J. Nucl. Mater. 274 (1999) 47

[2] T. Wiss and Hj. Matzke, Rad. Measurements 31 (1999) 507

[3] R. Fromknecht, J.P. Hiernaut, Hj. Matzke and T. Wiss, Nucl. Instr. Meth. B, 166 & 167 (2000) 163

[4] K.E. Sickafus, Hj. Matzke, Th. Hartmann, K. Yasuda, J. A. Valdez, P. Chodak III, M. Nastasi and R. Verrall, J. Nucl. Mater. 274 (1999) 66

Contact (4.4): Thierry Wiss • tel.: +49 7247 951 447
fax: +49 7247 951 591 • wiss@itu.fzk.de

5. Measurement of Radioactivity in the Environment

In the the Fifth Framework Programme, a new project "Measurements of Radioactivity in the Environment" has been started at ITU to support the DG Environment of the European Commission. This project will take into account the implementation of Articles 35 and 36 of the Euratom treaty and the OSPAR (OSlo-PARis convention) strategy on the management of radioactive substances.

The first task within this project is to establish a standardisation between the Member States for the methodology covering the environmental monitoring of the atmospheric, terrestrial and aquatic environments. Therefore the nuclides as well as the environmental media (sediments, water, particulate etc.) and different species (algae, biota and so on) will be classified according to their importance as transport and diffusion media of radioactivity in the environment.

Agreement between the member states on harmonisation of procedures for sampling, sample preparation, analysis and reporting of results should be achieved. ITU will provide its expertise to assist the DG Environment and upon their request also the Member States, other OSPAR partners or EU candidate member states.

The DG Environment may call upon ITU for technical assistance in order to carry out sampling and/or to plan analytical campaigns, in particular in pursuance of verification exercises conducted by DG Environment related to Article 35. Another important aspect of this programme is the intervention in the case of accidental releases of radioactivity, in which circumstances reproducibility and rapidity are more important than absolute sensitivity.

An extensive literature search has been carried out on the transport and diffusion mechanisms of radionuclides in the marine environment, which is of primary interest for the DG Environment since the OSPAR strategy is related to the radioprotection of the North-East Atlantic Ocean.

ITU will use its analytical techniques and facilities already existing for the detection of trace radioisotopes. These consist of methods for bulk and particle analysis based on mass spectrometric techniques as well as radiometric methods such as low background γ- and α-spectrometry, low-level liquid scintillation counting. A method based on electrodeposition prior to α-spectrometric determination has been validated and implemented. In the clean laboratory the methods for the preparation of different kinds of samples will be tested and wet and dry sample decomposition techniques will be used working with microwave digestion system and an oxygen plasma ashing device in a 100 – 10 class clean laboratory.

Contact (5.): Maria Betti • tel.: +49 7247 951 363
fax: +49 7247 951 186 • betti@itu.fzk.de

6. Spent Fuel Characterization in View of Long Term Storage

6.1 Development of a Flow Through Reactor to Study the Dissolution Rates of UO_2 and Irradiated Fuel.

Under oxidising conditions UO_2 is thermodynamically unstable. Surface oxidation of the UO_2 is followed by dissolution; both processes being influenced by a number of parameter like surface to volume ratios, pH, carbonate concentration. Furthermore depending on the redox conditions, precipitation of secondary uranium phases can be important [1,2].

The aim of the present work is to study the dissolution rates of UO_2 as a function of hydrogen carbonate concentration and to avoid, at the same time, any reprecipitation. Therefore a dynamic leaching set-up was used under oxidizing conditions at room temperature (Fig. 6.1). The dissolution rate is determined following the methods used for the analysis of mixed flow reactors (continuously stirred tank reactors) [3,4]. This equipment avoids secondary phase precipitation inherent to study of reaction kinetics in batch reactors.

The experiments were carried out using dense sintered material ($\rho \sim 95\%$ TD) and powders with different particle sizes (100-300 µm). Fig. 6.2 shows the linear range obtained from 0.025 to 0.08 ml min^{-1} in two carbonate media. The equilibrium dissolution rates obtained from the experiments under these conditions are 1.4×10^{-10} mol m^{-2} s^{-1} for the fragments and 5.0×10^{-10} mol m^{-2} s^{-1} for the powders. The small difference between these normalised dissolution rates is the results of the assumptions (constant diameter, spherical shape of the powders) used to calculate the surface area of the two types of sample. In these flow tests it is important to ensure that the measured uranium concentrations correspond to steady state, condition where aqueous uranium concentration must increase linearly with a decreasing flow rate and not to a solubility equilibrium [5,6].

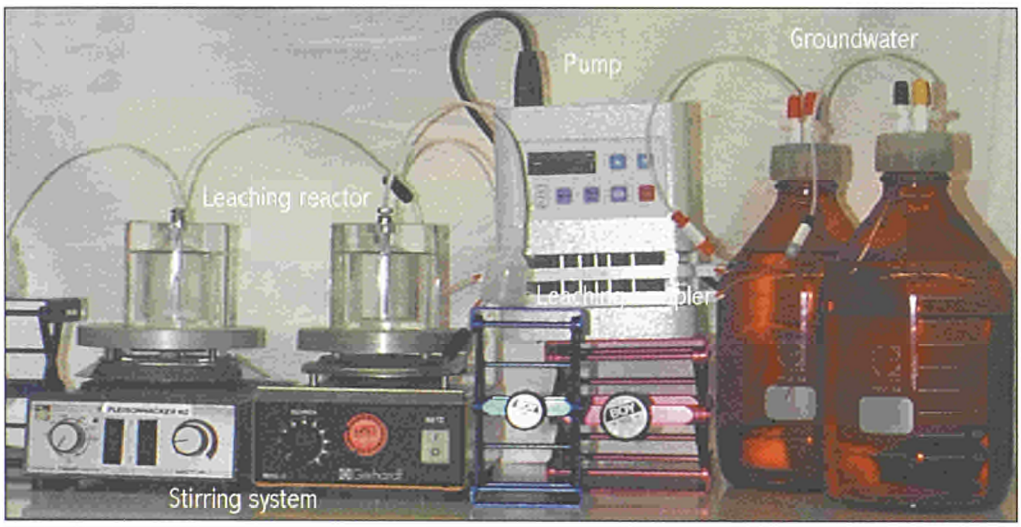

Fig. 6.1 Flow through reactor developed for dynamic leaching experiments on spent fuel.

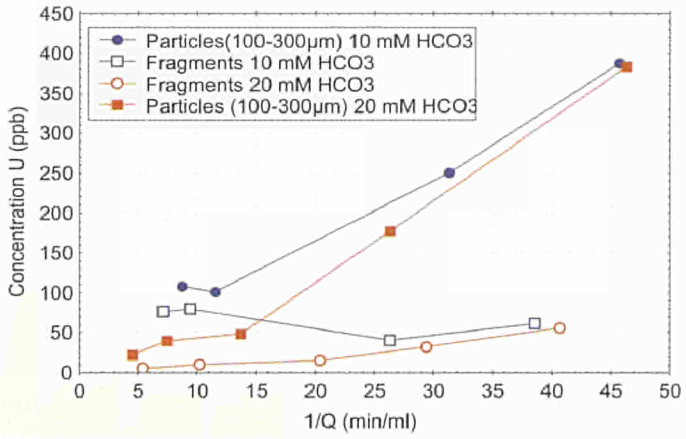

Fig. 6.2 Uranium concentration as function of the flow rate.

References

[1] R. S. Forsyth, L. O. Werme and J. Bruno, J. Nucl. Mater. 138 (1986) 1-15

[2] J. Quiñones, J. García, J.A. Serrano, P. Díaz. Mat. Res. Soc. Symp. Proc. Vol. 506 (1998) 247-252

[3] J. D. Rimstidt, P. M. Dove. Geochim. Et Cosmochim. Acta 50 (1986) 2509-2516

[4] O. Levenspiel. Ingeniería de las reacciones químicas (Ed. Reverte) 107-127 (1988).

[5] J. Bruno, I. Casas, E. Cera, J. de Pablo, J. Giménez and M. E. Torrero, Mater. Res. Soc. Symp. Proc. 553 (1995) 601-608

[6] I. Casas, J. Giménez, V. Marti, M. E. Torrero and J. Pablo, Radiochim. Acta 66/67 (1994) 23-27

Contact (6.1): Jean-Paul Glatz • tel.: +49 7247 951 321
fax: +49 7247 951 561 • glatz@itu.fzk.de

6.2 α-Radiolysis and α-Radiation Damage Effects on UO_2 Dissolution

Introduction

By the time the spent fuel containers in a geological repository may fail, i.e. after a few hundred years, α-decay will constitute almost entirely the radiation field in and around spent nuclear fuel. Although the repository is characterized by reducing conditions, the presence of products of the radiolytic process like H_2O_2, O_2 and OH radicals may cause oxidizing conditions near the fuel surface, which would enhance the dissolution of uranium. The activity of the spent fuel available today is dominated by β- and γ-decays; hence, it is not representative of aged fuel in the repository. In order to study the effects of radiolysis caused by α-emissions on the dissolution behaviour of UO_2-based fuel in contact with water, sintered unirradiated UO_2 pellets containing 0.1 w/o (labeled UO_2-01) and 10 w/o (labeled UO_2-10) of an oxide constituted mainly by the short-lived ^{238}Pu were fabricated and tested. The results were compared to those obtained for undoped unirradiated UO_2 (labeled UO_2-0). In parallel to leaching tests, characterization and radiation damage studies were performed on the α-doped UO_2, in order to investigate the build up of α-decay damage (He-ion and ~100 keV daughter recoil ion) in the structure.

The results of static batch leaching tests in deionized water at room temperature under an inert atmosphere have been described previously (TUAR-98, p. 98-100 and [1]).

A key factor in determining the dissolution behaviour of the fuel is the surface area exposed to water. During irradiation the structure of nuclear fuel is changed: cracks and bubbles are formed, and also modifications of the grain structure occur, e.g. the so-called rim structure, which is characterized by a significant amount of grain subdivision (~10^4 subgrains formed from each pre-existing grain) and increased porosity at the radial periphery of the fuel pellet. These modifications, which cause an increase of the surface area potentially exposed to water, are not reproduced in the unirradiated analogues used for laboratory experiments, including the α-doped UO_2. This work extends the results obtained previously to the investigation of α-radiolysis effects on the dissolution of U in the case of higher surface areas.

Experimental

The doping oxide used to fabricate the UO_2-10 and UO_2-01 had a specific α-activity of ~$3.76 \cdot 10^{11}$ Bqg^{-1} and was homogeneously distributed in the UO_2 matrix. The composition of the doping oxide, and the fabrication procedure of the sintered pellets have been described elsewhere (TUAR-98, p. 98-100 and [1]). Two types of specimens were prepared for these experiments: discs and powders. The discs, approximately 1 mm thick, were cut from the original pellets. One of the faces of the discs was polished, in order to perform meaningful surface characterization before and after leaching. The powders were prepared by crushing and sieving sintered pellets of the two doped materials and also of un-

doped UO_2-0 to obtain particles, labeled with the suffix "f", with particle size d ≤ 63 µm. Tab. 6.1 summarizes some properties of the samples.

Tab. 6.1 Summary of the samples used for the leaching experiments. The suffix "f" indicates the crushed samples. As an indicative value, the ratio of the sample surface to the leachant volume, S/V, calculated from the geometric area and assuming that all crushed particles are spheres and have the largest diameter is also reported.

Label	Additives (w/o)	α-activity (Bqg^{-1})	Particle size, d (µm)	Weigth (mg)	S/V m^{-1}
UO_2-0f	0	$1.10 \cdot 10^4$	d<63	77.2	65
UO_2-01f	0.1	$3.76 \cdot 10^8$	d<63	84.4	71
UO_2-10f	10	$3.76 \cdot 10^{10}$	d<63	90.5	76
UO_2-0	0	$1.10 \cdot 10^4$	disc, ~6 mm diam	390.0	4.1
UO_2-01	0.1	$3.76 \cdot 10^8$	disc, ~6mm diam	316.4	3.9
UO_2-10	10	$3.76 \cdot 10^{10}$	disc, ~6mm diam	317.7	3.9

The handling and the experimental procedures were the same for all the materials. In particular, before the leaching tests, the samples were annealed for several hours at 1000 °C in the sintering atmosphere to recover α-decay damage and the mechanical stresses accumulated during the sample preparation.

Static sequential leaching at room temperature in deionized water was performed on the samples in a glove box with N_2 atmosphere (< 10 ppm O_2). Care was taken to minimize the uptake of oxygen by the leachant. The leaching vessels were Pyrex glass tubes. The volume of leachant was 11 ml for the crushed samples, and 20 ml for the discs. The leaching times were 1, 10, 100, and 1000 h. At the end of each contact period, the liquid phase was separated from the powder by centrifuging. Fresh leachant solution was then introduced in the vessel for the next leaching time. The leachates were filtered through 0.50 µm membrane filters and acidified to stock until analysis. The leachates were analyzed using ICP-MS. In the case of UO_2-10 and UO_2-01, chromatographic separation was performed on line before ICP-MS in order to separate the ^{238}U and ^{238}Pu fractions. The next section will focus on the U results. The Pu results will be reported later.

The build up of α-decay damage in the material was analyzed by measuring the lattice parameter evolution as a function of time (hence of cumulative damage) using X-ray diffractometry (XRD). The evolution with time of the hardness of the material was measured using Vickers indentation.

Results

Figs. 6.3 and 6.4 show the amounts of U measured in the leachates as a function of leaching time for the crushed material and the discs, respectively. The data are expressed in mole m^{-2} and as cumulative values. The geometric surface was used for the normalization. In the case of crushed samples, it was tentatively assumed to have spheres with a diameter of 63 µm. Note that due to the logarithmic scale used, the error bars are smaller than the data points.

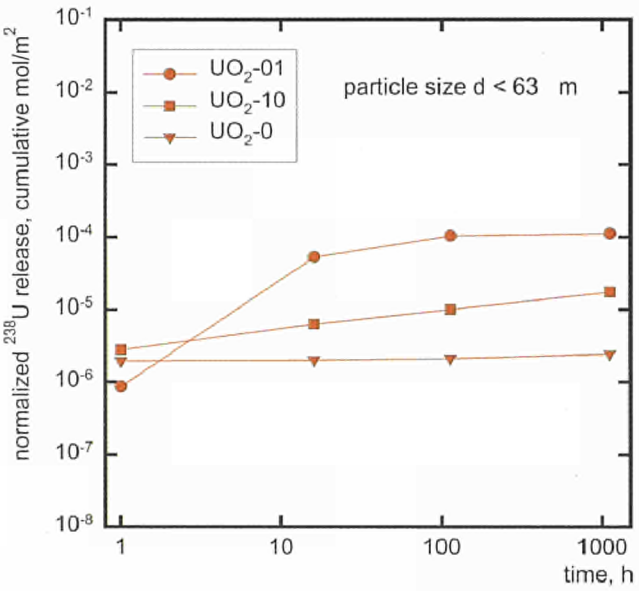

Fig. 6.3 Cumulative amounts of U per unit area released from the crushed materials as a function of leaching time.

The values shown in Fig. 6.3 for UO_2-01f and UO_2-10f are clearly higher than those for UO_2-0f except after 1 h of leaching. The initial release for the three samples is very similar. However, after longer leaching times the cumulative values for the α-doped materials increase, while those for undoped UO_2 remain essentially constant. The release after 10 and 100 h for UO_2-0f is in fact close to the detection limit of the set-up used to analyze the solutions. After 1111 h of leaching, the cumulative amount of U released by the α-doped samples is at least one order of magnitude higher than that for undoped UO_2. The highest cumulative release is measured from UO_2-01f.

Fig. 6.4 shows an even larger difference between the α-doped samples and the undoped UO_2. Differently from the behaviour of the crushed materials, which shows significant scatter of the datapoints, and similarly to the previous results from batch tests on monoliths (TUAR-98, p. 98-100 and

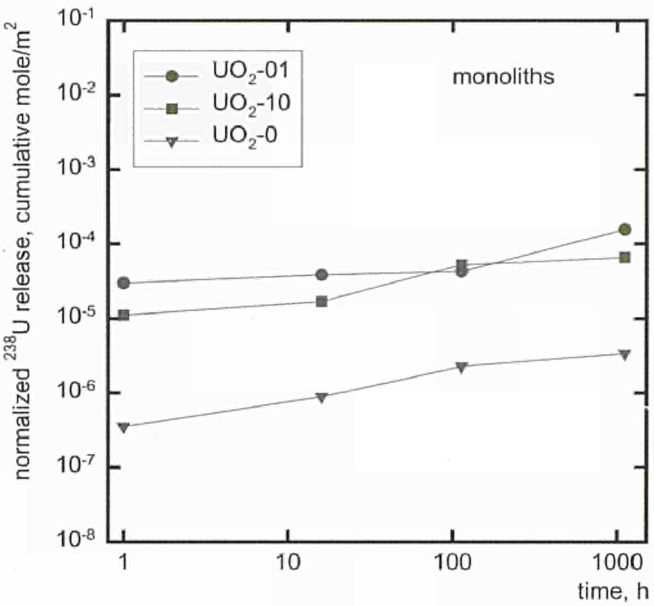

Fig. 6.4 Cumulative amounts of U per unit area released from disks of α-doped and undoped UO_2 as a function of leaching time.

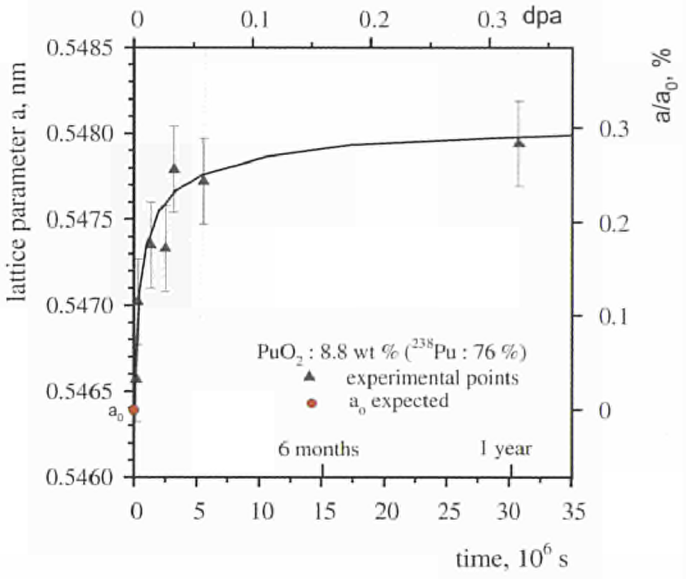

Fig. 6.5 Lattice parameter, a, as a function of time and displacements per atom (dpa axis) for the UO_2-10 material.

[1]) the behaviour of UO_2-10 and UO_2-01 shown in Fig. 6.4 is almost indistinguishable.
The normalized values of U released for UO_2-01f shown in Fig. 6.4 converge with those for the α-doped discs except for the shortest leaching time. Also the normalized values for UO_2-0f and UO_2-0 converge after the initial leaching period. The normalized values for UO_2-10f show instead a different behaviour and remain below those of UO_2-10 after all leaching times.

The conventional means of measuring radiation damage is to follow the increase of the lattice parameter. Fig. 6.5 shows the results of the XRD measurements on the UO_2-10 material. On the lower abscissa, the storage time is shown, while the upper abscissa shows the corresponding numbers of displacements per atom, dpa. On the left axis, the absolute values of the lattice parameter, a, are reported, and the right one shows the fractional changes, $\Delta a/a_0$, expressed in percent unit. The expected initial lattice parameter value, a_0, was calculated assuming that each fluorite type phase (i.e. UO_2 and PuO_2) contributes proportionally to its concentration to the resulting lattice parameter. The experimental results show an increase of the lattice parameter with time (corresponding to increasing damage). After 1 year, the lattice parameter value had increased by ~0.28%, to a dpa level of approximately 0.32. The UO_2-01 did not show, during the same time interval, appreciable variations of the lattice parameter. This was expected because of the 100-fold lower decay rate.

A similar behavior was observed by performing periodical Vickers hardness measurements. Whereas the UO_2-01 did not show significant variations of the hardness, the values measured for UO_2-10 increased, and after approximately 2 months reached a maximum value, corresponding to an increase of hardness of ~20%. After 12 months, it seemed that the hardness had reached an asymptotic level (similar to the saturation value in the case of the lattice parameter). Future measurements will determine if the hardness values will eventually decrease.

Conclusions

Enhanced U release from UO_2 samples containing different concentrations of a short-lived α-emitter was observed by performing static sequential leaching tests under anoxic conditions at room temperature in deionized water. This effect was observed on disc-shaped samples and also on crushed material. In the case of powders, the enhanced U release becomes apparent after leaching times longer than 1 h. A tentative normalization of the U concentration values to the geometric surface area produces convergence of the datapoints for α-doped UO_2 with increasing leaching times,

with the exception of UO_2-10f. The data for undoped UO_2 also tend to converge with increasing leaching periods. However, the normalized values for undoped UO_2 are clearly at least one order of magnitude below those for the α-doped samples. Ongoing and future work will extend the available information concerning radiolysis and surface area influences, including possible chemical effects due to the composition of the α-doping additive.

Reference

[1] V.V. Rondinella, Hj. Matzke, J. Cobos, T. Wiss; Mat. Res. Soc. Symp. Proc. 556 (1999) 447-454

Contact (6.2): Vincenzo V. Rondinella • tel.: +49 7247 951 279 fax: +49 7247 951 591 • rondinella@itu.fzk.de

6.3 Corrosion Measurements on α-doped UO_2 with Electrochemical Techniques

The determination of the leach rates of spent fuel in groundwater is essential for the evaluation and design of a repository for final fuel storage. Given the limitations related to the handling of irradiated fuel, spent fuel dissolution experiments combined with more detailed studies using non-irradiated chemical analogues are very useful. Irradiated fuel is characterised by intense radioactivity that increases with burn-up. This causes the radiolysis of the surrounding leachant and leads to the formation of oxidising chemical species like O_2, H_2O_2 or OH radicals, which can enhance fuel dissolution [1,2]. But the radiation inventory of today's spent fuel is different from aged fuel in a repository after 500-1000 y where α-emitters will predominate over β- and γ-emitters. The study of the effect of α-radiolysis on spent fuel dissolution is therefore of high importance. Leaching results on non-irradiated UO_2 fuel and non-irradiated UO_2 fuel doped with 0.1 w/o and 10 w/o of the α-emitter ^{238}Pu fabricated at ITU have shown an increase of the leaching rate by almost two orders of magnitude in the presence of α-radiation (TU-AR-98, p. 98-100).

In the present study, electrochemical free corrosion potential measurements were carried out in groundwater under anoxic conditions using the same materials. Electrodes were prepared by glueing fuel pieces onto a gold-coated brass holder followed by vacuum impregnation of the sample with a low viscosity resin. After mechanical polishing of the electrodes (see Fig. 6.6) they were used for the experiments.

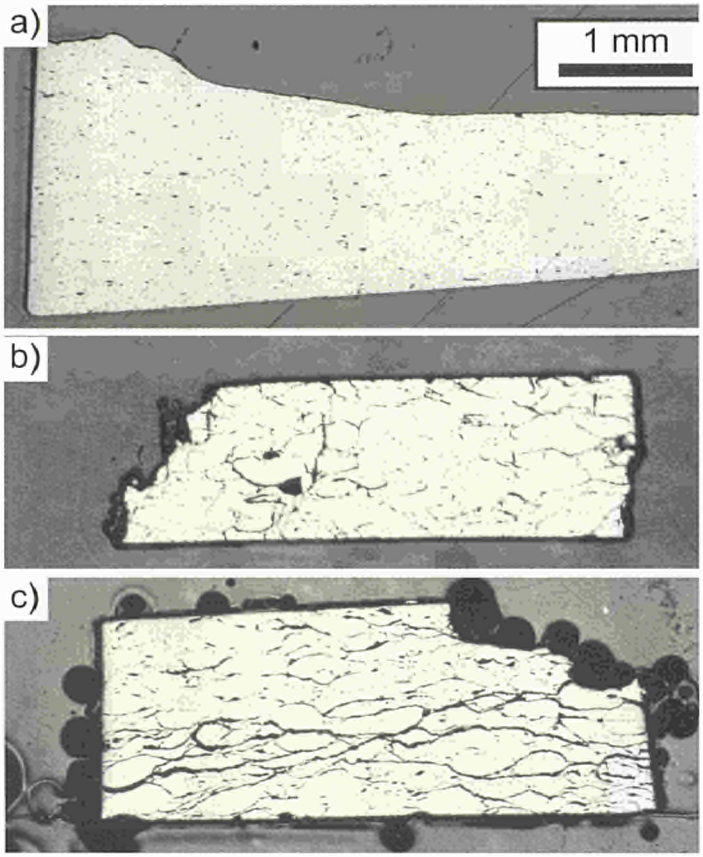

Fig. 6.6 Micrographs showing the surface of electrodes used for electrochemical free corrosion potential measurements: a) non-irradiated UO_2, b) non-irradiated UO_2 containing ~0.1 w/o ^{238}Pu with an α-activity of $2.7 \cdot 10^6$ Bq·cm^{-2} at the surface, c) non-irradiated UO_2 containing ~10 w/o ^{238}Pu with an a-activity of $2.7 \cdot 10^8$ Bq·cm^{-2} at the surface.

The groundwater (composition see Tab. 6.2) was purged with argon or nitrogen for 1 h to reduce the oxygen content. The experiments were carried out in a glove box under pure nitrogen atmosphere.

Fig. 6.7 shows the free corrosion potentials of α-doped UO_2 compared with non-irradiated UO_2.

Comparing the results obtained from non-irradiated UO_2 and the 10 w/o ^{238}Pu-doped UO_2 a strong effect on the corrosion potential is visible. The potential of the highly Pu-doped specimen is ~200 mV higher than that of UO_2.

Tab. 6.2 Average composition of the groundwater used for free corrosion potential measurements.

Ion	Concentration mg/l
Ca^{2+}	9.9
Mg^{2+}	6.1
Na^{+}	9.4
K^{+}	5.7
Cl^{-}	8.4
Si^{4+}	30.0
SO_4^{2-}	6.9
HCO_3^{-}	65.3

These high corrosion potentials are of course explained by the presence of oxidising species or oxygen in the solution. Comparing the redox potential E_h in solution, which is a measure of the oxidative behaviour of the solution, no significant difference is visible. Therefore it has to be concluded that due it's short range, the intense α-irradiation of ^{238}Pu has formed oxidising species very close to the surface. Those species should have cause an oxidation of the UO_2 surface demonstrated by the increased corrosion potential.
The corrosion potential is proportional to the logarithm of the dissolution rate of UO_2. Assuming a factor of 80 mV/decade [3] an over two orders of magnitude higher dissolution rate for the highly α-doped specimen is found, similar to the increase detected in the leaching experiments [TUAR-98, p. 98-100].

In contrast to the leaching test, the free corrosion potential of the low doped UO_2 is in the first two days even lower than that of the undoped UO_2, and after 56 hours the potentials are not significantly different. The slight differences might be explained by the redox potential in case of the 0.1 w/o ^{238}Pu-doped specimen which is 50 mV higher. Furthermore there are indications for an electrochemical effect of Pu, which will lower the corrosion potential [TUAR-99, Ch. 6.4].

More detailed investigations at α-doped material containing e.g. ^{233}U instead of ^{238}Pu are necessary to separate the chemical from radiolysis effects. Differential measurements with doped and undoped material carried out under the same conditions in the same solution will also be very useful to clarify the influence of the different parameters.

References

[1] H. Christensen, S. Sunder, D.W. Shoesmith, J. Alloys Comp. 213/214 (1994) 93

[2] S. Sunder, D.W. Shoesmith, H. Christensen, N.H. Miller, J. Nucl. Mat. 190 (1992) 78

[3] B. Grambow et al., Final Report for contract FI4W-CT95-0004 EU-R&D programme 1994-1998 Nuclear Fission safety, Source term for performance assessment of spent fuel as a waste form, in press.

Contact (6.3): Detlef Wegen tel.: +49 7247 951 364 fax: +49 7247 561 detlef.wegen@itu.fzk.de

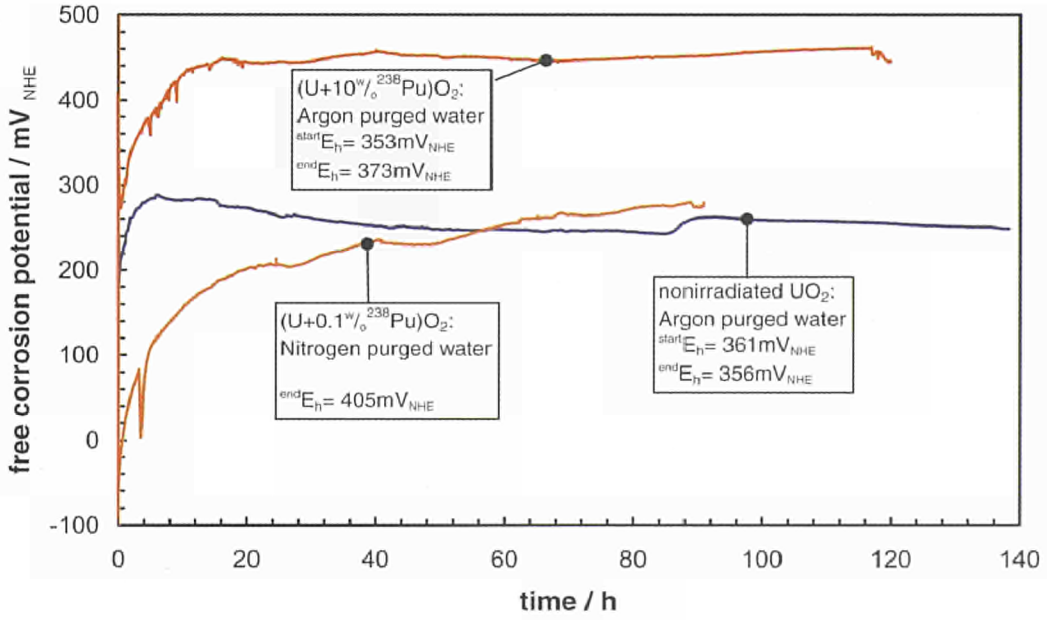

Fig. 6.7
Free corrosion potential of non-irradiated UO_2 and of α-doped UO_2 in groundwater under anoxic conditions.

6.4 Source Term for Performance Assessment of Spent Fuel as a Waste Form

During the present reporting period the SCA programme on a *Source Term for Performance Assessment of Spent Fuel as a Waste Form* was concluded. ITU contributions to this project were focussed on the dissolution behaviour of spent UO_2 and MOX fuel, or of unirradiated UO_2 and SIMFUEL by experimental and by modelling techniques in a large number of groundwater compositions typical for European repositories in salt, granite and clay formations. The experimental data and models are integrated in a consistent description of the electrochemistry, geochemistry and radiation chemistry process involved in spent fuel dissolution.

Electrochemical dissolution mechanism are relevant for groundwaters under oxic and anoxic conditions, in certain cases even at negative redox potential, whereas solubility controlled dissolution prevails under reducing conditions. Under oxidising, and possibly also under anoxic conditions, in the strong radiation fields of fresh spent fuel, the dissolution mechanism comprises an oxidation of the fuel surface followed by the dissolution of the oxidised layer. An oxidative dissolution threshold was defined kinetically at the potential where equal rates of electrochemical and solubility limited dissolution are measured. This threshold is E_{corr} = 150 mV_{NHE} free corrosion potential for unirradiated UO_2 in groundwater.

The free corrosion potential of spent fuel with burn-ups higher than 20 GWd/tU were measured for the first time at

Tab. 6.3 The free corrosion potentials measured on spent fuels and unirradiated UO_2.

fuel		conditions				free corrosion potential			corrosion rate			
							after electrochemical reduction		extrapolation of anodic Tafel line to E_{corr}			derived from impedance data
type	burn up GWd/tU	electrolyte	$C(O_2)$ ppm	initial pH	T °C	$E_{init.}$ mV_{SHE}	$^{max}E_{corr.}$ mV_{SHE}	$^{mean}E_{corr.}$ mV_{SHE}	initial $^{ext.}v_{UO2}$ $mg \cdot m^{-2} \cdot d^{-1}$	max $^{ext.}v_{UO2}$ $mg \cdot m^{-2} \cdot d^{-1}$	mean $^{ext.}v_{UO2}$ $mg \cdot m^{-2} \cdot d^{-1}$	$^{EIS}v_{UO2}$ $mg \cdot m^{-2} \cdot d^{-1}$
UO_2 !	31.5	synthetic groundwater	< 2	8	22 - 28	321	168	158	3.3	0.04	0.03	
			< 2	7.6	22 - 25	379	204	162	17	0.11	0.03	(22) *
UO_2	45.2	synthetic groundwater	< 2	8	22 - 28	291	260	209	1.4	0.56	0.13	(4) *
UO_2 !	53.1	synthetic groundwater	< 2	7.6	22 - 25	384	239		20	0.31		
UO_2 !	53.1	95% sat. NaCl	< 2	7.2	22 - 28	341	190	180	5.8	0.08		
MOX	21.1	95% sat. NaCl	< 2	7.2	22 - 28		-225	-272				
UO_2		synthetic groundwater	0.05	8.4	23			296			1.6	1.3
UO_2		synthetic groundwater	0.05	7.7	60		364	346		11.2	6.7	5.8
			0.05	7.5	60			328			4.0	17.5
UO_2		95% sat. NaCl		6.8	22		226	200 ↑		0.21	0.1	
			2	6	25		299	297↗		1.7	1.6	
			0.2	6	25			254			0.5	
UO_2		95% sat. NaCl	3.4	3.8	25		543	527↗		1940	1220	
			0.2	3.8	25			373			14	

! :samples with conductive pathways to underlying metal holder

( ) * : surface area estimated A_{fuel} = 0.15 cm^2

ITU. Tab. 6.3 shows a summary of free corrosion potentials and corrosion rates of irradiated UO_2 and MOX fuels in comparison to unirradiated UO_2.

The free corrosion potentials measured on spent UO_2 fuel are in the same range as those of unirradiated UO_2 and higher than the oxidative dissolution threshold indicating an electrochemical dissolution mechanism. MOX fuel has a different behaviour with a very low free corrosion potential. Areas of Pu-rich agglomerates are surrounded by the normal UO_2 phase. Therefore a galvanic coupling between the different phases seems to be possible. As a result, a mixed potential between the free corrosion potentials of the pure phases, Pu-rich agglomerates and UO_2, will be obtained. This also influences the dissolution rates. The corrosion rate of the more noble partner (UO_2) will be decreased while the other (Pu-rich agglomerates) will dissolve faster. In the case that the two materials have different active surface areas the one with the larger surface will be less affected. Such an effect was observed during the leaching tests on spent fuel rodlets with pre-set defects (TUAR-98, p. 101). To clarify this behaviour further investigations are necessary.

Corrosion rates obtained from free corrosion potential measurements and impedance measurements are in good agreement. But to compare these results with those from chemical leaching experiments the active surface area must be known. Initial porosity measurements show that this inner surface area can be very large relative to the outer geometric surface, which will result in much lower effective corrosion rates.

Contact (6.4): Detlef Wegen · tel.: +49 7247 951 364 fax: +49 7247 561 detlef.wegen@itu.fzk.de

6.5 Spent Fuel Characterisation for Interim Dry Storage – STEP 2

The objective of the project is the study of the behaviour and interaction of fuel with its surroundings during intermediate storage. The project is carried out under a contract with the Central Research Institute of Electric Power Industry (CRIEPI) Japan and has been previously (September 1999) extended for two years, covering now a seven years period, from 1997 until 2003.

The work has proceeded this year with the investigation of BWR-UO_2, PWR-UO_2 and PWR-MOX spent fuels under realistic storage conditions, including the following studies:

- Isotope composition of actinides and fission products.
- Fuel thermophysical properties, such as specific heat and thermal diffusivity.
- Leaching tests on powder and spent fuel fragments have started, as well as sample preparation for fission gas release measurements during thermal annealing and mechanical tests (microindentation).
- Long-term oxidation experiments have begun. Results on the oxidation of irradiated UO_2 fragments up to the transformation to U_3O_8 powder have been obtained at 350 °C, while the experiments at 400 °C were already started. XRD analyses for examination and identification of the appeared intermediate phases were proposed.

Contact (6.5): Dimitrios Papaioannou, +49 7247 951 375, fax: +49 7247 951 561, dimitri.papaioannou@itu.fzk.de

7 Safeguards Research and Development

With the 5th framework programme, the emphasis of the Institute's safeguards activities has changed. More importance has been given to actual research work, however still continuing service oriented tasks. This is reflected in the following chapters, which cover research results of immediate relevance to the traditional safeguards area, environmental sampling and high performance trace analysis which are in direct response to needs expressed by the safeguards authorities (Euratom and IAEA), and to nuclear forensics and covering also the analytical support.

7.1 Improvement of Measurement Technology and Methodology for Fuel Cycle Facilities

Plutonium dioxide and plutonium nitrate are the most important products from nuclear fuel reprocessing. The accurate assay of this material is of strategic importance to nuclear material safeguards. Neutron coincidence counting has proven to be a very elegant, non-destructive method. However, the uncertainty of some coefficients used in the evaluation of results limit the achievable accuracy. Therefore research work was carried out to redefine these parameters.

7.1.1 Accurate measurement of the specific ^{240}Pu-effective mass of ^{238}Pu and ^{242}Pu

The concept of a ^{240}Pu-effective mass, m_{240eff}, commonly adopted as measured in passive neutron-coincidence (PNCC) measurements on Pu-bearing materials accounts for the fact that three plutonium isotopes – ^{238}Pu, ^{240}Pu and ^{242}Pu – contribute to the measured neutron coincidence rate. The quantity m_{240eff} is expressed as a weighted sum of the spontaneously fissioning Pu isotopes 238, 240 and 242:

$$m_{240eff} = \gamma_{238} \cdot m_{238} + m_{240} + \gamma_{242} \cdot m_{242}$$

where the coefficients γ_{238} and γ_{242} proportion the contributions of the isotopes 238 and 242 per unit mass to the neutron coincidence response relative to that from ^{240}Pu.
In the course of previous parameter studies on PNCC at ITU it had been realized that the uncertainties associated with available coefficients γ_{238} and γ_{242} might represent a source of potential systematic error in high-accuracy PNCC measurements. This has led us to undertake a careful experimental determination of the specific ^{240}Pu-effective masses of ^{238}Pu and ^{242}Pu from measurements on isotopically enriched $^{238}PuO_2$, $^{240}PuO_2$ and $^{242}PuO_2$ samples containing between 20 mg and 440 mg of the respective enriched Pu isotope. Effective γ-coefficients were determined at ITU for the Euratom OSL neutron-gamma counter and, for comparison, at AEA Harwell for the Harwell N95 high-efficiency neutron coincidence counter. Table 7.1 summarizes the results for the obtained empirical γ-coefficients.

Tab. 7.1 Results for the determined empirical γ-coefficients.

Coefficient	OSL-Counter		N-95	Previous Values
	GW=64µs	GW=128µs	GW=88µs	
γ_{238}	2.707 ±0.011	2.714 ±0.011	2.718 ±0.010	2.52...2.57
γ_{242}	1.658 ±0.005	1.667 ±0.005	1.664 ±0.003	1.66...1.71

For the OSL counter the coefficients were determined for two different coincidence inspection intervals (gate width = GW) of 64 and 128 µs. Measurements with the Harwell N95 counter were carried out at a gate width of 88 µs. The close agreement of the measured γ-coefficients for the two counters suggests an encouraging insensitivity to details of the respective counter assemblies. To good approximation, the determined specific ^{240}Pu-effective coefficients for ^{238}Pu and ^{242}Pu can therefore be viewed as universal constants in the determination of m_{240eff}, and they are recommended for general use in the assay of plutonium by means of PNCC in chambers of similar moderator design.

7.1.2 Improved methodology for high-accuracy Pu assay by passive neutron coincidence counting

In the Euratom on-site laboratories passive neutron coincidence counting (PNCC) is utilized as the main routine analytical technique for the Pu assay in powder and pellet samples. Previous careful measurements and model calculations performed at ITU have revealed that the effect of neutron multiplication cannot be ignored even for the small sample sizes (gram) involved in the respective measurements, and

that the measured instrument response needs to be corrected for it in order to reach unbiased Pu assay results of high accuracy.

The magnitude of the neutron multiplication depends on numerous sample parameters such as sample amount, density, isotopic composition, U/Pu ratio etc. Such a multi-parameter dependence makes it difficult or impractical to follow the traditional procedure of using calibration curves for the quantification of measurement results. Instead, we have adopted an approach of calculating sample-specific correction factors for each measured sample, based on the computer-modeling of the neutronic behaviour of the sample using the neutron-transport code MCNP. The necessary input information on relevant sample properties are obtained from the parallel gamma and neutron measurements on the samples.

The ultimate goal of this approach is to reduce and to simplify the calibration efforts of analytical PNCC measurements to a normalization measurement against a single reference sample. This procedure has been successfully tested with PNCC measurements on a series of PuO_2 samples, where the Pu content of the samples could be determined with an absolute accuracy of better than 0.2%.

Contact (7.1.1-7.1.2):
Herbert Ottmar • tel.: +49 7247 951 372
fax: +49 7247 951 191 • ottmar@itu.fzk.de

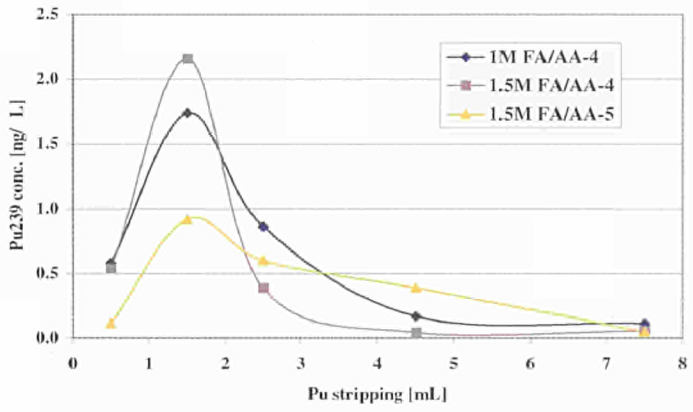

Fig. 7.1 Back-extraction of Pu from TOPO column using formic acid/ascorbic acid

7.1.3 Improvement of sample preparation for thermal ionisation mass spectrometry

Modern analytical requirements challenge instrument sensitivity and chemical sample preparation. Decreasing sample size calls for improved chemical separation techniques. Thermal ionisation mass spectrometry is a very accurate method, however requiring chemically pure samples. The application of tri-octyt-phosphine-oxide (TOPO) as column based extractant on silica gel support was implemented for the separation of U and Pu with high recovery rates. Pu back extraction is achieved with a combination of ascorbic and formic acids. Fig. 7.1 shows the elution curves of Pu using different media. The method was validated for samples down to 10 pg of Pu and 100 pg of U. Filament preparation from formic acid media results in an improvement of sensitivity by a factor of three due to much higher ionisation yields, consequently opening the possibility to further reduce the amount of material required for a measurement.

Contact (7.1.3):
Klaus Mayer • tel.: +49 7247 951 545
fax: +49 7247 951 191 • mayer@itu.fzk.de

7.2 Environmental Sampling

7.2.1 Implementation of techniques for particle characterization and detection of radioactive traces

In the framework of the programme 93+2 started in 1993 by IAEA for the detection of undeclared nuclear activities from the analysis of environmental samples, methods for the detection of particles containing fissile materials have been implemented. Of particular importance is the analysis of particles containing nuclear material in swipe samples. According to Article 9 of the Model Protocol Additional (INFCIRC/540) to the agreement between States and IAEA for the application of safeguards, Member States shall provide the Agency with access to locations specified by the Agency itself to carry out "wide-area environmental sampling". Some of the Member States have already ratified the additional protocol and the environmental sampling has been added to routine safeguards inspections.

In order to further develop and improve the methods for particle analysis, working standards were produced at ITU using reference uranium oxide powder. In 1999, uranium oxide particles of ~1 µm diameter with four different enrichments (^{235}U weight percentage 0.5%, 1%, 3% and 10%) were produced; starting from certified reference materials U-005, U-010, U-030 and U-100 (NBS standard). These particles were characterised by Scanning Electron microscopy (SEM) for their morphological properties and verified by Secondary Ion Mass Spectrometry (SIMS) for their isotopic composition [1]. (see Fig. 7.2). Both techniques reveal no agglomeration effects are present.

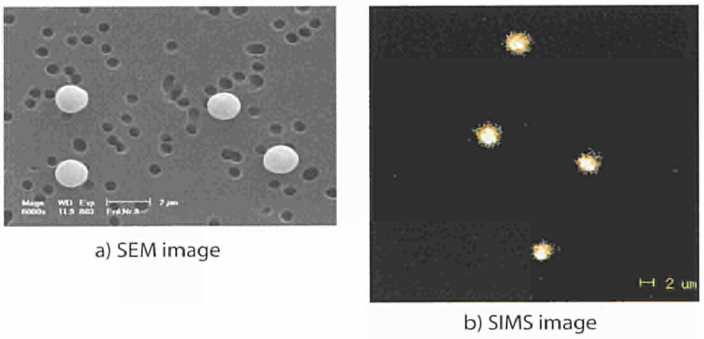

a) SEM image

b) SIMS image

Fig. 7.2 Images obtained by Scanning Electron Microscopy (a) and by Secondary Ionisation Mass Spectrometry (b) on control particles

These control particles were used in order to develop a method based on fission tracks compatible with SIMS/SEM analysis. The method has been applied to a swipe sample collected in an enrichment plant. In Fig. 7.3, an example of fission tracks produced by particles containing uranium is given. Subsequently, the particles will be analysed by SEM/SIMS. This new development will be implemented in 2000.

A method based on the development of α-tracks has been used to detect hot particles which then have been characterised by SIMS [2]. The same method will be applied to swipe samples collected in hot cells in order to identify particles from α-emitters in the samples.

x(mm)	y(mm)	Tracks
1,68	0,66	ca.25
3,45	2,08	20
7,25	2,58	20
8,29	2,18	10 + 20
10,21	2,20	14
12,08	3,28	ca. 30
2,51	3,93	9
10,45	3,65	17
7,91	5,47	12
15,59	5,24	ca. 40
1,36	7,30	15
0,59	7,24	ca. 30
16,23	9,01	11
14,55	8,55	12
12,30	8,44	10
7,73	9,12	27
3,60	9,50	> 100
9,50	9,41	22
14,34	9,43	30

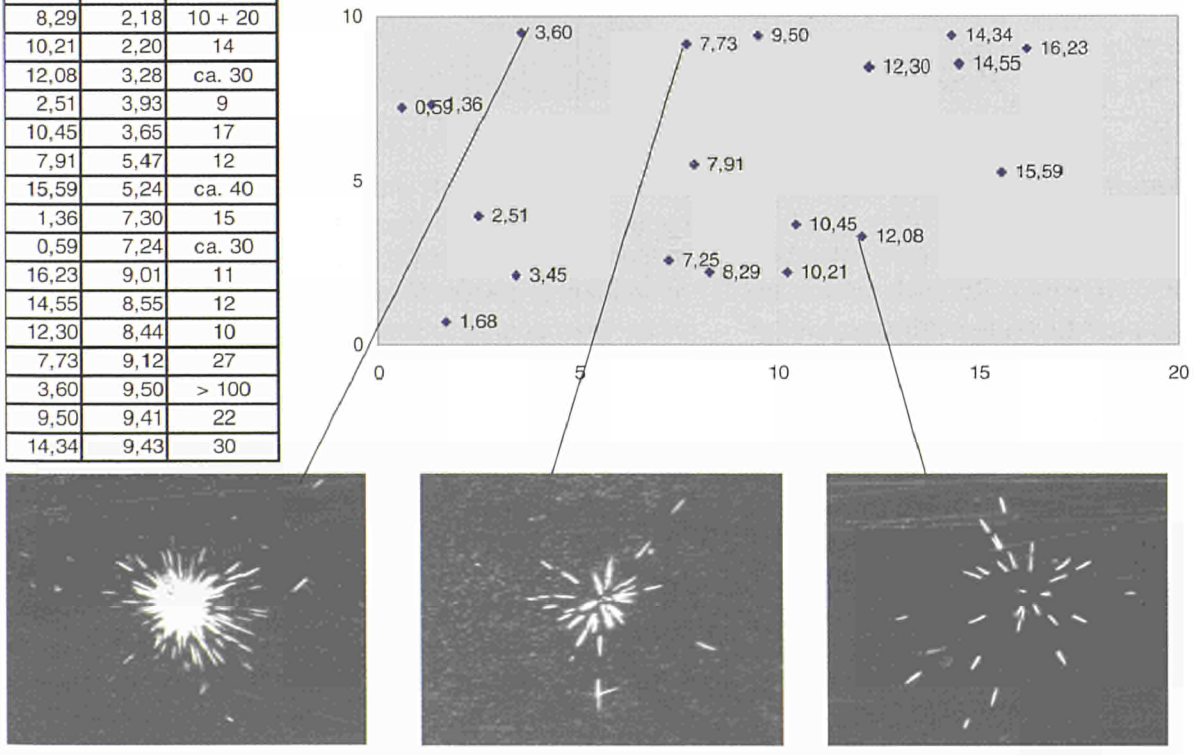

Fig. 7.3 Example of fission tracks produced by particles containing uranium.

A systematic study of the parameters affecting the preparation of swipe samples for particle analysis by SIMS has been started. The aim of this investigation is to find the recovery rate of particles from the swipe by determining the repartitioning of particles between swipe and solvent used for solid/liquid extraction of the particles from the swipe tissue. In order to increase the sample throughput, a prototype of an automatic sample changer for the SIMS that can load eight samples, has been constructed and will be installed in 2000 for testing.

Real swipe samples collected outside hot cells were provided by Euratom and IAEA. They have been analysed for their total content in fission products and actinides by low background γ-spectrometry and by ion chromatography inductively coupled plasma mass spectrometry (IC-ICP-MS) in order to understand if samples collected outside hot cells provide an indication of the activity performed in the cell itself. The results are still under evaluation.

References

[1] N. Erdmann, M. Betti, O. Stetzer, G. Tamborini, J.V. Kratz, N. Trautmann, J. van Geel; "Production of monodispersed uranium oxide particles and their characterisation by SEM and SIMS"; Spectrochimica Acta Part B, (submitted for publication).

[2] G. Tamborini, M. Betti, P. Carbol , L. Koch, "Secondary ion Mass Spectrometry for the detection of Radionuclides in particles from soil samples", in "Environmental Radiochemical Analysis" (Ed.) G.W.A. Newton, Royal Society of Chemistry, Cambridge 1999, 382-393

Contact (7.2.1): Maria Betti • tel.: +49 7247 951 363
fax: +49 7247 951 186 • betti@itu.fzk.de

7.2.2 Particle analysis with the Philips XL 40 scanning electron microscope

The new Philips XL40 scanning electron microscope (SEM) has been equipped with a "Gun Shot Residues" programme enabling automatic operation of the SEM in a combination of back-scattered electron (BSE) and energy dispersive X-ray fluorescence (EDX) modes for identifying and analysing selected particles of interest. The software has been adapted to allow the range of elements identifiable to extend to plutonium and uranium.

The program enables the microscope to operate unattended, for example, overnight, and to scan up to eight different swipe-test samples, providing a separate protocol for each with a list of the particles of interest. The sample is divided up into fields, each of which is scanned by the beam and the heavy metal particles detected by the BSE signal. The microscope then returns to each particle individually and makes an elemental analysis by EDX, producing a printout of particle composition, position and size. It can also automatically produce a secondary electron image of each particle if required.

An example of such an analysis is reproduced in Fig. 7.4. This shows a schematic image of the sample with the particles containing uranium indicated by the yellow crosses, and a summary protocol of the number of particles found. One particle has been chosen as an example and the high resolution secondary electron image is shown, revealing a complex surface structure, together with the EDX spectrum revealing the particle to contain uranium.

A new EDX detector is being fitted to the Philips XL 40 which also enables the analysis of the light elements carbon, nitrogen, oxygen and fluorine to be made.

Contact (7.2.2): Ian Ray • tel.: +49 7247 951 378
fax: +49 7247 951 191 • ray@itu.fzk.de

7.3 Illicit Trafficking and Forensic Analysis

Nuclear forensics deals with the identification and determination of characteristic parameters that help to identify the origin of nuclear material. Studies have been carried out to optimise the analytical methodology and to further improve international collaboration in this area. In parallel the compilation of known parameters from open sources and confidential information into the database continued. Furthermore, ITU provided essential contributions to the work of the International Technical Working Group on Nuclear Smuggling.

7.3.1 Relational database for identification of nuclear material of unknown origin

In the framework of ITU's activities for analytical identification of nuclear material of unknown origin, the relational database system dedicated to support and guidance of such analyses was updated and extended. Continuing the

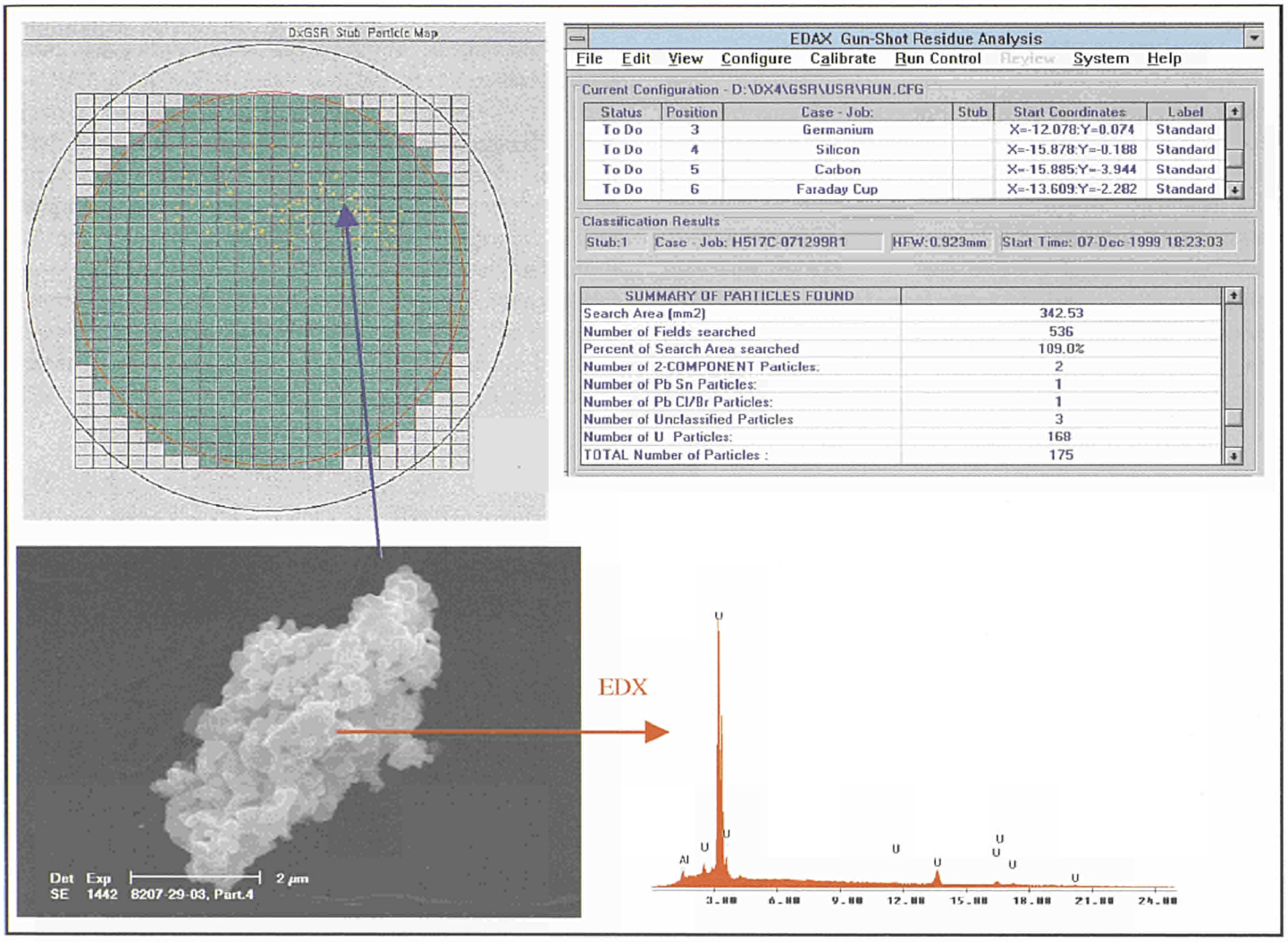

Fig. 7.4 Example of the automated identification and preliminary analysis of particles of interest using the modified "gun shot residues" programme.

co-operation with the Bochvar All-Russia Research Institute for Inorganic Materials (VNIINM) in Moscow, two guest scientists again stayed at ITU for one month each and made essential contributions for extending the database structure to

- time-dependent distribution parameters of nuclear materials and to
- update on analytical methods

In addition, the user interface of the database system was upgraded and now includes graphical output of nuclear fuel dimensions. A complete update of open literature data on macroscopic characteristics of fuel used in European power reactors has been done as well. All corresponding data have been cross-checked and transformed to the relational table system used as database backbone (TUAR-96, p. 135; TUAR-98, p. 33-35, 104). A symmetric update of the common database sector was done at VNIINM Moscow in October 1999.

Additional data covering characteristic parameters of special nuclear materials used in the Czech Republic, Hungary and Bulgaria are now available and are being implemented in the database. In the course of the step-by-step diagnostic analysis of a vagabonding material they allow for excluding a range of origins and intended use from the above mentioned countries.

Negotiations with Framatome and Belgonucleaire were completed and initiated important database contributions covering parameters characteristic for nuclear material manufactured in their respective production facilities.

Contact (7.3.1): Arndt Schubert • tel.: +49 7247 951 406 • fax: +49 7247 951 191 • schubert@itu.fzk.de

7.3.2 International technical working group on nuclear smuggling (ITWG)

At the last meeting of the International Technical Working Group on nuclear smuggling (Helsinki, 9 +10 June 1999) a task to set up a Model Action Plan (MAP) was given to ITU. MAP should list all actions following the seizure of illicit trafficking of nuclear materials. From earlier reports given to ITWG by the FBI of US and the Metropolitan Police of London (Scotland Yard) the initial steps following the detection were defined. Further, the experience of ITU gained in analysing seized material were included. In a meeting of the task group complemented by STUK, Finland and the IAEA the structure of the MAP was laid down (see Tab. 7.2). It served as the basis for the two demonstration exercises described below.

In the framework of the ITWG a **round robin test on PuO_2,** oxide powder was conducted to demonstrate the potential of nuclear forensics in identifying unknown nuclear materials. Fig. 7.5 explains the methodology used by ITU to identify the fabrication plant and the date where the PuO_2 was fabricated, the reprocessing plant that recovered the Pu from spent fuel and the nuclear power station that had discharged the fuel. ITU had the advantage of having an elaborated database to which the analytical results could be at-

Tab. 7.2 Key elements of the Model Action Plan (MAP) developed by a task group of ITWG

1.	Cordon off site and guard by **law enforcement** service present (customs or police)
2.	Call competent service (technical) to confirm the **nuclear or radioactive nature** of the material and to determine whether a nuclear or radiation hazard exists
3.	Inform a central authority authorized to initiate an **action plan** (in accordance with national institutions and legislation). Such an action plan should include institutions having competence in at least the following: – Public Health and environmental contamination – Radiation protection – Criminal investigation – Nuclear material categorization in the field – Nuclear material safeguards – Specialised laboratory for NDA – Laboratory for in-depth analysis – Storage and transport of nuclear and radioactive material – Point of Contact for IAEA Illicit Trafficking Database
4.	Perform **On-site** actions which should cover: – Health physics examinations – Law enforcement actions – On-site categorization by mobile NDA instrumentation – Safe storing of the material until transportation – Preparation for and transport to (eventual re-packing) national central and specialised laboratory
5.	Perform investigations at the **specialised national laboratory**
6.	If the national laboratory is not in a position to carry out certain analysis a sample of the material could be shipped to an **external specialised laboratory**
7.	Compare results again with appropriate database. Possibly request for further investigations
8.	Write an analytical "expert opinion" of the analysed seized material for the national law enforcement authorities where the seizure occurred
9.	Compile a synopsis and evaluation of all evidence by the national legal authority where the seizure occurred
10.	Organize treatment and closure of the case by the national courts
11.	Return the the material to the last legal owner in accordance with an international agreement and existing non-proliferation legislation

tributed. This finally led to full disclosure of the PuO_2 history. (see also highlight article p. !!!!).
The microstructural examination led to the interesting result that the material consisted of four different PuO_2 components, which can be characterised as follows:

Component A: PuO_2 platelets in the size range 1.0 µm to 16.0 µm with an unusually rough surface structure. This component formed the largest fraction of the total sample (> 90 %) and contained no Am which could be detected by EDX (< 1.0 at.%). The PuO_2 grain size was very small, typically 25 nm.

Component B: PuO_2 platelets in the size range 0.5 µm to 5.0 µm with flat regular surfaces, and a much larger PuO_2 grain size, typically 0.2 µm.
Component C: A fibrous form of PuO_2 which had a very small grain size and was a very minor component of the sample.

These three components are illustrated in Fig. 7.5. There was a further component consisting of irregular PuO_2 platelets typically 5.0 µm in size which contained a significant Am level (> 3.0 at.%) measured by EDX. This could represent a late fraction in the precipitation process.

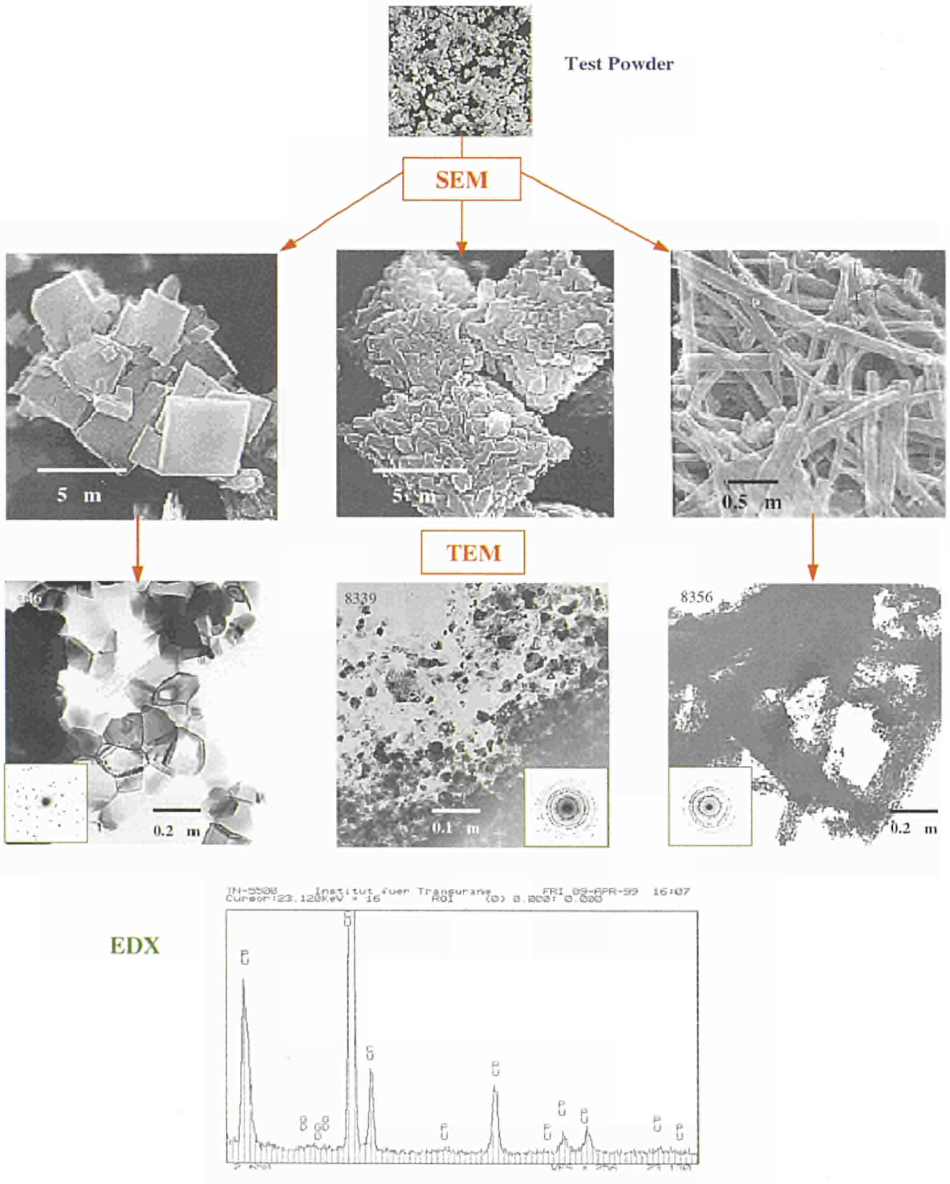

Fig. 7.5 Three components contained in the PuO_2 test sample

Since component A formed over 90% of the mixture the other components could not interfere with the analysis, but it seems unlikely that component B with the significantly larger grain size came from the same original batch of material.

Contact (7.3.2): Lothar Koch • tel.: +49 7247 951 424
fax: +49 7247 951 596 • koch@itu.fzk.de

7.3.3 Assistance to Central and East European countries

In the framework of the co-operation with Central and East European countries to combat nuclear trafficking of nuclear material three respective PHARE projects covering assistance to the Czech Republic, Hungary and Bulgaria under the acronym FONSAFE (FOrensic Nuclear analysis for SAFEguards) have been completed in 1999. To perform a maximum fraction of fissile material characterisation in the country of seizure, if possible directly on-site, the projects include an appropriate upgrade of local nuclear analysis capabilities complemented with queries to the ITU nuclear material database. Upon request of the nuclear regulatory authority of the partner country in-depth analyses of subsamples are made at ITU's dedicated laboratories in order to reveal the origin of the material.

After selection of the most appropriate technical solution for each project the delivered equipment has been thoroughly tested on samples stemming from previous cases of vagabonding material seized in the respective countries.

In the **Czech Republic** the updated capacity for trace analysis in nuclear materials was applied to generate complementary trace element data characteristic for nuclear material available at the Nuclear Research Institute (NRI) Rez near Prague. Those data were filed to the ITU database as a guidance tool to support nuclear forensic analysis. A selected sample material was shipped to ITU and used for complementary mass spectrometric analyses as well as for preparing a routine transport procedure which in future can be invoked on short notice. One mass spectrometry expert spent three stays at ITU to become acquainted with the working procedures for ICPMS, GDMS as well as TIMS.

Bulgarian experts were invited to ITU and had the possibility to familiarize with the application of portable gamma spectrometry for U/Pu categorization. In Bulgaria - after testing of the equipment with HEU material previously seized in the country - a demonstration was organised applying the system to a non-destructive enrichment measurement of nuclear fuel pellets.

In **Hungary** the same basic configuration was chosen for a more complex exercise aimed at demonstrating the full procedure of response to a seizure of nuclear material of unknown origin at a simulated Hungarian border checkpoint. This demonstration exercise was organized and guided by the Hungarian Atomic Energy Authority calling on intervention of the Hungarian border guards, customs, and police. For the first on-site analyses experts from the Frederic Joliot-Curie National Institute for Radioprotection and Radiohygiene and for on-site characterization experts from the Institute of Isotopes and Surface Chemistry of the Hungarian Academy of Sciences were involved (Fig. 7.6).

Fig. 7.6 L. Lakosi and J. Zsigrai (spectrometrists from the Institute of Isotopes of the Hungarian Academy of Sciences, Budapest) performing non-destructive categorization using a portable gamma spectrometer.

They successfully applied the equipment provided within the project. The exercise was the first in the frame of the Model Action Plan of the International Technical Working Group on nuclear smuggling (ITWG), see Tab. 7.2.

In all three projects, the basis for an efficient interface for complementary analyses to be performed at a dedicated EU laboratory (as ITU) with participation of experts from the partner countries was created. The projects can also be used as model for further broadening ITU's co-operation with other Central and East European countries, in particular with the candidates for EU extension.

A TACIS project on counteracting the illicit trafficking of nuclear materials in the **Ukraine** was started this year in collaboration with the Ukrainian Ministry for Environmental Protection and Nuclear Safety. The project envisages to upgrade the capabilities of the Institute for Nuclear Research in Kiev in order to execute the on-site characterisation of nuclear materials (U/Pu categorisation) and to do more detailed non-destructive analysis in that institute, being assigned officially this role by government decree. The project is carried out in close collaboration with the Delegation of the European Commission and the TACIS monitoring team in Kiev and has two further beneficiaries: the Ukrainian Customs Authorities and the Ukrainian Law Enforcement. The training requirements of the latter two organisations with respect to reacting to real cases of seizure of nuclear material were assessed and a specific training programme is under development. Training courses will be organised in February 2000 in collaboration with the Finnish Radiation and Nuclear Safety Authority (STUK). A handbook for the Ukrainian Nuclear Regulatory Administration on the appropriate response procedures, in line with the Model Action Plan of the International Technical Working Group (see Tab. 7.2), will also be developed under the project. In order both to gather the essential input for this handbook and to validate the initial procedures, a demonstration exercise was organised in Odessa, using seized material. The detection, radioprotection, criminal investigation and nuclear material characterisation were executed on the spot, involving all relevant authorities and using highly sensitive mobile equipment for the determination of the isotopic composition of the real material. Western participants came from IAEA, Scotland Yard, STUK and ITU. For this exercise the portable equipment was brought to the spot by the ITU representatives and operated by the trained spectrometrists from INR. Some INR personnel will also receive further training at ITU on nuclear analytical techniques for the more detailed (destructive analytical) investigation of the material, after transport by IAEA of a representative subsample to ITU. Finally an agreement on the exchange of data on the civil Ukrainian nuclear fuel cycle was signed in order to complete the ITU database on nuclear materials (section 7.3.1). In addition, it gives the Ukrainian authorities the possibility to issue specific queries to the database and to perform optimised source attribution of seized nuclear material.

Improving the analytical capabilities at the Bochvar Institute (VNIINM) in Moscow, **Russia,** is the objective of another TACIS project. Three different laboratories are being set-up for nuclear forensic purposes, for safeguards analysis and for metrological support. Several Russian analysts were trained at ITU (see section 7.5). A conceptual study in the implementation of the laboratories into VNIINM's existing structures was successfully completed. Instrumentation for upgrading the laboratories was ordered.

Contact (7.3.3): Klaus Mayer • tel.: +49 7247 951 545 • fax: +49 7247 951 191 • mayer@itu.fzk.de

7.3.4 New developments

The **concept of a "Microstructural Fingerprint"** of a material has been developed in ITU as a complement to the "Isotopic Fingerprint" in the characterization of samples in Nuclear Forensic Science. In the examination of unknown specimens of nuclear materials the primary parameter of importance is the "Isotopic Fingerprint" of the sample, mainly the ratios of the different isotopes of U and Pu which are present. In some cases, however, where no clear isotopic signature is found, or where there is a mixture of materials present, the isotopic fingerprint alone is not sufficient for a unique identification to be made.

The microstructural fingerprint of a material consists of a specific set of data resulting from a microscopic **(optical, SEM, TEM, EDX)** investigation which is characteristic of its physical and mechanical state and its mechanical and thermal history. This data comprises, for example: particle morphology and size distribution, grain size distribution, porosity, dislocation density, precipitation and crystallography. This fingerprint, once established, can be used for comparison purposes for identifying an unknown illicit sample with a known reference, or for eliminating materials of known origin as possible sources. Even where no reference samples

are available for comparison, much information about the material can be deduced from the microstructure using established principles of materials science. For example, the dislocation density and character gives information about whether the material has been deformed during manufacture and to what extent, and the grain size distribution provides clues about process temperatures and reaction rates.

The microstructural information is particularly important in the case of powder samples because they can be mixed with other compounds with the deliberate intention of confusing the chemical or isotopic analysis of suspect materials. However the microstructural fingerprint of a component cannot be altered unless the whole material is completely reprocessed. An example of the application of the microstructural fingerprint is given in the highlight article p. 32, where a plutonium oxide powder of unknown origin is compared with a reference sample. Though the platelets size distributions determined by SEM are only slightly displaced, the PuO_2 grain size distributions are very significantly different, thus excluding the unknown material as coming from the same source as the reference sample.

The **production mode and age of Pu** are of primary interest in nuclear forensic investigations as this information is essential for the determination of the origin of seized nuclear material. The isotopic composition of plutonium is a function of the conditions of irradiation (reactor type) and its duration. By comparing measurement results to calculated isotopic ratios (obtained through codes like ORIGEN2 or SCALE), the production mode can be identified. Pu isotopic composition in the test samples was determined by thermal-ionisation mass spectrometry. In our investigations the following reactor types were considered: heavy-water-reactor (HWR), light-water-reactor (LWR), graphite-moderated-reactor (RBMK), fast breeder reactor (FBR) and research reactors (MTR and Triga) (see Fig. 7.7). The age of the plutonium was determined by accurately assaying its daughter products, i.e. ^{241}Am, ^{234}U, ^{235}U, ^{236}U using isotope dilution mass spectrometry and respective decay calculations.

The ***n*(^{18}O)/*n*(^{16}O) ratio in UO_2** fuels may serve as a characteristic parameter in origin determination of seized nuclear material. Small variations in oxygen isotopic ratios are observed in nature. This reflects in uranium oxide produced at different geographic locations. The oxygen isotopic ratio measurements of UO_2 samples were carried out by two different methods: Thermal Ionisation Mass Spectrometry (TIMS)

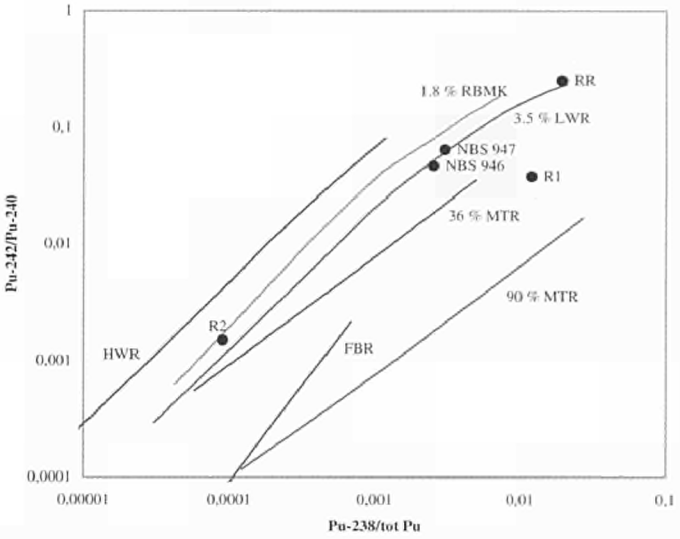

Fig. 7.7 Isotopic ratios of plutonium as produced in different reactor types: calculated (solid lines) and measured (data points)

and by Secondary Ionisation Mass Spectrometry (SIMS). Using the measured variations in $n(^{18}O)/n(^{16}O)$ ratios samples of different origin can clearly be distinguished (Fig. 7.8).

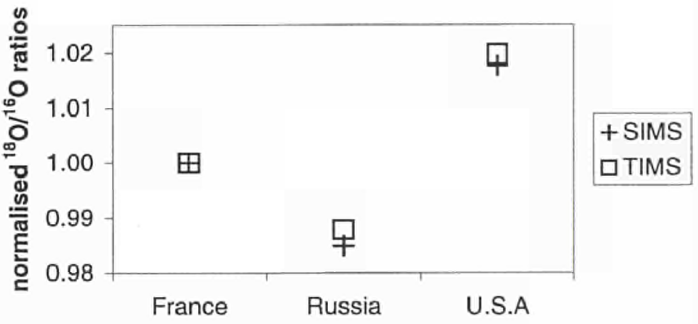

Fig. 7.8 Normalised $n(^{18}O)/n(^{16}O)$ ratios measured by TIMS and SIMS.

Contact (7.3.4): Ian Ray • tel.: +49 7247 951 378
fax: +49 7247 951 191 • ray@itu.fzk.de

7.4 Analytical Support to Euratom and IAEA

Considerable effort was spent in the continuation of the analytical support to the safeguards authorities. Both on-site laboratories made significant progress, the installation phase in the LSS was completed while the OSL has been passing gradually into operation. Measurement of samples at ITU and in field was continued.

7.4.1 Laboratoire sur site (LSS), La Hague

General status of the project

The LSS project is being executed according to schedule. The construction phase has been made under the supervision of the engineering firm SGN (Société Générale pour les techniques Nouvelles) and was completed by the middle of the year. The testing of the infrastructure started in September and general safety relevant tests were performed within two weeks in October with the participation of ITU staff. The hand-over of the laboratory (Mise à Disposition) was officially announced on November, 6. This is a legal milestone where the responsibility of the LSS is transferred to COGEMA and further on EURATOM. The authorization to connect the Lab to active area was given by the French Safety Authority (DSIN) on November, 12. An agreement between COGEMA and EURATOM concerning waste treatment has been finalized. Scientific equipment was installed and first functional tests were carried out by ITU experts. Figs. 7.9, 7.10, 711 show the implementation of the LSS [1]

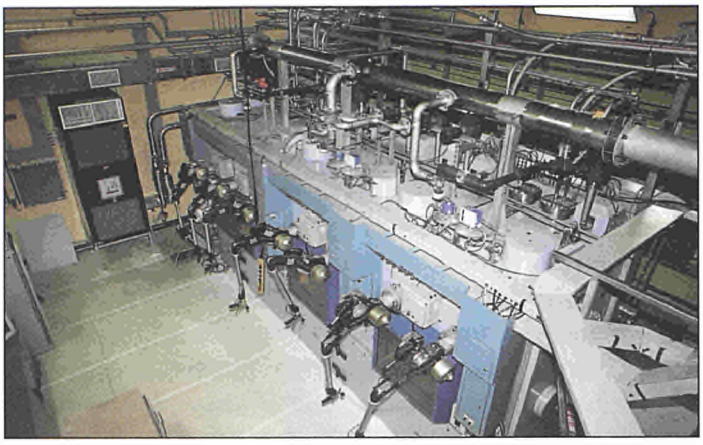

Fig. 7.9 LSS Hot cell suite for the analysis of reprocessing input samples

Fig. 7.10 LSS Mass Spectrometry Laboratory

ITU contribution

The on-site activities started in May 1999 with the implementation of the entire EURATOM equipment including four Hybrid K-Edges, a gamma-ray measurement station (all equipped with sample changers designed by ITU), a combined neutron-gamma counter, a Compact K-Edge, three PAAR densitometers, the fully automated IDA box (Isotope Dilution Analysis) housing a specially adapted Zymark laboratory robot, a Thermal Ionization Mass Spectrometer and additional small analytical devices built mainly in house. An internal computer network used as expert system (TUI

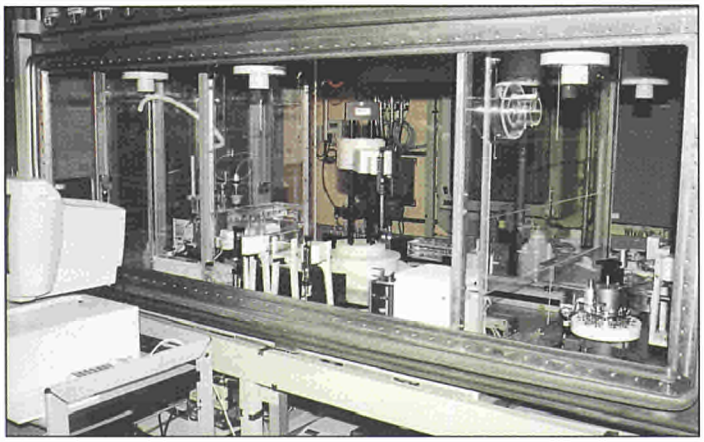

Fig. 7.11 LSS Robotised Isotope Dilution Analysis Box for preparation of samples prior to mass spectrometry

Analysis Management System, TAMS) developed at ITU for the specific application was also installed during the same period. All the electrical connections and specific assembling work, i. e. shielded integration of EURATOM material in the hot cell suite and use of telemanipulators in hot cell suite and PuO_2 chain were performed by ITU specialists. In order to cope with site requirements, special training was organized. Site specific procedures were applied for accessing the laboratory, still considered non-radioactive. Following the implementation, inactive commissioning started and was successfully completed by end of September. All the equipment listed above was powered, tested and calibrated where possible. At the end of the reporting period, the LSS was ready for active commissioning, which is foreseen to start in early 2000. The laboratory is expected to start operation by April 2000.

After completion of safety relevant tests involving EURATOM analytical equipment, ITU concentrated on the managerial side of the project. The interfaces between Euratom and ITU as well as the respective responsibilities were defined in a note of understanding. The laboratory responsible and his deputy have been proposed by ITU for nomination by ESD to COGEMA.

On the other side, ITU started together with COGEMA to implement a Quality Management system including specific procedures and working instructions. The interfaces between the plant operator and the LSS have been established. This will be amended and completed during active commissioning taking into account operational aspects.

The whole team of ITU inspector analysts successfully followed site specific training. Two sessions of a week duration were organized on site by INSTN (Institut National des Sciences et Techniques Nucléaires) followed by a general tour to the site of COGEMA La Hague.

References

[1] P. Daures, K. Mayer, H. Ottmar, , P. Richir, U. Blohm-Hieber, W. Kloeckner, Implemention of an on-site safeguards analytical laboratory: the "Laboratoire Sur Site" (LSS), Sixth International Conference on Facility Operations-Safeguards Interface, Jackson Hole, Wyoming, September 20-24,1999.

Contact (7.4.1.): Pascal Daures • tel.: +49 7247 951 211 fax: +49 7247 951 191 • daures@itu.fzk.de

7.4.2 On Site Laboratory (OSL), Sellafield

The OSL saw, during the reporting period, the finalisation of a long series of tests on equipment in the laboratory, aiming at the demonstration of safety, the so-called inactive commissioning. Many of these tests were repeated after having introduced radioactive material in the laboratory in the framework of the active commissioning. By the end of 1999 all types of samples apart from spent fuel solutions could be analysed in the on-site laboratory.

Inactive Commissioning

Early this year intense activities were carried out to allow to complete inactive commissioning. These were of technical and organisational nature, in particular:

- inactive testing of scientific equipment and establishing of appropriate test reports
- comprehensive testing of services vital to laboratory operation (electricity, ventilation, pressurised air etc.)
- BNFL provides services to the OSL services such as sample delivery, sample excess, waste disposal and maintenance. This was formalised by amending the agreement (Doc. Ref. OSL/93/1) between BNFL and ESD.
- a complete cycle of maintenance on OSL equipment was carried out to demonstrate its safe operation.

This phase of OSL activities was completed with the presentation of the Inactive Safety User Commissioning **Report** (summarising results and observations) and an Active Safety User Commissioning **Schedule** (describing the planned activities) to the respective safety committee within BNFL. Both documents were approved. After connecting the OSL to the active ventilation, radioactive material could be entered into the laboratory.

Since then the OSL is considered to be an active laboratory leading into active commissioning phase.

Active Commissioning

The active commissioning was carried out gradually. It started with a period where only uranium samples were handled and all related manipulations and procedures were tested with respect to safety, accuracy and practical applicability.

Fig. 7.12 Official inauguration of the OSL by W. Gmelin (left) and J. van Geel (second from left)

The scientific instrumentation was calibrated using well characterised standards and reference materials. Quality control material was analysed prior to measurements of real samples. After having successfully completed all tests, Uranium Safeguards samples have been analysed routinely.

Subsequently, plutonium commissioning was started. Again, first the equipment was calibrated, and the procedures were carefully verified. A intercomparison method using all available techniques for plutonium analysis was performed, covering Neutron Counting, Product Hybrid K-Edge and Isotope Dilution Mass Spectrometry. PuO_2 and Pu-nitrate safeguards samples have been analysed routinely.

Commissioning of reprocessing input sample analysis, the most delicate type of samples to be handled in the OSL, has been started.

A large proportion of this year's activities was allocated to integrate the OSL into BNFL's system for sample delivery, return of excess sample, waste disposal, accountancy and means of communication for these areas. These interfacing issues showed to be much more complex than expected, requiring the preparation of additional OSL procedures, updating of software modules and changes of managerial tools.

Finally the OSL was officially opened on the 13th of October by the director of the Euratom Safeguards Directorate, W. Gmelin in the presence of the director of ITU, J. van Geel and the director of Sellafield site, Gordon Adams (former Member of the European Parliament).

Training of inspector analysts

A series of lectures was organised for the inspector analysts on topics such as fundamentals of radiochemistry and nuclear physics, fuel cycle, reactor types, analytical techniques, radioprotection and conventional safety. The training activities in measurement techniques continued also this year in order to train new colleagues and to retrain other colleagues to improve versatility. The lectures as well as the practical training was given by ITU senior scientists.

Courses on OSL data management system and for the accountancy of fissile material were organised at ITU. Training on site specific-aspects was conducted by BNFL, being of fundamental importance for work in Sellafield's controlled areas.

Data management

The data management system of the OSL has been specifically designed and developed. It was thoroughly tested in the pre-OSL at ITU. Some modules, however, are unique in the OSL:

- Accountancy Management System (AMAS) to control fissile material holding and criticality
- AMAS-satellite program (ASAT) to monitor transfers of radioactive material in barcoded containers

These new modules were implemented before starting active commissioning and have been subject to validation processes.

Contact (7.4.2): Hans-Günther Schneider
tel.: +49 7247 951 211 • fax: +49 7247 951 191
schneider@itu.fzk.de

7.4.3 In-field verification activities

In order to carry out verification measurements on samples of reprocessing input solution, inspector analysts from ITU traveled on a regular basis to the reprocessing plant at La Hague, France. The measurement campaigns cover the whole year with ITU staff performing analyses on a weekly basis, perform instrument maintenance and calibration. Input samples are measured using the EURATOM Hybrid K-Edge instrument.

Last year, more than 800 samples have been measured at La Hague, leading to a total number of measurements of almost 1300 as shown in Tab. 7.3

Tab. 7.3 Evolution of the number of samples analyzed at La Hague

Year	Number of input samples	Number of measurements (total)	Effective working days	Measurements per day (average)
1989	15	33	11	3.00
1990	107	234	66	3.55
1991	175	317	98	3.24
1992	199	335	85	3.94
1993	305	435	104	4.18
1994	407	597	109	5.48
1995	573	917	144	6.37
1996	618	1067	156	6.84
1997	663	1068	171	6.25
1998	785	1246	172	7.24
1999	898	1298	154	8.43

The mobile COMPUCEA instrument was operated by specialized ITU staff to directly support inspection campaigns at **low enriched uranium** (LEU) fuel production facilities in Spain, France, Sweden, Belgium and the UK. The instrument is specifically dedicated for uranium enrichment and concentration measurements. More than 200 samples were measured in only 8 inspection weeks. The measurement results were communicated to the inspectors within 2 days.

Contact (7.4.3.): Klaus Mayer • tel.: +49 7247 951 545 fax: +49 7247 951 191 • mayer@itu.fzk.de

7.5 Training

In the framework of the Environmental Monitoring and High Performance Trace Analysis (HPTA) projects, a two days training course was organised in 1999. Inspectors from IAEA and Euratom attended the course where lectures on strategy and objectives of the projects for safeguards implementation, but also on swipe sampling, analytical methods, particle characterisation and interpretation of results. A written exercise about planning a sampling campaign and a practical exercise of swipe sampling, also inside hot cells, have been performed at ITU's laboratories to complement the theoretical part of the course. The inspectors also had the possibility to visit the laboratories (clean laboratory and SIMS laboratory) where the samples are analysed and to discuss with the expert analysts.

Training on the use of the hybrid K-Edge technique was provided to Euratom using the instrument installed at COGEMA La Hague. Furthermore, specific training on the in-field application of the COMPUCEA was given to a Euratom inspector.

In the framework of a TACIS project, seven analysts from the Bochvar Institute in Moscow were trained in active and passive radiometric measurement techniques. Alpha spectrometry, high resolution gamma spectrometry, neutron coincidence counting, X-ray fluorescence and K-edge densitometry were subject to lectures and to many practical exercises in the laboratory.

Contact (7.5): Klaus Mayer • tel.: +49 7247 951 545 • fax: +49 7247 951 191 • mayer@itu.fzk.de

Publications and Contributions to Conferences

Books and Periodicals

17 of these publications (marked by an asterisk) had been submitted or presented at conferences in 1998 and appeared in print in 1999.

Allgeier H.J., Schenkel R.
Wissenschaft in den Dienst des europäischen Bürgers stellen. Die Gemeinsame Forschungsstelle im Aufbruch
Jahrbuch der Atomwirtschaft 30 (1999) 43-53

**Amoretti G., Caciuffo R., Santini P., Lander G.H., Kulda J., de V. du Plessis P.*
Polarized Neutron Scattering Study of the Magnetic Response across TN in a Single Crystal of UO_2
Journal of Applied Physics 85 No. 8 (1999) 4524-4526

Apostolidis C., Edelmann F.T., Kanellakopulos B.
Organoactinide Chemistry: Polysilylated Actinidocenes of Thorium, Uranium, and Neptunium
Zeitschrift für Naturforschung 54b (1999) 960-962

Barrero Moreno J.M., Betti M., Nicolaou G.
Determination of Caesium and its Isotopic Composition in Nuclear Samples Using Isotope Dilution-Ion Chromatography-Inductively coupled Plasma Mass Spectrometry.
Journal of Analytical Atomic Spectrometry 14 (1999) 875-879

Behr T.M., Sgouros G., Stabin M.G., Béhé M., Angerstein C., Blumenthal R.D., Apostolidis C., Molinet R., Sharkey R.M., Koch L., Goldenberg D.M., Becker W.
Studies on the Red Marrow Dosimetry in Radioimmunotherapy: an Exerimental Investigation of Factors Influencing the Radiation-induced Myelotoxicity in Therapy with β-, Auger/Conversion Electron-, or α-Emitters
Clinical Cancer Research 5(10 Suppl) (Oct 1999) 3031s-3043s

Behr T.M., Béhé M., Stabin M.G., Wehrmann E., Apostolidis C., Molinet R., Strutz F., Fayyazi A., Wieland E., Gratz S., Koch L., Goldenberg D.M., Becker W.
High-Linear Energy Transfer (LET) α versus Low-LET β Emitters in Radioimmunotherapy of Solid Tumors: Therapeutic Efficacy and Dose-limiting Toxicity of ^{213}Bi versus ^{90}Y-labeled CO17-1A Fab' Fragments in a Human Colonic Cancer Model
Cancer Research 59 No. 11 (Jun 1999) 2635-2643

Bernhoeft N., Sato N., Roessli B., Aso N., Hiess A., Lander G.H., Endoh Y., Komatsubara T.
Magnetic Fluctuations Above and Below T_c in the Heavy Fermion Superconductor UPd_2Al_3
Physica B 259-261 (1999) 614-620

Betti M., Tamborini G., Koch L.
Use of Secondary Ion Mass Spectrometry in Nuclear Forensic Analysis for the Characterization of Plutonium and Highly Enriched Uranium Particles
Analytical Chemistry 71 No. 14 (1999) 2616-2622

Bourdarot F., Bombardi A., Burlet P., Calemczuk R., Lander G.H., Lapierre F., Sanchez J.P., Mattenberger K., Vogt, O.
Collapse of the Magnetic Ordering and Structural Anomalies in the $U_xLa_{1-x}S$-System: Neutron Diffraction and Specific Heat Measurements
European Physical Journal B 9 (1999) 605-611

Bourva L.C.A., Croft S., Ottmar H., Weaver D.R.
MCNP Modelling of a Combined Neutron/Gamma Counter
Nuclear Instruments & Methods in Phys. Res. A 426 (1999) 503-517

Caciuffo R., Amoretti G., Santina P., Lander G.H., Kulda J., de V. du Plessis P.
Magnetic Excitations and Dynamical Jahn-Teller Distortions in UO_2
Physical Review B 59 No. 21 (1999) 13892-13900

**Caciuffo R., Griveau J.C., Kolberg D., Wastin F., Rinaldi D., Panchula A., Canfield P.*
Static and Dynamic Magnetic Response of $CeFe_2$
Journal of Applied Physics Vol. 85 No. 8 (1999) 6229-6231

Capone F., Colle Y., Hiernaut J.P., Ronchi C.
Mass Spectrometric Measurement of the Ionisation Energies and Cross Sections of Uranium and Plutonium Oxide Vapors
The Journal of Physical Chemistry A 103 No. 50 (1999) 10899-10906

**Chauvin N., Konings R.J.M., Matzke Hj.*
Optimisation of Inert Matrix Fuel Concepts for Americium Transmutation
Journal of Nuclear Materials 274 (1999) 105-111

Couturier O., Faivre-Chavet A., Filippovich I.V., Saï-Maurel C., Bardiès M., Mishra A.K., Gauvrit M., Blain G., Apostolidis C., Molinet R., Abbe J.-C., Bataille R., Wijdenes J., Chatal J.-F., Chérel M.
Validation of ^{213}Bi-α Radioimmunotherapy for Multiple Myeloma
Clinical Cancer Research 5(10 Suppl) (1999) 3165s-3170s

Dervenagas P., Hiess A., Lander G.H., Wastin F., Rebizant J.
Neutron Diffraction Study of the Magnetic Structure of $U_{0.1}Np_{0.9}Ru_2Si_2$
Solid State Communications 109 (1999) 35-39

Dervenagas P., Kaczorowski D., Bourdarot F., Burlet P., Czopnik A., Lander G.H.
Neutron Diffraction on a UGa_3 Single Crystal
Physica B 269 (1999) 368-372

**Fernandez A., Richter K., Somers J.*
Preparation of Spinel ($MgAl_2O_4$) Spheres by a Hybrid Sol-Gel Technique
Innovative Materials. Advanced Energy Technologies (1999) 167

**Fernandez A., Richter K., Closset J.C., Fourcaudot S., Fuchs C., Babelot J.F., Voet R., Somers J.*
Fabrication of Targets for the Transmutation and Incineration of Actinides
Innovative Materials. Advanced Energy Technologies (1999) 539-546

**Gouder T.*
Photoemission Study of the 5f Localization in Thin Films of Pu
Journal of Electron Spectroscopy and Related Phenomena 101-103 (1999) 419-422

Haas D., Somers J., Charollais F.
Innovative Fabrication of Fuels and Targets for Pu Recycling and Minor Actinide Transmutation
atw Atomwirtschaft 44 No. 12 (1999) 709-714

**Hiess A., Bernhoeft N., Langridge S., Vettier C., Huth M., Jourdan M., Adrian H., Lander G.H.*
Magnetic Properties of UPd_2Al_3 Thin Films Investigated by Resonant Magnetic X-ray Scattering
Physica B 259-261 (1999) 631-633

**Hiess A., Coad S., Buschinger B., Trovarelli O., Boucherle J.X., Givord F., Hansen T., Lelievre-Berna E., Suard E., Geibel C., Steglich F.*
Magnetism in $R_2T_3X_9$ (R = Ce,Yb,U;T = Rh,Ir; X = Al,Ga) Intermetallic Compounds
Physica B 259-261 (1999) 343-344

Javorsky P., Havela L., Wastin F., Griveau J.C., Bednarczyk E., Rebizant J., Sanchez J.P., Vulliet P.
Magnetic and Transport Properties of NpNiSn
Journal of Alloys and Compounds 283 (1999) 16-20

Kern S., Robinson R.A., Nakotte H., Lander G.H., Cort B., Watson P., Vigil F.A.
Crystal-field Transition in PuO_2
Physical Review B Condensed Matter 59 No. 1 (1999) 104-106

Köbler U., Hoser A., Kawakami M., Chatterji T., Rebizant J.
An Unified View of the Spin Dynamics in Two- und Three-Dimensional Magnetic Systems
Journal of Magnetism and Magnetic Materials 205 (1999) 343-356

Langridge S., Paixao J.A., Bernhoeft N., Vettier C., Lander G.H., Gibbs Doon, Sorensen S.Aa., Stunault A., Wermeille D., Talik E.
Changes in 5d-Band Polarization in Rare-Earth Compounds
Physical Review Letters 82 No. 10 (1999) 2187-2190

Lee S.H., Majkrzak C.F., Sinha S.K., Stassis C., Kawano H., Lander G.H., Brown P.J., Fong H.F., Cheong S.W., Matsushita H., Yamada K., Endoh Y.
Search for Orbital Moments in Underdoped Cuprate Metals. A Sisyphian Task.
Physical Review B Condensed Matter 60 No. 14 (1999) 10405-10417

Lindbaum A., Gratz E., Heathman S., Méresse Y.
Compressibility of YMn_2, Y_6Mn_{23}, YMn_{12} und $ScMn_2$ Studied by Synchrotron Powder Diffraction
Journal of Physics Condensed Matter 11 (1999) 1189-1198

Lucuta P.G., Matzke Hj., Andrews H.R., Verrall R.A.
Simulated Fission Radiation Effects in UO_2 and SIMFUEL
Innovative Mater. Advanced Energy Technologies (1999) 455-462

Magill J., Peerani P.
Proliferation Issues.
In: NRG, Thorium as a Waste Management Option, Chapt. 2.6
H. Gruppelaar, J.-P. Schapira (Eds), (1999) 137-140

Magill, J., Peerani, P.
(Non-) Proliferation Aspects of Accelerator Driven Systems
Journal de Physique IV, Vol. 9 (1999) Pr7-167–Pr7-181

Mannix D., Langridge S., Lander G.H., Rebizant J., Longfield M.J., Stirling W.G., Nuttall W.J., Coburn S., Wasserman S., Soderholm L.
Experiments on Transuranium Compounds with X-ray Resonant Exchange Scattering
Physica B Condensed Matter 262 (1999) 125-140

Mannix D., Lander G.H., Rebizant J., Caciuffo R., Bernhoeft N., Lidström, E., Vettier C.
Unusual Magnetism on NpO_2: A Study with Resonant X-ray Scattering
Physical Review B Condensed Matter 60 No. 22 (1999) 15187-15193

**Marmeggi J.C., Curat R., Bouvet A., Lander G.H.*
Phonon Softening in Alpha-Uranium Associated with the CDW Transition
Physica B 263-264 (1999) 624-626

Martin-Martin A., Pereira L.C.J., Lander G.H., Rebizant J., Wastin F., Spirlet J.C., Dervenagas P., Brown P.J.
Neutron-Diffraction Studies of Single Crystals of U_2T_2In (T = Ni, Pd, Pt)
Physical Review B Condensed Matter 59 No. 18 (1999) 11818-11825

Matzke Hj., Rondinella V.V.
"Diffusion in Carbides, Nitrides, Hydrides and Borides"
Serie Landolt-Börnstein, Group III, Volume 33, Ed. D.L. Beke, Subvolume B 1, Chapter 5
Diffusion in Carbides, Hydrides and Borides (1999) 5-1 - 5-62

Matzke Hj.
Range, Energy Loss, Energy Straggling and Damage Production for Alpha Particles in Uranium Dioxide
Journal of Nuclear Materials 270 (1999) 49-54

Matzke Hj.
Cooperation and Exchange in Research on Nuclear Fuel – A Success Story of the Past 25 Years
Journal of Nuclear Fuel 32 (1999) 24-25

**Matzke Hj.*
Ceramics in Fission Energy - Current Developments and Problems
Innovative Materials. Advanced Energy Technologies (1999) 357-368

**Matzke Hj., Rondinella V.V., Wiss T.*
Materials Research on Inert Matrices: a Screening Study
Journal of Nuclear Materials 274 (1999) 47-53

Mayer K., Tolbert M.E.M., Wellum R., Deron S., Perrin R.E., Mitterrand B.
Preparing for the Future Today
Journal of Nuclear Materials. Management, Spring (1999) 4+18

Méresse Y., Heathman S., Rijkeboer C., Rebizant J.
High Pressure Behaviour of PuBi Studied by X-ray Diffraction
Journal of Alloys and Compounds 284 (1999) 65-69

Mogensen M., Pearce J.H., Walker C.T.
Behaviour of Fission Gas in the Rim Region of High Burn-up UO_2 Fuel Pellets with Particular Reference to Results from an XRF Investigation
Journal of Nuclear Materials 264 (1999) 99-112

Musella M., Ronchi C., Sheindlin M.
Dependence of the Melting Temperature on Pressure up to 2000 Bar in Uranium Dioxide, Tungsten and Graphite
International Journal of Thermophysics 20 No. 4 (1999) 1177-1188

Nikula T.K., McDevitt M.R., Finn R.D., Wu C., Kozak R.W., Garmestani K., Brechbiel M.W., Curcio M.J., Pippin C.G., Tiffany-Jones L., Geerlings M.W., Apostolidis C., Molinet R.; Geerlings M.W. Jr., Gansow O.A., Scheinberg D.A.
Alpha-Emitting Bismuth Cyclohexylbenzyl DTPA Constructs of Recombinant Humanized Anti-CD33 Antibodies: Pharmacokinetics, Bioactivity, Toxicity and Chemistry
The Journal of Nuclear Medicine 40(1) 166-176

Norreys P.A., Santala M., Clark E., Zepf M., Watts I., Beg F.N., Krushelnick K., Tatarakis M., Dangor A.E. et al., J. Magill et al.
Observation of a Highly Directional Gamma-ray Beam from Ultrashort, Ultraintense Laser Pulse Interactions with Solids
Physics of Plasmas 6 No. 5 (1999) 2150-2156

Paixao J.A., Pereira L.C.J., Estrela P., Godinho M., Almeida M., Paolasini L., Bonnet M., Rebizant J., Spirlet J.C.
Magnetization Density Distribution in U_2Co_2Sn
Journal of Physics: Condensed Matter 11 (1999) 2115-2125

Paixao, J.A., Robinson, R.A., Lander, G.H., Brown, P.J.
Magnetic Site Susceptibilities in UPdSn
Journal of Physics Condensed Matter 11 (1999) 2127-2138

Paolasini L., Caciuffo R., Roessli B., Lander G.H., Myers K., Canfield P.
Iron Spin Waves in YFe_2 and UFe_2
Physical Review B Condensed Matter 59 No. 10 (1999) 6867-6872

Paolasini L., Vettier C., de Bergevin F., Yakhou F., Mannix D., Stunault A., Neubeck W., Altarelli M., Fabrizio M., Metcalf P.A., Honig J.M.
Orbital Occupancy Order in V_2O_3: Resonant X-ray Scattering Results
Physical Review Letters 82 No. 23 (1999) 4719-4722

**Pereira L.C.J., Almeida M., Estrela P., Godinho M., Rebizant J., Spirlet J.C., Pinto R.P., Amado M.M., Braga M.E., Sousa J.B.*
Magnetic and Transport Properties of U_2Pt_2In Single Crystals
J. of Magnetism and Magnetic Materials 196-197 (1999) 885-887

Prokes K., Svoboda P., Kolomiets A., Sechovsky V., Nakotte H., de Boer F.R., Winand J.M., Rebizant J., Spirlet, J.C.
Magnetic Structure of U_2Pt_2Sn
Journal of Magnetism and Magnetic Materials 202 (1999) 451-457

Ronchi C., Sheindlin M., Musella M., Hyland G.J.
Thermal Conductivity of Uranium Dioxide up to 2900 K from Simultaneous Measurement of the Heat Capacity and Thermal Diffusivity
Journal of Applied Physics 85(2) (1999) 776-789

**Ronchi C., Heinz W., Musella M., Selfslag R., Sheindlin M.*
A Universal Laser-Pulse Apparatus for Thermophysical Measurements in Refractory Materials at Very High Temperatures.
International Journal of Thermophysics 20(3) (1999) 987-996

**Rondinella V.V., Matzke Hj., Cobos J., Wiss T.*
Alpha-Radiolysis and Alpha-Radiation Damage Effects on UO_2 Dissolution under Spent Fuel Storage Conditions 1998
Materials Research Society Symposium Proceedings Vol. 556 (1999) 447-454

Sickafus K.E., Hanrahan R.J., McClellan K.J., Mitchell J.N., Wetteland Ch.J., Butt D.P., Ramsey K.B., Blair T.H., Chidester K., Matzke Hj. et al.
Burn and Bury – Option for Plutonium
American Ceramic Society Bulletin 78 (1999) 69-74

Sickafus K.E., Matzke Hj., Hartmann Th., Yasuda K., Valdez J.A., Chodak P., Nastasi M., Verrall R.
Radiation Damage Effects in Zirconia
Journal of Nuclear Materials 274 (1999) 66-77

**Tamborini G., Betti M., Carbol P., Koch L.*
Secondary Ion Mass Spectrometry (SIMS) for the Detection of Radionuclides in Particles from Soil Samples
"Environmental Radiochemical Analysis" (1999) 382-393

Vogt O., Löhle J., Mattenberger K., Rebizant J.
Magnetic properties of $Pu_xY_{1-x}Sb$ single crystals
Physica B 259-261 (1999) 265-266

Walker C.T.
Assessment of the Radial Extent and Completion of Re-crystallisation in High Burn-up UO_2 Nuclear Fuel by EPMA
Journal of Nuclear Materials 275 (1999) 56-62

**Walker C.T.*
Electron Probe Microanalysis of Irradiated Nuclear Fuel: An Overview
Journal of Analytical Atomic Spectrometry 14 (1999) 447-454

Watson G.M., Gibbs Doon, Lander G.H.
Recent Highlights of X-ray Magnetic Scattering Studies from Surfaces
Japanese Journal of Applied Physics 38 Suppl. 38-1 (1999) 14-17

**Wiss T., Matzke Hj.*
Heavy Ion Induced Damage in $MgAl_2O_4$, an Inert Matrix Candidate for the Transmutation of Minor Actinides
Radiation Measurements 31 (1999) 507-514

Ziegler H., Mayer K.
Development of an Optimized Method for Faster and More Reliable Automated U/Pu/Np Separations
Radiochimica Acta 86 (1999) 123-128

Conferences

International Waste Management Symposium '99
February 28-4 March, 1999 Tucson, AZ (USA)

Glatz J.P., Giménez J., Bottomley D.
Leaching of High Burn-up UO_2 and MOX Fuel Rods with Pre-set Cladding Defects
Proceedings on CD-ROM

90th Annual Meeting of the American Association for Cancer Research
April 10-14 Philadelphia, PA (USA)

Behr T.M., Béhé M., Stabin M.G., Molinet R., Apostolidis C., Koch L., Becker W.
Radioimmunotherapy (RIT) with alpha-emitters: Therapeutic efficacy and dose-limiting toxicity of ^{213}Bi- versus ^{90}Y-labeled CO17-1A Fab' in a human colonic cancer model
Proceedings of the American Association for Cancer Research Annual Meeting, Vol.40 (March 1999) p. 644

29. Journées des Actinides
April 15-17, 1999 Luso (Portugal)

Amoretti G., Caciuffo R., Santini P., Lander G.H., Kulda J., de V. du Plessis P.
UO_2 Ten Years after: A Polarized Neutron Scattering Experiment on Single Crystal

Bombardi A., Grenier B., Burlet P., Lander G.H., Regnault L.-P., Mattenberger K., Vogt O.
Observation of Ferromagnetic Correlation in Diluted UTe

Bourdarot F., Bombardi A., Burlet P., Calemczuk R., Lander G.H., Lapierre F., Sanchez J.P., Mattenberger K., Vogt O.
Magnetic Ordering and Structural Anomalies in the $U_xLa_{1-x}S$ System

Brooks M.S.S.
Calculated Properties of the U-N-C System

Coad S., Paolasini L., Dervenagas P., Mannix D., Lander G.H., Bernhoeft N., Hiess A., Brown P.J., Burlet P., Bourdarot F., Rebizant J., Kaczorowski D., Czopnik A., Troc R.
Neutron and X-ray Studies of UGa3 Single Crystals

Coad S., Hiess A., McMorrow D., Lander G.H., Aeppli G., Fisk Z., Stewart G.
Magnetic Response in UBe_{13}

Colinau E., Wastin F., Rebizant J.
Mössbauer Investigations in $Np_2T_3X_4$ Compounds

Colineau E., Wastin F., Rebizant J.
Electronic and Magnetic Properties of $NpPd_2Ge_2$

Gouder T., Havela L., Wastin F.
PuSe: Photoelectron Spectroscopy on Thin Layers

Gouder T., Wastin F.
Photoelectron Spectroscopy on Thin Films of Pu: Temperature Dependence

Heathman S., Haire R.G., Le Bihan T., Lindbaum A., Litfin K., Méresse Y.
High Pressure X-ray Diffraction Studies of Pure Americium Metal up to 100 GPa

Kolberg D., Wastin F., Rebizant J., Schoenes J.
Magnetic Properties of $Pu_xU_{1-x}Sb$ Single Crystals

Litfin K., Heathman S., Mattenberger K., Schoenes J.
Optical Properties and X-ray Diffraction of US, USe and UTe up to 40 GPa

Mannix D., Caciuffo R., Bernhoeft N., Lander G.H., Rebizant J., Lidström E., Vettier,C.
Light on the Mysterious Magnetism on NpO_2

Marmeggi J.C., Currat R., Bouvet A., Lander G.H.
The Transition into the CDW State in Alpha-Uranium

Martin-Martin A., Pereira L.C.J., Lander G.H., Rebizant J., Brown P.J.
Neutron Scattering Investigation of Single Crystal U_2Pt_2In

Wastin F., Rebizant J., Colineau E.
Short Review of the Transuranium Ternary Intermetallic Compounds Database

Performance and Technology, 14. Plenary Meeting International Working Group on Water Reactor Fuel April 27-29, 1999 Vienna (Austria)

Matzke Hj.
Research Related to Water Reactor Fuels at the Joint Research Centre of the European Commission

Conference of the European Microbeam Analysis Society
May 3-7. 1999 Konstanz (Germany)

Bottomley P.D.T., Brémier S., Glatz J.P., Walker C.T.
EPMA of Melted UO_2 Fuel Rods Irradiated to a Burn-up of 23 GWd/tU
Proceedings Mikrochimica Acta Supplement

21. ESARDA Symposium on Nuclear Material Management
May 4-6,1999 Sevilla (Spain)

Bibilashvili Yu., Kositsyn V., Chorokhov N., Chkaboura I., Dolgov Yu., Koch L., Mayer K.
Methodology of the Analysis of Nuclear Materials of Unknown Origin at VNIINM Moscow
Proceedings EUR 18963 EN (1999) 821-829

Blohm-Hieber U., Mayer K., Ottmar H., Schneider H.G.
Revised Analytical Strategy for the Euratom On-Site Laboratory at Sellafield
Proceedings EUR 18963 EN (1999) 197-204

Dolgov Yu., Bibilashvili Yu., Chorokhov N., Schubert A., Janssen G., Mayer K., Koch L.
Installation of a Database for Identification of Nuclear Material of Unknown Origin at VNIINM Moscow
Proceedings EUR 18963 EN (1999) 831-838

Mayer K., Ottmar H., Cromboom O., Castelyn K.
Analysis of MOX Samples using Chemical and Radiometric Methods - A Method Comparison
Proceedings EUR 18963 EN (1999) 605-607

Ottmar H., van Belle P., Croft S., Chard P.M.J., Bourva C.-A., Blohm-Hieber U.
An Empirical Measurement of the Specific ^{240}Pu-Effective Mass of ^{238}Pu and ^{242}Pu
Proceedings EUR 18963 EN (1999) 311-319

Schenkel R., Mayer K.
Measurement Methodologies and Modern Verification Systems - Similarities and Synergies
Proceedings EUR 18963 EN (1999) 39-45

Schubert A., Mayer K., Schenkel R., Koch L.
The Bilaterial Workshop on Nuclear Forensics 1998, held by ITU Karlsruhe and VNIINM Moscow
Proceedings EUR 18963 EN (1999) 839-844

IAEA Symposium on MOX Fuel Cycle Technologies for Medium and Long-Term Deployment: Experiences, Advances, Trends
May 17-21, 1999 Vienna (Austria)

Cook P., Palmer I., Walker C.T., Stratton R.
PIE of BNFL's First Commercially Irradiated SBR MOX Fuel
Proceedings IAEA-SM-358/16

Haas D., Somers J., Charollais F., Fuchs C., Fourcaudot S.
Fabrication and Characterization of MOX Fuels with High Plutonium Content Using Alternative Processes

Enlarged Halden Program Group Meeting
May 24-29, 1999 Loen (Norway)
Proceedings Halden Report

Matzke Hj., Kinoshita M.
Recent Progress in Investigations of high Burnup Fuel at ITU Karlsruhe in Relation to the Irradiation IFA-601

Sonoda T., Matzke Hj., Kinoshita M.
High Burnup Rim Project (IV) Threshold Burnup of Rim Structure Formation

International Workshop on Orbital and Spin Magnetism of Actinides (IWOSMA)
June 4-5, 1999 Warrington (United Kingdom)

Brooks M.S.S.
Orbital Magnetism in Itinerant Magnets

Ichas V., Rebizant J., Spirlet J.C., Griveau J.C.
Strong Pressure Effects on the Resistivity of PuTe

Lander G.H.
Spin and Orbital Moments by Neutron Diffraction

46th Annual Meeting of the Society of Nuclear Medicine
June 6-10, 1999 Los Angeles CA (USA)

Adam C., Schumacher C., Becker K., Handschuh G., Nikula T., Apostolidis C.,Fischer K., Schwaiger M., Senekowitsch-Schmidtke R.
Binding of a Bi-213 labeled monoclonal antibody targeting a tumor specific mutant E-cadherin in different tumour models
Journal of Nuclear Medicine vol.40 No.5 SUPPL. (May 1999) p. 107 (abstract)

Behr T.M., Sgouros G., Stabin M.G., Béhé M., Angerstein C., Blumenthal R.D., Apostolidis C., Molinet R., Sharkey R.M., Koch L., Goldenberg D.M., Becker W.
Factors influencing the radiation-induced myelotoxicity of beta-, Auger/conversion electron- or alpha-emitters
Journal of Nuclear Medicine vol.40 No.5 SUPPL. (May 1999) p. 314 (abstract)

Behr T.M., Béhé M., Stabin M.G.,Wehrmann E., Apostolidis C., Molinet R., Koch L., Goldenberg D.M., Becker W.
Experimental studies of the therapeutic efficacy and toxicity of alpha- as compared to beta-emitters in radioimmunotheraphy.
Journal of Nuclear Medicine vol.40 No.5 SUPPL. (May 1999) p. 313 (abstract)

3. International Conference on Accelerator Driven Transmutation Technologies and Applications
June 7-11, 1999 Prague (Czechoslovakia)

Magill J., Peerani P., van Geel J.
Basic Aspects of Sub-Critical Systems based on Thin Actinide Films

Workshop on Impact of Fuel Chemistry on Fission Product Behaviour
June 16-17, 1999 Mol (Belgium)

Gouder T., Black L.
Sputter Deposition of U-Ni Films

Miserque F., Gouder T., Wegen D., Bottomley D.
Electrochemistry of UO_2 Thin Films

Workshop on FMCT-Verification-Detection of Clandestine Activities
June 21-22, 1999 Stockholm (Sweden)

Schenkel R.
Is it Possible to Detect Clandestine Reprocessing Activities?

Kozloduy NPP - Energy, Environment and Society
July 1-3, 1999 Sofia (Bulgaria)

Lassmann K.
Nuclear Power Reactors: Worldwide Status

22. Rare-Earth Research Conference
July 11-15, 1999 Argonne, IL (USA)

Paolasini L., Lander G.H.
Iron Magnetism in Cubic Laves Phase Itinerant Ferromagnets
Journal of Alloys and Compounds

10. International Conference on Radiation Effects in Insulators
July 19-23, 1999 Jena (Germany)

Fromknecht R., Hiernaut J.P., Matzke Hj., Wiss T.
He-ion Damage and He-release from Spinel $MgAl_2O_4$
Proceedings Nucl. Instrum. Meth. in Phys. Research

Matzke Hj., Lucuta P.G., Wiss T.
Swift Heavy Ion and Fission Damage Effects in UO_2 Nuclear Instruments Methods in Physics Research
Proceedings Nucl. Instrum. Meth. in Phys. Research

40. Annual Meeting of the Institute of Nuclear Materials Management
July 25-29, 1999 Phoenix, AZ (USA)

Mayer, K., Ottmar, H.
Certified Reference Materials for Radiometric Safeguards Analytical Measurements: A Demanding Issue
Journal of the Institute of Nuclear Materials Management

Ottmar H., Mayer K., Richir P., Daures P.
Streamlined Reprocessing Input Verification Measurements in the Euratom On-Site Laboratory at La Hague
Journal of the Institute of Nuclear Materials Management

International Conference on Strongly Correlated Electron Systems
August 24-28, 1999 Nagano (Japan)
Proceedings Physica B

Bernhoeft B., Roessli B., Sato N., Aso N., Hiess A., Lander G.H., Endoh Y., Komatsubara T.
Order Parameter Symmetry in UPd_2Al_3

Coad S., Hiess A., Paolasini L., Bernhoeft N., Dervenagas P., Kaczorowski D., Czopnik A., Troc R., Lander G.H.
Magnetic Excitations in UGa_3

Lidström E., Hiess A., Mannix D., Dervenagas P., Wastin F., Rebizant J., Lander G.H.
The Magnetic Properties of $(U_{1-x}Np_x)Ru_2Si_2$ Investigated by Neutron and Resonant X-ray Magnetic Scattering

Paolasini L., Vettier C., De Bergevin F., Yakhou F., Mannix D., Neubeck W., Stunault A., Altarelli M., Fabrizio M., Metcalf P.A, Honig J.M.
Direct Observation of Orbital Ordering in V_2O_3 by X-ray Resonant Scattering Technique

Paolasini L., Hiess A., Hennion B., Lander G.H., Panchula A., Canfield P.
Ferro-Antiferro Interactions in the Cobalt Doped $CeFe_2$

International Conference on Future Nuclear Systems Global '99 "Nuclear Technology – Bridging the Millenia"
August 29–September 3, 1999 Jackson Hole, WY (USA)
Proceedings on CD-ROM - 1999, American Nuclear Society (ANS)

Boucharat N., Somers J., Haas D., Walker C.T.
Fabrication of Macrosphere Targets using a Combination of Sol-Gel and Powder Blending Techniques

Chauvin N., Konings R.J.M., Matzke Hj.
Optimization of Minor Actinide Fuels for Transmutation in Conventional Reactors (PWRs, FRs)

Chauvin N., Matzke Hj., Konings R.
Trends for Optimisation of MA Targets

Cobos J., Rondinella V.V., Matzke Hj., Martinez-Esparza A., Wiss T.
The Effect of Alpha-Radiolysis on the Dissolution Behaviour of UO_2

Conti A., Ottaviani J.-P., Konings R.J.M., Schram R.P.C.
Long-Lived Fission Product Transmutation Studies

Haas D., Somers J., Fuchs C., Fourcaudot S., Voet R., McGinley J.
Fabrication of Fuels for Incineration and Transmutation: Review of Achievements and Ongoing Developments

Haas D., Konings R.J.M., Konrad R., Heusener G., Rouault J., Schram R.P.C., Vambenepe G.
The EFTTRA European Collaboration for the Development of Fuels and Targets for Transmutation: Status of Recent Development

Schram R.P.C., Bakker K., Boshoven J.G., Dassel G., Hein H., van der Laan R.R., Neeft E.A.C., Konings R.J.M., Konrad, R.
Irradiation Experiments and Fabrication Technology of Inert Matrix Fuels for the Transmutation of Actinides

Somers J., Glatz J.P., Haas D., Wegen D.H., Fourcaudot S., Fuchs C., Plancq D., Mühling G.
Status of the TRABANT Irradiation Experiment

8. International Conference on Muon Spin Rotation, Relaxation and Resonance
August 30-September 3, 1999 Les Diablerets (Switzerland)
Proceedings Physica B

Lander G.H.
X-rays and Neutrons as Complementary Probes to Muons in Magnetism: A View from Reciprocal Space

European Conference on Neutron Scattering
September 1-4, 1999 Budapest (Hungary)
Proceedings Physica B

Bombardi A., Grenier B., Burlet P., Lander G.H., Regnault L.P., Mattenberger K., Vogt O.
Observation of Ferromagnetic Correlation in Diluted UTe

Coad S., Hiess A., McMorrrow D., Lander G.H., Aeppli G., Fisk Z., Stewart G., Hayden S., Mook H.
Magnetic Response in UBe_{13}

Marmeggi J.C., Currat R., Bouvet A., Lander G.H.
Incommensurate Phase Associated with Soft Phonon-Mode Displacive Transition in Alpha-U

European Research Conference on Strongly Coupled Systems
September 4-10, 1999 St. Malo (France)

Gryaznov V., Iosilevski I., Yakub E., Fortov V., Hyland G.J., Ronchi C.
Improved Ionic Model of Liquid Uranium Dioxide

Secondary Ion Mass Spectrometry "SIMS XII"
September 6-10, 1999 Bruxelles (Belgium)

Tamborini G., Betti M., Erdman N., Stetzer O., van Geel J.
SIMS Characterisation of In-house Monidispersed Isotopic Standard Uranium Oxide Particles

3rd International Conference on Isotopes
September 6-10, 1999 Vancouver (Canada)

Magill J.
Nuclides 2000: An Electronic Chart of the Nuclides

International Conference on LWR Nuclear Fuel Highlights at the Beginning of the Third Millennium (TOPFUEL '99)
September 13-15, 1999 Avignon (France)

Haas D.
Innovative Fabrications of Fuels and Targets for Pu Recycling and Minor Actinides Transmutation

Haas D., Somers J., Charollais F.
Innovative Fabrication of Fuels and Targets for Pu Recycling and Minor Actinide Transmutation

7th International Conference on the Chemistry and Migration Behaviour of Actinides and Fission Products in the Geosphere
September 26-October 1, 1999 Incline Village, CA (USA)

Rondinella V.V., Matzke Hj., Cobos J., Wiss T.
Dissolution Behaviour of UO_2 Containing Alpha-Emitting Actinides
Proceedings Radiochimica Acta

Seminar on "European R&D on Materials for MA and LLFP Transmutation"
September 30-October 1, 1999 Cadarache (France)

Conti A., Ottoviani J.P., Matzke Hj., Casalta S.
Thermochemical Studies: Current Status on Am-oxides

Matzke Hj., Beauvy M.
Simulation of FP and Alpha-Decay by Ion Irradiation: Results and Transposition

Matzke Hj.
Highlights from GLOBAL '99

Neeft E., Matzke Hj.
Study of Damage Formation and Helium Diffusion in Spinel $MgAl_2O_4$ Following Ion Implantation

3rd International Seminar on WWER Fuel Perforance, Modelling and Experimental Support
October 4-8, 1999 Pamporovo (Bulgaria)

Elenkov D., Lassmann K.
The Development of the TRANSURANUS-WWER Version

Lassmann K., van de Laar J., Elenkov D.
Analysis of RIA Accidents for WWER Reactor Employing the TRANSURANUS Code

Manolova M., Elenkov D., Georgieva M., Boneva S., Simeonova V., Djourelov N., Georgiev S., Lassmann K., van de Laar, J.
Validation of the TRANSURANUS Code - WWER Version by the Updated Kola-3 Data Set

European Association of Nuclear Medicine (EANM) congress 1999
October 9-13, 1999 Barcelona (Spain)

Behr T.M., Béhé M., Stabin M.G., Angerstein C., Mach R., Hagemann L., Apostolidis C., Molinet R., Koch L., Rösch F., Becker W.
Radiopeptide therapy with cholecystokinin – B / Gastrin receptor ligands: dose-limiting toxicity and therapeutic efficacy of Auger / Conversion electron (^{111}In, ^{140}Nd) versus alpha (^{213}Bi) or conventional beta (^{90}Y, ^{153}Sm) emitters.
European Journal of Nuclear Medicine 26 (1999) 1212 (abstract)

9. Italian-Hungarian Symposium on Spectrochemistry - Urban Health: a Challenge for the Third Millennium
October 11-15, 1999 Siena (Italy)

Betti M.
Environmental Monitoring of Radioisotopes by Mass Spectrometric and Radiochemical Techniques

Menichetti L., Betti M., Barrero-Moreno J.M., Fuoco R.
Determination of Long-lived Radionuclides in Environmental Samples by Ion Chromatography Inductively Coupled Plasma Mass Spectrometry (IC-ICP-MS) (Poster)

Righi S., Betti M., Bruzzi L.
Monitoring of Natural Radioactivity in Working Places (Poster)

Rondinella V.V., Betti M., Bocci F., Hiernaut T.
IC-ICP-MS applied to the Separation and Determination of Traces of Plutonium and Uranium in Aqueous Leachates and Acid Rinse Solutions of UO_2 Doped with ^{238}Pu (Poster)

Tocci U., Betti M., Actis-Dato O.L., Aldave de las Heras L., Fuoco R.
Monitoring of Depth Distribution of Trace Elements by Glow Discharge Mass Spectrometry (Poster)

Meeting European Working Group on ot Laboratries and Remote Handling"
October 13-15, 1999 Karlsruhe (Germany)

Ronchi C., Sheindlin M.
New Facilities for High-Temperature Physical Property Measurements in Alpha-Gamma Active Materials

Wiss T., Ray I., Thiele H., Huber W., Matzke Hj.
Electron Microscopy for PIE: New Developments

5. European Commission Conference on Radioactive Waste Management and Disposal and Decommissioning (Euradwaste '99)
October 15-18, 1999 Luxembourg

Courson O., Malmbeck R., Pagliosa G., Römer K., Sätmark B., Glatz J.P.
Separation of Minor Actinides from a genuine An/Ln Fraction

Malmbeck R., Apostolidis C., Courson O., Molinet R., Pagliosa, G., Römer K., Sätmark B., Glatz J.P.
Advanced Reprocessing of Irradiated Fuel Using the PUREX, DIAMEX and SANES-Processes

9. International Conference on Radiation Shielding
October 17-22, 1999 Tsukuba (Japan)

Matsumura T., Sasahara A., Nicolaou G., Pellottiero D.
Neutron/Gamma Ray Source Measurement and Analyses of High Burnup UO_2/MOX Fuel Rods
Proceedings Journal of Nuclear Science and Technology

5. Inert Matrix Fuel Workshop
October 21-22, 1999 Paris (France)

Wiss T., Matzke Hj.
Radiation Damage Produced by Energetic Ions in Selected Inert Matrices

OECD/NEA/JAERI Workshop on Evaluation of Speciation Technology
October 26-28, 1999 Tokai-mura (Japan)

Wastin F.,Colineau E., Gouder, T., Rebizant, J., Lander G.H.
Transuranium Compounds Characterisation Facility at ITU-Karlsruhe

26. Annual Meeting of the Argentinian Nuclear Society
November 9-12, 1999 Bariloche (Argentina)

Bevilacqua A.M., Matzke Hj.
Propiedades mecánicas del UO_2 y del combustible irradido simulado SIMFUEL a alta temperatura

Matzke Hj.
Inert Matrix Fuel to Reduce the Radiotoxicity of Nuclear Waste

IAEA TC Meeting "Technical and Economic Limits to Fuel Burnup Extension"
November 15-19, 1999 Bariloche (Argentina)

Matzke Hj.
Recent Studies on the Formation of the RIM Structure and on Polygonization in LWR Fuel

1999 Winter Meeting of the American Nuclear Society November 14-18, 1999 Long Beach, CA (USA)

Iosilevski I., Hyland G., Ronchi C., Yakub E.
An Advanced Equation of State of UO_2 up to the Critical Point
Proceedings Transactions Vol. 81 (1999) 122-124

3. European ALARA Network Workshop November 15-18, 1999 München (Germany)

Wagner W.
ALARA in Fuel Element Production
EU document: Radiation Protection Series

25. Annual Conference SNE November 17-19, 1999 Granada (Spain)

Cobos J., Gimenez J., Glatz J.P., Matzke Hj., Casas I., De Pablo J.
Development of Flow through Reactors to Study the Dissolution Rates of the UO_2 and Irradiated Fuel

Fernandez A., Somers J., Haas D., Konings R.J.M., Boucharat N.
Transmutation and Incineration of Minor Actinides

Haas D., Fernandez A., Somers J., Konings R.J.M., Boucharat N., Charollais F., Fourcaudot S., Fuchs C., Voet, R.
Advanced Fuel and Target Fabrication

Rondinella V.V., Matzke Hj., Wiss T., Cobos J.
Oxidation Behaviour and Hydrogen Production of an Oxidic Corium Melt in Contact with Water

Report & Special Publications

Babelot J.-F., Chauvin N.
Joint CEA/ITU synthesis report on the experiment SUPERFACT 1
Technical Note TN-99/03

Magill J.
Nuclides 2000. An Electronic Chart of the Nuclides on Compact Disc
EUR 18737 EN (1999) , ISBN 92-828-6512-6

Schenkel R.; Richter J.; Magill J., Pel D.
Annual Report 98 – Institute for Transuranium Elements
EUR 18715-EN (1999) , ISBN 92-828-6589-0

Collaborations with External Organizations

ARGENTINA

Brazilian-Argentine Agency for Accounting and Control of Nuclear Materials (ABACC), Rio de Janeiro: Safeguards (E. Palacio, C. Feu Alvim, O. Mafra Guidicini)
Centro Atómico Bariloche: Simfuel mechanical properties, Pu sorption on rocks (A.M. Bevilacqua)
CNEA Buenos Aires: Diffusion in solids (F. Dyment)

ARMENIA

Armenian Nuclear Regulatory Authority, Yerevan: TRANSURANUS fuel pin code development (A. Martirossian)

AUSTRIA

International Atomic Energy Agency (IAEA), Vienna: Evaluation and automation of techniques for safeguards analysis (K. Lessmon); *Division of Safeguards Directorate:* Environmental analysis (E. Kuhn); *Seibersdorf Analytical Laboratory* (SAL): Cooperative Support Programme (Y. Kuno); *Division of Nuclear Fuel Cycle and Waste Management:* TRANSURANUS fuel pin code development (M. Samiei)
Technical University of Vienna: Resistivity of alloys and high-pressure effects (E. Gratz)

BELGIUM

Belgonucléaire: Ariane project: Inventory of high burn-up UO_2 and MOX fuel (M. Lippens); Post irradiation examinations (S. Pilate, Y. Vanderborck, M. Lippens, J. Basselier); Measurements of thermal conductivity of high burn-up MOX fuel (GERONIMO) (M. Lippens)
SCK-CEN, Mol: Doping of UO_2 films (S. van der Berghe); Mox programme (M. Verwerft, P. d'Hondt)
University Hospital Gent, Clinic for Radiotherapy and Nuclear Medicine: α-immunotherapy (F. Offner)
University of Leuven: Xe-implantation (H. Pattyn)
University of Liège: Single crystal growth, X-ray diffraction, and analysis (J.F. Desreux, L. Martinot, M.R. Spirlet)
University of Namur, Laboratoire Interdisciplinaire de Spectroscopie Electronique: Surface spectroscopy and electrochemistry (R. Caudano, J. Riga)
Virga Jesse Clinik, Hasselt: α-immunotherapy (D. Vanstraelen)

BRASIL

Brazilian-Argentine Agency for Accounting and Control of Nuclear Materials (ABACC), Rio de Janeiro: Safeguards (E. Palacio, C. Feu Alvim, O. Mafra Guidicini)

BULGARIA

Committee on the Use of Atomic Energy for Peaceful Purposes, Sofia: TRANSURANUS fuel pin code development (P. Ardenska); Illicit trafficking; FONSAFE (N. Todorov)
Institute of Nuclear Research and Nuclear Energy, Bulgarian Academy of Science, Sofia: Fuel rod modelling and performance, FERONIA (D. Elenkov); Illicit trafficking, FONSAFE (A. Strezov)

CANADA

AECL *Chalk River:* Gas release, SIMFUEL production and property studies, oxygen potential of UO_2 fuel (R. Verrall); behaviour of Rb and Cs in SIMFUEL (W. Hocking),
University of Kingston: Inert matrices (P.G. Lucuta)

CZECH REPUBLIC

Nuclear Research Institute Rez plc, Rez: TRANSURANUS fuel pin code development (F. Pazdera);
Central Analytical Laboratory: Illicit trafficking, FONSAFE (F. Sus)
State Office for Nuclear Safety, Prague: TRANSURANUS fuel pin code development (P. Krs); Illicit trafficking, FONSAFE (L. Bartak)
University of Prague: Magnetic and electrical measurements (V. Sechovsky, L. Havela, P. Jaworsky); Gas release measurements (V. Balek)

DENMARK

Risø National Laboratory: Neutron scattering (B. Lebech)

FINLAND

STUK: Finnish Centre for Radiation and Nuclear Safety: Illicit trafficking, FONSAFE (E.: Kainulainen)
VTT Energy Aerosol Technology: shared cost actions 'Revaporisation of Phebus PF samples' (J. Iokiniemi, A. Auvinen); Spent fuel source term (K. Oilila)

FRANCE

Commissariat à l'Énergie Atomique (CEA)

CEA, Cadarache: Transmutation of actinides - irradiation experiments: DNR (Ch. Bonnet, J.L. Faugère, S. Pillon, J.-C. Garnier, D. Warin, A. Languille, J. Rouault, M. Salvatores); PHEBUS PF programme, ThO_2 tube production (R. Zeyen); Bundle post irradiation examinations and sample post-test analysis (M. Schwartz, R. Zeyen); Melting point of PHEBUS pf corium (M. Schwartz); Examination of FP deposits of PHEBUS PF by mass spectrometry (M. Schwartz); Inert matrices (M. Beauvy and N. Chauvin); shared cost action 'Corium Interaction Thermochemistry' (B. Adroguer, M. Barrachin); Thermophysical measurements on ECRIX material 'MgO-AmO_2' (T. Albiol, Y. Croixmarie)

CEA, Marcoule: Partitioning of actinides, DIAMEX process (C. Madic); Characterization of transuranium cyano-complexes (D. Meyer, C. den Auwer); behaviour of He in waste glasses (D. Ghaleb)

CEN, Grenoble: Neutron diffraction, magnetic studies; transport properties and Mössbauer studies (P. Burlet, N. Bernhoeft, J.P. Sanchez, D. Braithwaite and F. Bourdarot)

CEA Palaiseau: Radiation Damage (A. Dunlop)

CEN, Saclay: Neutron diffraction (J.M. Mignot, B. Hennion); Post-irradiation examinations (J.I. Blanc, F. Couvreur)

CERCA, Romans: MTR fuel development (J.P. Durand, B. Lelievre)

CNRS, Lab. de Cristallographie, Grenoble: Crystallography of phase transitions (J.C. Marmeggi); Orsay: Basic studies on spent UO_2 fuel (J.C. Dran); ARAMIS accelerator, radiation damage, ion implantation (L. Thomé)

COGEMA, La Hague: Laboratoire sur Site (G. Decobert)

Velizy: *Branche Retraitement et Combustible:* Development of MOX fuels (J. Nigon, J.L. Guillet, Mme M. Trotabas)

Électricité de France (EDF)

Septen, Villeurbanne: Transmutation of actinides (G. Vambenepe); Div. Recherche, Paris: RIM effect (M. Baron); Chemical and mechanical interactions fuel/cladding (thermal reactor) and determination of mechanical properties of irradiated UO_2 (M. Baron)

ESRF, Grenoble: Synchrotron studies on actinides (C. Vettier, G. Grübel, P. Carra)

FRAMATOME, Nuclear Fuel Division, Lyon: Post-irradiation examinations (P. Blanpain, E. Van Schel, O. Gentil)

Grand accélérateur National d'ions Lourds, GANIL, Caen: Radiation damage in inert matrices) (M. Toulemonde)

ILL, Grenoble: Polarized neutron diffraction and neutron inelastic scattering (P.J. Brown, A. Hiess)

Institut National de la Santé et de la Recherche Médicale (INSERM), Nantes: α-immunotherapy by Bi-213 (J.F. Chatal)

OECD Nuclear Energy Agency, AEN-NEA, Paris: Database on fuel performance (E. Sartori)

SICN, Veurey-Voroize: automated bismuth-213 generator (Mr. Huguet)

Subatech, Ecole des Mines, Nantes: production of Ac-225 (H. Gutbrod)

GERMANY

Bundesministerium für Umwelt, Naturschutz, und Reaktorsicherheit: Vagabonding nuclear material (J. B. Fechner); Treatment of nuclear fuels (H. Dumpich);

Bundesministerium für Bildung und Forschung: Environmental sampling (H. Remagen)

Deutsches Krebsforschungszentrum, Biophysik und Medizinische Strahlenphysik, Heidelberg: α-immunotherapy (G. van Kaick)

Forschungszentrum Jülich, Institut für Festkörperforschung: spin dynamics in UO_2 (U. Köbler)

Forschungszentrum Karlsruhe (FZK)

Hauptabteilung Zyklotron (HZY): production of Ac-225 (H. Schweikert)

Institut für Nukleare Entsorgung (INE): shared cost action: Spent fuel source term (T. Fanghaenel)

Institut für Nukleare Festkörperphysik (INFP): Radiation damage studies, RBS analyses, channeling, ion implantation (R. Fromknecht, G. Linker)

Institut für Technische Chemie (ITC): Susceptibility and crystal preparation (B. Kanellakopulos)

Projekt Nukleare Sicherheitsforschung (PSF): Irradiation experiment CAPRA-TRABANT (G. Heusener)

Technologie Transfer: KEIM initiative (J. Wüst)

Hahn-Meitner-Institut (HMI), Berlin: High-energy ion implantation (S. Klaumünzer)

Heinrich Hein Universität Düsseldorf: Klinik für Hämatologie, Onkologie und klinische Immunologie: α-immunotherapy (R. Haas)

Max-Planck Research Group 'Theory of Complex and Correlated Systems', Dresden: Theory of the Kerr-effect (P.M. Oppeneer)

Siemens/KWU, Erlangen: Post-irradiation fuel rod examination (R. Manzel)

Technische Hochschule Darmstadt; Theory of actinides (L. Sandratskii)

Technischer Überwachungsverein Bayern e.V., München: TRANSURANUS fuel pin code development (G. Sauer)

Technischer Überwachungsverein Hannover/Sachsen-Anhalt e.V.: TRANSURANUS fuel pin code development (H. Märtens, D. Bour)
Technischer Überwachungsverein Norddeutschland e.V., Hamburg: TRANSURANUS fuel pin code development (J.F. Schriek)
Technischer Überwachungsverein Südwest e .V., Mannheim: TRANSURANUS fuel pin code development (I. Brestrich)
Technische Universität München: Mössbauer and μSR studies (M. Kalvius, W. Potzel, L. Asch)
Nuklearmedizinische Klinik und Poliklinik der TU München: α-immunotherapy (R. Senekowitsch-Schmidtke)
Universität Göttingen, Zentrum Radiologie: α-immunotherapy (T.M. Behr, W. Becker)
Universität Heidelberg, Medizinische Klinik und Poliklinik V, Heidelberg: α-immunotherapy (G. Egerer)
Universität Mainz, Institut für Kernchemie: Analytical techniques for particle characterization (J.V. Kratz)
Universität München-Garching: High-energy ion implantation (W. Assmann)

HUNGARY

Hungarian Academy of Sciences, Institute of Isotopes, Budapest: Forensic nuclear analysis for safeguards (J. Safar)
KFKI Atomic Energy Research Institute, Budapest: TRANSURANUS fuel pin code development (S. Elo)
Hungarian Atomic Energy Commission, Budapest: TRANSURANUS fuel pin code development (M. Gado), Illicit trafficking, FONSAFE (I. Czoch)

ISRAEL

Technion, Haifa: Waste glass studies (Y. Eyal)

ITALY

Centro Ceramico Bologna: Leaching studies, Indentation techniques (L. Esposito)
Centro Legnaro/Padova: RBS, Ion implantation, H-analysis on leached waste matrices (G. Della Mea, V. Rigato)
ENEA: Partitioning and Transmutation, Accelerator Driven Systems (G. Gherardi)
TGW: Technical Working Group on accelerator driven systems (ADS) (C. Rubbia)
University of Ancona: Neutron and bulk magnetization studies (R. Caciuffo)
University of Aquila, Physics Department: Theory of optical properties (P. Monachesi)
University of Bologna, Ravenna, Environmental Science: Measurements of environmental radioactivity (Prof. Bruzzi)
University of Padova: Analysis of glass surfaces (P. Mazzoldi)
University of Pisa, Chemistry Department: Instrumental analytical techniques for traces analysis (R. Fuoco)
University of Parma, Physics Department: Theory of oxides (G. Amoretti)

JAPAN

Central Research Institute of Electricity Producing Industries (CRIEPI), Tokyo: Preparation and characterization of minor actinide alloys (T. Inoue); Pyro-reprocessing studies (T. Inoue, T. Koyama); Spent fuel characterization for interim dry storage (T. Matsumura), Rim effect studies (M. Kinoshita), Measurements of thermal conductivity of irradiated fuel up to high burnup (M. Kinoshita)
JAERI, Tokai Mura: Radiation damage in oxide fuels (K. Fukuda)
Nuclear Material Control Center, Tokai: Safeguards (T. Tsujino)
Tohoku University, Inst. for Materials Research, Sendai, Japan: Reduction of Np metal, solid states physics (Y. Shiokawa)
Tokohu University, Sendai, Japan: Studies of heavy fermion uranium compounds (N. Sato, T. Komatsubara, Y. Endoh)

KOREA

Korean Atomic Energy Research Institute (KAERI): PIE of high burn-up fuels (W.-H. Kim)

THE NETHERLANDS

Interfaculty Reactor Institute, Delft: Gas release (A. van Veen); Neutronics of thin fissile layers (H. van Dam)
Mallinckrodt, Medical bv, Petten: α-immunotherapy (G. Ensing):
NRG, Petten: Transmutation of fission products (H.U. Staal, R. Schram)

NORWAY

OECD Halden Reactor Project: High Burnup Rim Effect irradiation (E. Kolstad)

POLAND

Institute of Atomic Energy, Otwock/Swierk: TRANSURANUS fuel pin code development (M. Szuta)
Institute for Low Temperature and Structure Research, Warsaw: Bulk properties and neutron scattering (R. Troc, W. Suski, D. Kaczorowski)

PORTUGAL

Instituto Tecnológico e Nuclear (ITN), Sacavem: Physical chemistry of actinides (A. Pires de Matos, M. Almeida, J.C. Warenborgh)
University of Coimbra: Neutron and X-ray studies (J.A. Paixão)

ROMANIA

Institute for Nuclear Research, Nuclear Fuel Performance Analysis, Pitetsi: TRANSURANUS fuel pin code development (G. Horhoianu)

RUSSIA

Academy of Sciences, IVTAN, Moscow: Equation of uranium dioxide (I. Iosiliewski); Studies on high-melting materials (V. Fortov)
All Russia Research Institute of Inorganic Materials (A.A. Bochvar Institute), Moscow: Setting up of three laboratories for safeguards, metrology, nuclear forensics (A. Petrov)
ENIL, Moscow: Thermophysical properties of high temperatures (E. Volkov))
Flerov Laboratory, Dubna: Radiation damage in ceramics (V.A. Skuratov)
GOSATOMNADZOR; Moscow: Nuclear Safeguards (A. Dimitriev)
High Temperature Institute, Moscow: Thermodynamic database (V. Yungman, L. Gorokhov)
Institute of Chemical Physics, Chernogolowka: Critical Point of UO_2 (V. Gryaznov)
MINATOM, Moscow: Nuclear Safeguards (N. Redin)
Nuclear Power Plant, Leningrad: PIE, non destructive examinations (V.C. Shevchenko)
Nuclear

SLOVAK REPUBLIC

Nuclear Power Plant Research Institute, Trnava: TRANSURANUS fuel pin code development (M. Cvan)

SOUTH AFRICA

University of Witwatersrand, Johannesburg: Transport measurements (P. du Plessis)

SPAIN

Ministerio de Industria y Energia, CIEMAT, Instituto de Technologica Nuclear, Madrid, TRANSURANUS fuel pin code development (J. Lopez Jimenez)
ENRESA: Waste management, leaching tests (J.A. Esteban-Hernandez)

SWEDEN

SKB: Spent fuel disposal (K. Spahiu)
University of Uppsala: Solid state theory of actinides (B. Johansson, O. Eriksson)

SWITZERLAND

ETH, Zürich: Single crystal growth, magnetic, optical and transport properties, preparation of U and Th compounds (O. Vogt, P. Wachter, K. Mattenberger)
Katonsspital Basel, Institut für Nuklearmedizin, α-immunotherapy (H.R. Mäcke)
Paul-Scherrer-Institut, Villigen TRANSURANUS fuel pin code development (C. Hellwig); Post-irradiation structural investigations by electron microscopy, PHEBUS PF FPT1 bundle post irradiation examination (D. Gavillet); Inert matrix studies (M. Burghartz)

UKRAINE

Ministry for environmental protection and nuclear safety of Ukraine: Illicit trafficking, FONSAFE (A. Smyshliaiev)
State Scientific and Technical Centre on Nuclear and Radiation Safety, Kyiv: TRANSURANUS fuel pin code development (M. Yeremenko)
University of Odessa: Liquid state models (E. Yakub)

UNITED KINGDOM

AEA Technology, Winfrith: shared cost action 'Revaporisation effects of PHEBUS samples (B. Bowsher)
Birkbeck College: neutron and magnetization studies (K. McEwen)
BNFL, Sellafield: On-site laboratory (R. Strong, J. Reed); PIE examination of MOX spent fuel (S. Fisher); Melting point of irradiated MOX (S. Fisher); Fuel fabrication (J. Edwards, C. Brown)
BFNL Eng. Department, Risley: Laboratory infrastructure (R. Johnson)
NNC, Risley: Engineering design support (B. Rowney)
NCC, Workington: QA consultancy (W.G. Smith)
Rutherford Appleton Laboratory, Chilton: Neutron Synchrotron studies (N. Bull, S. Langridge)

University of Bristol, Interface Analysis Centre: Surface corrosion (G. Allen)
University of Glasgow, Dept. of Physics and Astronomy/Rutherford Appleton Laboratory: Laser induced fission (K.W.D. Ledingham)
University of Liverpool: X-ray and neutron scattering (W.G. Stirling)
University of Oxford: Preparation of multilayers (M. Wells, R. Ward); UO_2 surface properties (A. Castell, C. Muggelberg)
University of Warwick: Compton scattering (M.J. Cooper); Equation of state of irradiated fuel (G. Hyland); Radiative properties at high temperatures (G. Hyland)

UNITED STATES OF AMERICA

Argonne National Laboratory, IL: Neutron scattering and X-ray arbsorption spectroscopy (L. Soderholm)
Battelle Pacific Nothwest Laboratories, Richland, WA: Irradiation damage studies (W. Weber)
Brookhaven National Laboratory, NY: High-resolution and magnetic X-ray scattering (D. Gibbs)
Colorado State University, Fort Collins, CO: Studies of oxides (S. Kern)
Eichrom Industries, Inc. Actinium-225 production (M.J. Gula)
Lawrence Berkeley National Laboratory, CA: Synchrotron studies of actinide surfaces and thin films (D. Shuh)
Lawrence Livermore National Laboratory, CA: Forensic nuclear analysis (S. Niemeyer)
Los Alamos National Laboratory, NM: Materials preparation and photoemission (B. Cort, A.J. Arko, A. Lawson); Radiation damage in ceramics (K. Sickafus)
Memorial Sloan Kettering Cancer Center, New York, NY: α-immunotherapy by Bi-213 (D.A. Scheinberg)
National Institute of Health, Bethesda, MD: α-immunotherapy by Bi-213 (M.W. Brechbiel)
Oak Ridge National Laboratory, TN: Material preparation, high pressure X-ray and optical studies (R.G. Haire, J.R. Peterson); Radiation damage in ceramics (S.J. Zinkle)
Rennsselaer Polytechnic Institute, Gaerttner Lab. Actininium-225 production (G. Xu)
University of Maryland, Baltimore, MD: Studies of surfaces (G. Watson)
University of of Michigan, Ann Arbor, MI: High resolution TEM, radiation damage (R. Ewing, L.M. Wang)
University of West-Virginia, Morgantown, WV: Actinide theory (B.R. Cooper)

UZBEKISTAN

Physical Technical Institute, Tashkent: Radiative properties of UO_2 at high temperatures (T. Salikhov)

List of Contributors

A – The Institute in Overview

ITU'S Programme
U. Huber, W. Janssens

Highlights
F. Wastin, J. Rebizant, G. Lander (H1); S. Heathman (H2); J. Magill (H3); C. Ronchi, J.-P. Hiernaut (H4); J. Spino, D. Papaioannou (H5); B. Sätmark, O. Courson, J.-P. Glatz, R. Malmbeck (H6); V.V. Rondinella, Hj. Matzke, T. Wiss, J. Cobos-Sabaté, M. Wallenius (H7); K. Mayer (H8); I. Ray, A. Schubert, K. Mayer, L. Koch (H9)

Review Article
L. Koch, J.-P. Glatz, R.J.M. Konings, J. Magill

Input & Output
W. Janssens, J.-F. Babelot, J. Richter, U. Huber

B – Activities in Progress

1. Alpha-Immunotherapy
L. KOCH, C. Apostolidis, W. Janssens, R. Molinet, T. Nikula

2. Basic Actinide Research
G.H. LANDER, A. Bombardi, M.S.S. Brooks, S. Coad, E. Colineau, T. Gouder, J.C. Griveau, S. Heathman, V. Ichas, D. Kolberg, K. Litfin, D. Mannix, A. Martín-Martín, J. Rebizant, F. Wastin, Hj. MATZKE, M. Cheindlin, J.-P. Hiernaut, C. Ronchi

3. Safety of Nuclear Fuels
J.-P. GLATZ, D.W. Bottomley, S. Brémier, D. Papaioannou, J. Spino, A.D. Stalios, E. Toscano, C.T. Walker, D.H. Wegen, D. HAAS, F. Charollais, R. Konings, J. Somers, Hj. MATZKE, M. Cheindlin, K. Laßmann, M. Musella, I. Ray, C. Ronchi, V.V. Rondinella, T. Wiss

4. Partitioning and Transmutation
J.-P. GLATZ, O. Courson, M. Ougier, R. Malmbeck, B. Sätmark, A. D. Stalios, C.T. Walker, D.H. Wegen, D. HAAS, N. Boucharat, A. Fernandez, R. Konings, J. Somers, Hj. MATZKE, T. Wiss

5. Measurement of Radioactivity in the Environment
L. KOCH, M. Betti, L. Aldave, O. Actis-Dato, D. Solatie, N. Erdmann

6. Spent Fuel Characterization in View of Long Term Storage
J.-P. GLATZ, D. Papaioannou, D.H. Wegen, B. Sätmark, Hj. MATZKE, J. Cobos-Sabaté, V. V. Rondinella, T. Wiss

7. Safeguards Research and Development
L. KOCH, J.M. Barrero, M. Betti, F. Bocci, P. Daures, P. Carbol, N. Erdmann, K. Mayer, H. Ottmar, H.-G. Schneider, A. Schubert, O. Stetzer, G. Tamborini

Glossary, Acronyms and Abbreviations

ABACC: Agência Brasileiro-Argentina de Contabilização e Controlo dos Materiais Nucleares
Argentinian-Brazilian Agency for Accounting and Control of Nuclear Material
ACTINEAU: Incinération des actinides dans les réacteurs à eau
ADS: Accelerator driven systems
ALI: Annual limits of intake (of radioactive substances)
ANS: American Nuclear Society
a/o: (at.%) atomic percent

BNFL: British Nuclear Fuel plc, Springfields (United Kingdom)
BOC: t-butyloxycarbonyl
BOL: Beginning of life (of a fuel pin)
BSE: Back-scattered electron
BTP: propyl-bis-triazinylpyridine
BWR: Boiling water reactor

CAPRA: Consommation accrue de plutonium dans les (réacteurs) rapides
CEA: Commissariat à l'Énergie Atomique (France)
CEN: Centre d'Études Nucléaires
CERN: Conseil Européen pour la Recherche Nucléaire, Geneva, Switzerland
CIT: Corium interaction thermochemistry
COGEMA: Compagnie générale des matériaux nucléaires, Vélizy (France)
COMPUCEA: Combined product-uranium concentration and enrichment assay
CORDIS: Community research and development information service, Luxembourg
CRIEPI: Central Research Institute of the Electric Power Industry, Tokyo (Japan)

DAC: Diamond anvil cell
DESY: Deutsches Elektronen-Synchrotron, Hamburg (Germany)
DIAMEX: Diamide extraction process
DIDPA: diisodecyl phosphoric acid
DIN: Deutsche Industrienorm; Deutsches Institut für Normung
DMDBTDMA: Dimethyl-dibutyl-tetradecyl-methylen-diamide
DOTA: 1,4,7,10-tetraazacyclododecane-1,4,7,10-tetraacetic acid
DOVITA: Dry reprocessing, oxide fuels, vibropac, integral, transmutation of actinides
DQS: Deutsche Gesellschaft zur Zertifizierung von Qualitätssicherungssystemen
Deutsche Gesellschaft zur Zertifizierung von Managementsystemen mbH
DSIN: Direction de la Sûreté des Installations Nucléaires (France)
DTPA: diethylenetriaminepentaacetic acid

EAEC: European Atomic Energy Commission
EBR: Experimental breeder reactor, Argonne National Laboratory (USA)
ECN: Energie Centrum Nederland, Petten (Netherlands)
ECSAM: European Commission's safeguards analytical measurements
EDAX: Energy-dispersive analysis with X-rays
EDF: Électricité de France
EDX: Energy-dispersive X-ray analysis
EFQM: European Foundation for Quality Management
EFTTRA: Experimental feasibility for targets and transmutation
EIS: Electrochemical impedance spectroscopy
EMPA: Electron micro-probe analysis (also EPMA)
EOL: End-of-life (of a fuel pin)
EOS: Equation of state
EPMA: Electron probe micro-analysis (also EMPA)
ESARDA: European safeguard research and development association
ESD: European Safeguards Directorate, Luxembourg
ESO: Euratom Safeguards Office
ESRF: European Synchrotron Radiation Facility, Grenoble (France)
ETH: Eidgenössische Technische Hochschule, Zürich (Switzerland)
EURATOM: European Atomic Energy Community
EXAFS: Extended X-ray absorption fine structure

FACT: Formation of actinides
FBR: Fast breeder reactor
FCCI: Fuel clad chemical interaction
FCMI: Fuel Clad Mechanical Interaction
FERONIA: fuel rod modelling and performance project
FNR: Fast neutron reactor
FONSAFE: Forensic nuclear analysis for safeguards
FP: Fission products

FWP: Framework programme
FZK: Forschungszentrum Karlsruhe (Germany)

GDMS: Glow discharge mass spectrometry (spectrometer)
GSP: Gel supported precipitation
GWd/tM: Gigawatt-day per (metric) ton metal
GWd/tU: Gigawatt-day per (metric) ton uranium (metal)

HASYLAB: Hamburger Synchrotronstrahlungslabor (Germany)
HBRP: High burnup rim project
HEHA: 1,4,7,10,13,16-hexacarboxylmethyl-1,4,7,10,13,16-hexaazacyclooctadecane
HFR: High flux reactor, Petten (Netherlands)
HLW: High level waste
HLLW: High level liquid waste
HPTA: High performance trace analysis

IAEA: International Atomic Energy Agency, Vienna (Austria)
IC-ICP-MS: Ion chromatography inductively coupled plasma mass spectrometry
IDA: Isotope dilution analysis
IDMS: Isotope dilution mass spectrometry
ILL: Institut Max von Laue - Paul Langevin, Grenoble (France)
IMF: Institut für Materialforschung, FZK (Germany)
INE: Institut für Nukleare Entsorgungstechnik, FZK (Germany)
INR: Institut für Neutronenphysik und Reaktortechnik, FZK (Germany)
INRAM: Infiltration of radioactive materials
INRNE: Institute for Nuclear Research and Nuclear Energy, Bulgarian Academy of Science
INSERM: Institut National de la Santé et de la Recherche Médicale
INSTN: Institut National des Sciences et Techniques Nucléaires, La Hague (France)
INTAS: International Association for the promotion of Cooperation with Scientists
from the Independent States of the former Soviet Union
IPSN: Institut de Protection et de Sureté Nucléaire, Cadarache (France)
ISO: International Organisation for Standardisation
ISTC: International Science and Technology Center, Moscow (Russia)
ITU: Institute for Transuranium Elements, Karlsruhe (Germany)
ITN: Instituto Tecnológico e Nuclear, Savacem (Portugal)
ITWG: International technical working group on nuclear smuggling

IVTAN: Institute for High Temperature Physics, Moscow (Russia)

JAERI: Japan Atomic Energy Research Institute (Japan)
JEF: Joint evaluated file, decay library, NEA-OECD, Paris
JRC: Joint Research Centre, European Commission

KAERI: Korea Atomic Energy Research Institute, (Republic of Korea)
KEDG: K-edge densitometer
KNK II: Kompakte Natriumgekühlte Kernreaktoranlage (Germany)
KWU: Kraftwerk-Union AG, Germany

LET: Linear-energy-transfer
LLB: Laboratoire Léon Brillouin, Gif-sur-Yvette, CEA-Saclay (France)
LLFP: Long-lived fission products
LMR: Liquid metal reactor
LSS: Laboratoire sur site, La Hague (France)
LWR: Light water reactor

MA: minor actinides (Np, Am, Cm)
MIMAS: Micronized master blend
MOX: Mixed oxide fuel of uranium and plutonium
MS: Mass spectrometer (Mass Spectrometry)
MSKCC: Memorial Sloan Kettering Cancer Center, New York (USA)
MTC: Medullary thyroid carcinoma
MTD: Maximum tolerated dose
MWd/kgM: Megawatt day per kg of (heavy) metal
MWd/kgU: Megawatt day per kg of uranium

NDA: Non-destructive assay (analysis)
NDT: Non-destructive testing
NEA: Nuclear Energy Agency, OECD, Paris (France)
NILOC: Nitride fuel with low oxygen and carbon content (irradiation experiment)
NIMPHE: Nitrures mixtes dans Phénix à joint helium
NNC: National Nuclear Corporation, Ltd. Risley (U.K.)
NRI-CAL: Nuclear Regulatory Institute Rez near Prague, Central Analytical Laboratory
NSLS: National Synchrotron Light Source, Brookhaven, NY (USA)

OECD: Organization for Economic Cooperation and Development, Paris (France)
ORACLE: Relational database program

ORIGEN: The Oak Ridge National Library-Isotope Generation and Depletion Code
ORNL: Oak Ridge National Laboratory, Oak Ridge, TN (USA)
OSL: On-site laboratory
OSPAR: joint meeting of the Oslo and Paris Commissions

PCI: Pellet clad interaction
PDF: Portable document format
PHARE: Pologne-Hongrie: Aide à la Reconstruction Économique
PHEBUS: French test reactor, Cadarache (France)
PHEBUS-FP: Programme to study fission product release and their distribution in the primary circuit
PHENIX: French prototype fast reactor
PIE: Post-irradiation examination
PIMPOM: Plutonium inert matrix in the POMPEI device
PNCC: Passive neutron-coincidence counting
PSI: Paul Scherrer Institut, Würenlingen, (Switzerland)
PUREX: Plutonium and uranium recovery by extraction
PWR: Pressurized water reactor

QM: Quality Management

RBMK: Reactor Bolshoi Moshchnosti Kanalnyi (high-power channel, graphite moderated, reactor (Russia)
RIAR: Research Institute of Atomic Reactors, Dimitrovgrad (Russia)
RKKY: Rutterman, Kittel, Kasuya, Yoshida interaction
RXMS: Resonant X-ray magnetic scattering

SANEX: Selective actinides(III) extraction
SBR: Short binderless route
SCA: Shared cost action
SCK-CEN: Studiecentrum voor Kernenergie - Centre d'Etude de l'Energie Nucleaire, Mol (Belgium
SEM: Scanning electron microscopy
SGN: Société Générale pour les Techniques Nouvelles, (France)
SIMFUEL: Simulated high burnup fuel (with major non-volatile fission products)
SIMS: Secondary ion mass spectrometry
SOLMAS: Sol gel master blend
SONS: State Office for Nuclear Safety, Czech Republic
SQUID: Superconducting quantum interference device
SUBATECH: Laboratoire de physique subatomique et de technologies associés, Nantes (France)

SUPERFACT: minor actinide irradiation in Phenix (France)
TACIS: Technical Assistance to the Commonwealth of Independent States
TEM: Transmission electron microscopy
THORP: Thermal oxide reprocessing plant, Sellafield (U.K.)
TIMS: Thermal ionization mass spectrometry
TOPO: Trioctyl phosphine oxide
TRABANT: Transmutation and burning of actinides in TRIOX
TRANSURANUS: Fuel behaviour code (ITU), Karlsruhe (Germany)
TRIOX: HFR irradiation capsule, Petten (The Netherlands)
TRPO: Trialkyl phospine oxide
TRU: Transuranic waste
TRUEX: Aqueous process for transuranium extraction
TUAR: Institute for Transuranium Elements annual report, Karlsruhe (Germany)

UREX: Uranium extraction

VNIINM: All-Russia Research Institute of Inorganic Materials, Moscow (Russia)
v/o: (vol %) volume percent
VVER: (also WWER) Voda-Vodyanoi Energetichesky Reaktor Pressurized Water Reactor (PWR) built by Russia

w/o: (wt %) weight percent
WWER: (also VVER) Pressurized water reactor (PWR) built by Russia

XMCD: X-ray magnetic circular dichroism
XPS: X-ray induced photoelectron emission spectroscopy
XRD: X-ray diffraction
XRF: X-ray fluorescence analysis

Previous Annual Reports

TUSR	Period	COM Nr.	EUR-Nr.
1	Jan - Jun 1966	1580	–
2	Jul - Dec 1966	1522	–
3	Jan - Jun 1967	1745	–
4	Jul - Dec 1967	2007	–
5	Jan - Jun 1968	2172	–
6	Jul - Dec 1968	2300	–
7	Jan - Jun 1969	2434	–
8	Jul - Dec 1969	2576	–
9	Jan - Jun 1970	2664	–
10	Jul - Dec 1970	2750	–
11	Jan - Jun 1971	2833	–
12	Jul - Dec 1971	2874	–
13	Jan - Jun 1972	2939	–
14	Jul - Dec 1972	3014	–
15	Jan - Jun 1973	3050	–
16	Jul - Dec 1973	3115	–
17	Jan - Jun 1974	3161	–
18	Jul - Dec 1974	3204	–
19	Jan - Jun 1975	3241	–
20	Jul - Dec 1975	3289	–
21	Jan - Jun 1976	3358	–
22	Jul - Dec 1976	3384	–
23	Jan - Jun 1977	3438	6475 EN
24	Jul - Dec 1977	3484	7209 EN
25	Jan - Jun 1978	3526	7459 EN
26	Jul - Dec 1978	3582	7227 EN
27	Jan - Jun 1979	3657	7483 EN
28	Jul - Dec 1979	3714	7509 EN
29	Jan - Jun 1980	3822	7857 EN
30	Jul - Dec 1980	3846	8230 EN
31	Jan - Jun 1981	3898	8447 EN
32	Jul - Dec 1981	3927	8777 EN
33	Jan - Jun 1982	3990	9581 EN
34	Jul - Dec 1982	4048	10251 EN
35	Jan - Jun 1983	4094	10266 EN
36	Jul - Dec 1983	4117	10454 EN
37	Jan - Jun 1984	4150	10470 EN
38	Jul - Dec 1984	4165	11013 EN
39	Jan - Jun 1985	4201	11835 EN
40	Jul - Dec 1985	4263	11836 EN

TUSR	Period	COM Nr.	EUR-Nr.
86	Jan - Dec 1986	4302	12233 EN
87	Jan - Dec 1987		11783 EN
88	Jan - Dec 1988		12385 EN
89	Jan - Dec 1989		12849 EN
90	Jan - Dec 1990		13815 EN
91	Jan - Dec 1991		14493 EN
92	Jan - Dec 1992		15154 EN
93	Jan - Dec 1993		15741 EN
94	Jan - Dec 1994		16152 EN
95	Jan - Dec 1995		16368 EN
96	Jan - Dec 1997		17269 EN
97	Jan - Dec 1997		17746 EN
98	Jan - Dec 1998		18715 EN
99	Jan - Dec 1999		19054 EN

Previous Programme Progress Reports were confidential for a period of two years. Between 1977 and 1987 they had been made freely accessible after that period as EUR-Reports (on microfiches) and since 1988 they have been issued as regular EUR-Reports.

European Commission

EUR 19054 EN - Institute for Transuranium Elements - Annual report 1999
Editors: R. Schenkel, J. Richter, J. Magill, D. Pel
Luxembourg: Office for Official Publications of the European Communities
2000 - 164 pp. - 21.0 x 29.7 cm
Scientific and Technical Research series
ISBN 92-828-8985-8

Abstract

The 1999 annual report of the Institute for Transuranium Elements (ITU) of the JRC decribes progress made during the first year of the 5th Framework Programme.

In the first part of the report, an overview of the organisational structure together with staff and budget resources is given together with publications and patents for the reporting period. A brief description of the institutional and competitive activities is given. In addition to a review article on Partitioning and Transmutation studies at ITU, a series of highlight articles on important progress made during 1999 are presented on:

- Growth of single crystals of mixed actinide dioxides;
- New crystal phase of americium metal;
- "Switching" on nuclear reactions: laser induced fission of uranium;
- Volatile molecule of PuO_3 observed by sublimating plutonium dioxide;
- Application of the micro-X-ray diffraction technique to the rim zone in high burn-up fuels;
- Separation of minor actinides from lathanides;
- α-decay damage in UO_2: Long term storage behaviour in spent fuel;
- Inauguration of the "On-Site" laboratory in Sellafield; Plutonium round-robin test,

together with a review article on Partitioning and Transmutation studies at ITU is presented.

In the second part of the report, a more in-depth technical description of progress made in the last year is given. Topics covered focus on: Alpha-Immunotherapy Studies, Basic Actinide Research, Safety of the Nuclear Fuel, Partitioning and Transmutation, Measurement of Radioactivitiy in the Environment, Spent Fuel Characterisation in view of Long-Term Storage, and Safeguards Research and Development work.

A detailed list of publications and collaborations is given in the annex.

The mission of the JRC is to provide customer-driven scientific and technical support for the conception, development, implementation and monitoring of EU policies. As a service of the European Commision, the JRC funcitions as a reference centre of science and technology for the Union. Close to the policy-making process, it serves the common interest of the Member States, while being independent of special interests, whether private or national.

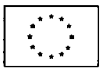

EUROPEAN COMMISSION
JOINT RESEARCH CENTRE

15 LC-NA-19-054-EN-C

OFFICE FOR OFFICIAL PUBLICATIONS
OF THE EUROPEAN COMMUNITIES

L-2985 Luxembourg